Samarth Educational Trust's

Arvind Gavali College of Engineering

Affiliated to Dr. Babasaheb Ambedkar Technological University, Lonere.
Approved by AICTE, New Delhi, Recognized by Govt. of Maharashtra, DTE Mumbai.

NAAC and NBA Accredited

PROPOSAL FOR AUTONOMOUS STATUS
A.Y. 2025-26

Name of Document	Particular
Achievements of Faculty Members	List of Faculty Achievements

Annexure No. 22

Dr. Sharad S. Mulik
PRINCIPAL

ARVIND GAVALI COLLEGE OF ENGINEERING EN-6545 SATARA

SAMARTH EDUCATIONAL TRUST
ARVIND GAVALI COLLEGE OF ENGINEERING
Approved by AICTE, New Delhi, Recognized by Govt. of Maha. DTE Mumbai &
Affiliated to MSBTE Mumbai ,Dr. Babasaheb Ambedkar Technological, University Lonere
AICTE ID: 1-4210711 AISHE Code: C-11245 DTE Code: EN-6545 DBATU Code: 6545 MSBTE Code: 1617
NBA Accredited NAAC Accredited
Address : Gat No.247, At.Panmalewadi,
Post.-Varye,Tal.& Dist.-Satara, Pin.- 415 015
Mob.: 9957100100, 9069700100
Email : agcenggsatara@gmail.com
Website: www.agce.edu.in

Ref. No.: AGCE/Office/2024-25/ **Date:27th Feb. 2025**

ACHIEVEMENTS OF FACULTY MEMBERS

The faculty of Arvind Gavali College of Engineering have demonstrated exceptional academic and research excellence. They have published numerous research papers, filed patents, presented at conferences, authored books, and secured external funding. These achievements showcase their expertise and dedication, enhancing the institution's reputation and research ecosystem, making it an ideal candidate for autonomous status.

Sr No	Activity	No of activities academic year wise					
		2023-24	2022-23	2021-22	2020-21	2019-20	2018-19
1	Number of Research Papers Published in Journals	17	27	08	13	11	07
2	Number of Patents Granted	05	05	02	02	01	
3	Number of Papers Published in National Conferences						
4	Number of Papers Published in International Conferences	01	50		02	34	40
5	Number of Books Authored	02		01	01		
6	Number of Book Chapters Authored		01				
7	Number of New Externally Funded Research Projects Received	31	24	25	21	16	14
8	Funds Received	5.74 Lakhs	11.26 Lakhs	4.98 Lakhs	6.98 Lakhs	4.83 Lakhs	3.10 Lakhs
9	Other Achievements	47	22	17	44	110	02
All faculty members achievement certificates Link for reference		View	View	View	View	View	View

Note: All faculty achievements documents are attached in the respective y[illegible] link above[illegible]ble for your reference.

ARVIND GAVALI COLLEGE OF ENGINEERING EN-6545 SATARA

Achievements of Faculty Members for the Academic Year 2020-21:

https://www.agce.edu.in/files/autonomy/af/2020-2021.pdf

1. Number of Research Papers Published in Journals:

Sr. No.	Name of the Faculty Member	Department	Award/Recognition	Details/Title of the Paper
1	Ms. D. S. Jadhav	Civil Engineering	Research Paper Published	Analysis of Factors Causing Cost Overruns in Residential Building Construction Projects
2	Ms. D. S. Jadhav	Civil Engineering	Research Paper Published	Effect of Time and Cost Overruns on Building Construction Projects
3	Ms. D. S. Jadhav	Civil Engineering	Research Paper Published	Influence of Buildability Factors on Flooring Labour Productivity
4	Mrs. Eva Gupta	Electrical Engineering	Research Paper Published	Fabrication and characterization of novel nitinol particulate reinforced aluminium alloy metal matrix composites (NiTip/AA6061 MMCs) [SCOPUS]
5	Mrs. Eva Gupta	Electrical Engineering	Research Paper Published	Finite element analysis of mechanical response of fracture fixation functionally graded bone plate at paediatric femur bone fracture site under compressive and torsional loadings [SCOPUS]
6	Mrs. Eva Gupta	Electrical Engineering	Research Paper Published	An Insight into the Simplified RP Transmission Network, Concise Baseline and SIR Models for Simulating the Transmissibility of the Novel Corona virus Disease 2019 (COVID-19) [SCOPUS]

ARVIND GAVALI COLLEGE OF ENGINEERING EN-6545 SATARA

7	Mrs. Eva Gupta	Electrical Engineering	Research Paper Published	Stochastic and deterministic mathematical 2odelling and simulation to evaluate the next COVID-19 pandemic control measures [SCOPUS]
8	Dr. G S Mirajkar	Electronics and Telecommunication Engineering	Research Paper Published	Early Detection of Tumors in MR Images in MR Images of the Human Brain: An Application Using Deep Learning Techniques [SCOPUS]
9	Dr. G S Mirajkar	Electronics and Telecommunication Engineering	Research Paper Published	Detection of deforestation change in SAR images using local features [Web of Science]
10	Dr. G S Mirajkar	Electronics and Telecommunication Engineering	Research Paper Published	Comparison of Image Processing Techniques for Classification of Red Blood Cell Structures [Web of Science]
11	Dr. G S Mirajkar	Electronics and Telecommunication Engineering	Research Paper Published	Brain Tumor Detection in MR Images of the Human Brain Using Biologically Inspired Orthogonal Wavelet Transform and Machine Learning [SCOPUS]
12	Dr. V. A. Pharande	Mechanical Engineering	Research Paper Published	Design of Tooling System to Reduce Cycle Time [SCOPUS]
13	Dr. A. N. Khadtare	Mechanical Engineering	Research Paper Published	Surface integrity studies for straight and inclined hole in micro-drilling of thermal barrier coated Inconel 718: A turbine blade application [SCOPUS]

2. Number of Patents Granted:

Sr. No.	Name of the Faculty Member	Department	Award/Recognition	Details/Title of the Patent
1	Dr. G S Mirajkar	Electronics and Telecommunication Engineering	Published Australian Patent	Semi-Automatic Approach for Tumor Segmentation in Human Brain MR Images
2	Dr. V. A. Pharande	Mechanical Engineering	Published Indian Patent	Retro-Fitment Kit for Three-Wheeler Auto Rickshaw to Convert IC

				Engine Into Electrical Drive Using Gear Box

3. Number of Papers Published in National Conferences: NIL

4. Number of Papers Published in International Conferences:

Sr. No.	Name of the Faculty Member	Department	Award/Recognition	Details/Title of the Papers
1	Mr. V. C. Khade	Electronics and Telecommunication Engineering	Presented Research Paper in International Conference on Communications and Cyber Physical Engineering (ICCCE 2021)	Maize Leaf Healthy and Unhealthy Classification Using Image Processing Technique and Machine Learning Classifiers
2	Mr. A. S. Shivade	Mechanical Engineering	Presented Research Paper in International Conference on Artificial Intelligence and Machine Learning (ICAIML 2020)	Modified Direct Clustering Algorithm for Group Formation in Cellular Manufacturing

5. Number of Books Authored:

Sr. No.	Name of the Faculty Member	Department	Award/Recognition	Details
1	Dr. V. A. Pharande	Mechanical Engineering	Published Book	Book Titled, "Customer Relationship Management" published by International Research Journal of Multidisciplinary Scope (IRJMS) ISSN: 2454 – 8499

6. Number of Book Chapters Authored: NIL

7. Number of New Externally Funded Research Projects Received:

Sr. No.	Name of the Faculty Member	Department	Award/Recognition	Details/Title of the Project
1	Dr. A. V. Gujar	Civil Engineering	Project Sponsored by Dhumal Construction Pvt. Ltd., Satara	Experimental Study on Effect of Glass Fiber in Glass Powder Cement Concrete
2	Dr. V. R. Thombare	Civil Engineering	Project Sponsored by JW Infra Pvt. Ltd., Satara	Effect of Granite and Marble Waste to Enhance the Properties of Silty Soil
3	Mr. R. N. Sapkal	Civil Engineering	Project Sponsored by Innovative Construction Pvt. Ltd., Satara	Strengthening of Beam and Column by Carbon Fiber Reinforced Polymer
4	Dr. V. S. Hingmire	Electronics and Telecommunication Engineering	Project Sponsored by Ajinkya Polymers and Engineering	IoT-Based Industrial Security System
5	Mr. V. T. Barkade	Electronics and Telecommunication Engineering	Project Sponsored by Prime Enterprises	Sanitizer Dispensing Robot
6	Dr. V. S. Hingmire	Electronics and Telecommunication Engineering	Project Sponsored by 3 Star IT Solutions, Satara	Smart Receptionist Using IoT
7	Dr. G. S Mirajkar	Electronics and Telecommunication Engineering	Project Sponsored by VRT Enterprises, Satara	Alexa Based Home Automation System
8	Dr. B. M. Nayak	Electrical Engineering	Project Sponsored by Ajinkya Electrosystems, Satara	Reverse Rotation Controller for Rotating Equipment
9	Dr. V. K. Bhosale	Electrical Engineering	Project Sponsored by Ravi Electricals, Satara	IoT-Based Induction Motor Monitoring System
10	Dr. G S Mirajkar	Electrical Engineering	Project Sponsored by Siddheshwar Electricals, Satara	IoT-Based Smart Energy Meter Monitoring and Billing System
11	Mr. Basavraj Nelogal	Electrical Engineering	Project Sponsored by Ajinkya Electrosystems, Satara	Induction Motor Rotation in Bidirectional Through A Remote ControlDevice
12	Mr. P. A. Pathak	Computer Science and Engineering	Project Sponsored by Sourcecode Technology, Pune	Online Grocery Market
13	Mr. V. T. Barkade	Computer Science and Engineering	Project Sponsored by Sourcecode Technology, Pune	Forest Fire Detection and Control

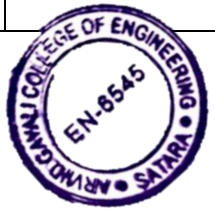

14	Mr. P. A. Pathak	Computer Science and Engineering	Project Sponsored by Rudra Architects Interior, Landscape, and Master Planners, Satara	Web Development of PTMPL Advertising
15	Mr. P. M. Tambe	Mechanical Engineering	Project Sponsored by Novel Industries, Satara	Performance Study of Electric Discharge Machine (EDM) Processes
16	Mr. P. M. Tambe	Mechanical Engineering	Project Sponsored by Paranjape Autocast Pvt. Ltd. Satara	Ladle Lining by Readymade Exothermic Sleeve
17	Mr. P. M. Tambe	Mechanical Engineering	Project Sponsored by Kavade Engineering Works, Satara	Polyster Let Off Machine
18	Mr. A. S. Shivade	Mechanical Engineering	Project Sponsored by Omkar Engineering, Tal. Wai, Dist. Satara	Compact Rolling and Bending Machine
19	Mr. P. R. Nikam	Mechanical Engineering	Project Sponsored by SBK Machinery & Consulting Services, Koregaon, Dist. Satara	Vertical Hydraulic Baling Machine
20	Mr. A. S. Shivade	Mechanical Engineering	Project Sponsored by Urja Setu, Dhankawadi, Pune	Automatic Painting Machine
21	Mr. P. R. Nikam	Mechanical Engineering	Project Sponsored by Shri Ganesh Industries, Karad	Pneumatic Operated Feeder

8. Funds Received During This Academic Year:

Sr. No.	Name of the Faculty Member	Department	Award/Recognition	Details/Title of the Project
1	Dr. A. V. Gujar	Civil Engineering	Project Sponsored by Dhumal Construction Pvt. Ltd., Satara	Rs. 20,000/-
2	Dr. V. R. Thombare	Civil Engineering	Project Sponsored by JW Infra Pvt. Ltd., Satara	Rs. 15,000/-
3	Mr. R. N. Sapkal	Civil Engineering	Project Sponsored by Innovative Construction Pvt. Ltd., Satara	Rs. 28,000/-

4	Dr. V. S. Hingmire	Electronics and Telecommunication Engineering	Project Sponsored by Ajinkya Polymers and Engineering	Rs. 18,000/-
5	Mr. V. T. Barkade	Electronics and Telecommunication Engineering	Project Sponsored by Prime Enterprises	Rs. 20,000/-
6	Dr. V. S. Hingmire	Electronics and Telecommunication Engineering	Project Sponsored by 3 Star IT Solutions, Satara	Rs. 22,500/-
7	Dr. G. S Mirajkar	Electronics and Telecommunication Engineering	Project Sponsored by VRT Enterprises, Satara	Rs. 12,000/-
8	Dr. B. M. Nayak	Electrical Engineering	Project Sponsored by Ajinkya Electrosystems, Satara	Rs. 15,000/-
9	Dr. V. K. Bhosale	Electrical Engineering	Project Sponsored by Ravi Electricals, Satara	Rs. 22,000/-
10	Dr. G S Mirajkar	Electrical Engineering	Project Sponsored by Siddheshwar Electricals, Satara	Rs. 20,000/-
11	Mr. Basavraj Nelogal	Electrical Engineering	Project Sponsored by Ajinkya Electrosystems, Satara	Rs. 22,000/-
12	Mr. P. A. Pathak	Computer Science and Engineering	Project Sponsored by Sourcecode Technology, Pune	Rs. 12,000/-
13	Mr. V. T. Barkade	Computer Science and Engineering	Project Sponsored by Sourcecode Technology, Pune	Rs. 16,000/-
14	Mr. P. A. Pathak	Computer Science and Engineering	Project Sponsored by Rudra Architects Interior, Landscape, and Master Planners, Satara	Rs. 12,000/-
15	Mr. P. M. Tambe	Mechanical Engineering	Project Sponsored by Novel Industries, Satara	Rs. 12,000/-
16	Mr. P. M. Tambe	Mechanical Engineering	Project Sponsored by Paranjape Autocast Pvt. Ltd. Satara	Rs. 2,50,000/-
17	Mr. P. M. Tambe	Mechanical Engineering	Project Sponsored by Kavade Engineering Works, Satara	Rs. 1,10,000/-

18	Mr. A. S. Shivade	Mechanical Engineering	Project Sponsored by Omkar Engineering, Tal. Wai, Dist. Satara	Rs. 8000/-
19	Mr. P. R. Nikam	Mechanical Engineering	Project Sponsored by SBK Machinery & Consulting Services, Koregaon, Dist. Satara	Rs. 25,000/-
20	Mr. A. S. Shivade	Mechanical Engineering	Project Sponsored by Urja Setu, Dhankawadi, Pune	Rs. 20,000/-
21	Mr. P. R. Nikam	Mechanical Engineering	Project Sponsored by Shri Ganesh Industries, Karad	Rs. 10,000/-

9. Other Achievement:

Sr. No.	Name of the Faculty Member	Department	Award/Recognition	Details
1	Ms. D. S. Jadhav	Civil Engineering	Attended Six Days Workshop	Attended Six Days Workshop on "NAAC Accreditation Process for University"
2	Ms. D. S. Jadhav	Civil Engineering	Participated in Webinar on “Tendering & Execution of Works"	Webinar on "Tendering & Execution of Works"
3	Ms. D. S. Jadhav	Civil Engineering	Participated in Two Day Workshop	Participated in Two Day Workshop on "COs, POs, PSOs Mapping and Attainment"
4	Dr. V. R. Thombare	Civil Engineering	Attended One Week Online Faculty Development Programme	Attended One Week Online Faculty Development Programme on "Research Opportunities in Environmental Engineering"
5	Dr. V. R. Thombare	Civil Engineering	Attended TEQIP 3 Sponsored Five Days Online FDP	TEQIP 3 Sponsored 5 Days Online FDP on "Recent Advances in Health 5.0 In-line with NEP 2020"
6	Mrs. S. S. Tokdar	Civil Engineering	Attended TEQIP 3 Sponsored Five Days Online FDP	TEQIP 3 Sponsored 5 Days Online FDP on "Recent

				Advances in Health 5.0 In-line with NEP 2020"
7	Mr. V. S. Nikam	Civil Engineering	Attended TEQIP 3 Sponsored Five Days Online FDP	TEQIP 3 Sponsored 5 Days Online FDP on "Recent Advances in Health 5.0 In-line with NEP 2020"
8	Mr. P. A. Pathak	Computer Science and Engineering	Attended TEQIP 3 Sponsored Five Days Online FDP	TEQIP 3 Sponsored 5 Days Online FDP on "Recent Advances in Health 5.0 In-line with NEP 2020"
9	Dr. V. K. Bhosale	Computer Science and Engineering	Attended TEQIP 3 Sponsored Five Days Online FDP	TEQIP 3 Sponsored 5 Days Online FDP on "Recent Advances in Health 5.0 In-line with NEP 2020"
10	Dr. V. K. Bhosale	Computer Science and Engineering	Attended One Day Webinar	Webinar on "Virtual Labs: Effective Tool for Teaching and Learning"
11	Mrs. R. M. Mandhare	Computer Science and Engineering	Attended TEQIP 3 Sponsored Five Days Online FDP	TEQIP 3 Sponsored 5 Days Online FDP on "Recent Advances in Health 5.0 In-line with NEP 2020"
12	Mrs. R. M. Mandhare	Computer Science and Engineering	Attended One Week Online Short-Term Training Programme	One Week Online Short-Term Training Programme (STTP) on "Deep Learning Tools & Application in Engineering & Science"
13	Mr. V. B. Gujar	Computer Science and Engineering	Participated in Quiz	Quiz on "R - Programming"
14	Mr. V. B. Gujar	Computer Science and Engineering	Participated in Online Quiz	Techno-Social Awareness Quiz on "Biodiversity"
15	Mr. V. B. Gujar	Computer Science and Engineering	Attended Online Webinar	Webinar on "Dynamic Routing Using Cisco Packet Tracer"
16	Mr. V. B. Gujar	Computer Science and Engineering	Attended Two Weeks Short Term Training Programme	Two Weeks Short Term Training Programme on "IT for Sustainability"
17	Mr. V. B. Gujar	Computer Science and Engineering	Attended One Day Webinar	Webinar on "Security Issues in Internet of Things (IoT)"
18	Ms. R. D. Shingade	Computer Science and Engineering	Attended TEQIP 3 Sponsored Five Days Online FDP	TEQIP 3 Sponsored 5 Days Online FDP on "Recent Advances in Health 5.0 In-line with NEP 2020"
19	Dr. B. M. Nayak	Electrical Engineering	Attended TEQIP-III sponsored Faculty Development Programme	TEQIP-III sponsored Faculty Development Programme (FDP) on “Industrial IoTs, Industry 4.0 & Disruptive Technologies”

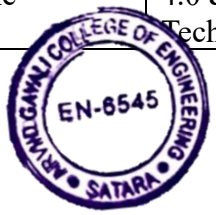

20	Dr. B. M. Nayak	Electrical Engineering	Attended TEQIP 3 Sponsored 5 Days Online FDP	TEQIP 3 Sponsored 5 Days Online FDP on "Recent Advances in Health 5.0 In-line with NEP 2020"
21	Mrs. Eva Gupta	Electrical Engineering	Attended TEQIP 3 Sponsored 5 Days Online FDP	TEQIP 3 Sponsored 5 Days Online FDP on "Recent Advances in Health 5.0 In-line with NEP 2020"
22	Mr. Jivajee Bichkar	Electrical Engineering	Attended TEQIP 3 Sponsored 5 Days Online FDP	TEQIP 3 Sponsored 5 Days Online FDP on "Recent Advances in Health 5.0 In-line with NEP 2020"
23	Mr. Basavraj Nelogal	Electrical Engineering	Attended TEQIP 3 Sponsored 5 Days Online FDP	TEQIP 3 Sponsored 5 Days Online FDP on "Recent Advances in Health 5.0 In-line with NEP 2020"
24	Ms. Hrutuja S. Bhutkar	Electrical Engineering	Attended TEQIP 3 Sponsored 5 Days Online FDP	TEQIP 3 Sponsored 5 Days Online FDP on "Recent Advances in Health 5.0 In-line with NEP 2020
25	Dr. G S Mirajkar	Electronics and Telecommunication Engineering	Attended TEQIP 3 Sponsored 5 Days Online FDP	TEQIP 3 Sponsored 5 Days Online FDP on "Recent Advances in Health 5.0 In-line with NEP 2020"
26	Dr. G S Mirajkar	Electronics and Telecommunication Engineering	Attended One Day Webinar	Webinar on "Antenna Design through Simulation Using TaraNG 19.1"
27	Dr. G S Mirajkar	Electronics and Telecommunication Engineering	Attended One Day Online Workshop	Online Workshop on "Academic Book Writing & Related Topics"
28	Dr. G S Mirajkar	Electronics and Telecommunication Engineering	Attended One Day Webinar	Webinar on "IEEE 802.11 and Building Wireless Community Networks"
29	Dr. G S Mirajkar	Electronics and Telecommunication Engineering	Attended One Day Webinar	One Day Webinar on "New Higher Education Policy and Digitization of Education"
30	Mr. V. T. Barkade	Electronics and Telecommunication Engineering	Attended TEQIP 3 Sponsored 5 Days Online FDP	TEQIP 3 Sponsored 5 Days Online FDP on "Recent Advances in Health 5.0 In-line with NEP 2020"
31	Ms. Tanuja Phadatare	Electronics and Telecommunication Engineering	Attended TEQIP 3 Sponsored 5 Days Online FDP	TEQIP 3 Sponsored 5 Days Online FDP on "Recent Advances in Health 5.0 In-line with NEP 2020"
32	Mr. Vivek Mohite	Electronics and Telecommunication Engineering	Attended TEQIP 3 Sponsored 5 Days Online FDP	TEQIP 3 Sponsored 5 Days Online FDP on "Recent Advances in Health 5.0 In-line with NEP 2020"

33	Mr. Pratik Mahajan	Electronics and Telecommunication Engineering	Attended TEQIP 3 Sponsored 5 Days Online FDP	TEQIP 3 Sponsored 5 Days Online FDP on "Recent Advances in Health 5.0 In-line with NEP 2020"
34	Dr. V. A. Pharande	Mechanical Engineering	Attended TEQIP 3 Sponsored 5 Days Online FDP	TEQIP 3 Sponsored 5 Days Online FDP on "Recent Advances in Health 5.0 In-line with NEP 2020"
35	Mr. S. S. Ghadage	Mechanical Engineering	Attended TEQIP 3 Sponsored 5 Days Online FDP	TEQIP 3 Sponsored 5 Days Online FDP on "Recent Advances in Health 5.0 In-line with NEP 2020"
36	Mr. P. B. Bamankar	Mechanical Engineering	Attended TEQIP 3 Sponsored 5 Days Online FDP	TEQIP 3 Sponsored 5 Days Online FDP on "Recent Advances in Health 5.0 In-line with NEP 2020"
37	Mr. A. V. Kamble	Mechanical Engineering	Attended TEQIP 3 Sponsored 5 Days Online FDP	TEQIP 3 Sponsored 5 Days Online FDP on "Recent Advances in Health 5.0 In-line with NEP 2020"
38	Mrs. M. N. Alatkar	Mechanical Engineering	Attended TEQIP 3 Sponsored 5 Days Online FDP	TEQIP 3 Sponsored 5 Days Online FDP on "Recent Advances in Health 5.0 In-line with NEP 2020"
39	Mr. Sandeep Pawar	Mechanical Engineering	Attended TEQIP 3 Sponsored 5 Days Online FDP	TEQIP 3 Sponsored 5 Days Online FDP on "Recent Advances in Health 5.0 In-line with NEP 2020"
40	Mr. P. R. Nikam	Mechanical Engineering	Attended TEQIP 3 Sponsored 5 Days Online FDP	TEQIP 3 Sponsored 5 Days Online FDP on "Recent Advances in Health 5.0 In-line with NEP 2020"
41	Mr. N. V. Ghadage	Mechanical Engineering	Attended TEQIP 3 Sponsored 5 Days Online FDP	TEQIP 3 Sponsored 5 Days Online FDP on "Recent Advances in Health 5.0 In-line with NEP 2020"
42	Mr. R. R. Kamble	Mechanical Engineering	Attended TEQIP 3 Sponsored 5 Days Online FDP	TEQIP 3 Sponsored 5 Days Online FDP on "Recent Advances in Health 5.0 In-line with NEP 2020"
43	Mr. P. M. Tambe	Mechanical Engineering	Attended TEQIP 3 Sponsored 5 Days Online FDP	TEQIP 3 Sponsored 5 Days Online FDP on "Recent Advances in Health 5.0 In-line with NEP 2020"
44	Mr. S. G. Chavan	Electronics and Telecommunication Engineering	Attended 40 Hours Self-Paced Certification Programme	40 Hours Self-Paced Certification Programme in "Python for Machine Learning"

ARVIND GAVALI COLLEGE OF ENGINEERING EN-6545 SATARA

Principal
Principal
Samarth Educational Trust
Arvind Gavali College of Engineering
Panmalewadi, Satara

1. Number of Research Papers Published in Journals

International Journal of Research in Engineering, Science and Management
Volume-3, Issue-7, July-2020
journals.resaim.com/ijresm | ISSN (Online): 2581-5792

Analysis of Factors Causing Cost Overruns in Residential Building Construction Projects

Diksha Jadhav[1*], B. A. Konnur[2], Sanjana Patil[3]
[1,3]*PG Student, Department of Civil Engineering, Government College of Engineering, Karad, India*
[2]*Associate Professor, Department of Civil Engineering, Government College of Engineering, Karad, India*
*Corresponding author: jadhav25diksha@gmail.com

***Abstract*: One of India 's key industrial industries are the construction industry and the largest driving force in India's national economy. Efficient project management of the construction is based on three main factors, namely time, cost and quality. Cost is a key factor in the project management life cycle and can be viewed as one of the project's most important factors and the driving force behind the project's performance. Cost overruns are common in construction and infrastructure projects. Most projects are subject to cost overruns, and thus exceed the contract's original value. In India, residential building projects are growing in size. However, completion of the projects at the allotted cost is challenging. This paper mainly focuses on residential construction projects. Data obtained from the questionnaire survey is used to identify the main causes of Cost Overruns. The data analysis is performed using the relative importance index (RII) method, and the ranking method identifies the factors that cause significant cost overruns in residential building projects.**

***Keywords*: Analysis, Cost overrun, Factors causing overruns, Relative importance index, Residential building construction project.**

1. Introduction

Project delays and cost overruns are a major concern in developing countries, where project execution faces many uncertainties. This leads to a lack of financial shortage funds, delays in infrastructure provision, development and thus increase the construction costs. Despite global economic development driven by globalization and technology, there is a need for a scientific and structured project management approach to ensure that project targets are met within time and budget constraints.

Cost overrun, also known as cost rise or budget overrun, entails additional costs incurred in excess of the budgeted sums due to underestimation of actual costs during the budgeting process.

Cost is one of the important indicators for the performance of the project. It is true, particularly for building projects in developing countries, because building construction projects in these countries are being carried out with limited financial resources. Many of the literature reviews on construction projects indicated that the common factors for project performance are usually considered to be expense, time and quality [Arditi et al, 1997; Frimpong et al 2003]; Atkinson (1999) referred to these factors as the 'iron triangle.' Songer and Molenaar (1997) found the project to be satisfactory if it had been completed on budget, on time, in compliance with customer standards, fulfilled the requirements, and achieved the standard of the workmanship.

Generally, a project is considered to be satisfactory if the project is completed within the specified cost or budget, if the project is performed by the target date, if the technical objective is met, and if the project participants are highly satisfied with the project outcome.

A. Definitions of Cost Overruns

a) Cost overrun: A cost overrun, also known as a cost increase or budget overrun, involves unexpected costs incurred in excess of budgeted amounts due to an underestimation of the actual cost during budgeting. [User Guide, 2005].
b) Cost overrun: The amount by which actual costs exceed the baseline or approved costs [Wideman, 2002].
c) Cost overrun: The difference between the original cost and the actual cost when the project is completed [Avots, 1983]. Actually, Avots, (1983) used the word growth instead of cost overrun.

B. Causes of Cost Overruns

- Conflicts and changes in design, inadequate planning, unpredictable weather conditions climate factors, fluctuations in the cost of building materials, poor coordination.
- Poor site management, incomplete design at the time of tender, additional work at owner's request, changes in owner's brief, equipment-related delays can be due to poor equipment planning, site/poor soil conditions.
- Lack of control inaccurate management of personnel and the whole agency, attitude, low moral motivation, labor, machinery and equipment.
- Lack of cost reports during construction stage, delays in issuing information to the contractor during construction stage, improper construction methods.
- Contractual claims, such as, extension of time with cost claims, Improvements to standard drawings

during construction stage.

- Technical personnel- shortages, strikes, Lack of experience, slow mobilization, absenteeism, poor communication.
- Omissions and errors in the bills of quantities, Delays in costing variations and additional works, ignoring items of abnormal rates during tender evaluation.
- Labor-related delays- increase in labor wages, poor communication, absentees or low motivation.
- Site management and site safety, financial delay, inadequate supervision, too many responsibilities Shortage of personnel Lack of experience, Poor quality, Poor planning, Lack of experience of local regulation.
- Materials-related delays inefficient communication damage materials poor quality of materials late delivery, Delay in procuring and arrangement of construction equipment by contractors.

2. Objective of the Study

The main objective of this analysis is to identify the major causes of cost overruns of construction projects using a case study in Satara City. It is noted that clients, consultants, and contractors do not give any priority to assess the cost overruns at the project's end. There are also few study and studies in Satara on this field. The main objectives of this research are:

- To study the concept of cost overrun from the available literature and identify the causes of cost overruns.
- To collect data by conducting Questionnaire survey.
- To identify the main factors causing cost overruns in residential building construction project using data analysis.

3. Methodology and Data Collection

This research is conducted in a number of stages, including literature reviews and research papers, data collection, discussion and conclusion. From the literature review, we identified 29 factors causing for Cost Overruns in Satara city. For data collection, a total of one hundred and twenty (120) sets of questionnaires were sent to the people working in the organization of the selected five residential construction sites located in Satara. The respondent's included Contractors, Clients, Quantity Surveyors, Project Managers, Engineers and Architects. The evaluation of Cost Overrun factors was carried out using the 4-point Likert scale from 1 to 4 as follows:

1. Can be neglected
2. Low influence
3. Medium influence
4. High influence

Out of 120, eighty (80) completed sets were received back. This was considered adequate for the analysis based on the assumption by Moser and Kalton (1971) that the result of a survey could be considered as biased and of little value if the return rate was lower than 30–40%. The respondents involved in the survey had several years of experience in handling several types of projects.

4. Data Analysis

Data analysis was carried out by calculating the Relative Importance Index (RII) using the following formula, adopted by Memon et al. in 2002, as the RII is the most suitable approach to perform the ranking analysis.

$$RII = \frac{\sum_{i=1}^{4} W * X}{A * N}$$

Where, RII = Relative Importance Index
W = Weighting given by respondents to each factor and its ranges from 1 to 4
X = Reaction frequency for each factor
A = Maximum weight (i.e. 4 in case)
N = Participants total no.

The ranking for various factors was calculated from RII results to identify the major factors causing cost overruns in building projects.

Table 1 shows the data analysis of the factors causing Cost Overruns. The relative importance index (RII) is calculated for each factor. The ranks are given based on the obtained value of RII respectively.

Table 1
Ranking of causes of cost overruns

S.No.	Causes of Cost Overruns	RII	Rank
1	Conflicts and changes in design.	0.631	10
2	Inadequate planning.	0.697	2
3	Unpredictable weather conditions climate factors.	0.569	21
4	Fluctuations in the cost of building materials	0.663	7
5	Poor coordination.	0.650	8
6	Poor site management.	0.678	5
7	Incomplete design at the time of tender.	0.566	22
8	Additional work at owner's request.	0.694	3
9	Changes in owner's brief.	0.634	9
10	Equipment-related delays can be due to poor equipment planning.	0.600	16
11	Site/poor soil conditions.	0.578	19
12	Lack of control inaccurate management of personnel and the whole agency, attitude, low moral motivation.	0.588	18
13	Labour, machinery & equipment.	0.622	11
14	Lack of cost reports during construction stage	0.578	20
15	Delays in issuing information to the contractor during construction stage	0.509	25
16	Improper construction methods.	0.594	17
17	Contractual claims, such as, extension of time with cost claims.	0.725	1
18	Improvements to standard drawings during construction stage.	0.616	13
19	Technical personnel- shortages, strikes, Lack of experience, slow mobilization, absenteeism, poor communication.	0.613	14
20	Omissions and errors in the bills of quantities	0.484	28

21	Delays in costing variations and additional works	0.472	29
22	Ignoring items of abnormal rates during tender evaluation.	0.519	24
23	Labour-related delays- increase in labour wages, poor communication, absentees or low motivation.	0.609	15
24	Site management and site safety.	0.497	27
25	Financial delay	0.500	26
26	Inadequate supervision, too many responsibilities Shortage of personnel Lack of experience, Poor quality, Poor planning.	0.619	12
27	Lack of experience of local regulation.	0.691	4
28	Materials-related delays inefficient communication damage materials poor quality of materials late delivery.	0.550	23
29	Delay in procuring & arrangement of construction equipment by contractors	0.672	6

5. Results and Discussions

From the data analysis, major eight factors having highest RII value were identified respectively. The results obtained from the study are shown in fig. 1 using bar chart representation.

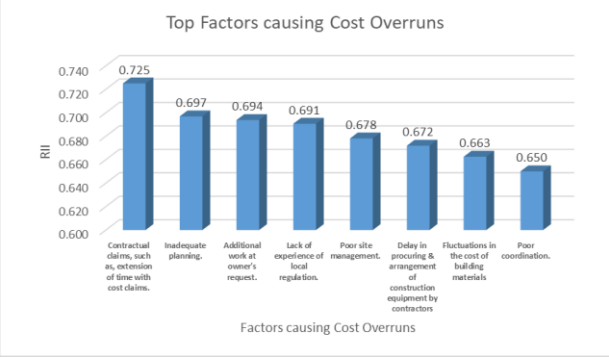

Fig. 1. Top factors causing cost overruns

The top factors causing Cost Overruns in the residential building construction projects from the survey are as follows.

1. Contractual claims, such as, extension of time with cost claims (RII-0.725) - Changes in construction projects can cause substantial adjustment to the contract duration and construction cost.
2. Inadequate planning (RII-0.697) – Poor planning can cause serious problems in many areas later in the project, including lack of business support and poor estimates.
3. Additional work at owner's request (RII-0.694) – This is the factor associated with the owner's request related to additional design or construction work.
4. Lack of experience of local regulation (RII-0.691)-It can occur if the concerned working team fails to deal with the local working techniques.
5. Poor site management (RII-0.678) - A poor project management structure will have an impact at all stages of the construction process leading to lack of solid project plan, Lack of team coordination and poor communication between members of the project team and the project sponsor.
6. Delay in procuring & arrangement of construction equipment by contractors (RII-0.672) – Due to lack of communication or other crises, the delay in arrangement of equipment's can occur.
7. Fluctuations in the cost of building materials (RII-0.663)- During periods of high development where the level of construction activity is unusually high in a particular region, there may be shortages of some construction materials. Sometimes the local market may not be able to supply the full demand of these construction materials.
8. Poor coordination (RII-0.650) – This is the major cause of cost overrun found in majority of studies.

6. Conclusion

The results of the study are the same as those of the previous studies. The concept of Cost Overrun and the causes of Cost Overrun in construction projects were studied. Civil professionals have reported that most projects are delayed due to cost overrun problems. Civil workers stated that the most of the projects gets delayed due to cost overrun issues. Contractual claims, inadequate planning, additional work issues, delay in procuring and arrangement of construction equipment's, poor site management, fluctuation in the cost of building materials are the major factors for Cost Overrun in residential building construction projects. The relative importance index (RII) can be used as an important cost overrun evaluation tool. The study offers knowledge and data to project managers and contractors to concentrate on key cost overrun factors in residential construction projects.

References

[1] Aftab Memon, Ismail Rehman, Ade Asmi Abdul Azis (2012), "Time & Cost performance in Construction Projects in Southern and Central Region of Peninsular Malaysia". International Journal of advances in applied sciences, Vol. 1, March 2012, pp. 45-52

[2] Ahsan, K., & Gunawan, I. (2010). Analysis of cost and schedule performance of international development projects. International Journal of Project Management, 28, 68-78. Anderson, J. D. (2006). Qualitative and quantitative research (Imperial COE, 1-3).

[3] Al-Khalil, M.I. & Al-Ghafly, M.A. (1999). "Important causes of delay in public utility projects in Saudi Arabia". Construction Management and Economics, 17(5), pp. 647- 655.

[4] Al-Momani, A.H. 2000. Construction delay: A quantitative analysis. International Journal of Project Management, 18(1), pp. 51-59.

[5] Apolot, Ruth, Alinaitwe, Henry & Tindiwensi, Dan. (2012), "An Investigation into the Causes of Delay & Cost Overrun in Uganda's Public Sector Construction Projects", Second International Conference on Advances in Engineering and Technology, pp 305-311.

[6] Assaf, S.A., Al-Khalil, M. & Al-Hazmi, M. (1995). Causes of delay in large building construction projects. Journal of Management in Engineering, 11(2), pp. 45-50.

[7] Azhar, N., Farooqui, R. U., & Ahmed, S. M. (2008). Cost overrun factors in construction industry of Pakistan. Proceedings from First International Conference on Construction in Developing Countries.

[8] Azis, A. A. A., Memon, A. H., Rahman, I. A., & Karim, A. T. A. (2012). Controlling cost overrun factors in construction projects in Malaysia.

Research Journal of Applied Sciences, Engineering and Technology, 5(8), 2621-2629.

[9] Baloyi, Lucius and Bekkar, Michiel (2011), "Couses of Construction Cost & Time Overruns:The 2010 FIFA World Cup Stadia in South Africa, Acta Structilia Journal, Vol. 1, 51-67.

[10] Kumaraswamy, M.M. & Chan, D.W.M. 1998. Contributors to construction delays. Construction Management and Economics, 16(1), pp. 17-29.

[11] M. Haseeb, Aneesa Bibi, Wahab Rabbani (2011), Causes & Effects of delays in Large Construction Projects of Pakistan, Kuwait chapter of arabian journal of buisiness & management review Vol. 1, No. 4 December 2011, pp 18- 42.

[12] Sambasivan, M. and Soon, Y. (2007) 'Causes and effects of delays in Malaysian construction industry', International Journal of Project Management, 25 (5), 517-526.

[13] S. Shanmugapriya (2013) Investigation of Significant Factors Influencing Time and Cost Overruns in Indian Construction Projects, International Journal of emerging Technology & advanced engineering, Vol. 3, Issue 10, October 2013.

[14] T. Subramani, P. S. Sruthi, M. Kavitha (2014), Causes of Cost Overruns in Construction, IOSR Journal of Engineering (IOSRJEN), 06(04), pp.01-07

[15] Walid Kholif, Hossam Hosny & Abdelmonem Sanad, (2013) "Analysis of Time & Cost Overruns in Educational Building Projects in Egypt.", International Journal of Engineering and Technical Research, Vol. 1, Issue 10.

[16] Yakubu Adisa Olawale (2010) "Cost and time control of construction projects: inhibiting factors and mitigating measures in practice" Construction Management and Economics, 28 (5), 509–526.

IJCRT.ORG ISSN : 2320-2882

INTERNATIONAL JOURNAL OF CREATIVE RESEARCH THOUGHTS (IJCRT)

An International Open Access, Peer-reviewed, Refereed Journal

EFFECT OF TIME AND COST OVERRUNS ON BUILDING CONSTRUCTION PROJECTS

[1]Diksha S Jadhav, [2]Pranali B Devthanekar

[1]Assistant Professor, [2]Assistant Professor

[1] Civil Engineering Department,

[1,]Sanjay Ghodawat University, Kolhapur,India

Abstract: The construction industry plays an important role in Indian economics. Successful completion of project depends upon two major factor time and cost .Hence, there is need to overcome cost and time overruns in construction projects. The objective of this study is to identify the factors causing time and cost overruns. To achieve this objective, a case study of residential construction project is taken. The questionnaire survey for 50 respondents is carried out. The data analysis is done using relative importance index(RII) method and the factors causing major overruns are found out by ranking method. Suitable measures are suggested to minimize the impact of time and cost overruns on the building construction projects.

Index Terms **-Time Overrun,Cost Overrun,Relative importance index, Construction project**

I. INTRODUCTION

Construction industry plays an important role for the economic development of any country. However this industry is facing severe problems which directly affects the time, cost and quality performances of construction projects. The construction projects are affected by number of factors during construction phase and post construction phase. As a result, successful completion of project within the desired time and cost is become a challenging task.

Cost overrun is described as the ratio of the change in the original contract amount to the original contract award amount. For the ease of comparison, the cost overrun can be converted into a percentage value. Mathematically it can be expressed as:

Cost overrun = Final Contract Amount – Original Contract Amount

Time Overrun is the phenomenon in which the project gets delayed beyond its expected completion time due to certain difficulties i.e. more time is required to finish the project than initially planned. The time overrun variable is defined as the difference between the estimated project duration and the actual time taken to complete the project. Time or Money used unnecessarily is of course 'time' and 'money' wasted.

Time and cost are the lifelines of every project. It is of supreme importance to study, analyze and evaluate the common factors leading to these constraints and suggest the best mitigation measures to overcome time and cost overrun constraints. Hence, an efficient control system must be employed to achieve desired results. Effective and meaningful control must begin at design stage and should be backed up by proper and scientific estimation and data analysis

II. OBJECTIVE OF THE STUDY

The main objective of this study is to identify the major causes of delays of building construction projects using a case study in Satara city. Accordingly, possible ways of minimizing them are suggested. It is noted that the clients, consultants, and contractors don't give importance to evaluate the time and cost overruns at the end of project. Also research and studies in this field in Satara are few. The specific objectives of the study are as follows:

1) To study the concept of time and cost overrun from the available literature.
2) To collect data by conducting Questionnaire survey.
3) To carry out data analysis using Relative importance index and thereby ranking of factors using Likert's Scale.
4) To recommend possible Solutions/Prevention to avoid cost and time overrun.

III. RESEARCH METHOD

Research method is the systematic stepwise process to carry out any survey work. This study is carried out through several phases that include literature reviews, research papers, data collection, discussion and conclusion. From the literature review 40 influencing factors were identified causing for time and cost overrun in residential construction projects.

For this purpose, a case study of residential construction project located in Satara city was selected.The data collection was carried out through questionnaire survey. The questionnaires were distributed to contractors, consultants and the staff involved in the respective project. The respondents involved in the survey had several years of experience in handling residential construction projects. Assessment of causes of time & cost overruns was carried out using 4-point Likert scale from 1 to 4 representing can be neglected, low influence, medium influence & high influence respectively. Data analysis was done calculating Relative Importance Index (RII) by following formula, adopted from Memon et al. 2002 as RII is best suitable method to do the ranking analysis.

$$\mathbf{RII} = \frac{\sum_{i=1}^{4} \mathbf{W} * \mathbf{X}}{\mathbf{A} * \mathbf{N}}$$

Where, RII = Relative Importance Index
W = Weighting given to each factor by respondents and its ranges from 1-4
X = Frequency of it response given for each factor A =Highest weight (i.e. 4 in case)
N = Total no. of participants.
From RII results, the ranking for different factors was determined to discover the influencing factors causing time overrun in construction projects.

IV. RESULTS

4.1 Data Collection

For data collection, a total of eighty(80) sets of questionnaires were sent to the people working in the organization of the selected residential construction site located in Satara. Out of 80, fifty (50) completed sets were received back which were evaluated with Microsoft Excel program in order to find the importance factors causing time & cost overrun in construction. Significance of major influencing factors causing construction time & cost overrun was identified in the questionnaire survey. Respondents were asked to rank the factors with 4-likert scale as:

1. Can be neglected
2. Low influence
3. Medium influence
4. High influence

4.2 Data Analysis

Data were analysed by using Relative Importance Index method (RII); the factors were ranked by dividing the factors in various phases such as before construction, during construction, external reasons, management problem, and shortage in resources.Following table shows the analysis of data by RII method and giving the ranks to each influencing factor. In table no.2, C & T means factor caused for Cost overrun & Time overrun.

Table 1. Data Analysis by RII

	INFLUENCING FACTORS	Weight (1-4)				RII	Rank
		1	2	3	4		
BEFORE CONSTRUCTION							
1	Inaccurate estimate of cost and time (C & T)	8	12	18	19	0.81	1
2	Poor bidding process (T)	19	9	14	8	0.555	8
3	Faulty designs (C & T)	8	11	13	18	0.705	2
4	Intentional low-bidding (C)	4	19	24	3	0.63	7
5	Improper site planning (T)	8	11	17	14	0.685	3
6	Delay in Approval of Drawings (T)	10	10	14	16	0.68	4
7	Land acquisition problem (T)	9	12	16	13	0.665	6
8	Errors in Contract Documents/ Schedule (T)	3	16	24	7	0.675	5
DURING CONSTRUCTION							
9	Redesigning (C & T)	5	12	27	6	0.67	3
10	Disputes and clashes on site (T)	8	18	12	12	0.64	4
11	Use of costly material/poor market survey (C)	8	13	15	14	0.675	2
12	Poor quality of work/ Rework (C & T)	10	5	15	20	0.725	1
13	Non adherence to the contract conditions (T)	6	27	13	4	0.575	7
14	Primitive technologies used (T)	15	10	9	16	0.63	5
15	Location of site/ lack of proper access(T)	11	16	18	5	0.585	6
EXTERNAL REASONS							
16	Irregular Flow of Finance (C & T)	2	10	27	11	0.735	1
17	Fluctuation in Price (C)	8	9	13	20	0.725	2
18	Cut in Water & Electrical Supply (T)	20	8	6	16	0.59	8
19	Weather Conditions (T)	3	24	14	9	0.645	7
20	Political & Other External Influence (T)	9	10	16	15	0.685	5
21	Wire/ Theft of Materials (T)	9	15	12	14	0.655	6
22	Government Influence (T)	12	9	8	21	0.69	4
23	Work Stay Due to Act of God (T)	8	10	16	16	0.7	3
MANAGEMENT PROBLEMS							
24	Lack of Experience (T)	8	12	15	15	0.685	7
25	Delay in Decision by Client (T)	12	10	8	20	0.68	8
26	Delay in Decision by Architect (T)	13	7	13	17	0.67	9
27	Delay in Decision by Consultant (T)	11	10	5	24	0.71	4
28	Delay in Decision by Contractor (T)	10	12	6	22	0.7	6
29	Delay in Payment for Work Order (T)	4	8	4	34	0.84	1
30	Inadequate Safety Measures/ Accidents (C & T)	5	16	12	17	0.705	5
31	Lack of Supervision (C & T)	8	20	5	17	0.655	10
32	Lack of Co-ordination between Different Parties involved (C & T)	5	15	11	19	0.72	3
33	Lack of Efficient Staff (T)	7	6	19	18	0.74	2
SHORTAGE IN RESOURCES							
34	Delays in Purchasing of Materials (C & T)	10	12	8	20	0.69	4
35	Delay in Supply of Material (T)	5	15	12	18	0.715	3
36	Delay in Procurement/ Supply of Equipments (T)	8	18	14	10	0.63	6

37	Equipment Breakdown/ Non Availability (T)	7	22	11	10	0.62	7
38	Improper Material Management (T)	6	14	8	22	0.73	1
39	Improper Labour Management (T)	4	14	16	16	0.72	2
40	Labour Strike (T)	12	15	4	19	0.65	5

V. DISCUSSION OF RESULTS

5.1 Before Construction

Based on the ranking, Figure 1 shows the top three most influencing factors caused for time and cost overrun before construction were:

a. Inaccurate estimate of cost and time(RII= 0.81) (C & T)
b. Faulty design (RII= 0.705) (C & T)
c. Improper site planning (RII= 0.685) (T)

5.2 During Construction

From fig. 2, based on ranking, during construction the top three most significant factors caused for both cost & time overrun were:

a. Poor quality of work / rework (RII-0.725) (C & T)
b. Use of costly material/poor market survey (RII-0.675) (C)
c. Redesigning (RII- 0.670) (C)

5.3 External Reasons

From figure 3, based on ranking, following are the top three external significant factors caused for both cost & time overrun were:

a. Irregular Flow of Finance (RII-0.735) (C & T)
b. Fluctuation in Price (RII-0.725) (C)
c. Work stay due to Act of God (RII-0.7) (T)

5.4 Management Problem

From Figure 4, based on ranking, the top three factors caused for time & cost overrun regarding management problem were:

a. Delay in Payment for Work Order (RII-0.840) (T)
b. Lack of Efficient Staff (RII-0.740) (T)
c. Lack of Co-ordination between Different Parties Involved (RII-0.720) (C & T)

5.5 Shortage in Resources

From Figure 5, based on ranking, following top three factors caused for cost and time overrun because of shortage in resources were:

a. Improper Material Management (RII-0.730) (T)
b. Improper Labour Management (RII-0.720) (T)
c. Delay in Supply of Material (RII-0.715) (T)

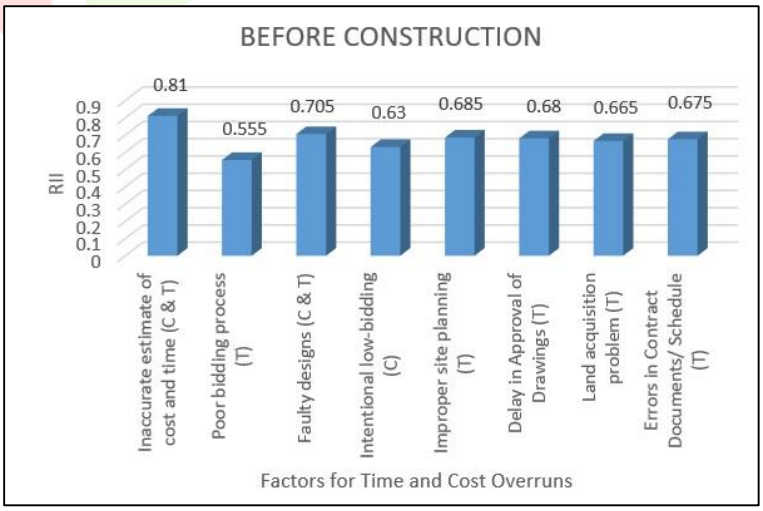

Figure 1. RII of influencing factors before construction

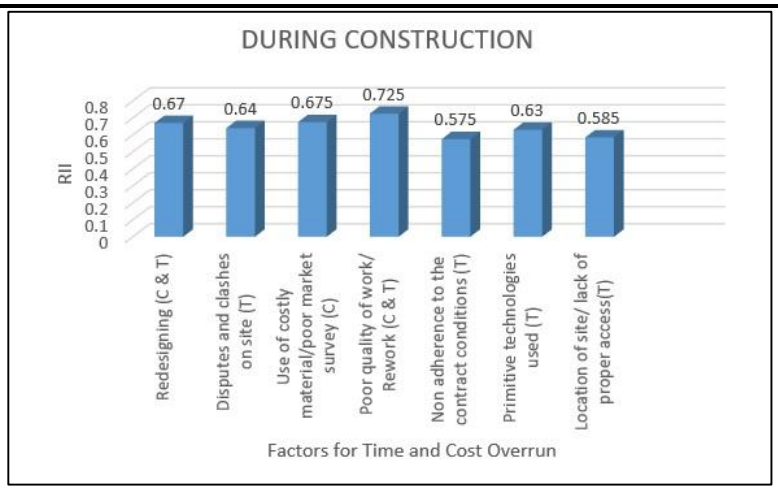

Figure 2. RII of influencing factors during construction

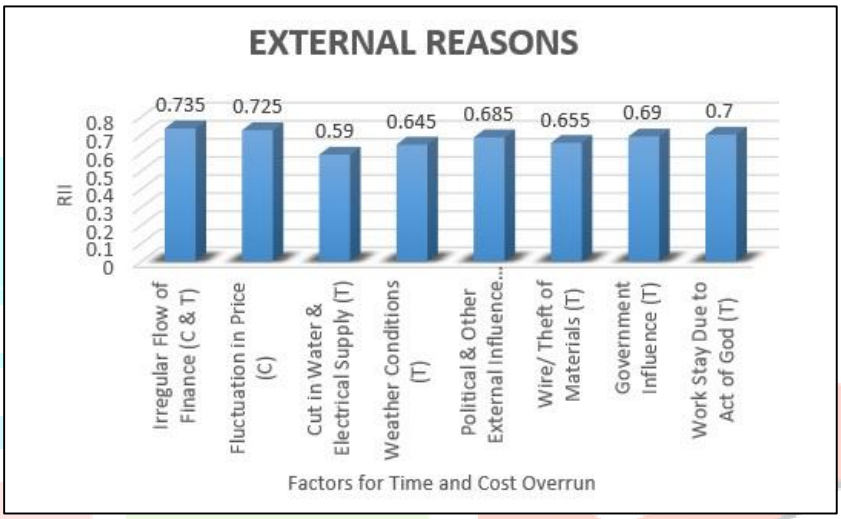

Figure 3. RII of influencing factors due to external reasons

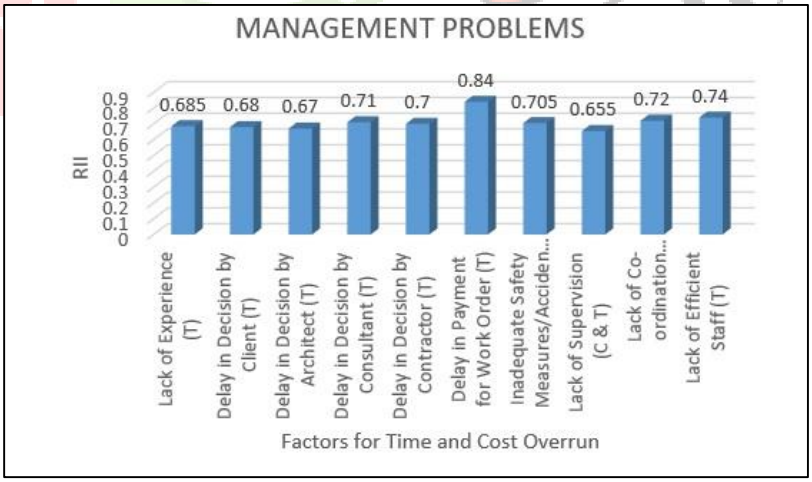

Figure 4. RII of influencing factors due to management problems

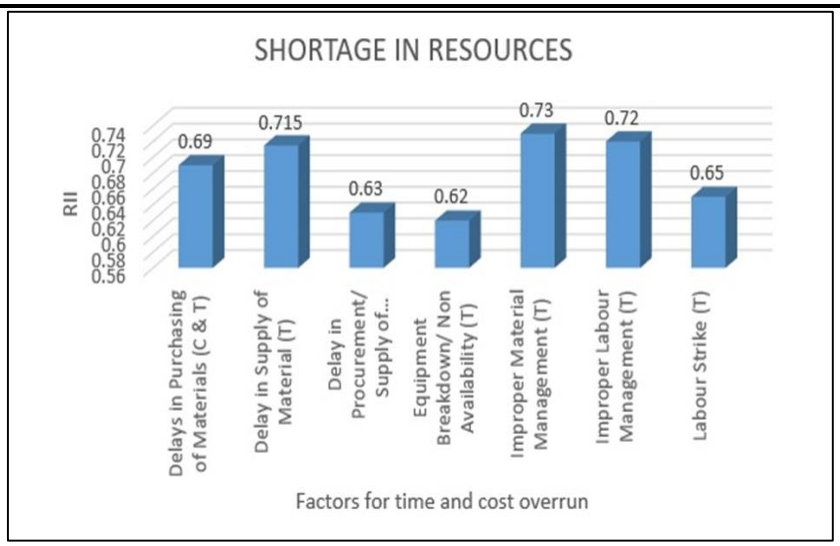

Figure 5. RII of influencing factors due to shortage in resources

VI. CONCLUSION

After doing the analysis using case study, most influencing factors caused for time & cost overruns are provided. The relative importance index (RII) can be used as an effective tool for analysis on time & cost overruns.The following learnings with some remedial measures for the observed causes of time & cost overruns are:

- Most of the labours working in construction site are coming from other state and having a poor knowledge regarding the new techniques in construction. Proper training programs can be adopted to increase the efficiency and skill of labours.
- Finally management also needs to increase the efficiency of works by conducting labour welfare, recognition programs for the motivation of labours.
- It will not possible to execute the construction projects within the desirable time and cost without sound implementation of planning. Hence, management needs to focus on effective and sound planning.
- The project manager should record whether all the activities are completed according to the estimated schedule weekly and then take the sign of the contractor. This practice may reduce time as well as cost overrun considerably.
- Industrial engineering and management techniques such as method study, value engineering, etc., can help in reducing time duration of activities and giving up of unnecessary items/activities
- 'Monitoring groups' can be established, which may consist of representatives of the project as well as inter-linked agencies and the parties concerned. The groups could monitor and review the progress of the complete system -the project and the inter-linked activities/projects.

REFERENCES

[1] Adam, A, Josephson, P, Lindahl, G. (2014) Implications of cost overruns and time delays on major public construction projects, Proceedings of the 19th International Symposium on the Advancement of Construction Management and Real Estate, 7-9Nov 2014

[2] Aftab Hameed Memon , Ismail Abdul Rahman , Ade Asmi Abdul Aziz (2012) " The cause factors of large project's cost overrun: a survey in the southern part of peninsular Malaysia" International Journal of Real Estate Studies, Volume 7, Number 2

[3] Ahsan, K., & Gunawan, I. (2010). Analysis of cost and schedule performance of international development projects. International Journal of Project Management 28(1), 68-7

[4] Albert, P.C. Chan., David Scott & Ada, P.L. Chan (2004), Factors affecting the success of a construction project, Journal of Construction Engineering and Management.

[5] B.V. Khode, S.V.Bhalerao(2018), A survey on assessment of time and cost overrun of Indian national highways project , IJCSMC, Vol. 7, Issue. 3, pg.33 – 42

[6] M. R. Apte (2016), Schedule overrun and cost overrun in the construction of private residential construction project: case study of pune India , International Journal of Technical Research and Applications Volume 4, Issue 2

[7] M.V. Raju, S.S. Asadi(2017), Evaluation of cost and time impacts to overruns in construction industry , International Journal of Civil Engineering and Technology

[8] N K Gupta(2018), Avoiding Cost Overruns of Residential Construction Projects in Western Part of Pune City, India , International Research Journal of Engineering and Technology
[9] Santosh Kumar Prajapati(2016), Impact of Cost and Time Overrun on Building Construction Projects, IJEDR ,Volume 4, Issue 4

International Journal of Research in Engineering, Science and Management
Volume-3, Issue-7, July-2020
journals.resaim.com/ijresm | ISSN (Online): 2581-5792

Influence of Buildability Factors on Flooring Labour Productivity

Pranali B. Devthanekar[1*], Diksha S. Jadhav[2], B. A. Konnur[3]
[1,2]*M.Tech. Scholar, Department of Civil Engineering, Government College of Engineering, Karad, India*
[3]*Associate Professor, Department of Civil Engineering, Government College of Engineering, Karad, India*
*Corresponding author: pran123434.pd@gmail.com

***Abstract*: Buildability is most important factor which impacts the labour productivity. Since Flooring is most important and repetitive activity in the construction of many types of industrial and residential buildings. Hence buildability factors in flooring considerably affect the labour productivity. In this study buildability factors involved in flooring are studied by selecting 40 building sites. Data collected from sites is analysed by using categorical regression analysis. The effects of factors such as geometry of room, screed thickness, tile area on buildability are discussed. Conclusions are drawn to show the impact of buildability on floor fixing operations. This study provides information to construction project managers or and site engineers to improve their labour productivity for the flooring activity on building sites.**

***Keywords*: Buildability, Categorical regression analysis, Flooring, Labour productivity.**

1. Introduction

In a production process, productivity is generally defined as the ratio of output to inputs. Productivity derives from the efficiency of the manufacturing process, in particular the efficiency with which labour and capital (men and machines) are used to turn inert materials into end products which are socially functional. Labour efficiency (i.e. the man-hour relationship and the quantity of work installed) is a significant measure of construction labour performance. Since labour is a key building resource. Construction labour productivity is described as "physical progress per hour." The cost time and quality of any construction project depend on the productivity. Building industry is a labour-intensive industry, and labour costs account for 30–50 percent of the overall project cost in most countries. A cornerstone of a good calculation is the cost of labour, which relies on assessing the projected efficiency of labour.

The accepted definitions of buildability developed by the Construction Industry Research and Information Association (CIRIA) in the UK, as: "Buildability is the extent to which the design of a building facilitates ease of construction, subject to the overall requirements for the completed building (CIRIA, 1983). Illingworth (1993) defined buildability as design and detailing which recognize the assembly process in achieving the desired result safely and at least cost to the client.

Moore (1996) modified Illingworth's (1984) definition as a "design philosophy, which recognizes and addresses the problems of the assembly process in achieving the construction of the design product, both safely and without resort to standardization or project level simplification."

Buildable designs lead to more labour productivity and lower construction costs (Dong 1996; Carter 1999; Williamson 1999). Design simplification is achieved through the implementation of the following three major buildability principles: (1) rationalization; (2) standardization; and (3) repetition of elements (Dong 1996). Design rationalization is defined as "the minimization of the number of materials, sizes, components or subassemblies," whereas standardization is "a design philosophy requiring the designed product to be produced from those materials, components, and subassemblies remaining after design rationalization has taken place" (Moore 1996b). The design repetition principle involves repeating bay layout, floor grids, dimensions of elements, and storey height.

2. Flooring Operation Overview

The Floor Tiling Productivity Monitoring Form has been designed to standardize the monitoring of productivity for floor tiling. Flooring involves following basic process-

A) Marking of reference and level lines
B) Preparation of sub-grade
C) Laying of mortar bed
D) Laying of tiles

A. Marking of reference and level lines

After completing the preparatory activities, a reference line is marked on room walls. On the basis of this reference line, a level for sub grade, mortar bed and the tile-finished surface are established taking into consideration the slope required & their thickness. Thereafter, respective level lines are transferred/marked on the walls with the use of line thread and indigo (Neel).

B. Preparation of sub-grade

The sub-grade, for flooring laid on the ground floor is known as "Base Concrete" whereas flooring laid over structural slabs, is known as "Cushioning layer". The base concrete shall be

either lime concrete or cement concrete of specified mix. The thickness of base concrete shall be as specified (normally up to 85-90mm).

C. Laying of mortar bed

Over properly laid sub-grade, the mortar layer is evenly and smoothly spread. Both cement mortar as well as lime mortar can be used for this purpose.

1. Preparation of mortar for bedding.
2. Spreading of mortar.

D. Laying of tiles

It consists of following operations:

1. Marking of layout lines
2. Plan/pattern for the tile application
3. Fixing of tiles

3. Objective of the Study

The main objective of this study is to identify the buildability factors which impacts on the flooring labour productivity. Major factors are identified by visiting the sites located in Kolhapur city. The specific objectives of the study are as follows:

- To study the concept of buildability from the available literature.
- To study construction labour productivity on the basis of activity level.
- To find out the impact of buildability factors on the flooring labour productivity by regression analysis using PhStat software.

4. Experimental Work

A. Data collection through interview for productivity calculation

For the flooring labour productivity calculation, 40 sites were visited and interviewed to collect the data of vitrified tile installation. 3 Major buildability factors were observed on the sites 1. Tile Size, 2. Screed Thickness, 3. Geometry of the room.

B. Productivity calculation

Data collection sites were located in Kolhapur city.

Productivity calculation is done by time study. Productivity is calculated in the by general formula output divided by input. Here output is tiled area and input is time required to complete the tiling the entire room.

Productivity = $\boldsymbol{Tiled\ Area}$ (m^2) /$\boldsymbol{required\ time\ in}$ ($\boldsymbol{hr}$)

For categorical regression analysis, tile size, screed Thickness are measured and geometry is observed weather it is rectangular or non -rectangular. Also, tiled area and time require to install the tiles are also recorded.

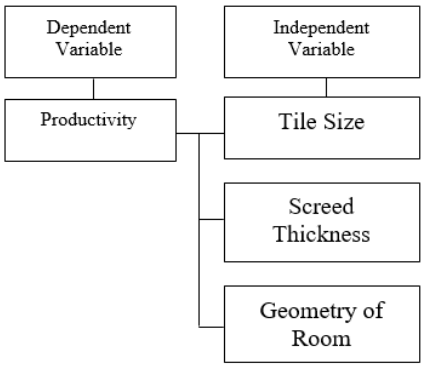

Fig. 1. Block diagram

The tile installation labour productivity data were collected at from 40 different construction sites located in the State of Maharashtra, Kolhapur.

Observations involved monitoring the overall activity within the trade, where the total productive labour inputs associated with completing the overall activity were recorded, therefore, a single labour productivity index, i.e., tiled area (m^2) per total productive labour input (man-hour, commonly abbreviated as mh), was achieved. The labour inputs collected at this level included both contributory time, i.e., time spent in cleaning and setting-out, preparing work areas, levelling, transporting and distributing tiles within the job site, and identifying element locations, and direct or effective time used to complete the activity, that is, preparation of base material, lifting, placing tiles, and securing ages in positions final checking and tamping.

The buildability factors explored included: the: tile size, quantity screed that is thickness of screed, and geometry of room. The variability of column sizes was expressed by the total number of different sizes encountered within the activity.

Regression analysis is a statistical technique that attempts to explore and model the relationship between two or more variables. Usually, the investigator seeks to ascertain the causal effect of one variable upon another. To explore such issues, the investigator assembles data on the underlying variables of interest and employs regression to estimate the quantitative effect of the causal variables upon the variable that they influence.

In this study the multiple categorical regression model formulated in the conceptual framework was used to show the relationship between the three independent variables of labour and the dependent factor. With the input from the secondary data, multiple regression analysis was conducted to reveal how independent factors impacted on labour productivity. That is regression analysis helped to understand how much the dependent variable changed, when one or more independent variables changed in the equation.

The smaller the p-value of the corresponding factor, the greater the extent of disagreement between the data and the null hypothesis, and the more significant the result is. In general, if the p-value of the regression coefficient is less than the significance level, i.e., p-value < 5%, the null hypothesis is

rejected in favor of the "alternate hypothesis (Ha)", that is, the regression coefficient of the corresponding buildability factor, i.e., the average rate of change of the factor in the model is significantly different from zero, and hence its effect on labour productivity is statistically significant (Sincich et al. 2002).

The quality of fit of the regression model, moreover, was assessed by the correlation and determination coefficients. The correlation coefficient (R) measures the strength of the linear correlation between the dependent and independent variables in the regression model, whereas the coefficient of determination (R2) indicates the percent of variance in the dependent variable, which can be explained by the independent variables of the model. The higher the coefficients of correlation and determination the better the quality of fit. The algebraic sign of the regression coefficient, on the other hand, denotes the direction of the corresponding buildability factor's effect on labour productivity, i.e., positive or negative.

5. Data Analysis

Flooring labour productivity parameters collected included the area (m^2) placed and its associated productive labour input (mh), for each installation method observed.

Flooring Labour Productivity:

$$\frac{Tiled\ Area\ (m^2)}{required\ time(mh)}$$

The screened data were entered into the spread sheet with which the regression analysis were conducted by using the PhStat software, a statistic add-in for Microsoft Excel.

Multiple categorical regression equation for the flooring activity.

Productivity= Size of tile + Screed Thickness + Geometry+ Error

Productivity=0.6654-0.0259(TS)+10.299(ST)

For shape factor 0

Productivity=0.6919-0.0259(TS)+10.299(ST)

For shape factor 1

TS-tile size and ST-screed Thickness and shape factor is assumed for the geometry of the room size While using the factor for rectangular 1 and for non-rectangular 0 factors is used.

A. Relationship between factors influencing labour productivity

Correlation and multiple regression analyses were conducted to examine the relationship between productivity and various potential predictors in labour.

Following is the regression model summary:

Table 1

Model	R	R Square	Adjusted R Square	Std. Error of the Estimate
1	0.93662138	0.8772	0.867031243	0.069550882

The multiple regression model with all three predictors produced R^2 = 0.08772, p<0.001. The research findings indicated that there was a strong positive relationship between the variables. The study also revealed that 89.24% of the labour productivity factors can be explained by the independent variables.

B. ANOVA test

Table 2

Model	Sum of squares(ss)	Degree of freedom(df)	Mean Square	F	Sigma
Regression	1.2446	3	0.4148	85.7	1.83614*E-16
Residual	0.1741	36	0.0048		
Total	1.4187	39			

6. Result and Discussion

The relationship between labour productivity and buildability factors was, therefore, quantified by regression model equation.

Productivity	=	0.6654- 0.0259(0.36) + 10.299(0.04) =1.068 For non- rectangular
Productivity	=	0.6919-0.0259(0.36)+10.299(0.04) =1.094 For rectangular

Average difference in productivity of the rectangular and non-rectangular room shape:

$$\frac{(1.094-1.068)}{1.094} * 100 = 2.4\%$$

In comparison with rectangular room shape installing tiles in non-rectangular is associated with an approximate average loss of 2.4% in labour productivity.

This investigation has determined the effects and relative influence of primary buildability factors affecting the vitrified tile installation labour productivity. Few published quantitative results exist, especially at this activity level, with which to compare the findings of this study, however, such data as exists have been examined and discussed.

O'Connor et al. (1987) and Alshawi and Underwood (1996) discussed the negative effect of the variability of element sizes on the complexity of the construction process. Nonetheless, their work was limited to general guidelines without any quantification of the impact of this factor on the productivity of the operation. The results obtained by this research show that, as the variability level of room sizes increases by one unit, labour productivity decreases, on average, by 2.4%.

The screed thickness has negative influence on labour productivity, whereas the area of tile has positive influence on the flooring labour productivity.

7. Conclusion

Because flooring is the small activity but it is repetitive and important activity involving skilled labours in every building related construction, improving labour productivity of this activity can help reducing the risk of labour costs overrun and increase the efficiency of operation. This study has focused on investigating and quantifying the influence of buildability factors on the flooring labour productivity.

The effects of variability of size of tile, thickness of screed and shape of room or geometry of room are determined and found to be significant on tile installation labour productivity.

As the size of tile increases time required for the installation will become less therefore productivity increases.

On the other hand, the thickness of screed affects the flooring labour productivity it depends on the weight of the tile which will lay on the screed, i.e. more the weight of tile more will be the thickness of screed. If Screed thickness is more, time required to work will be more and hence lesser the productivity.

As the geometry or shape of the room is non-rectangular time required for cutting and fitting the tiles is low as compared to rectangular room size therefore efficiency of installation operation significantly decreases.

The findings will substantiate the importance of applying the rationalization and standardization concept to the design stage of construction project. The effect of variability of the shape of room suggests that the designers should rationalize the shapes of room according to designer and architecture.

Practical recommendations are presented, which upon implementation can prove the buildability level of the activity and hence translate into higher labour productivity and lower labour costs.

The pattern of result may provide guidance to construction managers for effective activity planning and efficient labour utilization.

References

[1] Abulaziz M. Jarkas, “Effect of buildability on labour productivity: a practical quantification approach”, J. Constr. Eng. Manage., 2016, ASCE,142(2).
[2] Abdulaziz M. Jarkas and Camille G.Bitar “Factors affecting construction labour productivity in Kuwait”, J. Constr. Eng. Manage., 2012, ASCE, 138(7).
[3] Abdulaziz M. Jarkas. “Buildability Factors Influencing Concreting Labour Productivity”, J. Constr. Eng. Manage., 2012, ASCE,138(1).
[4] Abdulaziz M. Jarkas “Influence of Buildability Factors on Rebar Installation Labour Productivity of Columns”, J. Constr. Eng. Manage., 2012, ASCE, 138(2).
[5] Awad s. Hanna, Chul-Ki Chang, Jeffery a. Lackney, Kenneth T. Sullivan “Overmanning impact on construction labour productivity”, construction research congress., 2005, ASCE.
[6] Awad S. Hanna, P.E.; Craig S. Taylor; and Kenneth T. Sullivan “Impact of Extended Overtime on Construction Labour Productivity”. J. Constr. Eng. Manage., 2005, ASCE, 131(6).
[7] Awad S. Hanna, P. E, Chul-Ki Chang, Kenneth T. Sullivan, and Jeffery A. Lackney. “Impact of Shift Work on Labour Productivity for Labour Intensive Contractor” J. Constr. Eng. Manage., 2008, ASCE,134(3).
[8] Aryan Maarof Shamim Easeph “Construction Labour Productivity-Case Studies,” 2017.
[9] Adams, S. (1989). Practical Buildability. Butterworths, London.
[10] Ceramic Tiles-Definitions, Classification, Characteristics and marking Pressed ceramic tiles-specification IS 15622:2006.
[11] Handbook of Tiling work (Indian Railways 2015).
[12] Laying and finishing of cement concrete flooring tiles: IS 1443-1972.
[13] Particular specifications flooring work-CIDCO.
[14] R. B. Khanna, Production and operations management,” 2007.
[15] C. R. Kothari and Gaurav Garg, Research Methodology (Methods and Techniques),” 2004.

ScienceDirect

Materials Today: Proceedings

Volume 38, Part 5, 2021, Pages 3027-3034

Fabrication and characterization of novel nitinol particulate reinforced aluminium alloy metal matrix composites (NiTip/AA6061 MMCs)

Abhishek Chauhan [a], Umesh Kumar Vates [a], Nand Jee Kanu [b], Eva Gupta [c], Gyanendra Kumar Singh [d], Bhupendra Prakash Sharma [a], Srinivasa Rao Gorrepati [a]

Show more

https://doi.org/10.1016/j.matpr.2020.09.326

Get rights and content

Abstract

The composites of aluminium alloy metal matrix composites (AAMMCs) are extensively used to achieve the industrial demand. The present investigation deals with the manufacturing of AAMMCs reinforced with different weight percentage of nitinol particulates (NiTip) by using the powder metallurgy (P/M) technique. The weight percentage of the NiTip reinforcement is ranging from *0%, 4%, 8%,* and *12%.* The hardness and surface roughness of the NiTip/AA6061 metal matrix composites (MMCs) have been tested and compared with the results available in the published source to assess the novelty of the present investigation. The morphology of the NiTip/AA6061 MMCs is characterized using scanning electron microscopy (SEM). The experiment results exhibit that the surface roughness and hardness of the AAMMCs increase with increase in the percentage of NiTip content. This can also be due to the superior matrix-reinforcement interfacial bonding. The SEM results exhibit the homogenous distribution of the NiTip in AAMMCs.

Introduction

To increase the overall performance of automobile and aerospace components, the demand of light weight composite materials is increasing day by day. Among the different kinds of composites available in the market, composites of aluminium alloy metal matrix composites (AAMMCs) are extensively used to achieve the industrial demand because it has properties like light weight, corrosion to resistance, good wear resistance and good electrical conductivity. The metal matrix composites (MMCs) are very attractive materials for the applications of the automotive, aerospace, and marine industries due to their better physical as well as mechanical properties [1]. The tribological and mechanical behaviors of the MMCs of aluminium alloy could be exceptionally enriched by means of including reinforcing particles in the aluminium alloy [1]. For the MMCs, there is another type of reinforcement, i.e., nitinol (NiTi), also known as shape memory alloy (SMA), and it offers the MMCs with good properties both in terms of functional as well as mechanical properties. Most of the MMCs provide the opportunity to enhance their properties to meet particular requirements, which renders this type of material pretty special in evaluation to conventional unreinforced materials [1], [2]. Particulate-reinforced composites are especially attractive because of their less complicated manufacturing processes, reasonable costs, and nearly isotropic properties compared to continuously strengthened MMCs.

Various fabrication methods are used for manufacturing of different types of MMCs. The traditional casting techniques to produce MMCs are not wider applicable to get benefits in intricate shaped components [3]. Various manufacturing techniques were introduced to fabricate composites of various particulate-reinforced MMCs, e.g., stir casting, mechanical alloy operation, compression molding, squeezed casting, disintegrated melt accumulation, intrusion, and auto-propagation of high-temperature fusion processes. P/M based aluminium alloy metal matrix composites reinforced with nitinol particles (NiTip/AA6061 MMCs) have received big interest because of its shape changing behaviour with temperature. Nitinol has various applications as shown in Fig. 1 [1]. In Fig. 2 U-shaped component with shape memory effect in multistage form is illustrated [2]. Powder metallurgy (P/M) techniques include both regular methods as well as processes based on additive manufacturing. The regular operations include conventional sintering, metal infusion moulding, spark plasma sintering, and self-propagating synthesis at high temperature. On the other hand, P/M processes for additive manufacturing include selective ray liquefying, electron ray liquefying, selective ray sintering, ray-engineered net shaping. In fact, the majority of efforts to produce novel nitinol (shape memory alloy) particulate (NiTip)

reinforced aluminium alloy (AA6061) matrix composites, i.e., NiTip/AA6061 MMCs so far are mainly focussed on NiTip which could enhance the mechanical properties of aluminium alloy metal matrix composites (AAMMCs). The manufacturing processes include mainly casting, hot vacuum pressing, and consolidated ultrasonic techniques.

In this study, the aluminium alloy (AA6061) has been selected as a base material to manufacture the crucial aero craft and automobile components having light weight. Nano particles of nitinol (NiTip) are being reinforced in the matrix of AA6061 to improve the mechanical properties of basic aircraft components. Instead of stir-casting method, powder metallurgy (P/M) process is used to avoid considerable residual and thermal stresses. The purpose of the research is to fabricate NiTip/AA6061 MMCs using P/M processes with desired mechanical and microstructural characteristics by reinforcement of NiTip in the AA6061 matrix. Thus, nano particles of NiTip are mixed with AA6061 to fabricate NiTip/AA6061 MMCs by further pressing and sintering. It is evident that the percentage of NiTip in the AA6061 matrix has certain impact over mechanical properties such as hardness, toughness, malleability, ductility, and surface roughness quality of overall NiTip/AA6061 MMCs.

Section snippets

Materials

In the present investigation, the aluminum alloy AA6061 is used as a base material in powder form. Nano particles of nitinol (NiTip) are used as reinforcement. Nitinol is also known as nickel-titanium (often while in the proportion *50:50*). The present investigation falls under the particulate reinforced metal matrix composites (PMMCs). PMMCs are most commonly manufactured either by liquid metallurgy route or by powder blending and consolidation techniques. Other processing routes include …

Hardness test

The effect of percentage composition of NiTip in AA6061 matrix is directly influenced

with the hardness of the sample as shown in Fig. 6. The hardness and surface roughness test results are determined by an average of three consecutive measurements. Rockwell hardness test is selected for our circular NiTip/AA6061 MMCs specimens. There are other benefits for choosing Rockwell hardness tester as well, e.g., it does not require specimen preparation such as segregation, grinding, and integration. …

Summary and discussions

It is evident that from the last five decades, high strength to weight fraction is required in the aerospace, marine, automobile, and surgical industries. Researchers and scientists are constantly put their effort to fulfill the present industrial and commercial demand for such shape memory alloys (SMAs) reinforced MMCs. To reduce the reasonable cost, the desired mechanical properties of such high strength to weight fraction aerospace components, SMAs such as NiTip could be the suitable option …

Declaration of Competing Interest

The authors declare that they have no known competing financial interests or personal relationships that could have appeared to influence the work reported in this paper. …

Special issue articles Recommended articles

References (8)

A. Bhardwaj *et al.*
Mater. Sci. Eng., C (2019)

J. Ma *et al.*
Sci. Rep. (2017)

J.W. Mwangi *et al.*
J. Manuf. Processes (2019)

E.F.A. Zeid
J. Mater. Res. Technol. (2019)

There are more references available in the full text version of this article.

Cited by (28)

Mechanical behavior of shape memory alloy fiber reinforced aluminum matrix composites

2021, Materials Today Communications

Show abstract

Four-Dimensional Printing of Multifunctional Photocurable Resin Based on Waste Cooking Oil

2022, ACS Sustainable Chemistry and Engineering

Investigation of Mechanical and Tribological Behaviors of Aluminum Based Hybrid Metal Matrix Composite and Multi-Objective Optimization

2022, Materials

Nonlinear static and dynamic performance of CNT reinforced and nanoclay modified laminated nanocomposite plate

2022, AIP Advances

Nonlinear static analysis of CNT/nanoclay particles reinforced polymer matrix composite plate using secant function based shear deformation theory

2022, Smart Science

Modeling and Optimization of IoT Factors to Enhance Agile Manufacturing Strategy-based Production System Using SCM and RSM

2022, Smart Science

View all citing articles on Scopus

View full text

ScienceDirect

Materials Today: Proceedings

Volume 38, Part 5, 2021, Pages 2817-2823

Finite element analysis of mechanical response of fracture fixation functionally graded bone plate at paediatric femur bone fracture site under compressive and torsional loadings

Nand Jee Kanu [a], Devendra Patwardhan [b], Eva Gupta [c], Umesh Kumar Vates [d], Gyanendra Kumar Singh [e]

Show more

https://doi.org/10.1016/j.matpr.2020.08.740

Get rights and content

Abstract

The previous investigations clearly demonstrated that nearly *25%* of the paediatric injuries are due to fracture of bones. Children are more prone to paediatric injuries due to their childish behaviour. Their bones are subjected to axial compressive stresses due to their weight as well as torsional and bending stresses with maximum values at fracture sites of paediatric femur (PF) bones. The present investigation compares commercially available fracture fixation (FF) bone plate made up of titanium alloy with newly developed functionally graded (FG) prosthetic bone plate (graded stepwise in thickness direction using isotropic hydroxyapatite (Ha) and titanium (Ti) materials) for the treatment of fractured paediatric femur bones. The static stress analyses are carried out using finite element method (FEM) for the children under age group of *0–3 years*. Furthermore, the combined compressive and

torsional stresses are evaluated at *1%, 50%,* and *75%* healing stages of PF bones at their fracture sites using non-contacted bone-plate assemblies. The results favor the layered FG fracture fixation bone plates as they shield the PF bones from equivalent (von Mises) stresses as compared to the widely used FF bone plate made up of titanium alloy by (a) around *75–85%* under each loading, i.e., either compressive or torsional loading at a time in the contacted cortical PF bone-FF plate systems; and (b) around *0.5* to *4–4.5%* under each loading, i.e., either compressive or combined (both compressive and torsional loads) loading at a time in the non-contacted cortical PF bone-FF plate systems.

Introduction

The newly born infants or children under the age group of *0–3 years* are at higher risk of fatal paediatric injuries as per the report [1]. In our previous research work, we compared widely used and biocompatible fracture fixation (FF) plates made up of titanium alloys with recently developed FF plates made up of magnesium alloys [2].

The traditional FF plates are made up of biocompatible titanium alloys which have enough strength due to their high modulus to support fractured femur bones for their healing. As far as FF plates are concerned, the report suggests that they are developed to bear most of the loads and thus they shield the cortical fractured bone from equivalent (von Mises) stresses [3]. H. Fouad [3] discussed about non-contacted cortical bone-FF plate system and found significant improvement in stress shielding response of FG plates in presence of gap.

In the present investigation, finite element method is used to perform static analysis of fractured paediatric femur (PF) bones supported with FF bone plates. The newly developed functionally graded (FG) prosthetic bone plate is graded stepwise in thickness direction using suitable isotropic hydroxyapatite (Ha) and titanium (Ti) biomaterials in Abaqus 6.12 as shown in Table 1. Furthermore, PF bones assembled with FF plates are subjected to compressive and torsional loadings as well as combined loadings (both compressive and torsional loads) and the cortical bone-FF plate systems are analyzed in ANSYS for their static responses in case of children under age group of *0–3 years*. The FF bone plates are used to support fractured PF bones and assembled at a gap of *0.5 mm* to support healing at the fracture site of the PF bones.

Section snippets

Finite element modeling

The bone data (*0.5 mm* slice thickness, assigned for better geometrical accuracy) scanned in computer tomography (CT) is shared with medical imaging system (MIMICS) using digital imaging and communications in medicine (DICOM) format. The 3D data are shared with PTC Creo, and CATIA V5R19 to prepare assemblies of the cortical bone-FF plate systems before their analysis using ANSYS 15.0. The FF plates and screws mechanisms are improved with the advent of new biocompatible FG plates, which not only …

Study of static responses of the contacted cortical PF bone-FF plate systems in relation to ages of children

The FG prosthetic bone plate shields the PF bone from equivalent (von Mises) stresses in case of the children under age group of *0–3 years* more effectively as compared to FF bone plate modeled with titanium alloy as shown in Fig. 4 (a)-(d).

The deformation in FG prosthetic bone plate is significantly reduced by around *70–90%* under the compressive and torsional loads of *700 N* and *50 N.m,* respectively, as compared to FF bone plate modeled with titanium alloy (Fig. 4 (a)-(b)). Similarly, equivalent …

Summary of discussions and recommendations

The research provides an in-depth understanding of the advantages and limitations of contacted and non-contacted FF prosthetic bone plates such as FG and Titanium alloy bone plates when the entire system of cortical PF bone-FF bone plate assemblies are subjected to either compressive load or torsional load at a time, or either compressive load or combined load (both compressive and torsional loads) at a time. In all cases, newly developed FG bone plates are dominating over commercially …

Declaration of Competing Interest

The authors declare that they have no known competing financial interests or personal relationships that could have appeared to influence the work reported in this paper. …

Special issue articles Recommended articles

References (5)

H. Fouad
Med. Eng. Phys. (2011)

H. Fouad
Med. Eng. Phys. (2010)

There are more references available in the full text version of this article.

Cited by (13)

Comprehensive analysis of the behavior of waste cooking oil biodiesel in C.I. Engines modified using CuO nanoparticles with varying fuel injection pressure

2023, Materials Today: Proceedings

> *Citation Excerpt :*
> …The waste cooking oil biodiesel modified with copper oxide (CuO) nanoparticles [1,11,21,22,23,13–20] is obtained by rice-based waste cooking oil (Fig. 1). Average diameter of CuO nanoparticles is 305.45 ± 75.358 nm [24–28]. WCO20 biodiesel (rice bran oil) and diesel are combined 20:80 [29,30].…

Show abstract

Static bending of functionally graded single-walled carbon nanotube conjunction with modified couple stress theory

2022, Materials Today: Proceedings

Show abstract

American Journal of Infectious Diseases

Review

An Insight into the Simplified RP Transmission Network, Concise Baseline and SIR Models for Simulating the Transmissibility of the Novel Coronavirus Disease 2019 (COVID-19) Outbreak

[1]Eva Gupta and [2*]Nand Jee Kanu

[1]Amity University, Noida, India
[2]S.V. National Institute of Technology, Surat, India

Article history
Received: 04-05-2020
Revised: 26-06-2020
Accepted: 30-06-2020

Corresponding Author:
Nand Jee Kanu
S.V. National Institute of Technology, Surat, 395007, India
Email: nandssm@gmail.com

Abstract: The World Health Organization has reported about a Severe Acute Respiratory Syndrome, Coronavirus 2 (SARS-CoV2) (a virus of Wuhan, China pneumonia). The present investigation explores the transmissibility of the novel Coronavirus Disease (COVID-19) using some suitable mathematical models such as (a) a simplified Bats-Hosts-Reservoir (Wuhan Seafood Market)-People (BHRP) transmission network model useful in mapping the spread of the novel COVID-19 from its source (may be bats) to humans, (b) a concise baseline model based on individual behavioral response and control measures taken to control the transmission of the novel COVID-19 and (c) an exponential and the Susceptible-Infected-Recovered (SIR) models to predict the transmission of the pandemic on day-to-day basis. The basic Reproduction number (R_0) (for the next generation matrix) was derived to estimate the transmission of the novel COVID-19 using the simplified BHRP transmission network model. The logic estimates that around *2.30* persons could be affected by the reservoir and around *3.58* persons could be affected by the community (individual person to community population). On the other hand, the concise model based on real-time time-dependent data, such as day-to-day number of tests, appreciates the initiatives (control measures) of the Chinese government to break the transmission chain of the pandemic in the capital city of Hubei province. Furthermore, the basic Reproduction number (R_0) for India is reviewed to be in the range between *1.4* and *3.9* using the classical SIR model and thus, the transmission rate is the same as that of California and Washington. The review also outlines the epidemiological SIR model (based on real-time time-dependent data) which estimates about the equilibrium stage of the pandemic by the last week of May, 2020. The predictions of the age-structured epidemiological SIR model could be more accurate if data such as day-to-day number of tests are correctly fed during evaluation of the results. The present investigation emphasizes over the need of effective implementation of mitigatory strategies such as social distancing to prevent the transmission of the SARS-CoV2 outbreak in India.

Keywords: Novel Coronavirus, COVID-19, SARS-CoV2, Pandemic, Model, Transmission

Introduction

The novel Coronavirus (COVID-19) pandemic found its way from Wuhan Seafood Market, China (WHO, 2020a) and the outbreak of Severe Acute Respiratory Syndrome Coronavirus 2 (SARS-CoV2) has spread across the globe. The report indicates that SARS-CoV2 is identical to a bat coronavirus (reservoirs) (Zhou *et al*., 2020; Li *et al*., 2020a;

Huang *et al*., 2020; Fraser *et al*., 2004; Jung *et al*., 2020). The parameter such as basic Reproduction number (R_0) (for the next generation matrix) was evaluated using the inputs of time between different intervals of the novel COVID-19 pandemic and differences between birth and death rates (intrinsic evaluation rate) (Li *et al*., 2020a; Zhao *et al*., 2020a; 2020b). The next generation matrix (R_0) was modeled using ordinary differential equations and solved using the Markov Chain Monte Carlo methods (Chen *et al*., 2020; Wu *et al*., 2020a; Rao and Diamond, 2020).

The worldwide death toll from the novel COVID-19 pandemic has surged to over 486,128, as of 25th June 2020 (20:48 GMT+8), according to the source (NHCPRC, 2020). The concise baseline model was based on individual behavioral responses and control measures taken to control the transmission of the novel COVID-19 (TAC, 2020; CDC, 2019). Lin *et al*. (2020) mapped community transmission (individual person to community population) of the novel COVID-19 using a concise baseline model. Their model was based on key inputs such as individual behavioral responses and control measures taken by the government to control the transmission of the novel COVID-19. The authors did not forget to consider the efforts of the government such as initiatives to implement lockdown regulations, run quarantine centers, hospital conversion trends, etc., in their model to meet its objective. It is observed that during the initial few days, the symptoms of the novel COVID-19 are similar to the flu (Zhao *et al*., 2020c).

The novel COVID-19 spreads from an infected patient to a healthy person who comes in contact with him (patient) through tiny droplets from the nose, mouth and eyes, if the patient coughs, sneezes and speaks (Singhal, 2020; Ma *et al*., 2020; Araujo and Naimi, 2020; Salman and Salem, 2020; Luo *et al*., 2020). The incubation period of SARS-CoV2 is up to 14 days (Singhal, 2020; Linton *et al*., 2020; Lipsitch *et al*., 2020; Reich *et al*., 2009). India is having a large population density and thus the risk of transmission of the pandemic is quite high unless the Indian government implements mitigatory measures such as lockdown across the nation and social distancing to prevent the pandemic (Ma *et al*., 2013; Hethcote, 2000; Singh and Adhikari, 2020; Sahasranaman and Kumar, 2020; Bukhari and Jameel, 2020; Dey, 2020). The present review aims to explore the efficient mathematical modeling such as (a) the simplified Bats-Hosts-Reservoir (Wuhan Seafood Market)-People (BHRP) transmission network model, (b) a concise baseline model based on individual behavioral response and control measures and (c) an exponential and Susceptible-Infected-Recovered (SIR) models for in-depth understanding of the transmission of outbreak of the novel Coronavirus Disease (COVID-19). The modified age-structured epidemiological SIR model (based on real-time time-dependent data), which estimates about the equilibrium stage of the pandemic due to the sustained lockdown with some relaxation for effective implementation of social distancing measures, is also reviewed in-depth to emphasize over the need of mitigatory measures to prevent the transmission of the novel COVID-19 outbreak in India.

The Simplified Bats-Hosts-Reservoir (Wuhan Seafood Market)-People (BHRP) Transmission Network Model

Li *et al*. (2020a) mapped the initial outbreak of the virus of Wuhan pneumonia to the first few confirmed SARS-CoV2 infected patients and concluded with the evidence of community transmission. The data used in modeling were taken from the report published by these authors. The first case was reported on 07th December, 2019 in Wuhan, China (CAN, 2020; FT, 2020; BI, 2020; WHO, 2020b; MSN, 2020). Chen *et al*. (2020) performed analysis on the data of infected persons published until 01st January, 2020 as the Chinese central government took the step to shutdown the Wuhan Seafood Market from 01st January, 2020 after the outbreak of the novel Coronavirus (COVID-19) pandemic (WHO, 2020a).

The pandemic curve used in the modeling was plotted in the time interval between 07th December, 2019 and 01st January, 2020 with a simulation time step of 1 *day*. In a nutshell, the relationship between the variables on the x and y axes was established through a curve plotted using the Runge-Kutta method of fourth-order (tolerance level was set to 0.001). The fitting of the curve was best observed with the coefficient of determination (R^2). The transmission network model was based on the fact that SARS-CoV2 was carried from infected bats (I_B) Fig. 1a to some wild animals, or infected hosts (I_H), who were killed and sold in Wuhan Seafood Market, China (reservoir of the novel COVID-19) and shortly thereafter, people got infected from the SARS-CoV2 (Chen *et al*., 2019).

There were four categories of bats (B) such as Susceptible (S_B), Exposed (E_B), Infected (I_B) and Removed bats (R_B). The parameters such as birth rate (n_B) and population of bats (N_B) were used to calculate the population of infants bats (Λ_B). The parameters of infection of bats such as Incubation period ($1/\omega_B$) and

Infectious period ($1/\gamma_B$) were used in the modeling to understand the transmissibility of the novel COVID-19. Like bat, there were also four categories of hosts (H) such as Susceptible (S_H), Exposed (E_H), Infected (I_H) and Removed hosts (R_H). The parameters such as birth rate (n_H) and population of hosts (N_H) were used to calculate the population of infants hosts (Λ_H). The parameters of infection of hosts such as Incubation period ($1/\omega_H$) and Infectious period ($1/\gamma_H$) were used in the modeling to understand the transmissibility of the novel COVID-19. The S_B was supposed to get the novel COVID-19 from the I_B with the transmission rate of β_B and S_H was supposed to get the novel COVID-19 from the I_B and I_H with the transmission rates of β_{BH} and β_H, respectively. The other terms such as SARS-CoV2, buy rate and pervasiveness of SARS-CoV2 in sell activities were expressed as W (at Wuhan Seafood Market, the reservoir in our case), a and I_H/N_H respectively. Therefore, the rate at which the transmission of the novel COVID-19 (in Wuhan Seafood Market) from hosts took place was aWI_H/N_H (where N_H was used to express the population of hosts).

The model fills the gaps as much as possible as it also assumed the possibility of those persons with and without symptoms of SARS-CoV2 who might export SARS-CoV2 into the reservoir (W) with the transmission rates of μ_P and μ'_P, respectively. Such virus could result in W space in the reservoir at a rate of εW (where $1/\varepsilon$ was used to express the lifespan of the SARS-CoV2). It was assumed that there were five categories of persons (P), such as Susceptible (S_P) Exposed (E_P), Infected (I_P), Removed persons (R_P) and persons without symptoms (A_P) of the novel COVID-19. The parameters such as birth rate (n_P) and population of persons (N_P) were used to calculate the population of infants (Λ_P). The parameters of infection of persons such as incubation period ($1/\omega_P$) and latent period ($1/\omega'_P$) were used in the modeling of understand the transmissibility of the novel COVID-19. The other terms such as infectious periods of A_P and I_P were expressed as $1/\gamma_P$ and $1/\gamma'_P$, respectively, as well as the number of persons without symptoms was expressed as δ_P. The S_P was supposed to get the novel COVID-19 from the I_P and W with the transmission rates of β_P and β_W, respectively. The model was driven with some constant κ as it was expressed as a transmission coefficient of I_P and further assumed as the export potential of A_P was κI_P (where, $0 \le \kappa \le 1.$) (Chen *et al*., 2019).

The BHRP transmission network model was further simplified to a Reservoir (Wuhan Seafood Market)-People (RP) transmission network model due to the export of SARS-CoV2 from reservoir (Wuhan Seafood Market) in quick time. Therefore, bats and hosts were removed from the study and the overall ordinary differential equations were quite simplified. Chen *et al*. (2019) further modified the value of W using an impulse function (Chen *et al*., 2014a; Yi *et al*., 2019) for the simulation of transmission of the novel COVID-19, Equation (1):

$$Transmission = impulse\left(n, t_0, t_i\right) \tag{1}$$

where, the terms such as n, t_0 and t_i were used to express the transmission of SARS-CoV2 to Wuhan Seafood Market, beginning of the transmission study in simplified modeling and the time interval of transmission of the virus, respectively.

Chinese were celebrating the New Year during the outbreak of the novel COVID-19. The death rate and birth rate were negligible during the period. Chinese were travelling into and out from the capital city of Hubei province (People's Republic of China), so n_P was used to express the rate at which people were travelling into the city and m_P was used to express the rate at which people were travelling out from the city. Chen *et al*. (2014b) normalized the simplified RP transmission network model because both reservoir viruses and humans had different dimensions, Equation (2):

$$\begin{aligned} &s_P = \frac{S_P}{N_P}, e_P = \frac{E_P}{N_P}, i_P = \frac{I_P}{N_P}, a_P = \frac{A_P}{N_P}, r_P = \frac{R_P}{N_P}, \\ &w = \frac{\varepsilon W}{\mu_P N_P}, \mu'_P = c\mu_P, b_P = \beta_P N_P, b_w = \frac{\mu_P \beta_W N_P}{\varepsilon} \end{aligned} \tag{2}$$

where, the term c was used as the coefficient of relative shedding of A_P with respect to I_P.

The simplified RP transmission network model was expressed in its general form using the set of Equations (3):

$$\begin{aligned} \frac{ds_P}{dt} &= n_P - m_P s_P - b_P s_P\left(i_P + \kappa a_P\right) - b_W s_P w \\ \frac{de_P}{dt} &= b_P s_P\left(i_P + \kappa a_P\right) + b_W s_P w - \left(1-\delta_P\right)\omega_P e_P - \delta_P \omega'_P e_P - m_P e_P \\ \frac{di_P}{dt} &= \left(1-\delta_P\right)\omega_P e_P - \left(\gamma_P + m_P\right) i_P \\ \frac{da_P}{dt} &= \delta_P \omega'_P e_P - \left(\gamma'_P + m_P\right) a_P \\ \frac{dr_P}{dt} &= \gamma_P i_P + \gamma'_P a_P - m_P r_P \\ \frac{dw}{dt} &= \varepsilon\left(i_P + c a_P - w\right) \end{aligned} \tag{3}$$

The basic Reproduction number (R_0) (for the next generation matrix) was derived in the simplified RP transmission network model to describe the different stages of the novel COVID-19, such as its outbreak ($R_0 > 1$), stage of community transmission and the end of pandemic ($R_0 < 1$) (Chen *et al*., 2014a; Zhang *et al*., 2020; Chen *et al*., 2019; Cui *et al*., 2020).

The incubation and latent periods were substituted as 5.2 *days* and therefore, the term ω_P (or ω'_P) was taken as 0.1923 due to the 95% confidence level (Li *et al*., 2020a). On average, there was a delay of *5 days* before admitting any COVID-19 infected patients after they started complaining about symptoms of the pandemic (JMH, 2020; WHO, 2020c; 2020d). The parameters such as γ_P and δ_P were taken as 0.1724 (due to 95% confidence level (Li *et al*., 2020a)) and *0.5* (due to unavailability of the novel COVID-19 infected patients without symptoms), respectively. Both terms such as κ and c were set to *0.5*. Out of the *11 million* population of the city, *0.3 million* population was tested for symptoms of the novel COVID-19 (NENVN, 2020). It was estimated that *0.2 million* population was travelling out from the city per day to celebrate the festive season during the outbreak of the pandemic. Therefore, n_P and m_P were set to *0.0018/day* (as *0.1* times the fraction *0.2/11*) (CBN, 2020; WG, 2020). It was believed that SARS-CoV2 could remain active in the atmosphere up to *10 day*s in its host and therefore, the value of ε was assumed to be *0.1* and the pervasiveness of the SARS-CoV2 was assumed to be *0.00001* to the initial step of modeling (Chen *et al*., 2020). The above equations (3) of the simplified RP transmission network model were used to fetch the data of null COVID-19 spots $\left(\frac{\Lambda_P}{m_P},0,0,0,0,0\right)$. The next generation matrix (R_0) was calculated using Equation (4):

$$R_0 = FV^{-1} = \begin{bmatrix} 0 & \beta_P \frac{\Lambda_P}{m_P} & \beta_P \kappa \frac{\Lambda_P}{m_P} & \beta_W \frac{\Lambda_P}{m_P} \\ 0 & 0 & 0 & 0 \\ 0 & 0 & 0 & 0 \\ 0 & 0 & 0 & 0 \end{bmatrix} \begin{bmatrix} \frac{1}{\omega_P + m_P} & 0 & 0 & 0 \\ A & \frac{1}{\gamma_P + m_P} & 0 & 0 \\ B & 0 & \frac{1}{\gamma'_P + m_P} & 0 \\ D & E & G & \frac{1}{\varepsilon} \end{bmatrix} \quad (4)$$

where,

$$A = \frac{(1-\delta_P)\omega_P}{(\omega_P + m_P)(\gamma_P + m_P)},\ B = \frac{\delta_P \omega_P}{(\omega_P + m_P)(\gamma'_P + m_P)},\ D = \frac{(1-\delta_P)\mu\omega_P}{(\omega_P + m_P)(\gamma_P + m_P)\varepsilon}$$
$$+ \frac{\mu'\delta_P\omega_P}{(\omega_P + m_P)(\gamma'_P + m_P)\varepsilon},\ E = \frac{\mu}{(\gamma_P + m_P)\varepsilon}, and\ G = \frac{\mu'}{(\gamma'_P + m_P)\varepsilon}$$

The simplified RP transmission network model which was normalized further to provide the best fit to the curve (Fig. 1b) and it was found that the result of the model was in agreement with published data sources (R^2 = 0.512, $P < 0.001$). The values of R_0 were evaluated around *2.30* for those persons who were affected from reservoir and around *3.58* for those persons who were affected from community transmission (individual person to community population). On average, the value of R_0 of SARS-CoV2 was *2.9* (based on research in two such China's cities-Hong Kong and Beijing) and therefore, the transmission of SARS coronavirus was estimated to be much higher than Middle East Respiratory Syndrome (MERS) coronavirus (Riley *et al*., 2003; Dye and Gay, 2003; Zhou and Yan, 2003; Peak *et al*., 2017).

Overall, the normalized RP transmission network model was based on the input data sources that were published for only a few countries during the outbreak of the novel COVID-19 and thus it might not fit well into the situations in other countries. However, it throws light on mapping the transmission of the novel COVID-19 pandemic during its initial outbreak in the city of patient zero.

The Concise Baseline Model Based on Individual Behavioral Response and the Control Measures Taken by the Government to Prevent the Spread of the Novel COVID-19

Lin *et al*. (2020) adopted the framework (population size, *N*) which was based on two key parameters such as (a) the general reaction of the public about novel COVID-19 infected patients (who were either seriously ill or about to die), represented as *D* and (b) the progressive cases of infected patients in the zone, represented as *C*. There were four categories of persons such as Susceptible (*S*), Exposed (*E*), Infected (*I*) and Removed persons (*R*). It was needed then to discuss the rate of transmission of the novel COVID-19 in a model as the report was showing the number of the infected patients such as (a) *81%* of the patients were having mild symptoms, (b) *14%* of the patients were seriously ill and they had breathing problems and (c) *5%* of the patients were identified with respiratory failure (Wu and McGoogan, 2020).

Lin *et al*. (2020) modeled the zoonotic transmission (period around December, 2019) using a function, *F* for the outbreak of the pandemic, which was first encountered in November, 2019. The transmission function was equated with zero when the Chinese government took the step to shutdown the Wuhan Seafood Market on 01st January, 2020 after the outbreak of the novel coronavirus (COVID-19) pandemic (WHO, 2020a). They modeled initially to map the community transmission (individual person to community population) of the novel COVID-19 before the government imposed a lockdown across the city, using the set of Equations (5):

$$\begin{aligned}
S' &= -\frac{\beta_0 SF}{N} - \frac{\beta(t) SI}{N} - \mu S,\\
E' &= \frac{\beta_0 SF}{N} + \frac{\beta(t) SI}{N} - (\sigma + \mu) E,\\
I' &= \sigma E - (\gamma + \mu) I,\\
R' &= \gamma I - \mu R,\\
N' &= -\mu N,\\
D' &= d\gamma I - \lambda D, \text{ and}\\
C'' &= \sigma E
\end{aligned} \tag{5}$$

The parameter, $\beta(t) = \beta_0(1-\alpha)\left(1-\frac{D}{N}\right)^{\kappa}$ was used to express the effect of (a) control measures taken by the government to prevent the spread of the novel COVID-19 and (b) social distancing on the death tolls. The parameters such as *F*, *N*, *S*, β, α, κ, μ, σ^{-1}, γ^{-1}, *d* and λ^{-1} were used to express the count of the novel COVID-19 patients, the population length, suspected patients, the export rate initiative of the government to control the spread of the pandemic, the rate at which people were travelling into and out from the city, the latent time, the infectious time, the ratio of critical patients and the individual behavioral response, respectively. *5 million* emigrants (SCMP, 2020) were also involved in the modeling before the decision of lockdown was imposed. It was assumed that (a) the control measures were more effective from the fourth week of January, 2020 (α = 0.4249) until 29th January, 2020 and α = 0.8478 after 30th January, 2020) and (b) the population was travelling into and out from the capital city of Hubei province in between 31st December, 2019 and 22nd January, 2020.

Children aged between *0-17 years* are less critically affected by the novel COVID-19 so far. Only *10%* of the population thus, was not included in the modeling. The time between successive cases in the transmission chain of the pandemic and the incubation period were reported as *5 days* (Nishiura *et al*., 2020a; 2020b; Fine, 2003; SDT, 2012) and *4 days* (Guan *et al*., 2020), respectively. The infectious and latent periods were thus substituted as *4* and *3 days*, respectively. The results of the model were in good agreement with the previously published data (Zhao *et al*., 2020a; 2020b; Tuite and Fisman, 2020) as it involved real-time time-dependent data and critical cases instead of death rates only.

Lin *et al*. (2020) realized that the pandemic spread across the city at much higher rates Fig. 2 due to inadequate medical care infrastructure and health services. There was a delay of *14 days* between the first symptom of the novel COVID-19 and its official confirmation in the laboratory (Li *et al*., 2020b; Liu *et al*., 2020) for patients in the same age group (Fig. 3).

Lin *et al*. (2020) considered three different cases such as (a) when the government was not taking the outbreak of the novel COVID-19 pandemic seriously (α = 0) and there was then no individual behavioral response (*k* = 0), (b) when people were aware about the novel COVID-19 (thus, the official record of cumulative cases was trending down) and (c) when the government was on alert mode with all its task forces in action to prevent the spread and then the individual behavioral response reduced the cases of the novel COVID-19 patients (Fig. 4). They highlighted the third case which became a key element to break the transmission chain of the pandemic; and the estimated results of the simulation were in inline with the published data sources (Riou and Althaus, 2020; Bogoch *et al*., 2020; Imai *et al*., 2020; Mahase, 2020).

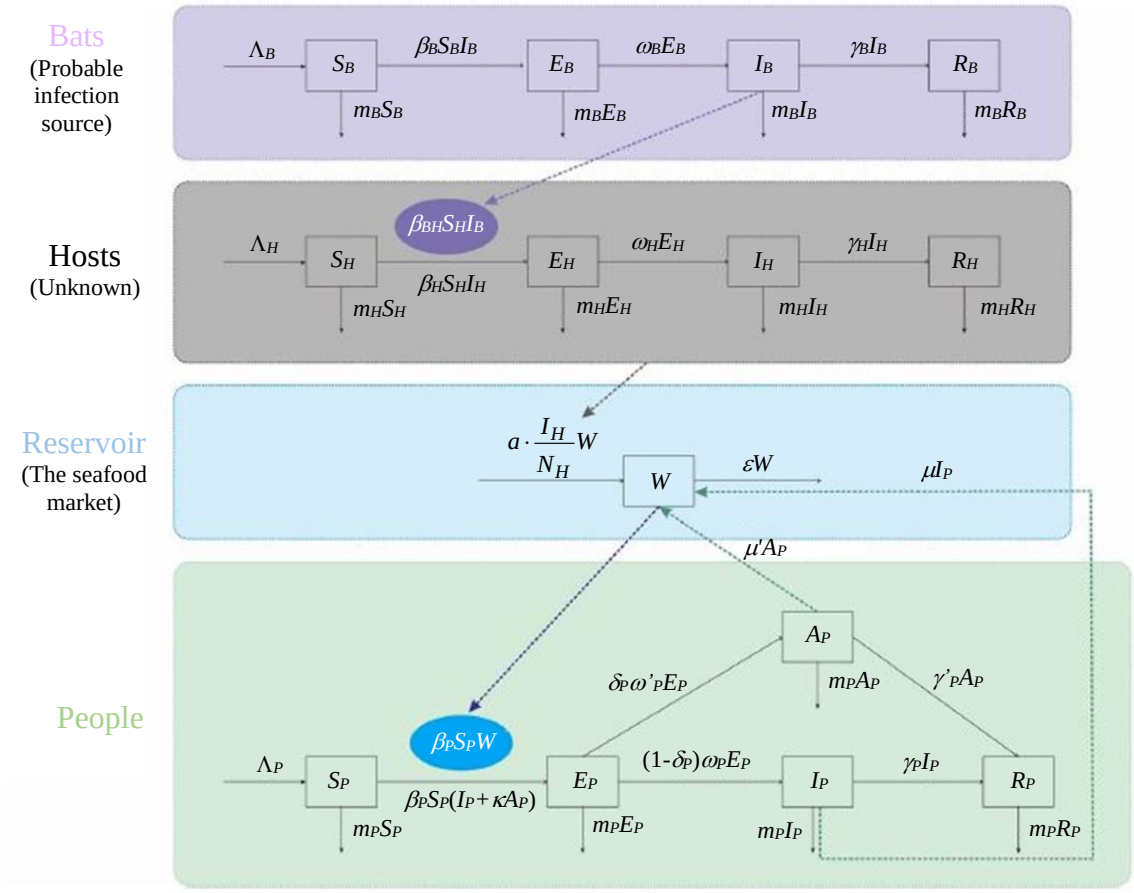

(a)

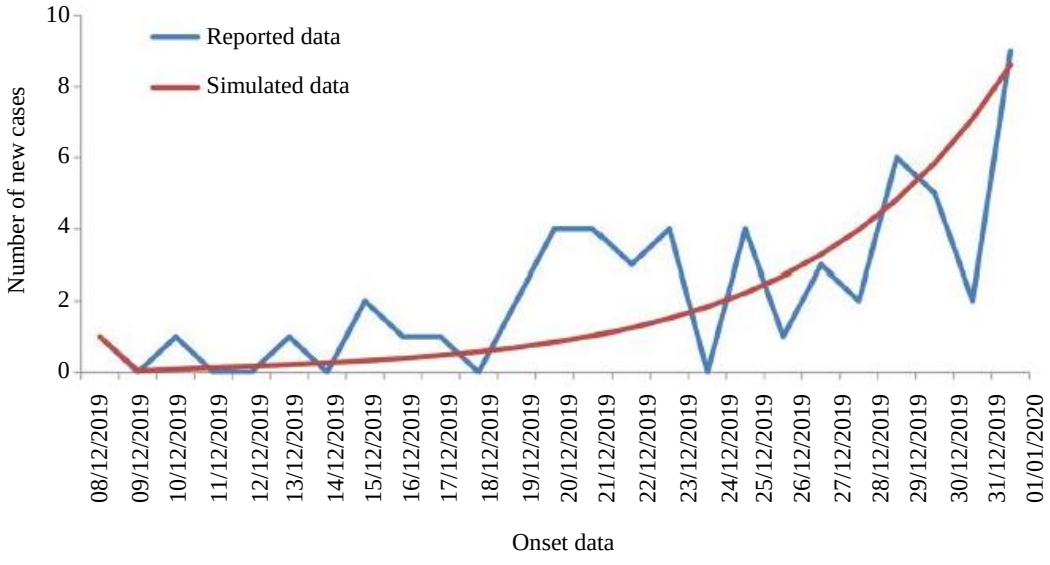

(b)

Fig. 1: The Bats-Hosts-Reservoir (Wuhan Seafood Market)-People (BHRP) transmission network model (Reprinted with permission from Ref. (Chen *et al*., 2020). Copyright 2020 Springer Nature). (a) The logic behind the transmission network model. (b) The response of simplified Reservoir (Wuhan Seafood Market)-People (RP) transmission network model

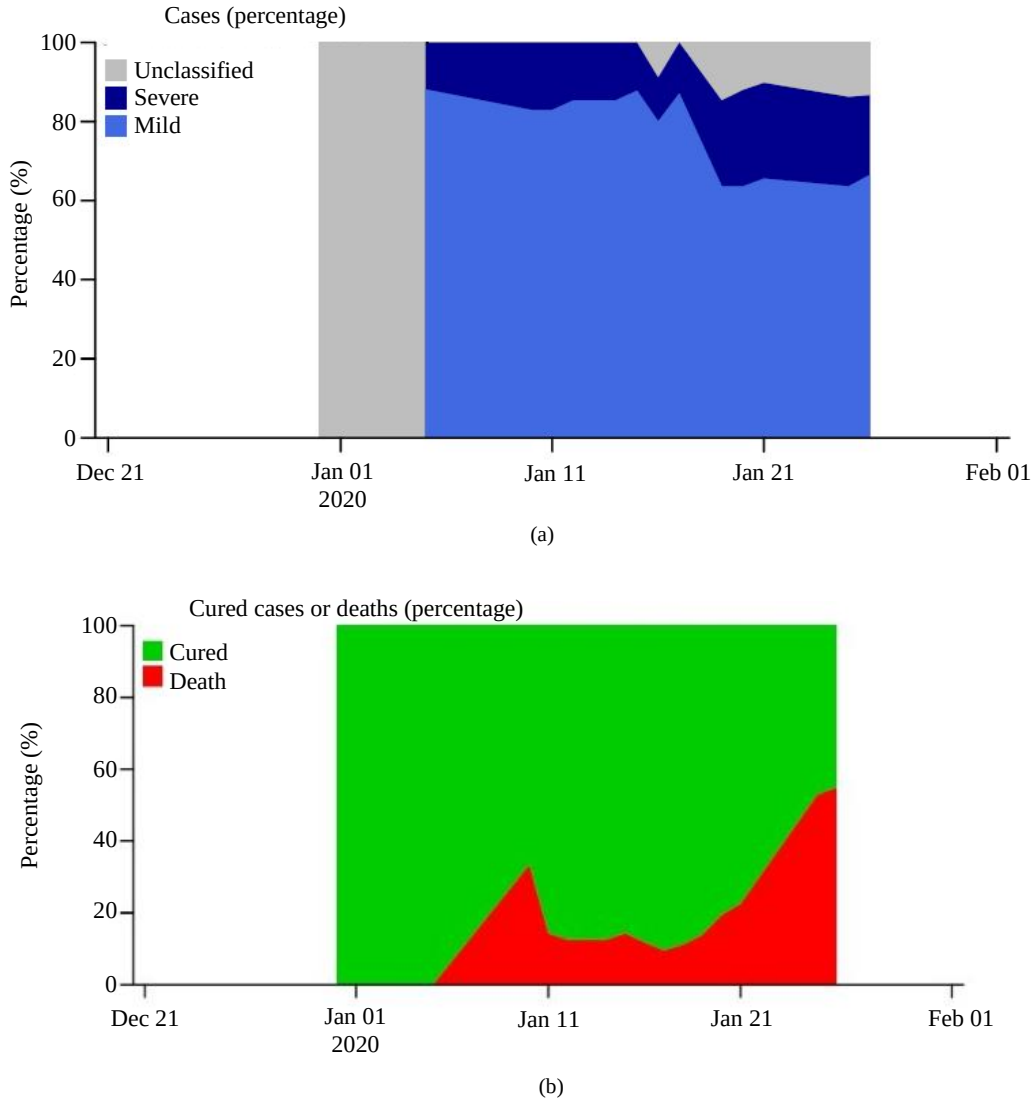

Fig. 2: The novel COVID-19 cases in Wuhan, China for the patients in the same age group (Reprinted with permission from Ref. (Lin *et al*., 2020). Copyright 2020 Elsevier). (a) The officially recorded severe and mild cases *(%)*. (b) The officially recorded cured and deaths cases

The concise baseline model did not rely on the conventional approach of fitting a curve to the dataset. It involved real-time time-dependent data which were based on testing facilities, availability of hospitals, etc. and thus, this framework was suitable for other countries including India as well.

The Epidemiological, Exponential and Susceptible-Infected-Recovered (SIR) Models to Investigate the Transmission of the Novel COVID-19 Outbreak in India

Ranjan (2020) estimated the basic Reproduction number (R_0) for India in the range between *1.4* and *3.9* using exponential and classical Susceptible-Infected-Recovered (SIR) models (Hethcote, 2000). The exponential model (Ma, 2020) was used in previous pandemics to estimate the transmission rate of disease Equation (6):

$$\frac{dI}{dt} = rI \tag{6}$$

After integration, the above equation was expressed in its general form Equation (7):

$$I(t) = I_0 \exp(rt) \tag{7}$$

The parameters, $I(t)$ and I were used to express the number of infected patients with time, t and the overall cumulative cases of cured and dead persons. The other parameter, I_0 was evaluated using the conventional approach of fitting a curve to the dataset (Rao and Vazquez, 2020).

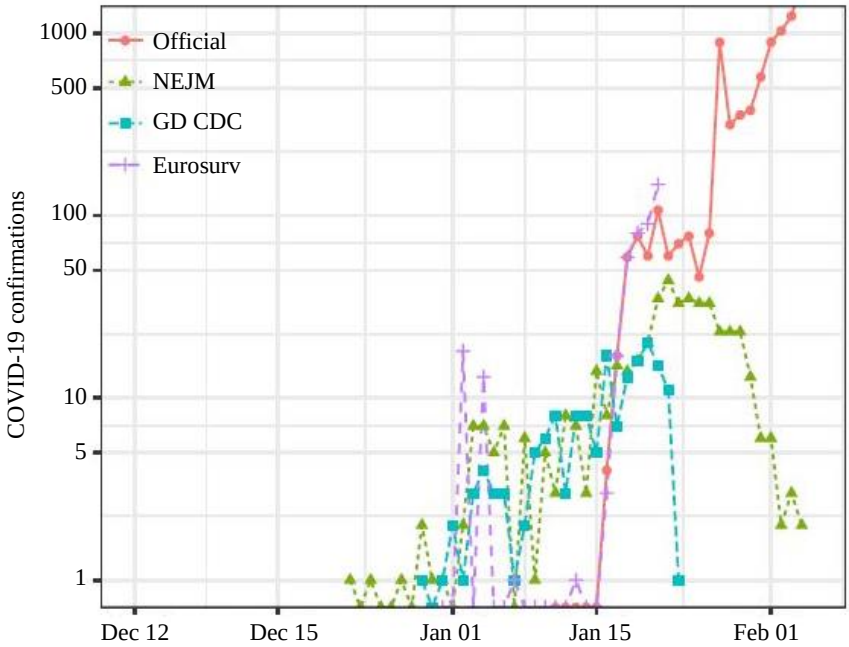

Fig. 3: The evaluation of previously published data such as (a) the officially recorded data was shown using red color (NHCPRC, 2020), (b) the data of (Li *et al*., 2020a) was shown using green color, (c) the data of (Liu *et al*., 2020) was shown using blue color and (d) the data of (Wu *et al*., 2020b) was shown using purple color (Reprinted with permission from Ref. (Lin *et al*., 2020). Copyright 2020 Elsevier)

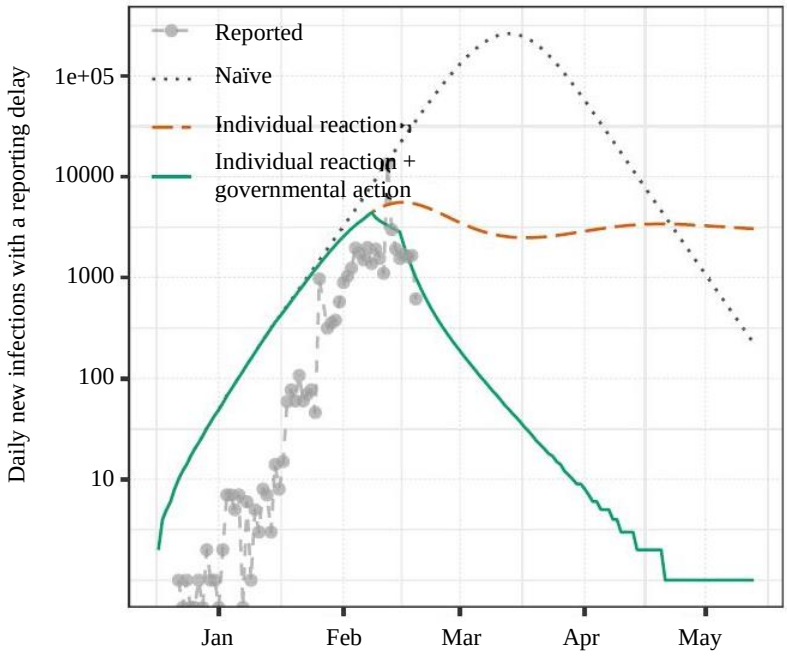

(a)

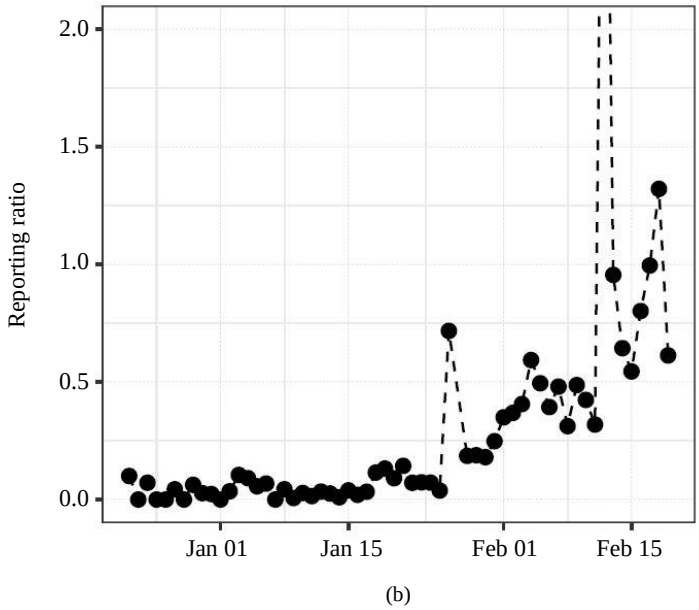

(b)

Fig. 4: The official and laboratory confirmation of the SARS-CoV2 test was delayed for two weeks after the onset of its symptoms (Reprinted with permission from Ref. (Lin *et al*., 2020). Copyright 2020 Elsevier). (a) The day-to-day reporting of new cases of the SARS-CoV2 was shown with three types of observational studies such as (i) when the government was not in action (shown using grey color), (ii) when there was individual behavioral response (shown using red color) and (iii) when the government was active and took initiatives to prevent spread of the pandemic and people were also aware about the novel COVID-19 (shown using green color); and the officially recorded data as well as data of Li *et al*. (2020a) was shown using dotted grey curve. (b) The graph was reconstructed on the basis of real-time time-dependent data such as the day-to-day number of tests, adequate medical care infrastructures and health services.

The epidemiological SIR model (evaluated using real-time time-dependent data) was based on three categories of persons such as Susceptible (*S*), Infected (*I*) and Recovered or Dead persons (R). The classical SIR model was expressed in its general form using the set of Equations (8):

$$\begin{aligned}
&\frac{dS(t)}{dt} = -\frac{\beta}{N}SI,\\
&\frac{dI(t)}{dt} = \left(\frac{\beta}{N}S - \gamma\right)I, \text{ and}\\
&\frac{dR(t)}{dt} = \gamma I
\end{aligned} \tag{8}$$

The parameters, β and γ were used to express the spread rate and the mean recovered rate, respectively. The entire population at a specific time, *t* was expressed as $N = S + I + R$ and that was unchanged during the prediction of transmission rate using the classical SIR model. The parameter such as the basic Reproduction number (R_0) (for the next generation matrix) was calculated using Equation (9):

$$R_0 = \frac{\beta}{\gamma}\left(1 - \frac{I_0}{N}\right) \tag{9}$$

Ranjan (2020) assessed the initial values of the parameters, β and γ at $R_0 = 0$ (Batista, 2020; McGee, 2020) as they assumed the equilibrium stage of the pandemic. They had used data available between 11th March, 2020 (*62* infected patients) and 23rd March, 2020 (*499* infected patients) for conducting the research using the exponential model. Furthermore, they had used data available from 10th March, 2020 to 30th March, 2020 (a period of *21 days*) for conducting the research using the classical SIR model. India has not entered the community transmission stage (third stage). The outcomes of the models were in good agreement with the first and second stages of the transmission of the pandemic. The transmission rate of India was the same as that of California and Washington (Fig. 5a). The variation in the trends of growth rates in different countries was due to the implementation of testing facilities to identify the patients. The exponential model was used to predict provisional and perpetual estimations about the novel COVID-19 cases in India. The values of I_0, r and the coefficient of determination, R^2 were *39.64*, *0.1887 and 0.9768*, respectively. The existing case of the novel COVID-19 was plotted against the estimated cases up to 06th April, 2020 (Fig. 5b). The comparison was also made between India (*5000* infected patients by 06th April, 2020) and Washington in Fig. 5b. The exponential model was unable to deliver the perpetual estimation about the novel COVID-19 cases, i.e., up to 30th April,

DOI: 10.3844/ajidsp.2020.89.108

2020 (Fig. 5c). The exponential model did not involve the initiatives (control measures such as lockdown imposed across the nation on 24th March, 2020 and social distancing was practiced as mitigatory measures) of the Indian government to break the transmission chain of SARS-CoV2 and that was why the estimation of the model was near to *0.5 million* cases by 30th April, 2020.

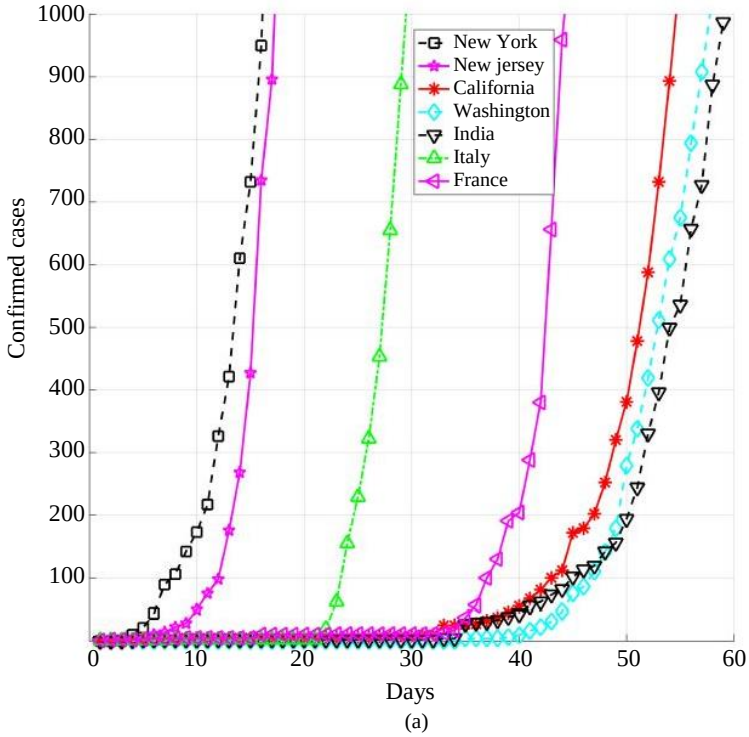

(a)

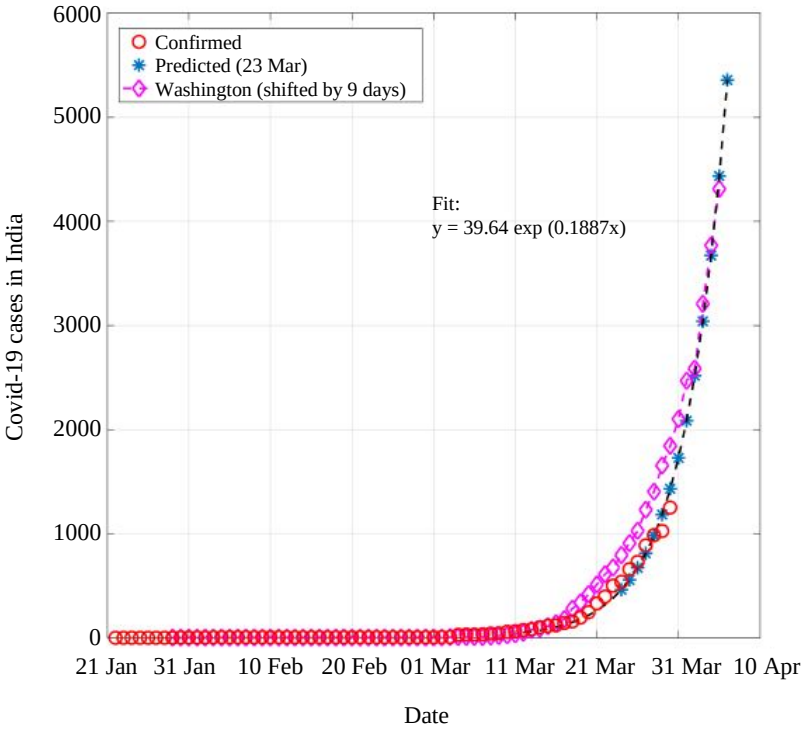

(b)

DOI: 10.3844/ajidsp.2020.89.108

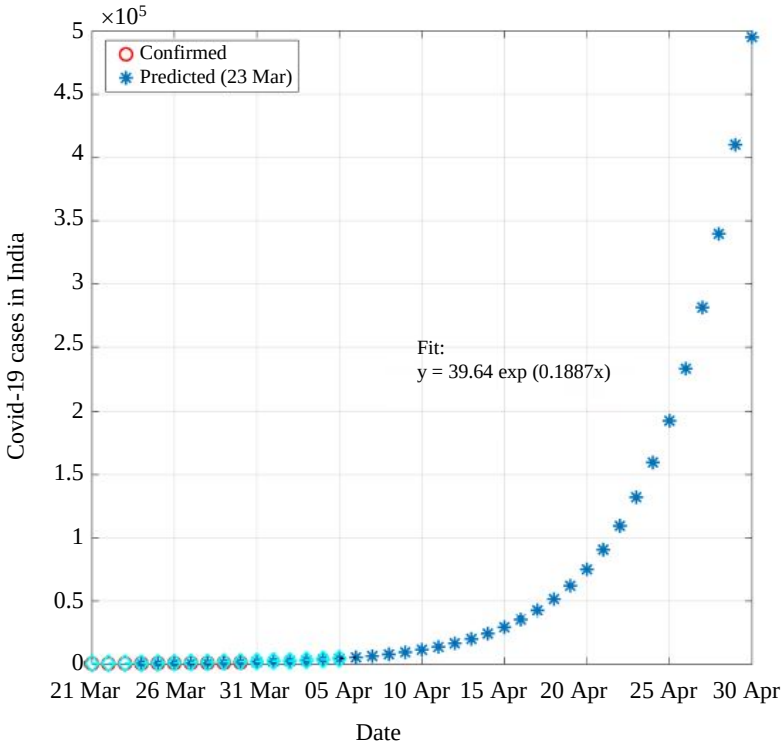

(c)

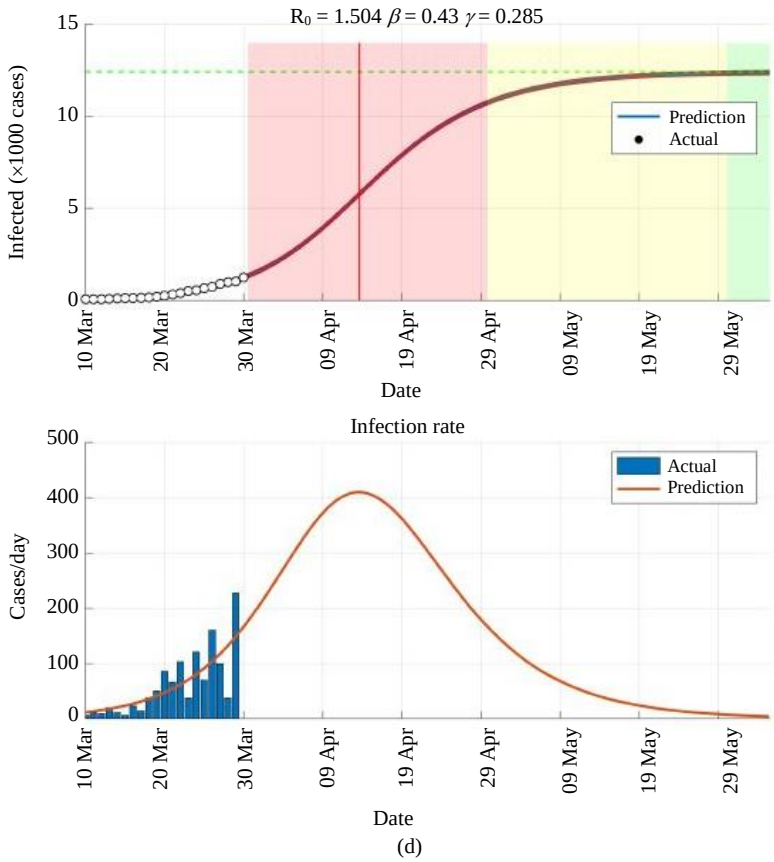

(d)

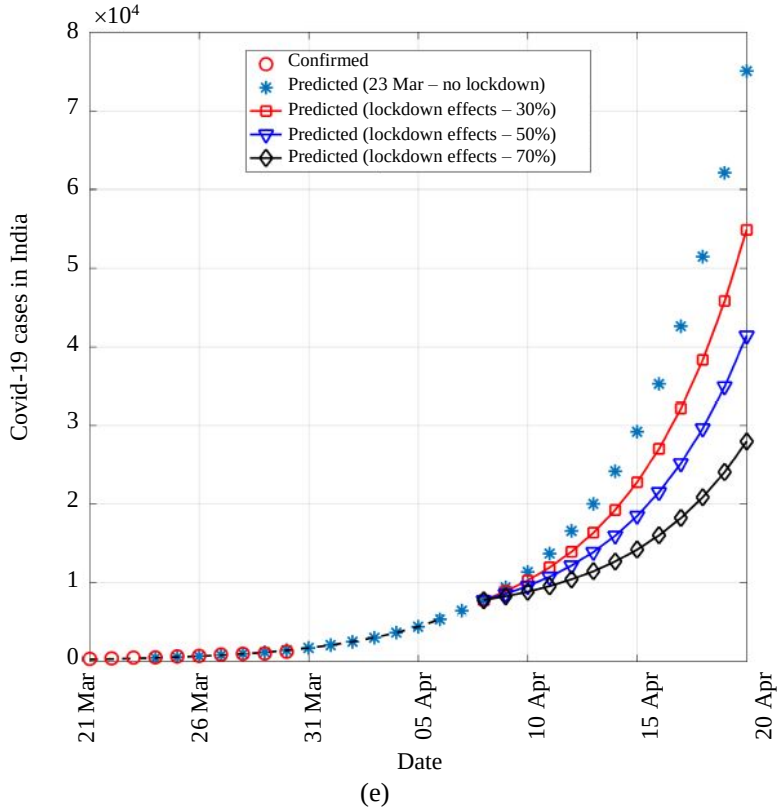

Fig. 5: The epidemiological exponential and SIR models (Reprinted with permission from Ref. (Ranjan, 2020). Copyright 2020 medRxiv). (a) The variation in trends of growth rates in different countries was due to their implementation of testing strategies. The growth rate of India was same as that of California and Washington using the exponential model. (b) The existing case of the SARS-CoV2 in India was plotted against the estimated cases up to 06th April, 2020. The comparison was also made between India (*5000* infected patients by 06th April, 2020) and Washington. (c) The exponential model did not involve the initiatives of the Indian government to break transmission chain of the SARS-CoV2 and that was why the estimation of the model was near to *0.5 million* cases by 30th April, 2020. (d) The classical SIR model was used to present a more realistic estimate of the SARS-CoV2. The effect of mitigatory social distancing was considered in the SIR model and the equilibrium stage of the pandemic was predicted around the last week of May, 2020. (e) The effects of mitigatory social distancing in few countries were outlined.

Ranjan (2020) therefore, switched over to the classical SIR model for the long term prediction of the novel COVID-19 cases and presented a more realistic estimate of the SARS-CoV2 (Fig. 5d) with the value of coefficient of determination, R^2 around *0.996*. The basic reproduction number (R_0) was estimated to be *1.504* (higher than the estimate of (Sahasranaman and Kumar, 2020); and close to the estimate of (Deb and Majumdar, 2020). Furthermore, the epidemiological SIR model considered the initiatives of the Indian government such as mitigatory social distancing to prevent the spread (Wu *et al*., 2020c) and suggested the equilibrium stage of the pandemic by the last week of May, 2020 (Fig. 5d). The impact of mitigatory social distancing Ridenhour *et al*., 2018; Chang *et al*., 2020; Mandal *et al*., 2020; Dhama *et al*., 2020) in a few countries was outlined in Fig. 5e.

The Analysis of Mitigatory Social Distancing to Investigate the Transmission of the Novel COVID-19 Outbreak in India using the Classical Susceptible-Infected-Recovered (SIR) Model

Singh and Adhikari (2020) studied the novel COVID-19 outbreak in India using the modified age-structured Susceptible-Infected-Recovered (SIR) model (Pontryagin, 1985; Box, 1976) by considering the initiative of the Indian government to implement mitigatory measures such as lockdown across the nation and social distancing (Ferguson *et al*., 2020; Bootsma and Ferguson, 2007; Hatchett *et al*., 2007; He *et al*., 2020) to prevent the pandemic. They assumed that persons within a specific age class (Prem *et al*., 2017) were equal with respect to their birth and death rates. The basic Reproduction number (R_0) was estimated on the basis of real-time time-dependent data, age groups and

mitigatory social distancing using the modified age-structured SIR model.

The persons were classified into different ages and thus in '*M*' groups expressed as $i = 1,2,\ldots M$. The persons within a specific age group were represented with '*i*' and they were classified into susceptible patients (S_i), asymptomatic patients $\left(I_i^a\right)$, symptomatic patients $\left(I_i^s\right)$, and removed patients (R_i).

Therefore, the sum of all these was the total number of persons within a specified age group (i) and thus $N_i = S_i + I_i^a + I_i^s + R_i$ (Anderson and May, 1991; Keeling and Rohani, 2008; Towers and Feng, 2012; Ferguson *et al*., 2006).

Thus, each N_i was expressed as the total number of persons (thus a constant with respect to time) Equation (10):

$$N = \sum_{i=1}^{M} N_i \tag{10}$$

The rate of transmission of disease in susceptible patients within a specific age group (i) was expressed using Equation (11):

$$\lambda_i(t) = \beta \sum_{j=1}^{M} \left(C_{ij}^a \frac{I_j^a}{N_j} + C_{ij}^s \frac{I_j^s}{N_j} \right),\ i, j = 1,\ldots M \tag{11}$$

where, the term, β was the chance of transmission of the novel COVID-19 due to social contact and C_{ij}^a and C_{ij}^s were used to express the cases of social contact between asymptomatic patients within a specific age group (j) and susceptible patients within a specific age group (i), respectively.

The cured rate, γ was not dependent on age and was the same for both asymptomatic (ratio, α) and symptomatic patients (ratio, $\bar{\alpha} = 1 - \alpha$).

Therefore, the growth of the pandemic was expressed using the age-structured SIR model Equation (12):

$$\begin{aligned} \dot{S}_i &= -\lambda_i(t) S_i, \\ \dot{I}_i^a &= \alpha \lambda_i(t) S_i - \gamma I_i^a, \\ \dot{I}_i^s &= \bar{\alpha} \lambda_i(t) S_i - \gamma I_i^s, \\ \dot{R}_i &= \gamma \left(I_i^a + I_i^s \right). \end{aligned} \tag{12}$$

The age group of the persons was expressed as the ratio of *Ni*/*N* and social contact was expressed using C_{ij}^a, and C_{ij}^s matrices. Furthermore, the symptomatic patients were supposed to have less contact as compared to the asymptomatic patients and thus, $C_{ij}^s = fC_{ij}^a \equiv fC_{ij,}$ (where, $0 \le f \le 1$).a

The people in self-isolation were supposed to remain in houses, work premises, school premises and other areas, thus the contact matrix was expressed using Equation (13):

$$C_{ij} = C_{ij}^H + C_{ij}^W + C_{ij}^S + C_{ij}^O \tag{13}$$

The contact matrix for a specific size of the population was expressed as $N_i C_{ij} = N_j C_{ji}$.

The mitigatory social distancing was modeled on a large-scale as a function of time, $u^W(t)$, $u^S(t)$ and $u^O(t)$, thus the time dependent contact matrix was expressed using Equation (14):

$$C_{ij}(t) = C_{ij}^H + u^W(t) C_{ij}^W + u^S(t) C_{ij}^S + u^O(t) C_{ij}^O. \tag{14}$$

During the lockdown across the nation, the social distancing measures were implemented effectively and thus a single household contact function was sufficient as shown using the linear Equation (15):

$$2u(t) = -\tanh\left(\frac{t - t_{on}}{t_w} \right) + \tanh\left(\frac{t - t_{off}}{t_w} \right) \tag{15}$$

The basic reproductive number was evaluated from null COVID-19 spots (where $S_i = N_i$) and infected persons were expressed using $2M \times 2M$ matrix, Equation (16):

$$J = \gamma(L - 1). \tag{16}$$

The next generation matrix, $2M \times 2M$ was expressed using Equation (17):

$$L = \begin{pmatrix} L^{aa} & L^{as} \\ L^{sa} & L^{ss} \end{pmatrix} \tag{17}$$

where, $L_{ij}^{aa} = \frac{\alpha\beta}{\gamma} C_{ij}^a \frac{N_i}{N_j}$, $L_{ij}^{as} = \frac{\alpha\beta}{\gamma} C_{ij}^s \frac{N_i}{N_j}$; and $L_{ij}^{sa} = \frac{\alpha\beta}{\gamma} C_{ij}^a \frac{N_i}{N_j}$, $L_{ij}^{ss} = \frac{\bar{\alpha}\beta}{\gamma} C_{ij}^s \frac{N_i}{N_j}$.

The identity matrix, I ($2M \times 2M$) was used to encompass both asymptomatic and symptomatic patients Equation (18):

$$I = \left(I^a, I^s \right) = \left(I_1^a, \ldots, I_M^a, I_{1,\ldots}^s I_M^s \right) \tag{18}$$

The dynamics of the above Equation (18) was expressed using Equation (19):

DOI: 10.3844/ajidsp.2020.89.108

$$I(t)=\exp\left[\gamma(L-1)t\right]I(0) \tag{19}$$

where, L was used to evaluate the eigenvectors, V and the diagonal matrix of eigenvalues, $\Lambda = diag(\Lambda_1,\ldots, \Lambda_{2M})$ to calculate the equation, $\exp[\gamma(L\text{-}1)t] = V\, diag\, [\exp\, \gamma(\Lambda\text{-}1)t]V^{-1}$.

In general, the span of L had to be greater than one for the spread of the pandemic and thus the basic reproductive number was expressed using Equation (20) (Diekmann *et al*., 2010):

$$R_0 \equiv \rho(L)=\max\left\{|\Lambda_1|,\ldots,|\Lambda_{2M}|\right\}. \tag{20}$$

The basic reproductive number was reasonably good to support the spread of the pandemic if the eigenvalue was real Equation (21):

$$\exp\left[\gamma(R_0-1)t\right] \tag{21}$$

The basic reproductive number was based on (a) the chance of transmission of disease on social contact, β, (b) the social contact matrix C_{ij} (c) the ratio of persons without and with symptoms of SARS-CoV2, α and (d) the ratio of symptomatic patients who were in self-isolation, f. The conversions such as (a) $N_i \rightarrow S_i(t)$ and (b) $C_{ij} \rightarrow C_{ij}(t)$ were done to transform the formulation into its linear form for time-based stability matrix, $L^{(t)}$. The time-based stability matrix, $L^{(t)}$ was expressed using Equation (22):

$$R_0^{eff}(t) \equiv \rho\left(L^{(t)}\right)=\max\left\{\left|\Lambda_1^{(t)}\right|,\ldots,\left|\Lambda_{2M}^{(t)}\right|\right\} \tag{22}$$

The cases of infected patients at any time, $t + \delta t$ were expressed Equation (23):

$$I(t+\delta t)=\exp\left[\gamma\left(L^{(t)}-1\right)\delta t\right]I(t) \tag{23}$$

The basic reproductive number played a significant role, $\left(\exp\left[\gamma(R_o^{eff}(t)-1)\delta t\right]\right)$, when the eigenvalue was real for its highest magnitude for the tremendous growth of the pandemic in a very short time, t. The end of the pandemic was shown with $R_0^{eff}<1$. The rise and fall of the spread of the SARS-CoV2 outbreak were shown with time constants such as $\gamma(R_0\text{-}1)$ and $\gamma\left(R_0^{eff}(t_{on})-1\right)$, respectively.

The predictions of the SARS-CoV2 outbreak in India without and with implementation of social distancing measures using the age-structured epidemiological SIR models were shown in Fig. 6 and 7, respectively. In the absence of mitigatory measures such as locking down across the nation and thus social distancing; the results were frightening (Fig. 6). Singh and Adhikari (2020) thus, emphasized over the various schemes of mitigatory measures such as successive lockdowns of *21 days* and *28 days* Fig. 7b and further *21 days*, *28 days* and *18 days* Fig. 7c (each scheme with a relaxation of some *5 days* and suggested to implement from 25th March, 2020); and if not possible then a single lock down of *49 days* starting from 25th March, 2020 would be required to impose across the nation to bring the equilibrium stage of the novel COVID-19 pandemic Fig. 7d.

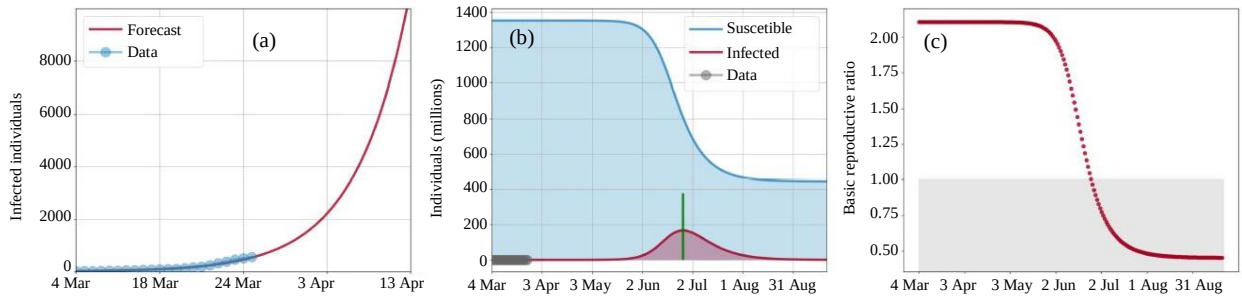

Fig. 6: The prediction of the SARS-CoV2 outbreak in India without implementation of social distancing measures using the age-structured epidemiological SIR model (Reprinted with permission from Ref. (Singh and Adhikari, 2020). Copyright 2020 arXiv). (a) The confirmed cases (shown using blue color) of the novel COVID-19 was plotted against the estimated cases (shown using red color) up to 25th March, 2020. (b) The prediction for the next five months, i.e., up to August, 2020 about the susceptible and infected cases was shown using blue and red colors, respectively. In the absence of mitigatory measures such as lock down across the nation and social distancing; the results were frightening (as shown using green bar). (c) The effective basic reproduction ratio was plotted against the time. **Note: All cases were assumed to be symptomatic during the prediction using the age-structured SIR model and thus $\bar{\alpha}=1$. The parameters such as β and γ were set to 0.0155 and 1/7, respectively*

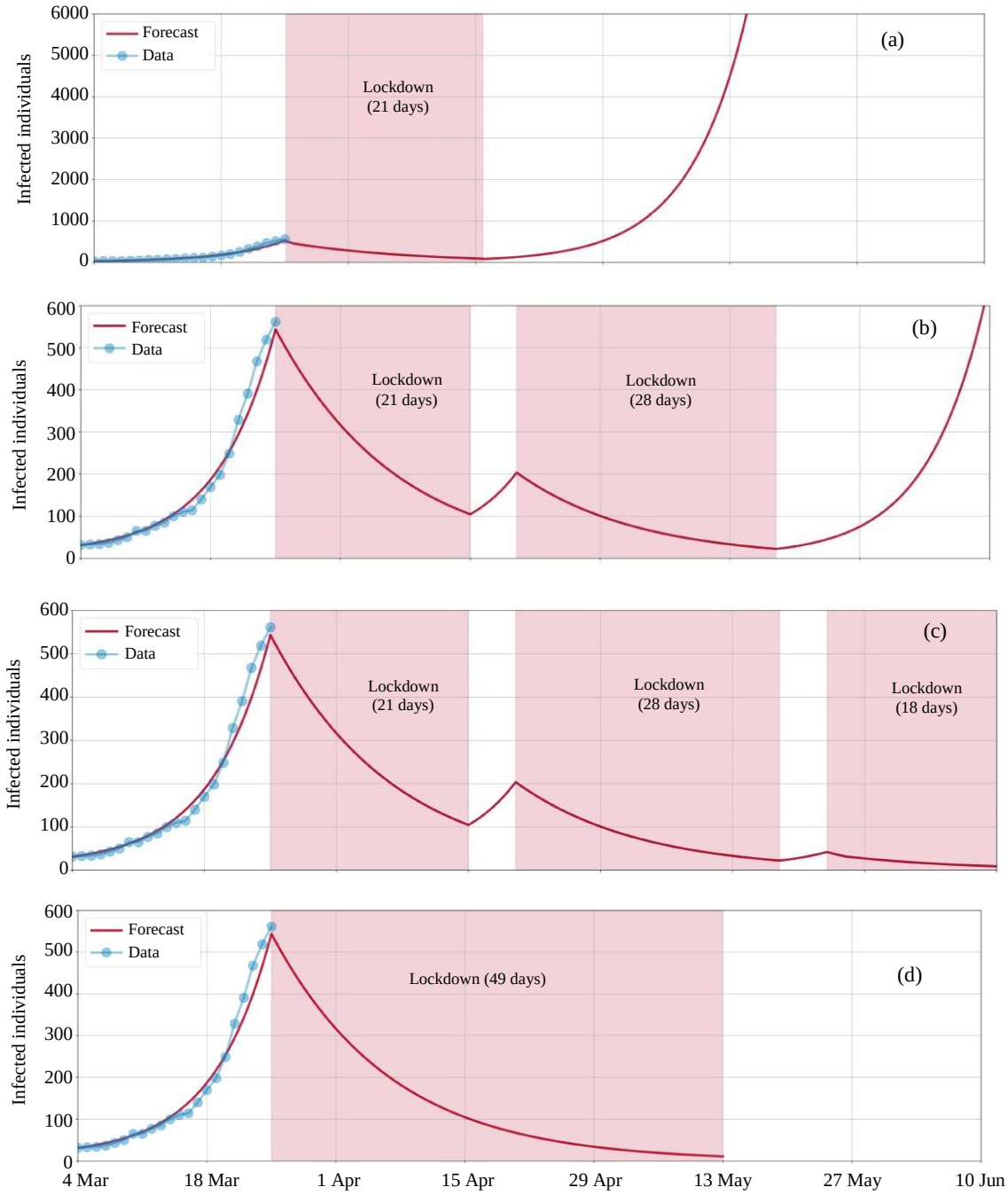

Fig. 7: The prediction of the SARS-CoV2 outbreak in India with effective implementation of social distancing measures using the age-structured epidemiological SIR model. The cases of infected patients were plotted against the various time intervals (Reprinted with permission from Ref. (Singh and Adhikari, 2020). Copyright 2020 arXiv). (a) A *21days* lockdown (from 25th March, 2020 until 14th April, 2020) was found to be insufficient after careful investigation to ensure the equilibrium stage of the pandemic by the end of May, 2020. (b) The outcome of the model was in favor of sustained lockdown with some relaxation for effective implementation of social distancing measures. It was found that the lockdown if imposed across the nation for further *28 days* after the relaxation period of *5 days* from 25th March, 2020, then the measure will be still insufficient to break transmission chain of the SARS-CoV2. (c) As per the scheme, it was found that three successive lockdowns with a gap of *5 days* as relaxation periods were required to bring the equilibrium stage of the pandemic. (d) An alternative scheme was also suggested herewith to impose a *49 days* lockdown across the nation to bring the number of infected cases below *10* or to ensure the equilibrium stage of the novel COVID-19 pandemic. **Note: All cases were assumed to be symptomatic during the prediction using the age-structured SIR model and thus* $\bar{\alpha} = 1$. *The parameters such as* β *and* γ *were set to 0.0155 and 1/7, respectively.*

The Scope and Limitation of the Mathematical Models Used to Investigate Transmission of the Novel COVID-19

Overall, the normalized RP transmission network model was based on the input data sources that were published for only a few countries during the outbreak of the novel COVID-19 and thus it might not fit well into the situations in other countries. The concise baseline model did not rely on the conventional approach of fitting a curve to the dataset. It involved real-time time-dependent data which were based on testing facilities, availability of hospitals, etc. and thus, this framework was suitable for other countries as well. However, the authors acknowledged that due to their limited knowledge of weather conditions, they could not connect it with the equations they have used in their concise modeling to understand the transmission of the pandemic. The exponential model was unable to deliver the perpetual estimation about the novel COVID-19 cases, i.e., up to 30th April, 2020 (section 4), as it did not involve the initiatives of the Indian government to break the transmission chain of the SARS-CoV2. The epidemiological SIR model will not be effective if India reaches the stage of community transmission due to poor implementation of the practice of social distancing. The modified age-structured epidemiological SIR model (section 5) was evaluated by considering both symptomatic and asymptomatic patients (Rothe *et al*., 2020) of SARS-CoV2. The prediction of the age-structured epidemiological SIR model were suggested to vary region-wise as it was based on data such as day-to-day number of tests.

During investigation of the transmission network models useful in mapping the transmission of the pandemic from its source, we realize the need of machine learning algorithms to identify infected symptomatic and asymptomatic patients during the lockdown periods, quickly based on a web based (artificial intelligence framework) participatory surveillance of the novel COVID-19 pandemic (implemented in cases of previous infectious diseases) (Rao and Vazquez, 2020; Neill, 2013; Rajalakshmi *et al*., 2018; Arabasadi *et al*., 2017; Kumar *et al*., 2013; Tomlinson *et al*., 2009; Ballivian *et al*., 2015; Braun *et al*., 2013; Bastawrous and Armstrong, 2013; Paolotti *et al*., 2014; Fabic *et al*., 2012; Liang *et al*., 2019).

Conclusion

The review finds the simplified Reservoir (Wuhan Seafood Market)-People (BHRP) transmission network model (section 2) as an effective tool to discuss the local transmission of the novel coronavirus disease (COVID-19). The simplified RP transmission network model was based on the next generation matrix (R_0). Using the model, it was estimated that the transmission of SARS coronavirus was much higher than Middle East respiratory syndrome (MERS) coronavirus.

The concise baseline model (section 3) based on the individual behavioral response and the control measures taken by the government to prevent the spread of the novel COVID-19 was found in close agreement with the previously published data and thus it throws light on mapping the transmission of the novel COVID-19 pandemic. The model did not rely on the conventional approach of fitting a curve to the dataset.

The epidemiological exponential and SIR models (section 4) revealed a similar exponential trend for the transmission of the novel coronavirus disease (COVID-19) in India, Washington and California. The classical model was derived based on the inputs available till 30th March, 2020 to predict the equilibrium stage of the pandemic by the last week of May, 2020. The outcomes of these models were based on real-time time-dependent data (reported on day-to-day basis) and thus found reasonably well to understand the transmission of the novel COVID-19 outbreak in India. The model, however, will not be effective if India reaches the stage of community transmission due to poor implementation of the social distancing strategies.

The modified age-structured epidemiological SIR model (section 5) was based on age groups and effective implementation of social distancing measures. The outcomes of the model were emphasizing about sustained lockdown across the nation with some relaxation to prevent the transmission of the novel COVID-19 outbreak to India. A *21 days* lockdown was found to be insufficient after careful investigation to ensure the equilibrium stage of the pandemic in May, 2020, instead, the outcomes of the model were emphasizing about sustained lockdown with some relaxation of a few days for effective implementation of social distancing measures. It has clearly demonstrated about the need of mitigatory measures such as successive lockdowns of *21 days* and *28 days* and further *21 days, 28 days and 18 days* (each scheme with a relaxation of some *5 days and* suggested to implement from 25th March, 2020), or alternatively a single lock down of 49 days starting from 25th March, 2020; which are required to impose across the nation to bring the equilibrium stage of the novel COVID-19 pandemic.

Author's Contributions

Eva Gupta: She has reviewed papers on epidemiological models for simulating the transmissibility of the novel coronavirus disease 2019 (COVID-19) outbreak to prepare and develop the entire research work to its publication.

Nand Jee Kanu: He has critically reviewed papers on epidemiological models for simulating the transmissibility of the novel coronavirus disease 2019 (COVID-19) outbreak to prepare and develop the entire research work to its publication.

Conflicts of Interest

The authors declare that there are no conflicts of interest.

Planning and Motivation

We reviewed the relevant articles on the novel coronavirus (SARS-CoV2) published online within the past few months with the aim to join the battle against Coronavirus Disease (COVID-19). The idea behind was to study efficient epidemiological models for simulating the transmissibility of the novel Coronavirus Disease 2019 (COVID-19) outbreak across the globe and understand the effective mitigatory measures to break the transmission chain of the pandemic.

Ethics

The author does not see any ethical issues that may arise after the publication of this manuscript.

References

Anderson, R.M. and R.M. May, 1991. Infectious Diseases of Humans: Dynamics and Control. 1st Edn., Oxford University Press, New York.

Arabasadi, Z., R. Alizadehsani, M. Roshanzamir, H. Moosaei and A.A. Yarifard, 2017. Computer aided decision making for heart disease detection using hybrid neural network-Genetic algorithm. Comput. Meth. Programs Biomed., 141: 19-26. DOI: 10.1016/J.CMPB.2017.01.004

Araujo, M.B. and B. Naimi, 2020. Spread of SARS-CoV-2 Coronavirus likely to be constrained by climate.

Ballivian, A., J.P. Azevedo and W. Durbin, 2015. Using Mobile Phones for High-Frequency Data Collection. In: Mobile Research Methods: Opportunities and Challenges of Mobile Research Methodologies, Toninelli, D., R. Pinter and P.D. Pedraza (Eds.), Ubiquity Press, London, pp: 21-39.

Bastawrous, A. and M.J. Armstrong, 2013. Mobile health use in low- and high-income countries: An overview of the peer-reviewed literature. J. Royal Society Med., 106: 130-142. DOI: 10.1177/0141076812472620

Batista, M., 2020. Estimation of the final size of the COVID-19 epidemic.

BI, 2020. Transit going in and out of Wuhan, China is being shut down to contain coronavirus. Business Insider.

Bogoch, I.I., A. Watts, A. Thomas-Bachli, C. Huber and M.U.G. Kraemer *et al*., 2020. Pneumonia of unknown etiology in Wuhan, China: Potential for international spread via commercial air travel. J. Travel Med., 27: 1-3. DOI: 10.1093/JTM/TAAA008

Bootsma, M.C.J. and N.M. Ferguson, 2007. The effect of public health measures on the 1918 influenza pandemic in U.S. cities. Proc. National Acad. Sci. USA, 104: 7588-7593. DOI: 10.1073/PNAS.0611071104

Box, G.E.P., 1976. Science and statistics. J. Am. Stat. Assoc., 71: 791-799. DOI: 10.2307/2286841

Braun, R., C. Catalani, J. Wimbush and D. Israelski, 2013. Community health workers and mobile technology: A systematic review of the literature. PLoS One, 8: e65772-e65772. DOI: 10.1371/JOURNAL.PONE.0065772

Bukhari, Q. and Y. Jameel, 2020. Will coronavirus pandemic diminish by summer?

CAN, 2020. Asia more Chinese cities shut down as novel coronavirus death toll rises. CNA Asia.

CBN, 2020. Wuhan has a permanent population of 2.87 million, ranking 15th in migration. China Business Network.

CDC, 2019. Flowchart to identify and assess 2019 novel coronavirus. CDC.

Chang, S.L., N. Harding, C. Zachreson, O.M. Cliff and M. Prokopenko, 2020. Modelling transmission and control of the COVID-19 pandemic in Australia.

Chen, S., D. Yang, R. Liu, J. Zhao and K. Yang *et al*., 2019. Estimating the transmissibility of hand, foot and mouth disease by a dynamic model. Public Health, 174: 42-48. DOI: 10.1016/J.PUHE.2019.05.032

Chen, T., R.K. Leung, R. Liu, F. Chen and X. Zhang *et al*., 2014a. Risk of imported Ebola virus disease in China. Travel Med. Infect. Dis., 12: 650-658. DOI: 10.1016/J.TMAID.2014.10.015

Chen, T., R.K. Leung, Z. Zhou, R. Liu and X. Zhang *et al*., 2014b. Investigation of key interventions for shigellosis outbreak control in China. PLoS One, 9: e95006-e95006. DOI: 10.1371/JOURNAL.PONE.0095006

Chen, T.M., J. Rui, Q.P. Wang, Z.Y. Zhao and J.A. Cui *et al*., 2020. A mathematical model for simulating the phase-based transmissibility of a novel coronavirus. Infect. Dis. Poverty, 9: 1-8. DOI: 10.1186/S40249-020-00640-3

Cui, J.A., S. Zhao, S. Guo, Y. Bai and X. Wang *et al*., 2020. Global dynamics of an epidemiological model with acute and chronic HCV infections. Applied Math. Lett., 103: 106203-106203. DOI: 10.1016/J.AML.2019.106203

Deb, S. and M. Majumdar, 2020. A time series method to analyze incidence pattern and estimate reproduction number of COVID-19.

Dey, S., 2020. Coronavirus: 15 lakh who flew back to India between Jan 18-Mar 23 under lens. The Times of India.

Dhama, K., K. Sharun, R. Tiwari, M. Dadar and Y.S. Malik *et al*., 2020. COVID-19, an emerging coronavirus infection: Advances and prospects in designing and developing vaccines, immunotherapeutics and therapeutics. Human Vaccines Immunotherapeutics.

Diekmann, O., J.A.P. Heesterbeek and M.G. Roberts, 2010. The construction of next-generation matrices for compartmental epidemic models. J. Royal Society Interface, 7: 873-885. DOI: 10.1098/RSIF.2009.0386

Dye, C. and N. Gay, 2003. Epidemiology modeling the SARS epidemic. Science, 300: 1884-1885. DOI: 10.1126/science.1086925

Fabic, M.S., Y.J. Choi and S. Bird, 2012. A systematic review of demographic and health surveys: Data availability and utilization for research. Bull. World Health Organization, 90: 604-612. DOI: 10.2471/BLT.11.095513

Ferguson, N.M., D. Laydon, G. Nedjati-Gilani, N. Imai and K. Ainslie *et al*., 2020. Impact of Non-Pharmaceutical Interventions (NPIS) to reduce COVID-19 mortality and healthcare demand. Imperial College COVID-19 Response Team, London.

Ferguson, N.M., D.A.T. Cummings, C. Fraser, J.C. Cajka and P.C. Cooley *et al*., 2006. Strategies for mitigating an influenza pandemic. Nature, 442: 448-452. DOI: 10.1038/NATURE04795

Fine, P.E.M., 2003. The interval between successive cases of an infectious disease. Am. J. Epidemiol., 158: 1039-1047. DOI: 10.1093/AJE/KWG251

Fraser, C., S. Riley, R.M. Anderson and N.M. Ferguson, 2004. Factors that make an infectious disease outbreak controllable. Proc. National Acad. Sci. USA, 101: 6146-6151. DOI: 10.1073/PNAS.0307506101

FT, 2020. Chinese villages build barricades to keep coronavirus at bay. Financial Times.

Guan, W.J., Z.Y. Ni, Y. Hu, W.H. Liang and C.Q. Ou *et al*., 2020. Clinical characteristics of 2019 novel coronavirus infection in China. New England J. Med.

Hatchett, R.J., C.E. Mecher and M. Lipsitch, 2007. Public health interventions and epidemic intensity during the 1918 influenza pandemic. Proc. National Acad. Sci. USA, 104: 7582-7587. DOI: 10.1073/PNAS.0610941104

He, F., Y. Deng and W. Li, 2020. Coronavirus disease 2019: What we know? J. Med. Virol.

Hethcote, H.W., 2000. The mathematics of infectious diseases. SIAM Rev., 42: 599-653. DOI: 10.1137/S0036144500371907

Huang, C., Y. Wang, X. Li, L. Ren and J. Zhao *et al*., 2020. Clinical features of patients infected with 2019 novel coronavirus in Wuhan, China. Lancet, 395. 497-506. DOI: 10.1016/S0140-6736(20)30183-5

Imai, N., A. Cori, I. Dorigatti, M. Baguelin and C.A. Donnelly *et al*., 2020. Report 3: Transmissibility of 2019-nCoV. British Med. J. Publishing Group.

JMH, 2020. Development of patients with pneumonia associated with new coronavirus. Ministry of Health Japan.

Jung, S.M., A.R. Akhmetzhanov, K. Hayashi, N.M. Linton and Y. Yang *et al*., 2020. Real-time estimation of the risk of death from novel Coronavirus (COVID-19) infection: Inference using exported cases. J. Clin. Med., 9: 523-523. DOI: 10.3390/JCM9020523

Keeling, M.J. and P. Rohani, 2008. Modeling infectious diseases in humans and animals. Princeton University Press.

Kumar, V.B., S.S.P. Kumar and V. Saboo, 2013. Dermatological disease detection using image processing and machine learning. Proceedings of the 3rd International Conference on Artificial Intelligence and Pattern Recognition, Sept. 19-21, IEEE Xplore Press, Lodz, Poland, pp: 1-6. DOI: 10.1109/ICAIPR.2016.7585217

Li, Q., X. Guan, P. Wu, W.X.L. Zhou and Y. Tong *et al*., 2020a. Early transmission dynamics in Wuhan, China, of novel coronavirus-infected pneumonia. New England J. Med., 382: 1199-1207. DOI: 10.1056/NEJMOA2001316

Li, R., S. Pei, B. Chen, Y. Song and T. Zhang *et al*., 2020b. Substantial undocumented infection facilitates the rapid dissemination of novel coronavirus (SARS-CoV2). Science.

Liang, H., B.Y. Tsui, H. Ni, C.C.S. Valentim and S.L. Baxter *et al*., 2019. Evaluation and accurate diagnoses of pediatric diseases using artificial intelligence. Nature Med., 25: 433-438. DOI: 10.1038/S41591-018-0335-9

Lin, Q., S. Zhao, D. Gao, Y. Lou and S. Yang *et al*., 2020. A conceptual model for the coronavirus disease 2019 (COVID-19) outbreak in Wuhan, China with individual reaction and governmental action. Int. J. Infect. Dis., 93: 211-216. DOI: 10.1016/J.IJID.2020.02.058

Linton, N.M., T. Kobayashi, Y. Yang, K. Hayashi and A.R. Akhmetzhanov *et al*., 2020. Incubation period and other epidemiological characteristics of 2019 novel coronavirus infections with right truncation: A statistical analysis of publicly available case data. J. Clin. Med., 9: 538-538. DOI: 10.3390/JCM9020538

Lipsitch, M., T. Cohen, B. Cooper, J.M. Robins and S. Ma *et al*., 2020. Transmission dynamics and control of severe acute respiratory syndrome. Science, 300: 1966-1970. DOI: 10.1126/SCIENCE.1086616

Liu, T., J. Hu, M. Kang, L. Lin and H. Zhong *et al*., 2020. Transmission dynamics of 2019 novel coronavirus (2019-nCoV).

Luo, W., M.S. Majumder, D. Liu, C. Poirier and K.D. Mandl *et al*., 2020. The role of absolute humidity on transmission rates of the covid-19 outbreak.

Ma, J., 2020. Estimating epidemic exponential growth rate and basic reproduction number. Infect. Dis. Model., 5: 129-141. DOI: 10.1016/J.IDM.2019.12.009

Ma, J., J. Dushoff, B.M. Bolker and D.J.D. Earn, 2013. Estimating initial epidemic growth rates. Bull. Math. Biol., 76: 245-260. DOI: 10.1007/S11538-013-9918-2

Ma, Y., Y. Zhao, J. Liu, X. He and Bo. Wang *et al*., 2020. Effects of temperature variation and humidity on the mortality of covid-19 in Wuhan, China. Sci. Total Environ., 724: 138226-138226. DOI: 10.1016/J.SCITOTENV.2020.138226

Mahase, E., 2020. Coronavirus: UK screens direct flights from Wuhan after US case. British Med. J.

Mandal, S., T. Bhatnagar, N. Arinaminpathy, A. Agarwal and A. Chowdhury *et al*., 2020. Prudent public health intervention strategies to control the coronavirus disease 2019 transmission in India: A mathematical model-based approach. Indian J. Med. Res., 151: 190-199. DOI: 10.4103/IJMR.IJMR_504_20

McGee, J., 2020. Fitviruscv19v3 (COVID-19 SIR Model). MATLAB Central File Exchange.

MSN, 2020. News Coronavirus explained: Death toll crosses 900, surpasses SARS and MERS. MSN News.

Neill, D.B., 2013. Using artificial intelligence to improve hospital inpatient care. IEEE Intell. Syst., 28: 92-95. DOI: 10.1109/MIS.2013.51

NENVN, 2020. Wuhan set up temperature detection points and checkpoints to strengthen the temperature detection of passengers departing from Han. North Evening New Vision Network.

NHCPRC, 2020. Daily briefing on novel coronavirus cases in China. National Health Commission of the PRC.

Nishiura, H., T. Kobayashi, Y. Yang, K. Hayashi and T. Miyama *et al*., 2020a. The rate of underascertainment of novel Coronavirus (2019-nCoV) infection: Estimation using Japanese passengers data on evacuation flights. J. Clin. Med., 9: 419-419. DOI: 10.3390/JCM9020419

Nishiura, H., N.M. Linton and A.R. Akhmetzhanov, 2020b. Serial interval of novel coronavirus (COVID-19) infections. Int. J. Infect. Dis., 93: 284-286. DOI: 10.1016/J.IJID.2020.02.060

Paolotti, D., A. Carnahan, V. Colizza, K. Eames and J. Edmunds *et al*., 2014. Web-based participatory surveillance of infectious diseases: The Influenzanet participatory surveillance experience. Clin. Microbiol. Infection, 20: 17-21. DOI: 10.1111/1469-0691.12477

Peak, C.M., L.M. Childs, Y.H. Grad and C.O. Buckee, 2017. Comparing nonpharmaceutical interventions for containing emerging epidemics. Proc. National Academy Sci. USA, 114: 4023-4028. DOI: 10.1073/PNAS.1616438114

Pontryagin, L.S., 1985. The mathematical theory of optimal processes and differential games. Trudy Matematicheskogo instituta im. V.A. Steklova RAN, 169: 119-158.

Prem, K., A.R. Cook and M. Jit, 2017. Projecting social contact matrices in 152 countries using contact surveys and demographic data. PLOS Comput. Biol., 13: e1005697-e1005697. DOI: 10.1371/JOURNAL.PCBI.1005697

Rajalakshmi, R., R. Subashini, R.M. Anjana and V. Mohan, 2018. Automated diabetic retinopathy detection in smartphone-based fundus photography using artificial intelligence. Eye, 32: 1138-1144. DOI: 10.1038/S41433-018-0064-9

Ranjan, R., 2020. Predictions for COVID-19 outbreak in India using epidemiological models.

Rao, A.S.R.S. and J.A. Vazquez, 2020. Identification of COVID-19 can be quicker through artificial intelligence framework using a mobile phone-based survey in the populations when cities/towns are under quarantine. Infection Control Hospital Epidemiol.

Rao, A.S.R.S. and M.P. Diamond, 2020. Deep learning of Markov model-based machines for determination of better treatment option decisions for infertile women. Reproductive Sci., 27: 763-770. DOI: 10.1007/S43032-019-00082-9

Reich, N.G., J. Lessler, D.A. Cummings and R. Brookmeyer, 2009. Estimating incubation period distributions with coarse data. Stat. Med., 28: 2769-2784. DOI: 10.1002/SIM.3659

Ridenhour, B., J.M. Kowalik and D.K. Shay, 2018. Unraveling R_0: Considerations for public health applications. Am. J. Public Health, 108: S445-S454. DOI: 10.2105/AJPH.2013.301704r

Riley, S., C. Fraser, C.A. Donnelly, A.C. Ghani and L.J. Abu-Raddad *et al*., 2003. Transmission dynamics of the etiological agent of SARS in Hong Kong: Impact of public health interventions. Science, 300: 1961-1966. DOI: 10.1126/SCIENCE.1086478

Riou, J. and C.L. Althaus, 2020. Pattern of early human-to-human transmission of Wuhan 2019 novel coronavirus (2019-nCoV). Eurosurveillance, 25: 2000058-2000058. DOI: 10.2807/1560-7917.ES.2020.25.4.2000058

Rothe, C., M. Schunk, P. Sothmann, G. Bretzel and G. Froeschl *et al*., 2020. Transmission of 2019-nCoV infection from an asymptomatic contact in Germany. New England J. Med., 382: 970-971. DOI: 10.1056/NEJMC2001468

Sahasranaman, A. and N. Kumar, 2020. Network structure of COVID-19 spread and the lacuna in India's testing strategy.

Salman, S. and M.L. Salem, 2020. The mystery behind childhood sparing by COVID-19. Int. J. Cancer Biomed. Res., 5: 11-13. DOI: 10.21608/JCBR.2020.79888

SCMP, 2020. 5 million left Wuhan before lockdown, 1000 new coronavirus cases expected in city. South China Morning Post.

SDT, 2012. Stan modeling language users guide and reference manual.

Singh, R. and R. Adhikari, 2020. Age-structured impact of social distancing on the COVID-19 epidemic in India.

Singhal, T., 2020. A review of coronavirus disease-2019 (COVID-19). Indian J. Pediatrics, 87: 1-6. DOI: 10.1007/S12098-020-03263-6

TAC, 2020. Expert: Better models, algorithms could help predict and prevent virus spread. The Australia Chronicle.

Tomlinson, M., W. Solomon, Y. Singh, T. Doherty and M. Chopra *et al*., 2009. The use of mobile phones as a data collection tool: A report from a household survey in South Africa. BMC Med. Inform. Decision Mak.

Towers, S. and Z. Feng, 2012. Social contact patterns and control strategies for influenza in the elderly. Mathe. Biosci., 240: 241-249. DOI: 10.1016/J.MBS.2012.07.007

Tuite, A.R. and D.N. Fisman, 2020. Reporting, epidemic growth and reproduction numbers for the 2019 novel Coronavirus (2019-nCoV) epidemic. Annals Int. Med.

WG, 2020. Population distribution. Wuhan Government.

WHO, 2020a. Novel Coronavirus-China. World Health Organization.

WHO, 2020b. Coronavirus disease 2019 (COVID-19) situation report-36. World Health Organization.

WHO, 2020c. Novel Coronavirus-Thailand (ex-China). World Health Organization.

WHO, 2020d. Novel Coronavirus-Japan (ex-China). World Health Organization.

Wu, J.T., K. Leung and G.M. Leung, 2020a. Nowcasting and forecasting the potential domestic and international spread of the 2019-nCoV outbreak originating in Wuhan, China: A modelling study. Lancet, 395: 689-697. DOI: 10.1016/S0140-6736(20)30260-9

Wu, J.T., K. Leung, M. Bushman, N. Kishore and R. Niehus *et al*., 2020b. Estimating clinical severity of COVID-19 from the transmission dynamics in Wuhan, China. Nature Med., 26: 506-510. DOI: 10.1038/S41591-020-0822-7

Wu, P., X. Hao, E.H.Y. Lau, J.Y. Wong and K.S.M. Leung *et al*., 2020c. Real-time tentative assessment of the epidemiological characteristics of novel coronavirus infections in Wuhan, China. Eurosurveillance, 25: 1-6. DOI: 10.2807/1560-7917.ES.2020.25.3.2000044

Wu, Z. and J.M. McGoogan, 2020. Characteristics of and important lessons from the Coronavirus disease 2019 (COVID-19) outbreak in China: Summary of a report of 72,314 cases from the Chinese center for disease control and prevention. J. Am. Med. Assoc., 323: 1239-1242. DOI: 10.1001/JAMA.2020.2648

Yi, B., Y. Chen, X. Ma, J. Rui and J.A. Cui *et al*., 2019. Incidence dynamics and investigation of key interventions in a dengue outbreak in Ningbo City, China. PLOS Neglected Tropical Dis., 13: e0007659- e0007659. DOI: 10.1371/JOURNAL.PNTD.0007659

Zhang, S., Q. Hu, Z. Deng, S. Hu and F. Liu *et al*., 2020. Transmissibility of acute haemorrhagic conjunctivitis in small-scale outbreaks in Hunan Province, China. Sci. Reports, 10: 119-119. DOI: 10.1038/S41598-019-56850-9

Zhao, S., Q. Lin, J. Ran, S.S. Musa and G. Yang *et al*., 2020a. Preliminary estimation of the basic reproduction number of novel Coronavirus (2019-nCoV) in China, from 2019 to 2020: A data-driven analysis in the early phase of the outbreak. Int. J. Infectious Dis., 92: 214-217. DOI: 10.1016/J.IJID.2020.01.050

Zhao, S., S.S. Musa, Q. Lin, J. Ran and G. Yang *et al*., 2020b. Estimating the unreported number of novel Coronavirus (2019-nCoV) cases in China in the first half of January 2020: A data-driven Modelling analysis of the early outbreak. J. Clin. Med., 9: 388-388. DOI: 10.3390/JCM9020388

Zhao, S., D. Gao, Z. Zhuang, M. Chong and Y. Cai *et al*., 2020c. Estimating the serial interval of the novel Coronavirus Disease (COVID-19): A statistical analysis using the public data in Hong Kong.

Zhou, G. and G. Yan, 2003. Severe acute respiratory syndrome epidemic in Asia. Emer. Infect. Dis., 9: 1608-1610. DOI: 10.3201/eid0912.030382

Zhou, P., X.L. Yang, X.G. Wang, B. Hu and L. Zhang *et al*., 2020. A pneumonia outbreak associated with a new coronavirus of probable bat origin. Nature, 579: 270-273. DOI: 10.1038/S41586-020-2012-7

American Journal of Infectious Diseases

Original Research Paper

Stochastic and Deterministic Mathematical Modeling and Simulation to Evaluate the Novel COVID-19 Pandemic Control Measures

[1]Eva Gupta, [2*]Nand Jee Kanu, [3]Amartya Munot,
[4]Venkateshwara Sutar, [1]Umesh Kumar Vates and [5]Gyanendra Kumar Singh

[1]Amity University, Noida, India & AGCE, Satara, India
[2]S. V. National Institute of Technology, Surat, India & JSPM Narhe Technical Campus, Pune, India
[3]S. A. P. D. J. Pathshala's Walchand Institute of Technology, Solapur, India
[4]JSPM Narhe Technical Campus, Pune, India
[5]Adama Science and Technology University, Adama, Ethiopia

Article history
Received: 12-10-2020
Revised: 12-11-2020
Accepted: 19-11-2020

Corresponding Author:
Nand Jee Kanu
S. V. National Institute of Technology, Surat, 395007, India & JSPM Narhe Technical Campus, Pune, 411041, India
Email: nandssm@gmail.com

Abstract:

Background: In India, the novel Coronavirus Disease (COVID-19) epidemic has grown to 17,00000 cases and around 38,000 deaths up to 30th July, 2020. The impacts of the Severe Acute Respiratory Syndrome Coronavirus 2 (SARS-CoV-2) pandemic in India were studied using modified age-structured stochastic and deterministic mathematical models.

Methods: A compartmental susceptible (S)-infected (symptomatic) (I_S) infected (asymptomatic) (I_N) recovered (R) i.e., SI_SI_NR model is developed, in which the flow of individuals through compartments is modeled using a set of differential equations. The outbreak of the novel COVID-19 pandemic is critically evaluated from all major angles using base, education, vaccination and education and vaccination models based on the modified SI_SI_NR transmission network model for their simulations in MATLAB and peak of infected cases (both symptomatic and asymptomatic cases) as well as end of pandemic is predicted in each case.

Result: The numerical investigations are done for both stochastic and deterministic studies using the modified SI_SI_NR transmission network model for effective prediction about the transmission of SARS-CoV-2 pandemic in India. The progress of the novel COVID-19 pandemic in India is estimated for various scenarios by varying the basic reproduction numbers from mean to extremes (general assumptions and strategies are inculcated through contact tracing based on the values of contact ratio operated for the basic reproduction numbers, 'R_0'). The efficacy and potential of the education programs and vaccination programs were established with the published datasets through a validation studies. Furthermore, the outbreak of the novel COVID-19 pandemic is predicted for majorly affected cities in India on the basis of different reproduction numbers 'R_0'.

Conclusion: The report presented herewith could be referred to revise the government policies to (a) implement mitigatory measures such as the practice of social distancing, partial city lockdown across the nation, etc., (b) implement a 100% daily number of tests to the susceptible population of the nation, (c) improve hospital facilities and the novel COVID-19 wards, (d) improve the recovery rate with the effective implementation of base, education, vaccination and education and vaccination model to attain the equilibrium stage of

pandemic at the earliest and (e) meet the objective of preventing the outbreak of the novel COVID-19 pandemic through the effective implementation of control and prevention strategies across the nation.

Keywords: COVID-19, SARS-CoV-2, Pandemic, Mathematical Model, Education, Vaccination

Introduction

The novel COVID-19 pandemic has presented a prodigious ultimatum before the whole world, with that tardy response from the WHO that resulted bedlam in the subcontinent of India and most of the other countries in the world. As of 30th July, 2020, there have been 18,000,000 confirmed cases of the novel COVID-19 and about 7,00000 reported deaths globally and, due to the rising economical unbalance, probably the countries around the world had to open financial markets. Due to which, there has been a great rise in the number of cases since the opening of the global market as there is no specific medication or vaccine approved by global medical authorities. The disease is transmitted by inhalation or contact with infected droplets or fomites and the incubation period during these days may range from 10-20 days. The disease can be fatal to elderly people and those with an underlying medical history (COVID-19 India, 2020; Hindustan Times, 2020a).

What is Already known on the Subject

The transmissibility of the disease outbreak is studied and it is observed that the strictness with which social distancing in India is followed, is insufficient to break the chain of the novel COVID-19. The impacts of the Severe Acute Respiratory Syndrome Coronavirus 2 (SARS-CoV-2) pandemic in India were studied using modified age-structured stochastic and deterministic mathematical models.

What does this Study Add

The major goal of the present investigation is to study the transmission of the novel COVID-19 pandemic in India for various possible scenarios based on general assumptions and strategies inculcated through contact tracing using the values of contact ratios which are operated for the basic reproduction numbers, 'R_0', with the aim to educate individuals to reduce the spread of the novel COVID-19 and vaccination program to assess their potential results in upcoming days.

The outbreak of the novel COVID-19 pandemic is critically evaluated from all major angles using base, education, vaccination and education and vaccination models based on the modified SI_SI_NR model.

The outspread of any epidemic depends on the infectivity of the pathogen and the available population that is considered as susceptible. For a novel pandemic, when the spread of the disease is not clear yet, here the mathematical modeling estimates the number of cases in the worst and the best cases. It can also aid to estimate the effect of preventive measures that are been applied against the novel COVID-19. By using the suppressive strategy, the major objective is to reduce the basic reproduction number, 'R_0' and maintain it below '1'. To prohibit further infection spread using mitigatory measures; the main objective is to contain the spread and reduce the effect of the pandemic. The novel COVID-19 pandemic is caused by the Severe Acute Respiratory Syndrome Coronavirus 2 (SARS-CoV-2). On 30th January, 2020, India witnessed its first case of the novel COVID-19. Currently, India is one of the most affected countries and has the highest number of cases in Asia continent. In the world, India was the third highest affected country after United States of America and Brazil, with over 100,000 confirmed cases on 19th May, 2020 and about 1,000,000 confirmed cases on 17th July, 2020. Whereas, in India the fatality rate is probably the lowest in the world at 2.11% as of 02nd August, 2020 and it is also steadily reducing with time. With that, the six cities - Delhi, Ahmedabad, Chennai, Mumbai, Pune and Kolkata have around 50% of the total cases reported in the country. By the 24th May, 2020, Lakshadweep was the only region that was unaffected by the novel COVID-19 pandemic. The recovery rate in India is 64.23% as on 02nd August, 2020 (COVID-19 India, 2020; Hindustan Times, 2020a; Wikipedia, 2020a).

In India, the speed of testing is raised from June, 2020 as shown in Fig. 1 and up to 31st May, 2020, a strict lockdown has been imposed across the nation by the government as mitigatory measures to restrict the spread of the pandemic. On 09th April, 2020, Indian Council of Medical Research (ICMR) further revised the testing strategy and allowed testing of people showing symptoms for a week in the hotspot areas of the country, regardless of travel history or local contact to the patient. There has been a rise in the number of cases in India during lockdown as due to the religious gathering in the country's capital territory, Delhi. The Government of India announced in the press release on 18th April, 2020, that 4,291 cases, which are about 29.8% of the total 14,378 confirmed cases of the novel COVID-19 in India, had connection with religious and social gatherings. These cases contributed to spread of the pandemic across 23 states and few of the nation's union territories. By 04th April, 2020, nearly about 22,000 people that were

in contact with the people who attended the social event were quarantined. In addition to that, pilgrims from Maharashtra state were sent by the state government back to Punjab. The total 609 of the around 4,000 stranded pilgrims who returned to Punjab from Nanded (a historical city in Maharashtra) were tested positive for the novel COVID-19, taking the state's infection tally to over 1,000 (Wikipedia, 2020a; Hindustan Times, 2020b).

The Indian government imposed the strict lockdown across the country to contain the spread of SARS-CoV-2 and built healthcare infrastructure to treat those who were affected. The lockdown was aggressive but vital. India's fast response to the pandemic was praised as comprehensive and robust by the United Nations (UN) as well as the World Health Organization (WHO). India has a vast experience in eradicating diseases like smallpox and polio. Owing to this, India is strong enough to deal with the outbreak of the novel COVID-19 as stated by Mr. Michael Ryan, (chief executive director of the WHO's health emergencies program). The lockdown was imposed by the government and as well as other agencies to contain the spread of SARS-CoV-2 and to help India to escape from the community transmission stage of the pandemic which could eventually make handling the situation very difficult and result in even more fatalities (Wikipedia, 2020a; Hindustan Times, 2020b; Livemint, 2020).

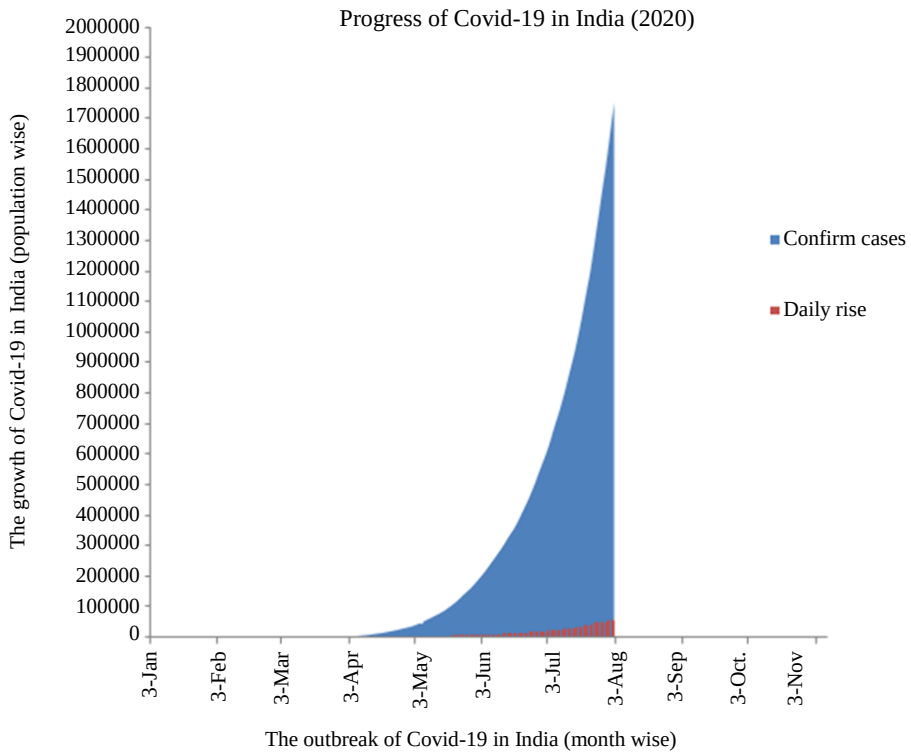

Fig. 1: Growth of the novel COVID-19 pandemic in India

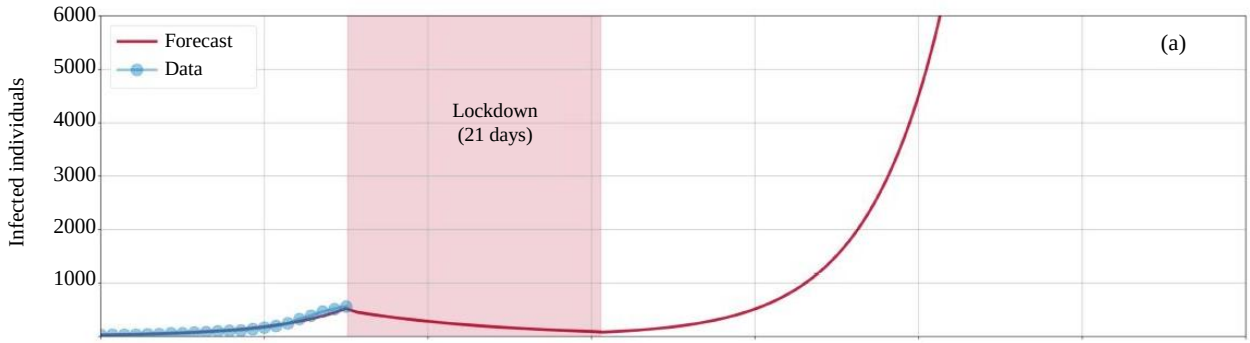

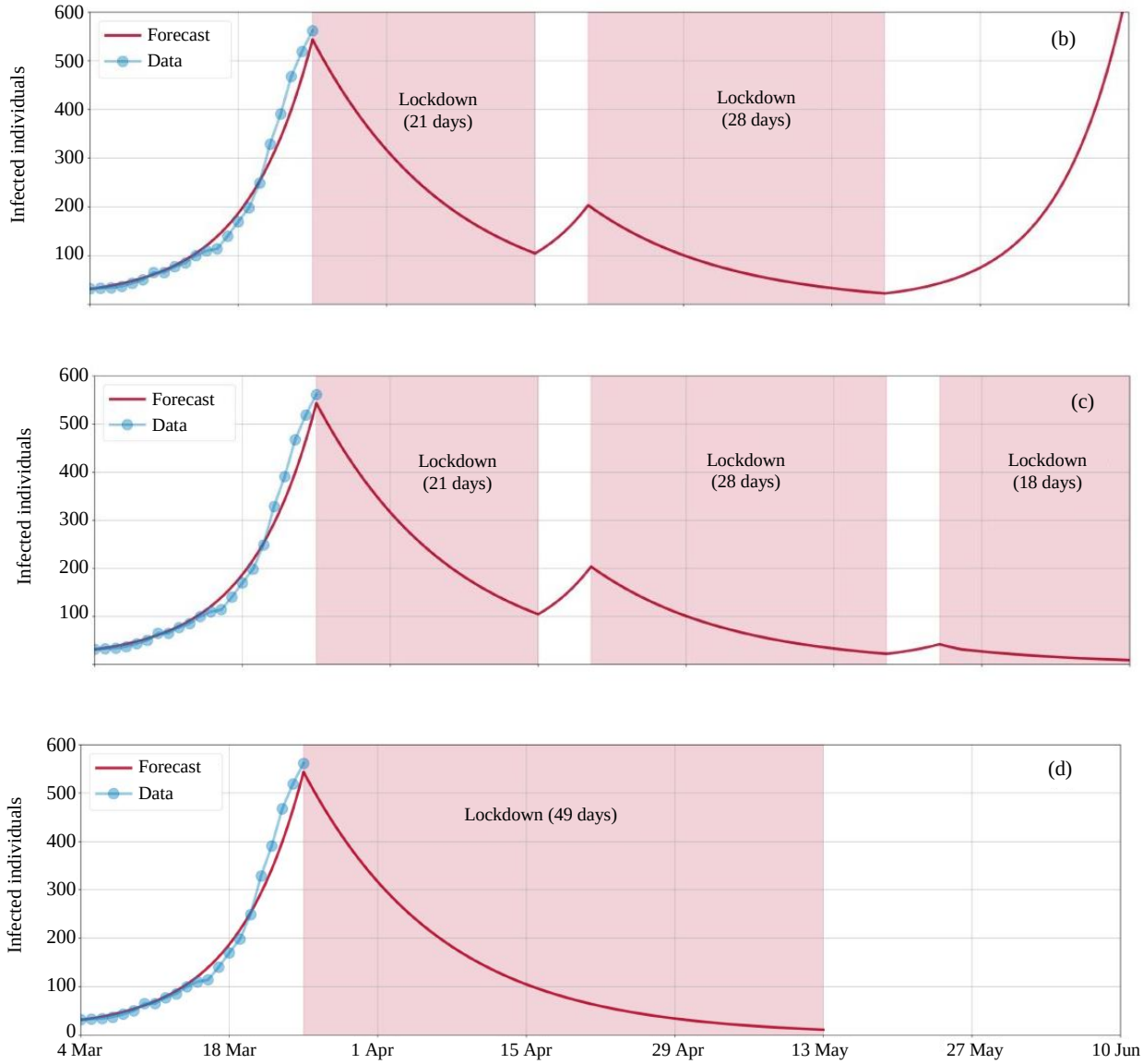

Fig. 2: The graphs of infected patients versus days as different schemes of series lockdowns (a), (b) and (c) and sustained lockdown (d) across the nation to restrict the chain of the novel COVID-19 pandemic in India using age-structured epidemiological Susceptible-Infected-Recovered (SIR) model (Reprinted with permission from (Singh and Adhikari, 2020). Copyright 2020 arXiv). *Note: Symptomatic cases were taken into consideration for the prediction of equilibrium stage of the pandemic. The inputs such as $\bar{\alpha}$, β and γ were taken as 1, 0.0155 and 1/7, respectively

A 21 day lockdown (from 25th March, 2020 to 14th April, 2020) was found to be insufficient after careful investigation to ensure the equilibrium stage of the pandemic by the end of May, 2020 (Fig. 2). The outcome of the model was in favour of sustained lockdown with some relaxation for effective implementation of social distancing measures. It was found that the lockdown is imposed across the nation for a further 28 days after the relaxation period of 5 days from 25th March, 2020 and then the measure will be still insufficient to restrict the transmission chain of the SARS-CoV-2 (Fig. 2). As per the scheme, it was suggested that three successive lockdowns with a gap of 5 days as relaxation periods were required to bring the equilibrium stage of the pandemic (Fig. 2) (Appendix A) (Singh and Adhikari, 2020).

As per the guidance of the Honorable Prime Minister of India, Shri Narendra Modi, there was a voluntary public curfew of 14 h on 22nd March, 2020. Later on it was followed as mandatory and strict lockdowns were

imposed in the major affected areas called as 'hotspots' in all major cities of the country. The nation further witnessed a strict 21 days nationwide lockdown from 24th March, 2020 as ordered by the Honorable Prime Minister of India. The nationwide lockdown was again extended up to 03rd May, 2020 by the Government of India on 14th April, 2020. This was later followed by another two-week extension with substantial relaxations. From 01st June, 2020, the government started "unlocking" the country (barring 'containment zones') in three unlock phases (Livemint, 2020; Singh and Adhikari, 2020; Inventiva, 2020a).

The factories and workplaces were shut down due to the nationwide lockdown which directly affected the livelihood of many migrant workers. Due to which, they were left with the only choice to turn back to their native villages. Thus, the Government of India asked the state government to set up relief camps for the migrant workers who are trying to return to their homes and issued orders for the protection of the rights of the migrant workers. It was admitted by the Supreme Court of India that the issues and problems of the migrant workers were still not completely solved. The Supreme Court ordered the state as well as the central government to provide free food, shelter and transport facilities to the migrant workers.

Most of the countries had lifted their lockdowns when the cases of novel COVID-19 started decreasing, but India has opted for a different plan. The WHO recommended the Government of India to test for SARS-CoV-2 for at least 14 days prior to lifting up the sustained lockdown to ensure positive rates were below the desired rate of 5%. As per the report from the Johns Hopkins University's Coronavirus Resource Centre, the average rate of daily positivity for the novel COVID-19 in India was around 8-10%. However, due to the unlock 1.0 on 07th June, 2020, it was raised to 8.2% and on the next day it was almost 9.2%. The increase in the positivity rate clearly throws light on the fact that the number of daily tests has been increased to unlock 1.0 in India. By May, 2020, India had done more than 10,00000 tests and the test positivity rate was just 3.8%. In June, 2020, Central Government of India chose to lift the lockdown and announced that it is mandatory for every citizen to maintain social distancing in the market and all other social places. The physical distancing norms were also strictly followed during multiphased lockdown. Still, the novel COVID-19 positive cases exponentially increased from a few hundred in March, 2020, to over 2,55000 when unlock 1.0 was declared in June, 2020 (Fig. 3) (Livemint, 2020; Singh and Adhikari, 2020; Inventiva, 2020a; 2020b; BBC News, 2020a; India Today, 2020a).

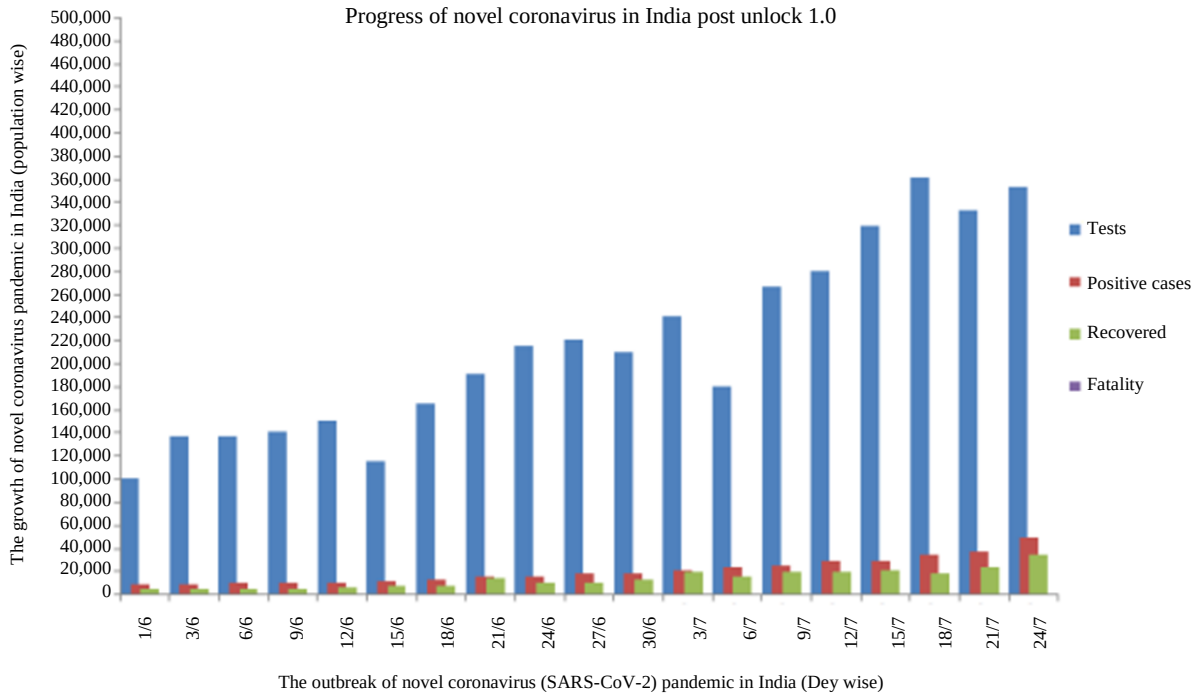

Fig. 3: The transmission of the novel Coronavirus Disease (COVID-19) post unlock 1.0 in India

Mathematical models can forecast the spread of the novel COVID-19 pandemic and help inform public health interventions. The suitable input parameters for various scenarios such as partial lockdown, full lockdown, mass vaccination program, public education program, etc., are considered on the basis of (a) basic assumptions and (b) reported statistical data in published sources. In the present investigation, both stochastic and deterministic approaches are used to discuss the transmission of SARS-CoV-2 outbreak in India to fulfill the objectives. The stochastic model is used to estimate the probability of potential outcomes by having a random variation in one or more inputs over time in the proposed mathematical model. The stochastic models mainly depend on the variations in the risk of exposure to the disease and all other dynamic factors of the illness. In the case of the deterministic models, the individuals in the population are arranged in a different subgroups or small compartments, which directly represent a specific stage of the pandemic. Here, the letters *M*, *S*, *E*, *I* and *R* are used to represent variables such as different age groups of persons, susceptible, exposed, infected and recovered patients, respectively. Later on, the transition rates from one stage to another stage are mathematically expressed in the form of derivatives and thus the model is formulated using differential equations. Although when building mathematical models, it can be assumed that the size of the population in each of the compartments is differentiable with respect to time and that the pandemic process is deterministic (Gupta and Kanu, 2020; Atkins, 2010). The major goal of the present investigation is to study the transmission of the novel COVID-19 pandemic in India for various possible scenarios based on general assumptions and strategies inculcated through contact tracing using the values of contact ratios which are operated for the basic reproduction numbers, 'R_0', with the aim to educate individuals to reduce the spread of the novel COVID-19 and vaccination program to assess their potential results in upcoming days. Furthermore, the transmission of the novel COVID-19 pandemic is also studied for majorly affected Indian cities on the basis of basic reproduction numbers (Atkins, 2010).

Research Methodology

Both deterministic and stochastic approaches are employed in the present mathematical investigations to study the transmissibility of SARS-CoV-2 pandemic in India. The Susceptible (*S*) -Infected (*I*) -Recovered (*R*) i.e., SIR model is a compartmental model. When a Susceptible (*S*) will come in an infectious contact with the infected individual, the susceptible will contract the disease and transition into the infected compartment. The symbol, '*I*' represents the number of infectious individuals. These are individuals who have been infected and can infect the Susceptible (*S*). The symbol, '*R*' portrays the number of removed individuals. These are individuals who have been infected and have recovered from the disease or died.

The present investigation analyzes the spread of the novel COVID-19 pandemic in India and its majorly affected cities. The transmission of SARS-CoV-2 pandemic is due to the contact structure among the people and thus is governed by the parameter, 'β' (contact ratio). The parameter 'β' directly shows the result of the effectiveness of the social distancing. The transmissibility of the disease outbreak is studied and it is observed that the strictness with which social distancing in India is followed, is insufficient to break the chain of the novel COVID-19 (Atkins, 2010).

The SIR model considers the specific types of diseases which could cause an infected one to infect a susceptible after they encounter with each other. The variables *S*, *I* and *R*, depict the population in every compartment for a particular instinct of time. The susceptible, infectious and removed individuals are a function of time and are represented by *S*(*t*), *I*(*t*) and *R*(*t*), respectively. The total number of individuals remains constant. The outbreak of such diseases in a specific population can be predicted by the mathematical model. The dynamics of the transition between these compartments can be modelled with the help of some parameters. These are 'β' and can be referred as transmission rates. The parameter, 'γ' is the reciprocal of the infectious period, which is the time duration in which the infected can transmit the disease (Gupta and Kanu, 2020; Atkins, 2010; Mazumder *et al*., 2020).

The distribution of population within these compartments at a given time, *t*, using the general SIR model are shown using a set of ordinary differential Equations (1) to discuss the transmission of the novel COVID-19 pandemic in India:

$$\left.\begin{aligned} &S + I + R = N;\\ &\frac{dS}{dT} = -\frac{\beta IS}{N};\\ &\frac{dI}{dT} = \frac{p\beta IS}{N} - I(\gamma + \mu);\\ &\frac{dR}{dT} = \gamma(I) \end{aligned}\right\} \quad (1)$$

The Modified SI_SI_NR Transmission Network Model for Modeling and Simulation of the Novel COVID-19 Outbreak in India

The SI_SI_NR transmission network model can be regarded as a derivative of the basic *SIR* model (Fig. 4). In the SI_SI_NR model, we include the asymptomatic compartment which turns the *SIR* model into the SI_SI_NR model (Fig. 5a). The modified SI_SI_NR transmission network model is partitioned into classes such as susceptible *S*(*t*), symptomatic infected $I_S(t)$, asymptomatic infected $I_N(t)$ and removed *R*(*t*); where $N + I_S + I_N + R = N$.

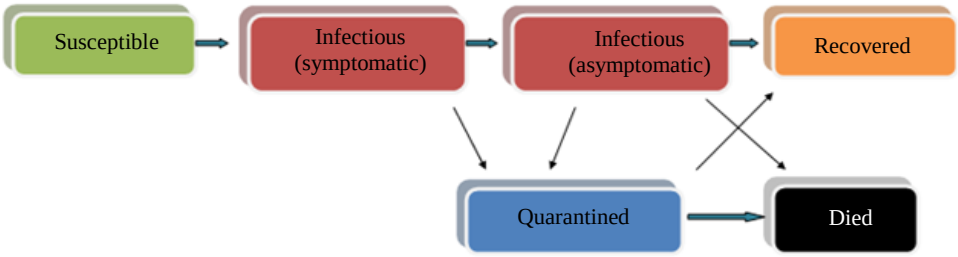

Fig. 4: The schematic representation of modeling of the novel Coronavirus (COVID-19) pandemic using SI_NI_NR model in India

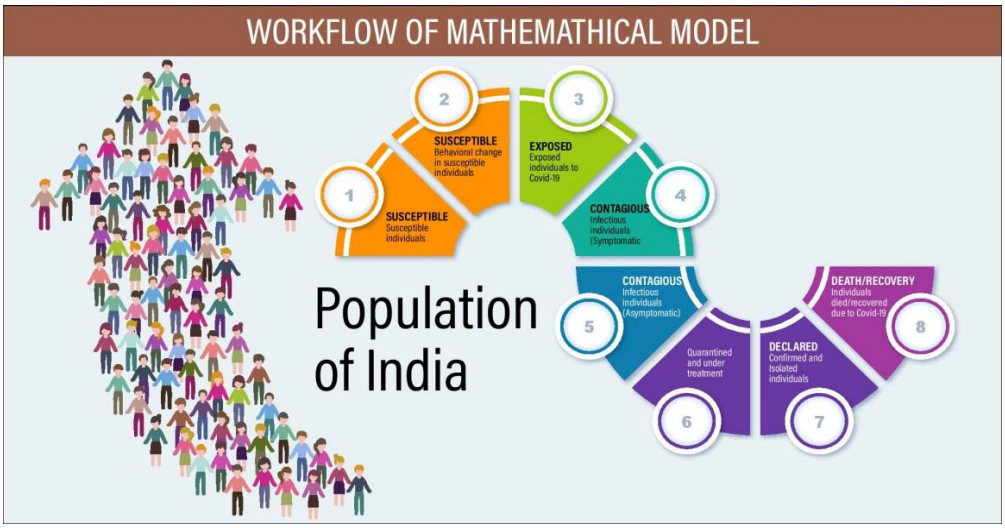

(a)

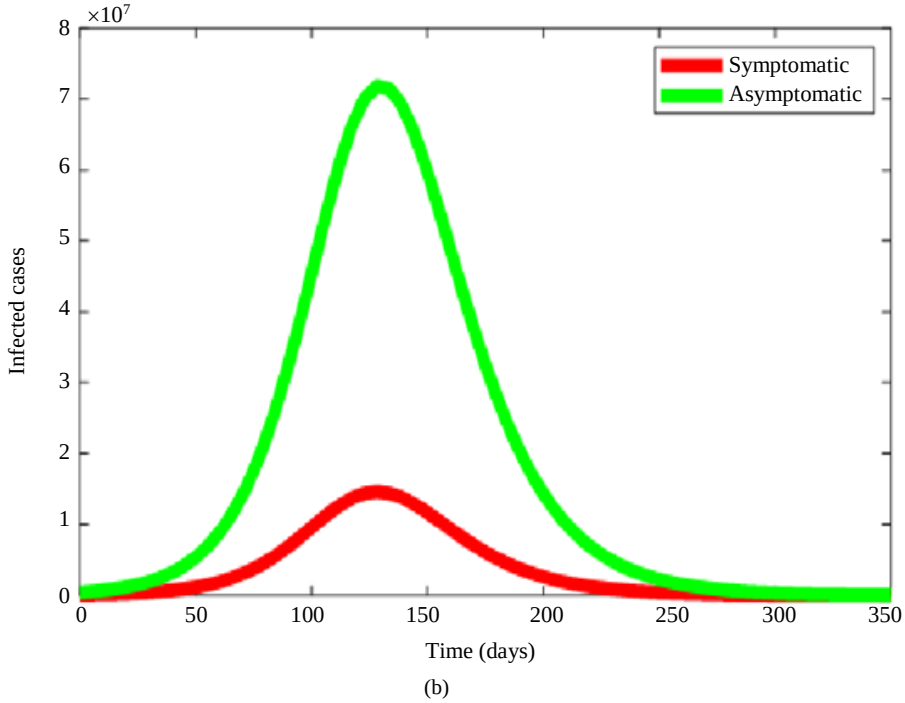

(b)

Fig. 5: The outbreak of SARS-CoV-2 pandemic in India. (a) The illustration of mathematical model of SARS-CoV-2 pandemic in India. (b) The transmission of the novel COVID-19 pandemic is shown with the graph of infected patients (both symptomatic and asymptomatic) versus time (days) using deterministic approach of SI_SI_NR transmission network model

Those contracting the disease entered into the infected classes at a rate of '*p*' i.e., the symptomatic class, or '(1-*p*)' entered into the asymptomatic class. Here, the infected individuals gets recovered from the infection and entered into the removed compartment at a rate of 'γ' or may die due to the illness at a rate of 'μ'. Those who are within the asymptomatic compartment exit into the removed category at the rate of 'γ' (Fig. 5b) (Gupta and Kanu, 2020; Atkins, 2010; Mazumder *et al*., 2020; Times Network, 2020; Pai *et al*., 2020).

Those contracting the disease entered into the infected classes at a rate of '*p*' i.e., the symptomatic class, or '(1-*p*)' entered into the asymptomatic class.

The distribution of population within these compartments at a given time, *t*, using the modified SI_SI_NR transmission network model are shown using the set of ordinary differential Equations (2) to discuss the transmission of the novel COVID-19 pandemic in India:

$$\left.\begin{aligned} &S + I_S + I_N + R = N \\ &\frac{dS}{dT} = -\frac{\beta\left(I_S + I_N\right)S}{N} \\ &\frac{dI}{dT} = \frac{p\beta IS\left(I + I\right)}{N} - I\left(\gamma + \mu\right) \\ &\frac{dI_A}{dT} = \frac{\left(1-p\right)\beta S\left(I_S + I_A\right)}{N} - \gamma I_A \\ &\frac{dR}{dT} = \gamma\left(I + I\right) \end{aligned}\right\} \quad (2)$$

The basic reproduction number, 'R_0', or basic reproductive number, or basic reproductive rate of an infection can be thought as the expected number of cases directly generated by one case in a population where all individuals are susceptible to infection. Here, the basic reproduction number, 'R_0' is calculated using the formula, $R_0 = \beta/(\gamma + \mu + \alpha)$, (where, '$\alpha$' represents persons who entered into the removed class and have resistance to fight against SARS-CoV-2 for a certain time, afterwards they will be considered a susceptible class) (Atkins, 2010; Tiwari, 2020; Rajesh *et al*., 2020).

The Outbreak of the Novel COVID-19 Pandemic in India

According to the report of the Hindustan Times, around 75% of the total novel COVID-19 cases in Punjab, 50% in Karnataka, 65% in Maharashtra and 75% in Uttar Pradesh were asymptomatic. Nearly 82% of the novel COVID-19 patients in Assam (reported at the time) were asymptomatic. On 20th April, 2020, the health ministry warned that 80% of all coronavirus patients were asymptomatic or showing mild symptoms. Around 80% are asymptomatic or show mild symptoms. Around 15% patients turned into severe cases and 5% cases turned into critical cases (India Today, 2020a; Mackolil and Mahanthesh, 2020; Bhola *et al*., 2020). As '*p*' represents the symptomatic class and '(1-*p*)' represents the asymptomatic class, therefore, we consider $p = 0.2$ as 80% cases are asymptomatic).

There is a period between which a person gets infected and is confirmed positive. Hence, the total number of infected people is greater than the total number of confirmed positives in an exponential growth phase and the total number of infected people is close to the total number of confirmed cases when the growth is halted. This is the reason many developed countries failed to halt the growth of the virus in the exponential phase. The incubation period for the novel COVID-19, which is the time between exposure to the virus (becoming infected) and symptom onset, is on average 5-6 days, however can be up to 14 days. Although the overall fatality rate is estimated to range from 2-3%, the disease can be fatal to elderly people (about 27%) whose age is more than 60 and those with an underlying medical history (Gupta and Kanu, 2020; Atkins, 2010). We assumed that the recovery rate 'γ' would remain constant for the Indian population around 0.1.

In Table 1, the contact ratio, 'β' is varied to depict the outbreak of novel COVID-19 as per the cases explored in the literature, so far for the outbreak of the novel of the COVID-19 pandemic in India (Atkins, 2010; Rihan and Anwar, 2012; Daughton *et al*., 2017; Chatterjee *et al*., 2020; Dhama *et al*., 2020). The recovery rate, 'γ' is taken constant which is around 0.1. It can be calculated by the formula (1/infectious period), the average death rate, 'μ' is taken as 0.025. The parameter '*p*' depicts the ratio of symptomatic infected to total infected and as 80% patients are asymptomatic, thus '*p*' is taken as 0.2.

Stochastic Model

The model presented here is modified with the inclusion of demographic stochasticity, which is defined as "fluctuations in population processes that arise from the random nature of events at the level of the individual". Although the probability of each event here is fixed, there is change in the outcomes because of the chance of individuals to get in contact with the infected ones. A deterministic model is the one which yields the same results under the same initial conditions. Stochastic models, on the other hand, include an element of randomness indicative of the real world. The main outcome of the analysis was to study the extinct of SARS-CoV-2 pandemic with the help of the stochastic model regardless of the value of the basic reproduction number (R_0). In the case of a very long time to extinction, the conclusion was that there may be the existence of a quasi-stationary probability distribution whose mean almost agrees with the deterministic pandemic equilibrium (when $R_0 > 1$).

Table 1: Inputs in the present investigation for the modeling of the novel COVID-19 pandemic in India

Symbols	Parameters	Values
β	Contact ratio	Varied
γ	Average recovery rate	0.100
μ	Average death rate due to the novel COVID-19	0.025
ρ	Ratio of symptomatic patients to total patients	0.200

Table 2: Data of most affected cities in India

City	Population	Active cases up to 28th July, 2020	β	γ	μ
Delhi	3,02,91,000	10,887	Varies	0.1	0.025
Pune	66,39,347	48,680	Varies	0.1	0.025
Mumbai	2,04,11,000	21,812	Varies	0.1	0.025
Chennai	1,09,7,1108	13,064 a	Varies	0.1	0.025
Ahmedabad	56,00,000	3,343	Varies	0.1	0.025

Using the modified SI_SI_NR transmission network model, we are considering five different events that can occur, each causing the numbers in the relative classes to increase or decrease by one (Gupta and Kanu, 2020; Atkins, 2010; Rihan and Anwar, 2012; Daughton *et al*., 2017; Chatterjee *et al*., 2020):

- Transmission occurs at rate $\beta Sp(I_S + I_S)/N$; Result $S \rightarrow S$-1and $I \rightarrow I$ +1
- Transmission occurs at rate $\beta S(1\text{-}p)(I + I)/N$; Result $S \rightarrow S$-1 and $I \rightarrow I$ +1
- Recovery occurs at rate γI_S; Result $I_S \rightarrow I_S$-1 and $R \rightarrow R$ +1
- Death occurs at rate μI_S; Result $I \rightarrow I$-1
- Recovery occurs at rate γI; Results $I_N \rightarrow I_N$-1 and $R \rightarrow R$ +1

As the transmission occurs at the rate $\beta Sp(I_S + I_N)/N$, initially, which results into $S \rightarrow S$-1 and $I \rightarrow I$ +1, one person gets removed from the group of susceptible and gets added to the group of infected ones. The same process is repeated when the transmissions occur at the rate $\beta S(1\text{-}p)(I + I)/N$. In case of the recovery rate γI_S (symptomatic as well as asymptomatic), one person is reduced from the group of infected group and gets added to the group of recovered ones. In case of death rate μI_S, one person gets reduced from the group of individuals of infected class and dies (Atkins, 2010). The following data were used as inputs to model the outbreak of the novel COVID-19 pandemic in various cities in India, stochastically.

Table 2 depicts the population and active cases of the most affected cities in India which includes Delhi, Pune, Mumbai, Chennai and Ahmedabad. Here, the value of contact ratio 'β' is varied to predict the outbreak of novel COVID-19 under different scenarios. We have plotted the outbreak of SARS-CoV-2 pandemic for the range of values of the basic reproduction number, 'R_0', from 1.25, 1.5, 2.0, 2.5 and 3.0 based on the values of contact ratio 'β' (Atkins, 2010; Rihan and Anwar, 2012; Dhama *et al*., 2020; Mandal *et al*., 2020) using the modified SI_SI_NR transmission network model to study the outbreak of the pandemic in-depth. The average recovery rate 'γ' is calculated to be 0.1 (1/infectious period). The average death rate 'μ' is taken as 0.025.

Validation of the Present Stochastic and Deterministic Models based on Modified SI_SI_NR Transmission Network Model with Datasets of Meningitis Epidemic Outbreak in University of Central Florida (UCF) Campus

Table 3 represents the values for the parameters which were used to plot the validation graphs. It contains the values of variables which include probability of transmission of infection, vaccination trial, contact rate and reproduction rate. The values of probability of transmission (q) of SARS-CoV-2 pandemic for four different models such as base, education, vaccination and education and vaccination models (Appendix B) are discussed herewith as per the meningitis outbreak case study (Atkins, 2010) to prove the efficacy of the present stochastic and deterministic MATLAB programs based on the modified SI_SI_NR transmission network model. As people get knowledge and awareness about protecting themselves from the infection, the contact ratio as well as the reproduction rate goes on reducing (Atkins, 2010).

Validation of the Stochastic Model

For small populations, a stochastic model may be more appropriate. In such a case, the stochastic model, which is concerned with mimicking the random or probabilistic event, would be more suitable.

In the stochastic model (Fig. 6), there are three curves which include: Number of susceptible (blue), number of infected (red) and number of recovered (yellow) plotted against the time (days). The curve for the susceptible cases here showed the number of susceptible around 50,000, which is the population of the University of Central

Florida campus (Atkins, 2010). The curve here depicts that the number of susceptible will reach to zero in a week. The second curve plotted (red) shows the number of infected ones. It depicts the number of infected cases which starts increasing from the fourth day of the spread of meningitis infection with probably 2,000 people getting infected. The number will rise till the sixth day with near about 4,800 people getting infected. Till the end of the second week of spread of infection, the number of people getting infected will start reducing and move towards the normal condition. The last curve (yellow) here shows the number of people in the campus who were recovered from the infection. The recovery of the infected started from the first week of infection spread. Till the end of the first week, almost 2,000 people got recovered from the infection. Later on, by the end of the second week, almost 4,000 people were recovered. By the end of month more than 5,000 people were recovered (Gupta and Kanu, 2020; Atkins, 2010). The present stochastic MATLAB programs based on the modified SI_SI_NR transmission network model are validated well under all three cases using the similar inputs for the meningitis outbreak case.

Validation of the Deterministic Model

In a deterministic model, the same results are observed for the same initial conditions every time. On the other hand, some randomness is always included in the stochastic model which depicts the real world situation. In Figs. 7-10, the deterministic curves represent the number of infected people versus the time (days). The blue-coloured curves plotted by (Atkins, 2010), are superimposed by the pink-coloured curves using the present deterministic MATLAB program based on the modified SI_SI_NR transmission network model.

Validation of the base Model

Here, the graph shows that if the infection continues to spread without any education or vaccination program, then by the end of the first week almost 4,000 people would be infected in a rapid manner. Later on, the number of infected persons will go on reducing almost after a week with 500 infected cases. Furthermore, by the end of the month, the situation in the university will be back to normal (Atkins, 2010).

Validation of the Education Model

In the model, the infection will start rising from the end of the first week with almost 200 people getting infected. The model depicts that if people were made aware about the spread of infection in the campus of university from the beginning itself, the overall growth of the infection could be definitely lowered.

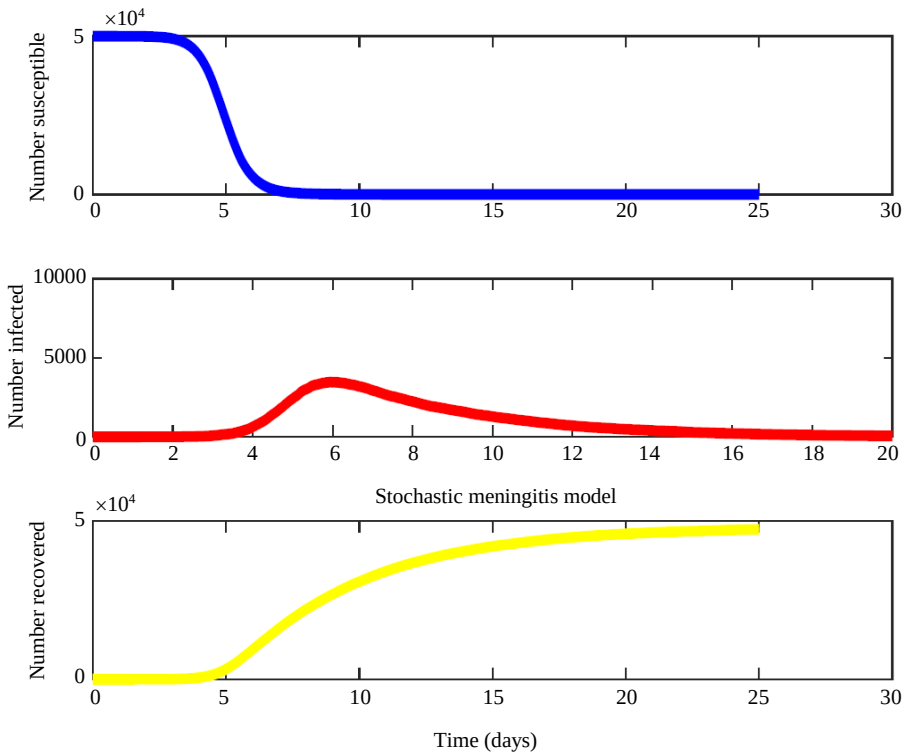

Fig. 6: Stochastic model for meningitis outbreak in University of Central Florida (UCF) campus

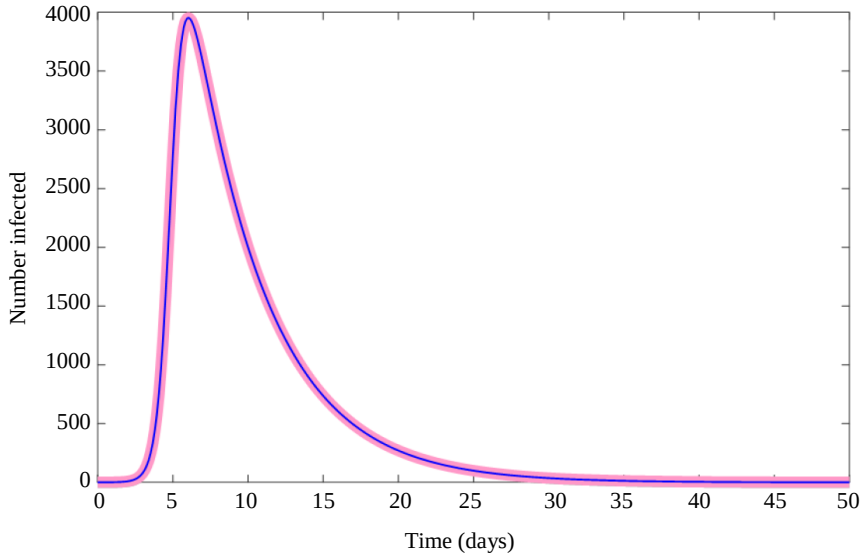

Fig. 7: Deterministic (base) model for meningitis outbreak in University of Central Florida (UCF) campus

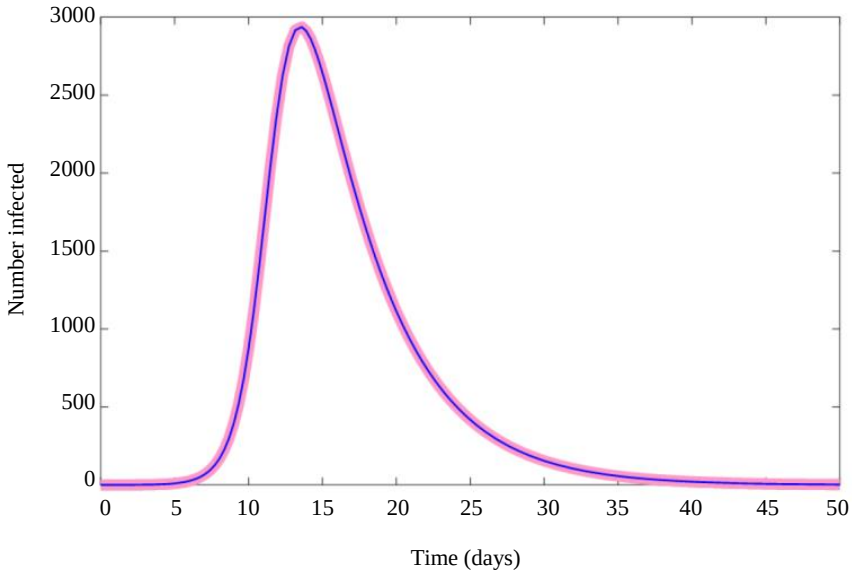

Fig. 8: Deterministic (education) model for meningitis outbreak in University of Central Florida (UCF) campus

Table 3: Parameters for the study of an outbreak of meningitis epidemic in University of Central Florida (UCF) campus

Parameters	Variable	Base model	Education model	Vaccination model	Education and Vaccination model
Probability of transmission of infection	q	0.10	0.05	0.1	0.05
Number of peoples vaccinated	v_0	0.00	10.00	51%	61%
Calculated contact ratio	β	2.34	1.05	1.15	0.46
Basic reproduction rate	R_0	7.80	3.50	3.8	1.5

As shown by the curve till the end of the second week, the maximum number of people will get infected. Almost 3,000 people will get infected by the end of the second week. Later on, the number of infected people will go on decreasing due to awareness about the prevention of the infectious disease. By the end of month the number of infected people will be lowered and the situation will be back to normal (Atkins, 2010).

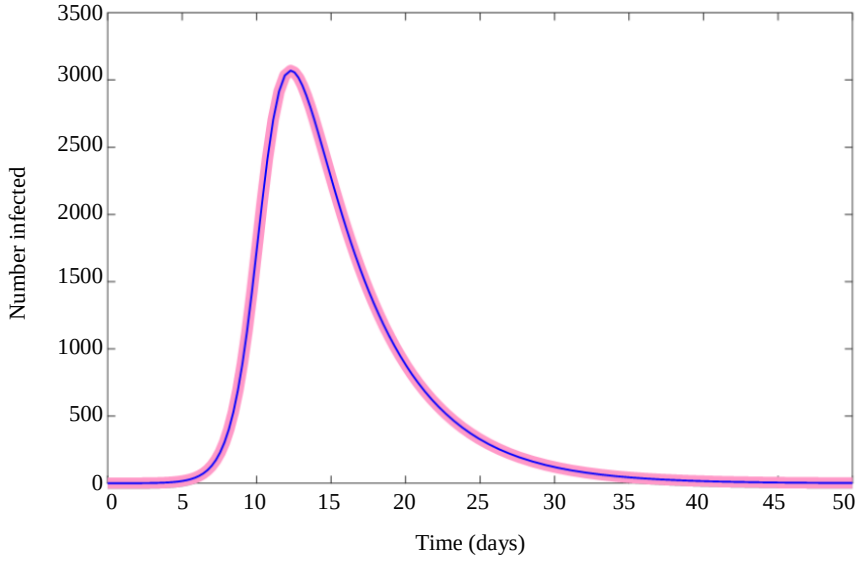

Fig. 9: Deterministic (vaccination) model for meningitis outbreak in University of Central Florida (UCF) campus

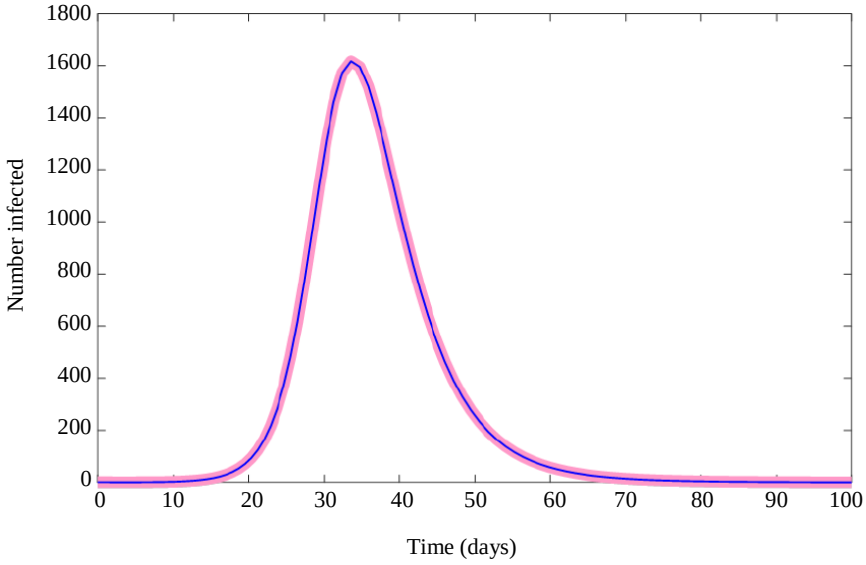

Fig. 10: Deterministic (education and vaccination) model for meningitis outbreak in University of Central Florida (UCF) campus

Validation of the Vaccination Model

The model depicted that the number of infected people will start rising by the end of the first week of infection with almost 100 cases.

As shown in Table 3, there would be 51% of people vaccinated, which resulted in the lower number of cases, i.e., around 3,000 (maximum) cases of infection by the second week. The number of people getting infected will start reducing by the second week of infection. By the end of the month, this situation will turn out to be normal (Atkins, 2010).

Validation of the Education and Vaccination Model

The model shows the result of the combined education and vaccination model. As shown in Table 3, there would be around 61% of people who will be aware about the preventive measures and would be vaccinated as well.

This will ultimately lower the number of maximum people getting infected and then it would be around 600 (maximum) cases of infection after almost 40 days. The rise in the number of infected people in this model will start late as compared to other models. By the third week, there would be almost 50 people getting infected.

After almost 40 days, the number of infected people will start lowering. Later on, after 3 months, the situation may be back to normal (Atkins, 2010).

Results

Deterministic Susceptible (S)-Infected (Symptomatic) (I_S) Infected (Asymptomatic) (I_N) Recovered (R) i.e., SI_SI_NR Models for Modeling and Simulation of the Outbreak of Novel Coronavirus Diseases (COVID-19) in India

In the present investigation, the basic reproduction number, 'R_0', are calculated using different values of contact rates, β, based on the novel deterministic susceptible (S)-infected (symptomatic) (I_S) infected (asymptomatic) (I_N) recovered (R) approach to discuss the transmission of the novel COVID-19 outbreak. A suitable computer routine is developed in MATLAB based on Ordinary Differential Equations (ODEs) in conjunction with Runge-Kutta method with a variable time step for efficient simulation of the growth of SARS-CoV-2 under control and prevention strategy program in India. The deterministic model is further classified into three submodels such as (a) base model, q = 0.1, (b) education model, q = 0.05, (c) education and vaccination model q = 0.1 for in-depth analysis of the outbreak of the pandemic (Atkins, 2010; Rihan and Anwar, 2012; Dhama *et al*., 2020; Mandal *et al*., 2020).

The spread of the novel COVID-19 pandemic is plotted for entire nation (Fig. 11). The graph, infected cases versus time (days) is plotted for SARS-CoV-2 outbreak to predict its behavior in due course of time. The mitigatory measures such as strict lockdown and partial lockdown across the nation are responsible to restrict the spread of pandemic. According to the graph the pandemic is approximately expected to end after 300 days from present day, i.e., 28th July, 2020. In Fig. 11, the 'R_0' is calculated around 1.25 following the deterministic strategies for entire India. The symptomatic cases are found to be around 80% less than asymptomatic cases (Atkins, 2010; Rihan and Anwar, 2012; Mandal *et al*., 2020). The suitable graph has been plotted on the basis of values of 'R_0' using deterministic mathematical models based on the modified SI_SI_NR transmission network model. The peaks of infected cases (both symptomatic and asymptomatic cases) as well as end of SARS-CoV-2 pandemic are estimated soon after 31st July, 2020 in the month of December, 2020 (Fig. 11) and by the end of March, 2021, respectively.

Impact of Community Transmission Phase of SARS-CoV-2 in India

As per the joint statement by Indian medical professional associations, nonuniform and rational strategies of lockdown across the nation such as movement of migrant workers, social gathering unlock 1.0 and 2.0, etc., resulted in community spread of the novel COVID-19 disease. India must be well equipped to counter the probability of community transmission of the COVID-19. Easing of lockdown will lead to more widespread and rapid transmission of coronavirus. Some of the experts suggested that India has already entered the community (Gupta and Kanu, 2020) transmission through the stage III of the novel COVID-19. As if one looks at the spread of people without a history of travel or history of contact, certainly there are several such cases.

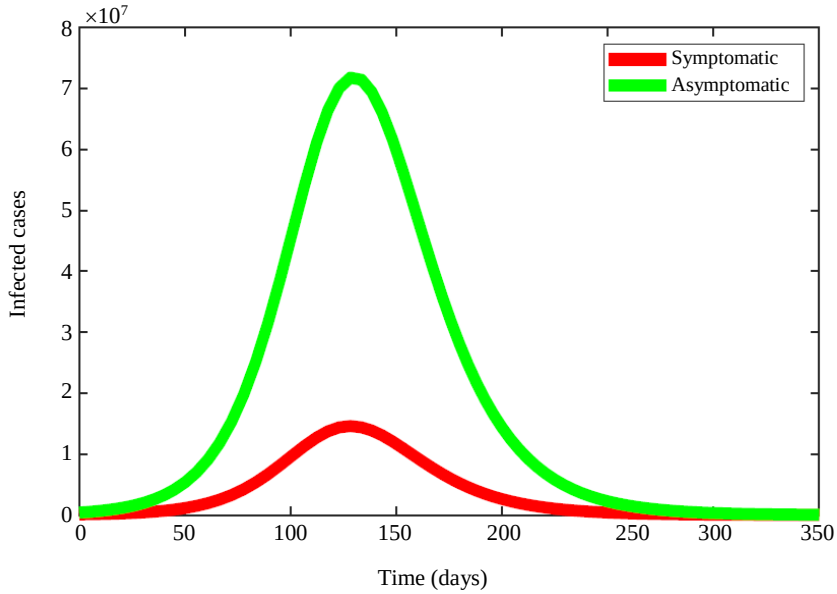

Fig. 11: Graphical simulation of the novel COVID-19 outbreak. Base model yields R_0 = 1.25 using β = 0.15625

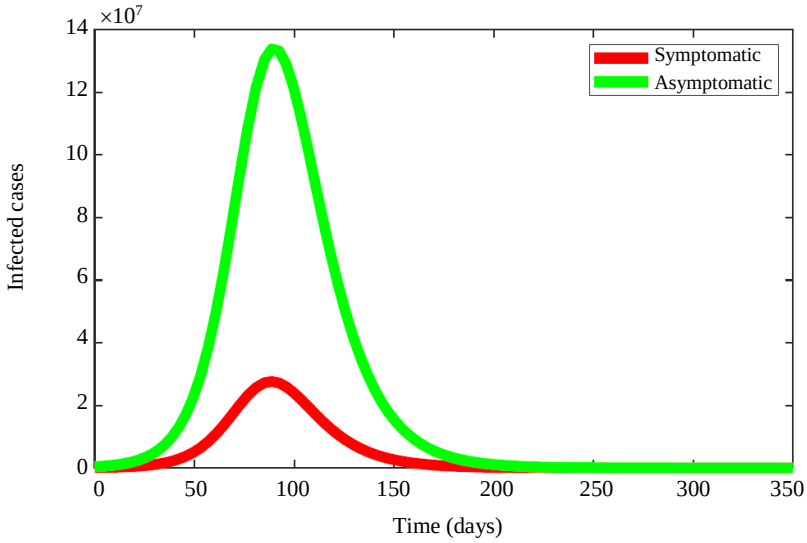

Fig. 12: Graphical simulation of the novel COVID-19 outbreak. Base model yields R_0 = 1.5 using β = 0.1875

Furthermore, governmental action and some misuse of mitigatory measures have influenced the spread of the pandemic (Fig. 12). As per the data reported in some published sources; the pandemic is modeled with the basic reproduction number, 'R_0', to validate the novel deterministic modeling approach of SARS-CoV-2 pandemic. The pandemic is predicted to end after 250 days from the present day, i.e., 28th July, 2020, using the current value of β = 0.1875. In Fig. 12, the 'R_0' is calculated around 1.5 following the deterministic strategies for the entire India (Atkins, 2010; Rihan and Anwar, 2012; Chang *et al*., 2020).

Social distancing is the only proven solution for halting corona virus growth as of now. Nation practices strict social distancing in the lockdown, but still due to several factors, we see failures in some lockdowns. Here 'β' is the transmission rate and 'γ' is the average recovery rate. With quarantine and isolation, the increasing number of infected slowly became constant. In the context of India, this model may be useful as a rigorous social distancing measure has been introduced and hence does not consider factors like age, etc. The parameter, 'β' governs the transmission efficiency of the virus in society, since lockdowns and social distancing measures focus on reducing the transmission, reduction in 'β' in different stages will reflect how better the lockdown was performed. The mitigatory measures imposed by Indian government have influenced the spread of pandemic (Fig. 13). With the further change in parameters such as contact rate, 'β' reported in some published sources, the pandemic is modeled for the basic reproduction number, 'R_0', to throw light on the novel deterministic modeling approach of SARS-CoV-2 pandemic. The pandemic is predicted to end after 200 days from the present day, i.e., 28th July, 2020, using the current value of β = 0.25. In Fig. 13, the 'R_0' is calculated around 2.0 following the deterministic strategies for the entire nation (Atkins, 2010; Rihan and Anwar, 2012; Sahasranaman and Kumar, 2020; Dhanwant and Ramanathan, 2020).

The testing of novel COVID-19 is essential in the direction of containing the spread of virus. The delays in testing may seriously reduce the ability of the population to protect it. The testing for the novel COVID-19 virus in India was inadequately conducted in the beginning, which might have not generated sufficient data on the number of people affected. Initially, only persons with a travel history to high risk countries were tested. Therefore, this case can be varied with different values of contact rate, β, as reported in some published sources; the pandemic is modeled for the basic reproduction number, 'R_0', to observe the transmission of the novel COVID-19 pandemic using the novel deterministic approach to prove the efficacy of the present model (Fig. 14).

The pandemic is predicted to end after 150 days from the present day, i.e., 28th July, 2020, using the current value of β = 0.3125. In Fig. 14, the 'R_0' is calculated around 2.5 following the deterministic strategies for the entire India (Atkins, 2010; India Today. 2020a).

As of 14th March, 2020, the National Institute of Virology, Pune, has tested around 5,900 samples from individuals across the country, which was quite low compared to other countries. It was also felt that community transmission may go undetected without adequate testing. Testing for community transmission began on 15th March, 2020. The Department of Health Research and the Indian Council of Medical Research (DHR-ICMR) have started testing random samples of people who exhibit flu-like symptoms and samples from

patients without any travel history or contact with infected persons. Later on, it was also decided to include all pneumonia cases, regardless of travel or contact history after the country saw a sharp increase in the number of cases. The ICMR further revised the testing strategy and allowed testing of people showing symptoms for a week in the hotspot areas of the country, regardless of travel history or local contact to the patient. Total 25,12,388 samples were tested by 20th May, 2020, out of which 1,06,750 have been confirmed positive. Finally, these are discussed with the contact rate, 'β' as reported in some published sources; the pandemic is modeled for the basic reproduction number, 'R_0', to observe the transmission of the novel COVID-19 pandemic using the novel deterministic approach to prove its efficacy (Fig. 15). The pandemic is estimated to reach its end after 100 days from the present day, i.e., 28th July, 2020, using the current value of $\beta = 0.375$. In Fig. 15, the 'R_0' is calculated around 3.0 following the deterministic strategies for the entire India (India Today, 2020a; Atkins, 2010; Rihan and Anwar, 2012; Ramola, 2020; The Times of India, 2020a).

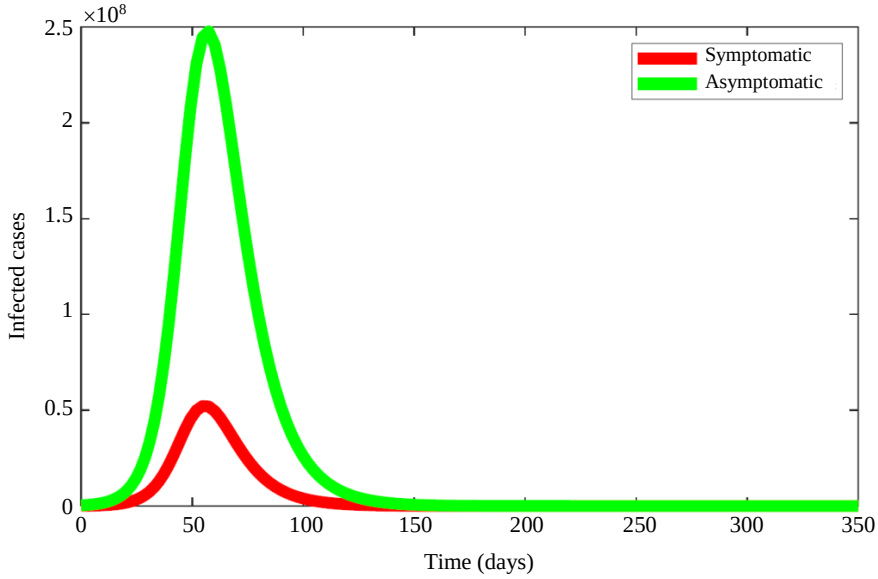

Fig. 13: Graphical simulation of the novel COVID-19 outbreak. Base model yields $R_0 = 2.0$ using $\beta = 0.25$

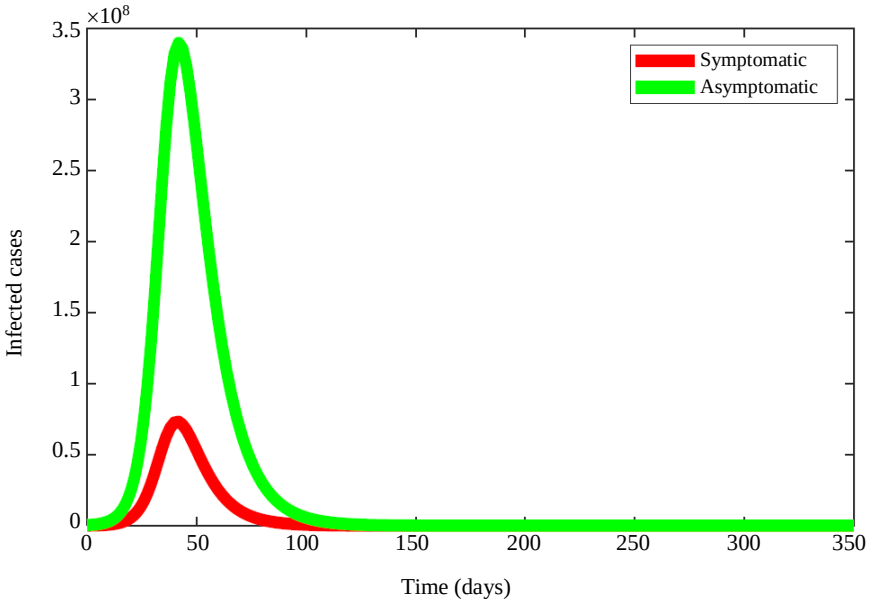

Fig. 14: Graphical simulation of the novel COVID-19 outbreak. Base model yields $R_0 = 2.5$ using $\beta = 0.3125$

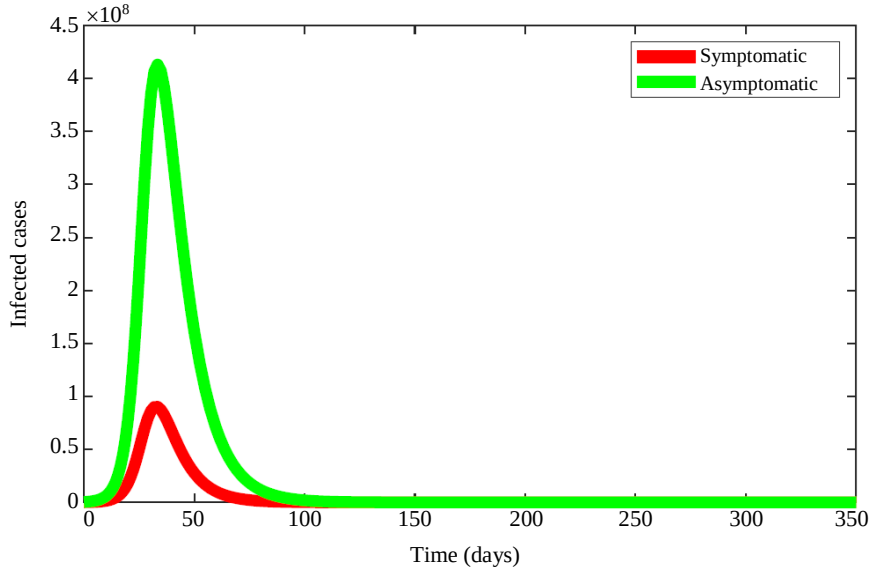

Fig. 15: Graphical simulation of the novel COVID-19 outbreak. Base model yields $R_0 = 3.0$ using $\beta = 0.375$

A mean is a number that in some sense represents the central value of a set of numbers. Mathematical average of two or more numbers is called as mean. There are many ways to compute the mean of a series of numbers. We use the sum of the given numbers in the arithmetic mean method. Geometric mean is computed by the average of a set of products. The arithmetic mean which is also called as mean or average that was found by summing the numbers in the data and dividing that sum by the number of count. Generally, the data is the result from an observational study, experiment or a survey (Wikipedia, 2020b).

In the above graphs, the outbreak of the novel COVID-19 pandemic is plotted for different values of R_0 = 1.25, 1.5, 2.0, 2.5 and 3.0. The outbreak of the novel COVID-19 pandemic is also plotted for the mean value of the above 'R_0'. In Fig. 16, the mean 'R_0' was found to be 2.05 and the corresponding 'β ' was found to be 0.25625. Furthermore, 'R_0' does not remain constant for SARS-CoV-2 pandemic. Its value depends upon many factors such as environmental conditions; frequency of contact between the infected and susceptible individuals, measures taken to contain the spread, etc. The pandemic is predicted to end after 125 days from the present day, i.e., 28th July, 2020, using the current value of $\beta = 0.25625$. The value of 'R_0' focuses light on the dynamics of the spread of disease. The mathematical models are used to determine the value of 'R_0' which also depends upon the other parameters used in mathematical modeling. Many popular presses have used 'R_0' which gave rise to misunderstandings related to its true meaning. Various mathematical models are used to calculate the value of 'R_0'. Each of these models may give a different estimate the value of 'R_0'. These values should be interpreted in the context of that model.

The value of 'R_0' can be used as a threshold, even if calculated with different methods. Whether the outbreak will die out or whether it will increase can be guessed using this number. If $R_0 < 1$, the outbreak will die out and if $R_0 > 1$, the outbreak will expand. In some cases, for some models, values of $R_0 < 1$ can still lead to self-perpetuating outbreaks. This is particularly problematic if there are intermediate vectors between hosts, such as malaria. Therefore, comparisons between values from the "Values of 'R_0' of well-known infectious diseases" table should be conducted with caution (Wikipedia, 2020b).

Education Model

A program including education would reduce the probability of transmitting an infection by half by increasing the awareness of people regarding maintaining social contact and improving personal hygiene.

We have not considered the vaccination but due to increased awareness between people, it would eventually give an effect of increased rate of vaccination to 10%. Fear of the novel COVID-19 has the country under its grip. Many state governments have ordered the closure of schools and colleges, movie halls, gyms, malls, etc. Air traffic has fallen, which is indicative of reduced economic activity. Many such happenings and signs of destructive effects of the novel COVID-19 have a direct effect on the behaviour of every citizen. People have become more aware about this virus and its spread. People are finding and comprehending the ways which will protect themselves and their families from the impact of this virus

(News18, 2020). We have plotted the graph from 15th June, 2021 onwards considering the value of 'β' to be 0.128125 (Fig. 17). The pandemic is predicted to end after 700 days from the present day, i.e., 28th July, 2020.

The Government of India managed to quickly spread the awareness regarding this virus by using every possible mode of communication. Ringtones were applied to spread the awareness regarding this virus and how to contain its spread. Observing the impact of this virus in other countries, containment was the only option. Passengers coming from abroad were screened for infection. Combating other weapons which helped in fighting the spread of this virus are building infrastructure for the infected patients, increasing the testing facilities and screening people who possibly may have come in contact with the infected individual. To maintain the confidence of people in the system, it is necessary to ensure that the supply of masks, sanitizers and drugs is available to each one (Atkins, 2010; Rihan and Anwar, 2012; News18, 2020; BBC News, 2020b).

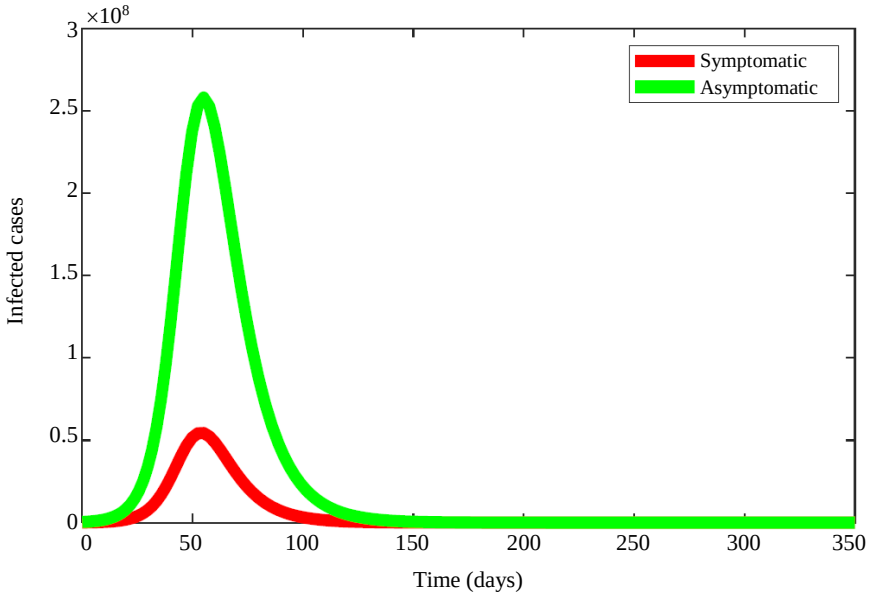

Fig. 16: Graphical simulation of the novel COVID-19 outbreak. Base model yields R_0 = 2.05 using β = 0.25625

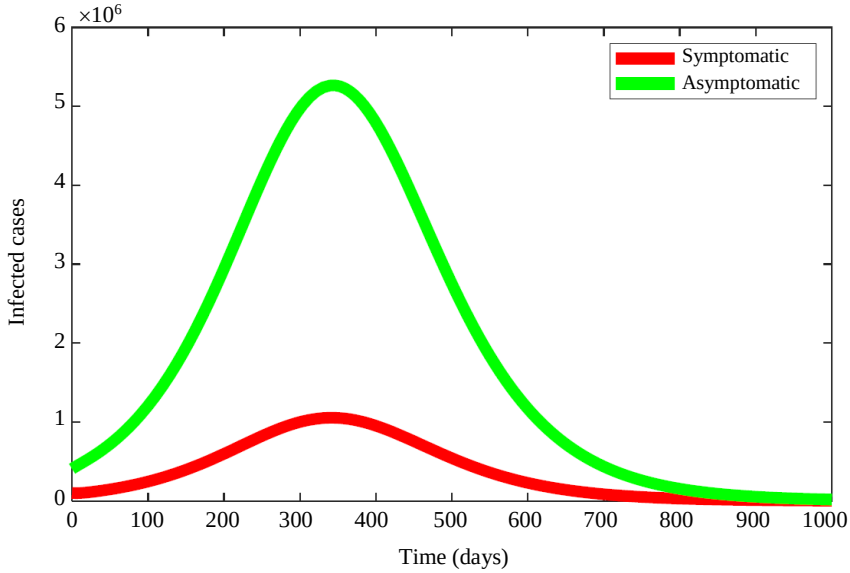

Fig. 17: Graphical simulation of the novel COVID-19 outbreak. Education model yields R_0 = 1.025 using β = 0.128125

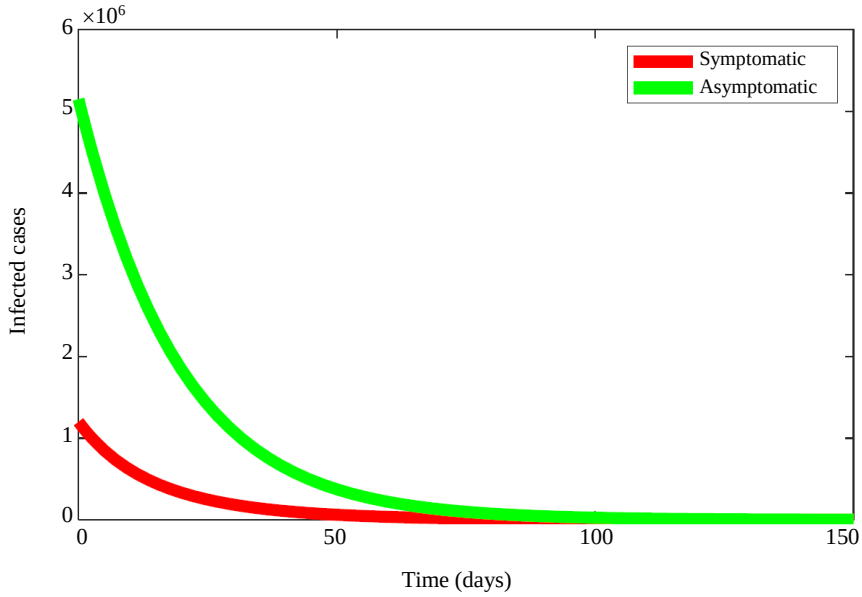

Fig. 18: Graphical simulation of the novel COVID-19 outbreak. Education and vaccination model yields R_0 = 1.025 Assuming 61% of the population is vaccinated

Education and Vaccination Model

Generally, a vaccine may take years to develop. According to the experts, we can expect the vaccine to be available by the end of February, 2021. We have assumed that 61% of the population of India would be vaccinated up to 15th June, 2021. Therefore, we have plotted the graph from 15th June, 2021and onwards considering the value of 'β ' to be 0.128125 (Fig. 18). The pandemic is predicted to end after 100 days from 15th June, 2021. The parameter, 'V_0' was considered 8,28,584,757. Research on the vaccine for the novel COVID-19 is happening at breakneck speed. At present, around 140 vaccines are in their early stage of development and about 24 numbers of vaccines are in their clinical trials on people. The vaccine developed by Oxford University is reported to trigger the immunity system to respond against the virus. According to the deal signed with AstraZeneca, 100 million doses will be supplied in the UK alone. A study performed in May in the United States of America resulted in the production of antibodies that could neutralize the novel COVID-19 in every eight patients taking part in the study. Other completely new approaches to vaccine development are in human trials (Ranjan, 2020).

Many research groups have designed the vaccine that has the potential to fight the novel COVID-19, but still a lot of work is left to do. These researchers must show that their vaccine is safe to be injected in the body. The vaccine should cause an immune response, which will work as a shield to the people and prevent them from getting sick. Furthermore, the vaccine should be able to be produced on a large scale so that billions of doses can be developed. The medicine regulatory frame must approve it before it is actually provided to the population. At last, the most difficult challenge is to immunize the world's population at a substantial scale (Atkins, 2010; The Times of India, 2020a; Deb and Majumdar, 2020).

City Wise Discussion on Transmission of the Novel Coronavirus Disease (COVID-19) Pandemic in India using Stochastic Susceptible (S)-Infected (Symptomatic) (I_S) Infected (Asymptomatic) (I_N) Recovered (R) (SI_SI_NR) Model

Stochastic Model Forecasting the Outbreak of the Novel COVID-19 in Delhi

The first case of the novel COVID-19 pandemic in the Indian capital, Delhi, was reported on 02nd March, 2020. Delhi has the third highest number of confirmed cases of the novel COVID-19 pandemic in India after Maharashtra and Tamil Nadu. The total 1,34,403 infected people were reported on 31st July, 2020, including 3,936 deaths and 1,19,724 recovered patients. On 22nd March, 2020, Delhi observed a 14 h voluntary public curfew named Janata curfew along with 75 districts in India at the directive from Honourable Prime Minister of India, prior to his order of nationwide lockdown from 24th March, 2020. Thousands of migrants from Uttar Pradesh and Bihar gathered at the bus stand and railway station to head back to their native places. More than 3,000 people from a social gathering were quarantined after

suspected contact with infected people, including foreigners. The Delhi government announced an operation known as SHIELD, i.e., **S**-sealing the area immediately, **H**-home quarantine to the people living in the area, **I** refers to isolation and contact tracing of people, **E** refers to essential supply of commodities, **L** refers to local sanitization and **D**-door to door health check upon order to restrict the spread of the novel COVID-19 pandemic in the containment zones or the hotspots around the state (Business Today, 2020).

The novel COVID-19 pandemic was widely spread in Dilshad Garden, from where the first success came. On 10th April, the government announced that Operation SHIELD was working quite successfully. This area became the novel COVID-19 free after implementation of the SHIELD operation. This operation also emerged successful in Vasundhara Enclave and Khichripur (The Times of India, 2020b; Wikipedia, 2020c).

An order was issued making 7 days home quarantine compulsory for all asymptomatic individuals who travelled into the city through domestic transport. Individuals who showed symptoms were immediately tested for the novel COVID-19 and were quarantined at the institutional level till the results were declared. If persons were found positive, they were moved to a hospital or any novel COVID-19 Care Centre. If they were found negative, they were instructed to follow the 14 days home quarantine. The details on containment zones and hotspots, testing facilities, key locations, e-pass procurement and relevant frequently asked questions were posted on this website. The information also included the locations of grocery shops, temporary relief centres and hunger relief centres in Delhi. On 24th June, 2020, the Delhi government set up the world's largest temporary novel COVID-19 care hospital of 10,000 beds, as the country grapples with rapidly rising cases (Wikipedia, 2020c).

The value of 'R_0' focuses light on the dynamics of the spread of disease and thus suitable graphs have been plotted using the above inputs to discuss the spread of the novel COVID-19 pandemic in the National Capital Region of Delhi (Fig. 19) using stochastic mathematical models based on the modified SI_SI_NR transmission network model. With an increase in the values of 'β' and thus 'R_0', the peaks of infected cases (both symptomatic and asymptomatic cases) as well as the end of SARS-CoV-2 pandemic are attended soon after 31st July, 2020 as discussed in Fig. 19. The first case (β = 0.15625; R_0 = 1.25) is more appropriate as it shows the peak of the novel COVID-19 pandemic in December, 2020 (Fig. 19a). The curve shows the zero case of pandemic by the end of March, 2021.

Stochastic Model Forecasting the Outbreak of the Novel COVID-19 in Pune

On 09th March, 2020, a couple who arrived in India from Dubai were tested positive for the novel COVID-19 and were the first confirmed case from Maharashtra. Three more people who were in contact with this couple were also tested positive on the next day. All five of them were taking treatment in Naidu Hospital. After 9 days on 18th March, 2020, the woman was tested positive in Pune. This woman had earlier travelled to France and Netherlands. An old woman who was in her late 60's was linked with a confirmed case also tested positive. The number of positive cases rose to 45 after cases were found in Pimpri-Chinchawad and Ratnagiri. The case found in Pimpri-Chinchwad had travelled to Singapore, Philippines and Sri Lanka. The latter case from Ratnagiri earlier travelled to Dubai.

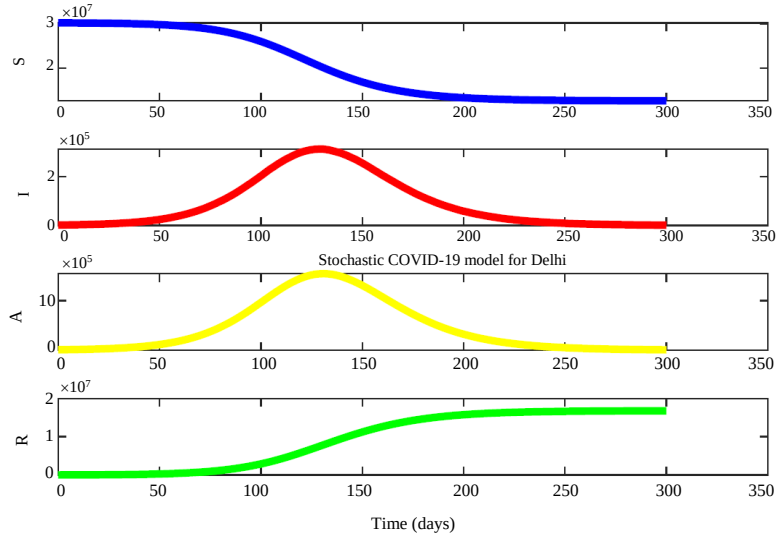

(a)

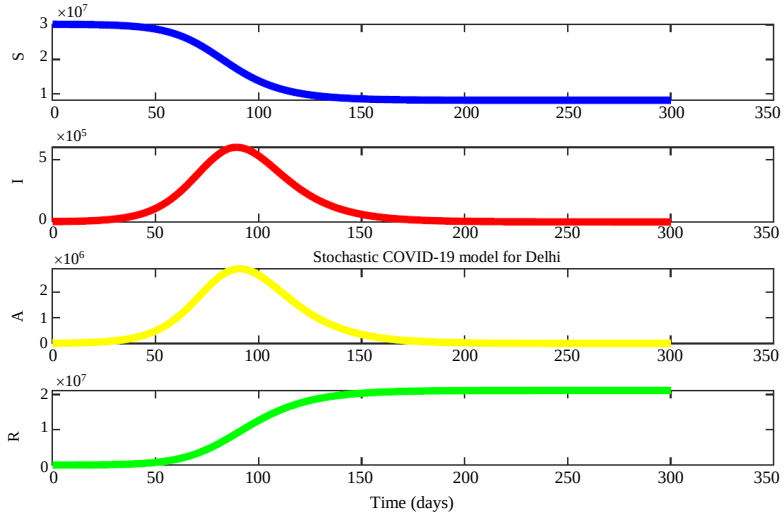
Stochastic COVID-19 model for Delhi
S
I
A
R
Time (days)

(b)

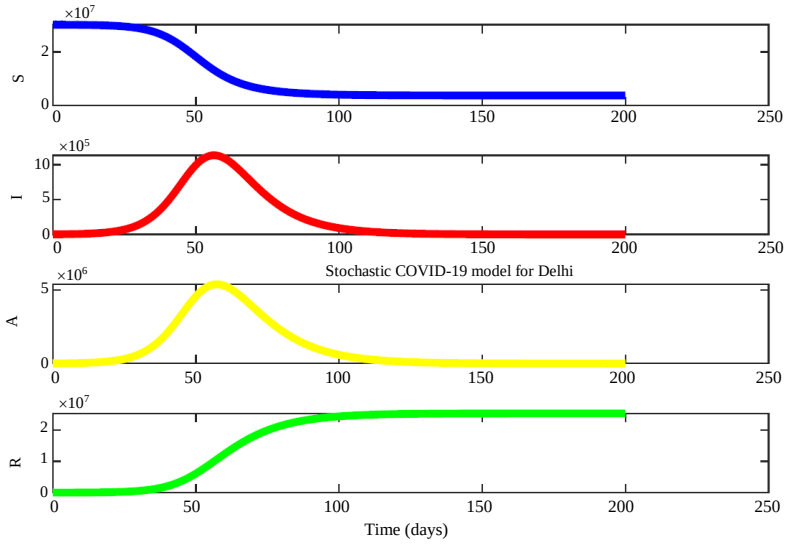
Stochastic COVID-19 model for Delhi
S
I
A
R
Time (days)

(c)

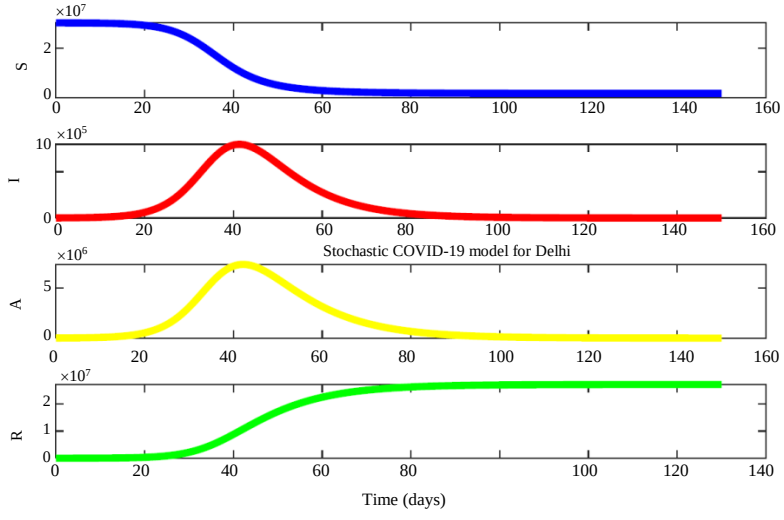
Stochastic COVID-19 model for Delhi
S
I
A
R
Time (days)

(d)

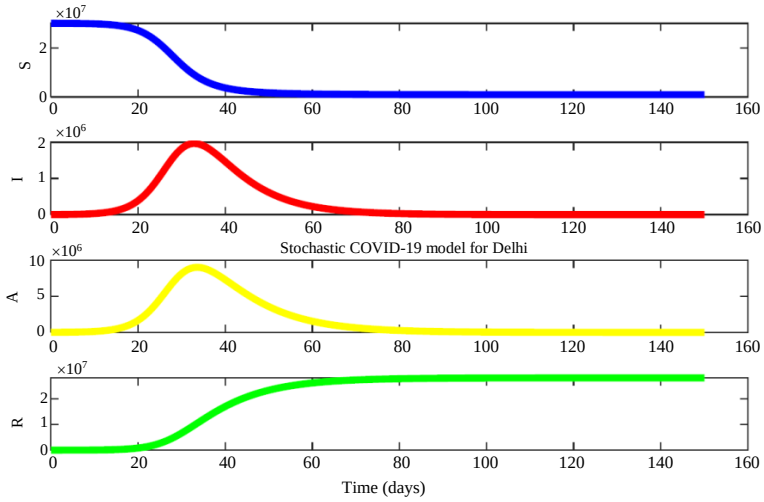

(e)

Fig. 19: The stochastic SI_SI_NR model of the novel COVID-19 for National Capital Region of Delhi considering sustained lockdown of 61 days, i.e., 25th March, 2020-31st May, 2020, unlock 0.1 and 0.2, as well as weekly lockdown in July, 2020 including night curfew and implementation of effective quarantine periods for travelers. (a) SI_SI_NR model based on the novel stochastic approach ($\beta = 0.15625$; $R_0 = 1.25$). (b) SI_SI_NR model based on the novel stochastic approach ($\beta = 0.1875$; $R_0 = 1.5$. (c) SI_SI_NR model based on the novel stochastic approach ($\beta = 0.25$; R_0 2.0). (d) SI_SI_NR model based on the novel stochastic approach ($\beta = 0.3125$; $R_0 = 2.5$). (e) SI_SI_NR model based on the novel stochastic approach ($\beta = 0.375$; $R_0 = 3.0$). Note: The parameters such as *S*, *I*, *A* and *R* are used to express susceptible, infected (symptomatic), infected (asymptomatic) and recovered patients, respectively

The population of Pune is estimated to be 6.8 million while Mumbai's population is much greater. Mumbai had the largest number of positive cases in Maharashtra as well as in India. The total positive cases in Mumbai were 84,524. On 03rd July, 2020, Pune city had 25% cases against Mumbai and a fatality rate of 3.32. Mumbai was reported to have a fatality rate 5.85% (India Today, 2020b).

Although Pune has better numbers as compared to Mumbai, it is on the same path as that of Mumbai. The total of infected people reported on 31st July, 2020 is 28,142 consisting of 872 deaths and 13,406 recoveries (The Hindustan Times, 2020a; NDTV, 2020).

As the value of 'R_0' focuses light on the dynamics of the spread of disease and thus suitable graphs have been plotted using the above inputs to discuss the spread of the novel COVID-19 pandemic in the Pune region of the Maharashtra state (Fig. 20) using stochastic mathematical models based on the modified SI_SI_NR transmission network model. Again, with an increase in the values of 'β ' and thus 'R_0', the peaks of infected cases (both symptomatic and asymptomatic cases) as well as the end of SARS-CoV-2 pandemic are attended soon after 31st July, 2020 as discussed in Fig. 20. For Pune city, the first case ($\beta = 0.15625$; $R_0 = 1.25$) is more appropriate as it shows the peak of the novel COVID-19 pandemic in December, 2020 (Fig. 20a). The curve shows the zero case of pandemic by the end of March, 2021.

Stochastic Model Forecasting the Outbreak of the Novel COVID-19 in Mumbai

Mumbai was the worst affected city in India, with about 100,000 cases. About half of the cases in the state emerged from the Mumbai Metropolitan Region (MMR). On 11th March, 2020, two people in Mumbai who were linked to the Pune couple tested positive. To prohibit the spread of coronavirus, various measures were taken by the Navi Mumbai civic body. According to the orders, roadside stores and commercial shops, outlets near public places and crowded places such as railway stations were closed on alternate days till the end of the March. Many measures to control the crowd and prohibit the spread of the coronavirus were taken by the administrative body. One of the measures to control the crowd and contain the spread of coronavirus was the order issued by the municipal commissioner to close shops, stores and roadside outlets, near footpaths and near crowded stations such as CBD Belapur, Nerul, Vashi, Sanpada, Kopar Khairane, Ghansoli and Airoli on alternate days (The Hindu, 2020a; The Hindustan Times, 2020b; Kumar, 2020).

Mumbai saw a delay in the diagnosis of the patients because the testing rate in Mumbai was low initially. Citizens wishing to be tested for the novel COVID-19 were sent back by municipal doctors. The same case was seen in Pune too. Due to the delay, the patient's condition was critical. This increased the number of serious patients and deaths.

DOI: 10.3844/ajidsp.2020.135.170

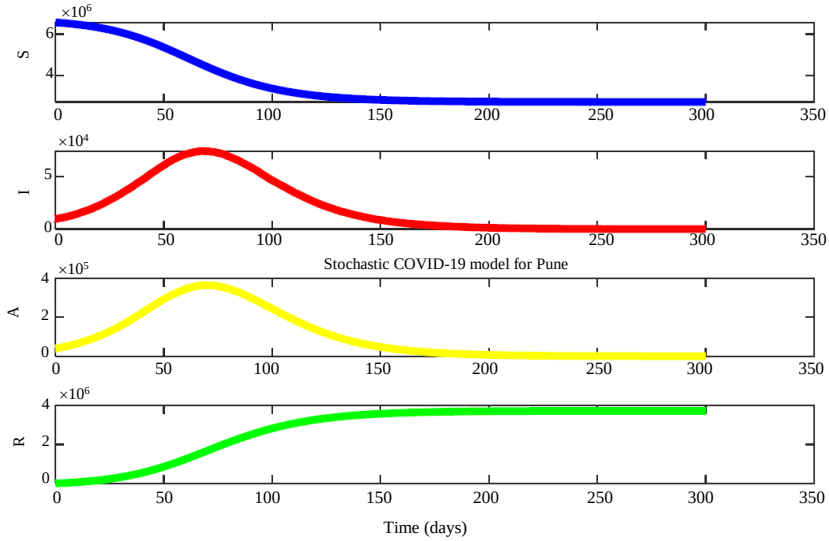

(a)

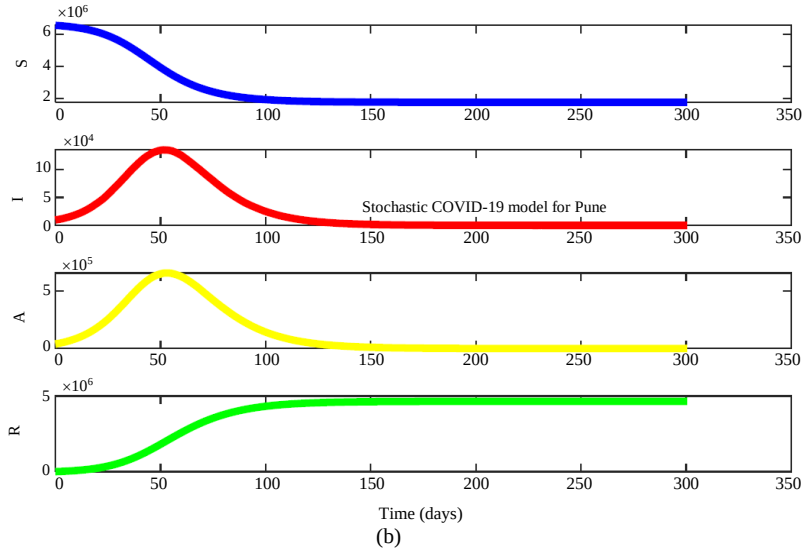

(b)

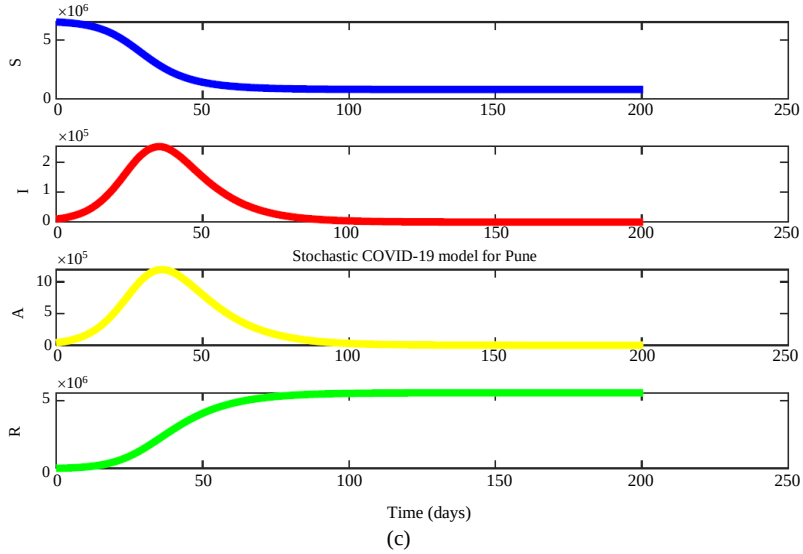

(c)

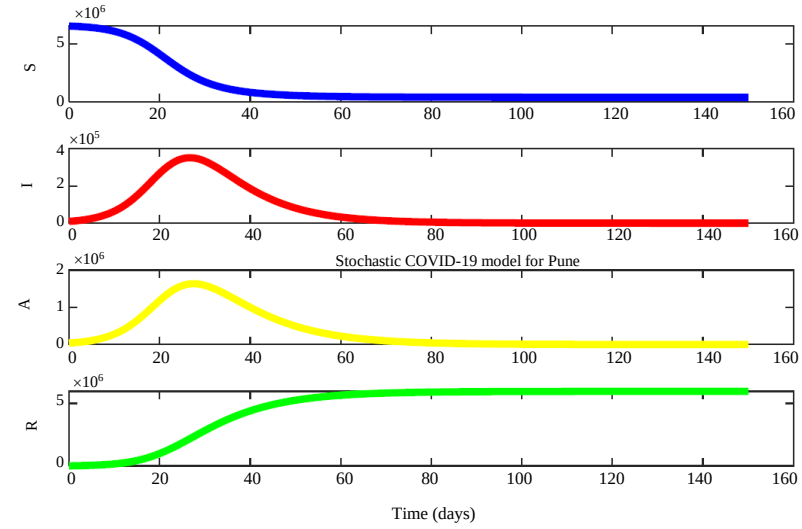

(d)

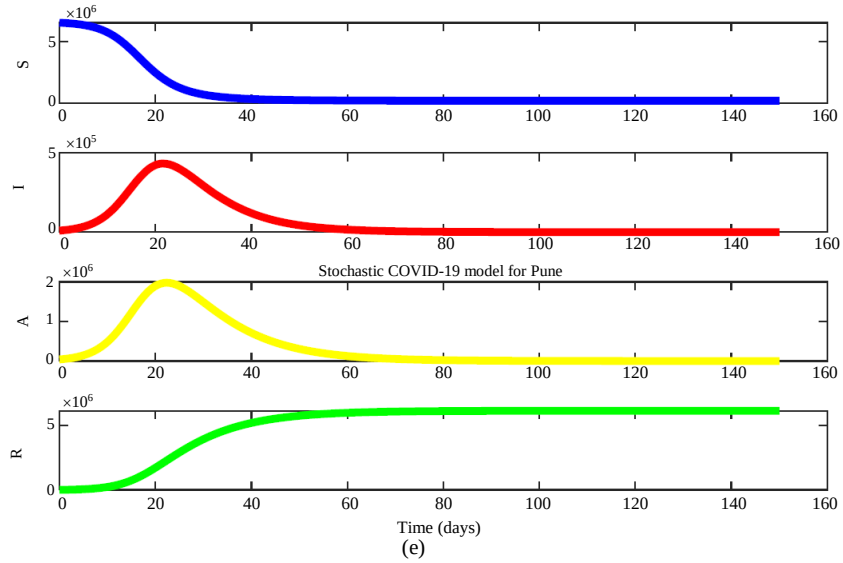

(e)

Fig. 20: The stochastic SI_SI_NR model of the novel COVID-19 for Pune considers a sustained lockdown of 61 days, i.e., 25th March, 2020-31st May, 2020, unlock 0.1 and 0.2, as well as weekly lockdown in July, 2020 including night curfew and implementation of effective quarantine periods for travelers. (a) SI_SI_NR model based on the novel stochastic approach (β = 0.15625; R_0 = 1.25). (b) SI_SI_NR model based on the novel stochastic approach (β = 0.1875; R_0 = 1.5). (c) SI_SI_NR model based on the novel stochastic approach (β = 0.25; R_0 = 2.0). (d) SI_SI_NR model based on the novel stochastic approach (β = 0.3125; R_0 = 2.5). (e) SI_SI_NR model based on the novel stochastic approach (β = 0.375; R_0 = 3.0). Note: The parameters such as *S*, *I*, *A* and *R* are used to express susceptible, infected (symptomatic), infected (asymptomatic) and recovered patients, respectively

The total of infected people reported on 31st July, 2020 is 1,14,284, consisting of 6,353 deaths. The discussion is made on the basis of the value of 'R_0' as it helps to understand the dynamics of the spread of disease and thus suitable graphs have been plotted using the above inputs to discuss the spread of the novel COVID-19 pandemic in the Mumbai region of the Maharashtra state (Fig. 21) using stochastic mathematical models based on the modified SI_SI_NR transmission network model. As discussed, with the increase in the values of 'β' and thus 'R_0', the peaks of infected cases (both symptomatic and asymptomatic cases) as well as the end of SARS-CoV-2 pandemic are attended soon after 31st July, 2020. For Mumbai city, the first case (β = 0.15625; R_0 = 1.25) is more appropriate in the current scenario as it shows the peak of the novel COVID-19 pandemic in December, 2020 (Fig. 21a). The curve shows the zero case of pandemic by the end of March, 2021.

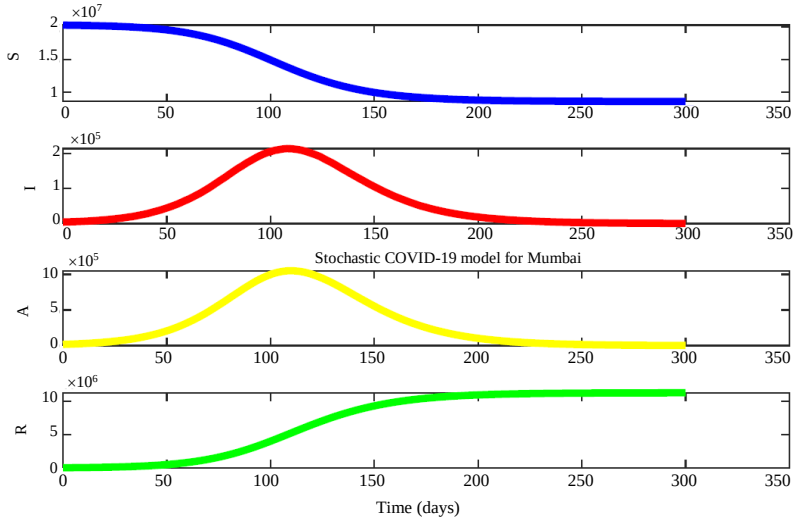
S
I
A
R
Stochastic COVID-19 model for Mumbai
Time (days)

(a)

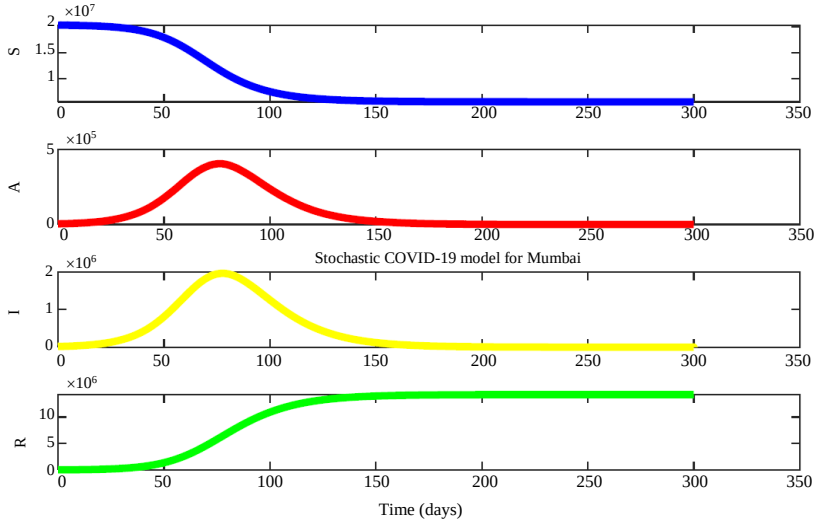
S
A
I
R
Stochastic COVID-19 model for Mumbai
Time (days)

(b)

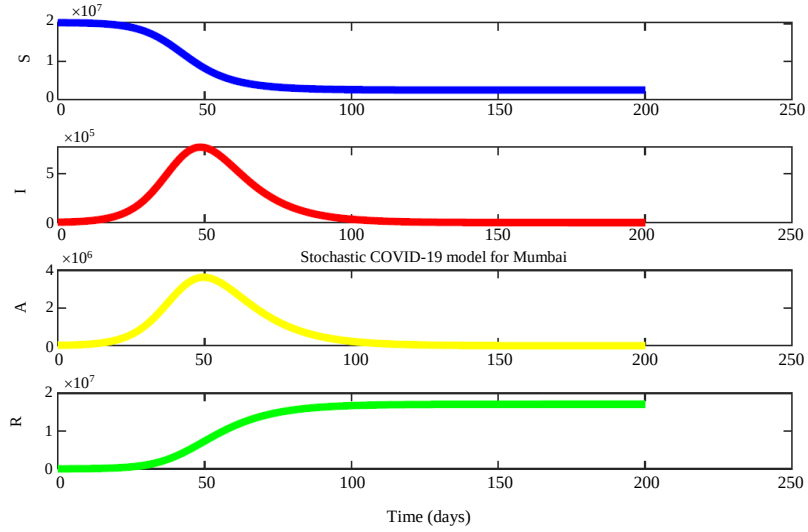
S
I
A
R
Stochastic COVID-19 model for Mumbai
Time (days)

(c)

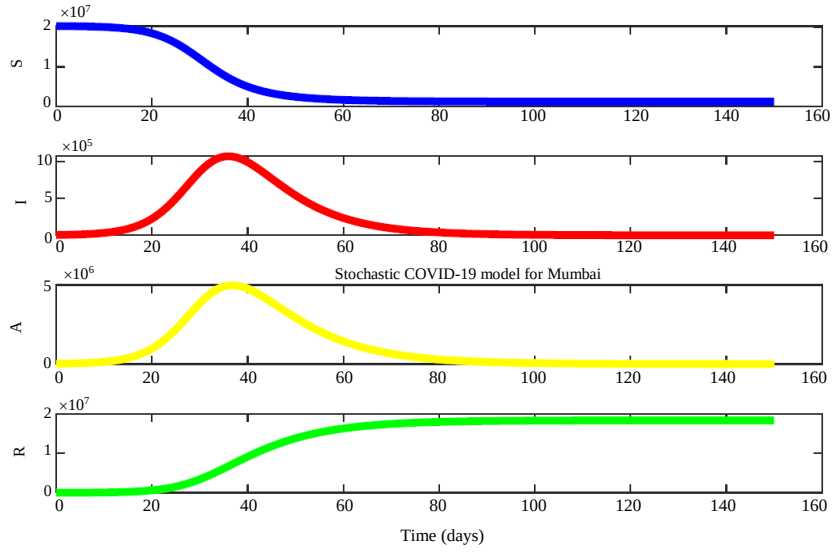

(d)

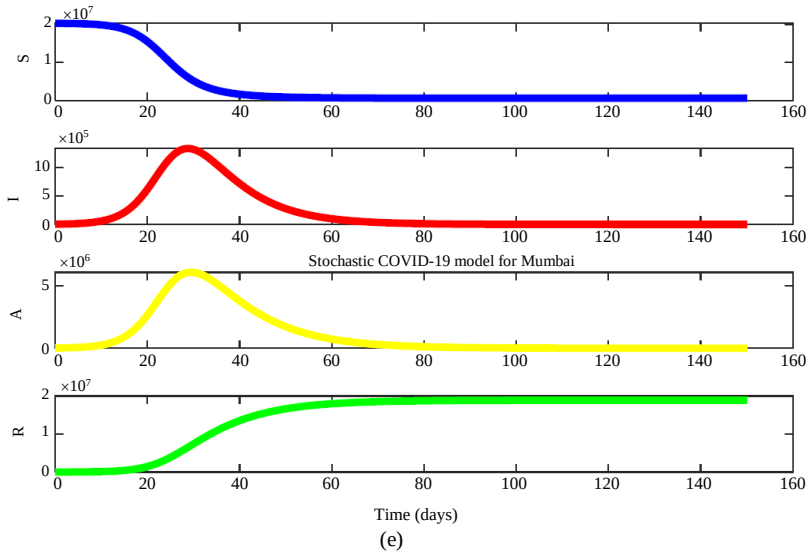

(e)

Fig. 21: The stochastic SI_SI_NR model of the novel COVID-19 for Mumbai considers a sustained lockdown of 61 days, i.e., 25th March, 2020-31st May, 2020, unlock 0.1 and 0.2, as well as weekly lockdown in July, 2020 including night curfew and implementation of effective quarantine periods for travelers. (a) SI_SI_NR model based on the novel stochastic approach (β = 0.15625; R_0 = 1.25). (b) SI_SI_NR model based on the novel stochastic approach (β = 0.1875; R_0 = 1.5). (c) SI_SI_NR model based on the novel stochastic approach (β = 0.25; R_0 = 2.0). (d) SI_SI_NR model based on the novel stochastic approach (β = 0.3125; R_0 2.5). (e) SI_SI_NR model based on the novel stochastic approach (β = 0.375; R_0 = 3.0). Note: The parameters such as *S*, *I*, *A* and *R* are used to express susceptible, infected (symptomatic), infected (asymptomatic) and recovered patients, respectively

Stochastic Model Forecasting the Outbreak of the Novel COVID-19 in Chennai

Tamil Nadu has the second highest number of confirmed cases in India after Maharashtra. Three cases were initially reported in Chennai. The first case was of an old man who was in his mid 60's. He travelled to New Zealand and came back in India. He was treated at a private hospital. Second case of an old lady was found in her mid 50's. She was admitted to Kilpauk Medical College Hospital. The third case was a 25-year-old man who had travelled to London and came back to India. He was been treated at Rajiv Gandhi Government Hospital. Furthermore, 17 cases in Tamil Nadu were reported positive, which also included two foreign nationals. All districts of the state were suffering from the novel COVID-19 pandemic. Chennai was the worst affected. More than fifty percent of the total confirmed cases in Tamil Nadu were from Chennai.

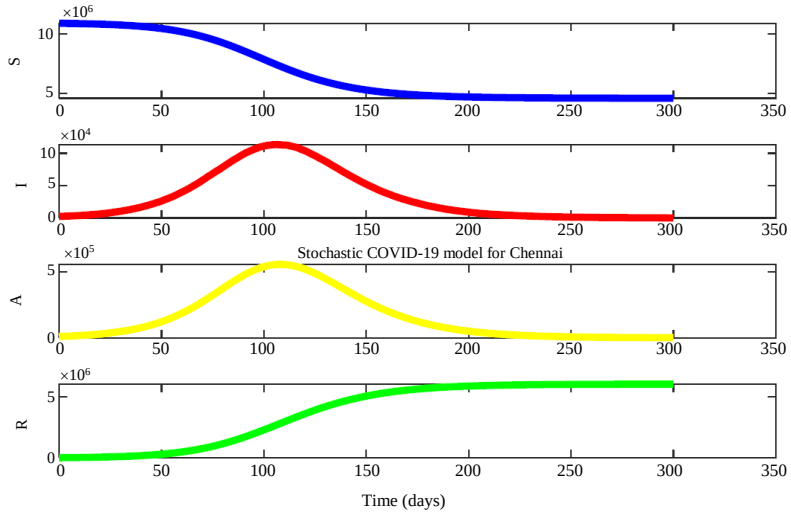
Stochastic COVID-19 model for Chennai
S
I
A
R
Time (days)

(a)

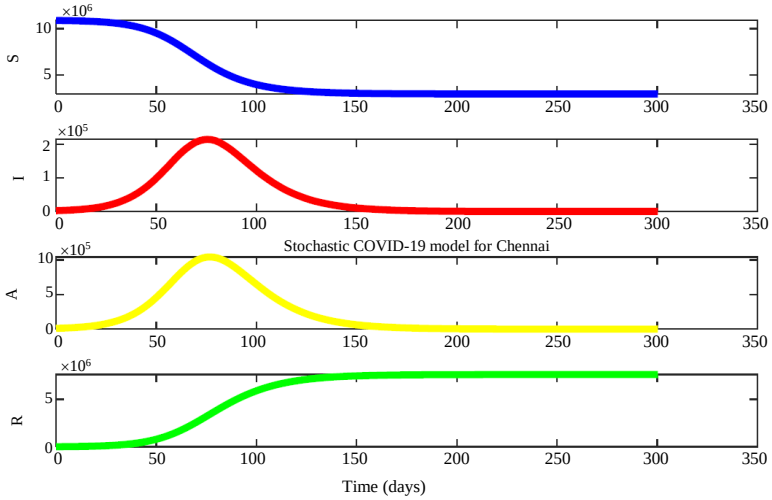
Stochastic COVID-19 model for Chennai
S
I
A
R
Time (days)

(b)

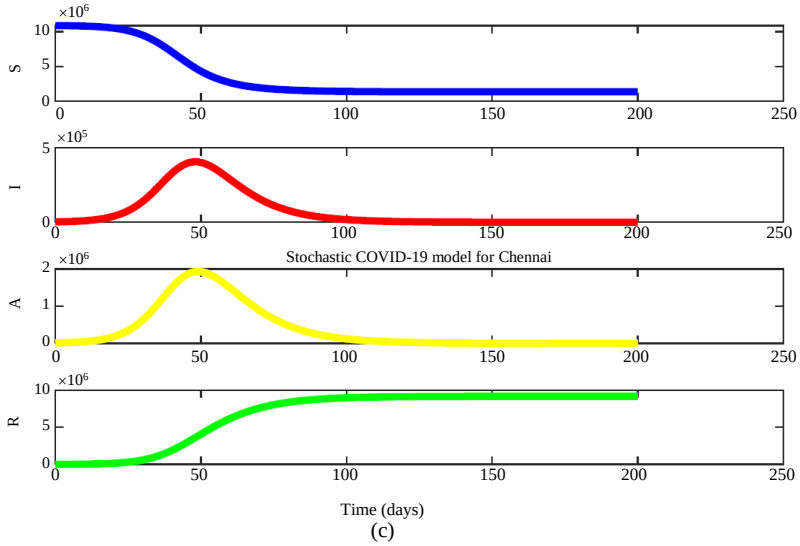
Stochastic COVID-19 model for Chennai
S
I
A
R
Time (days)

(c)

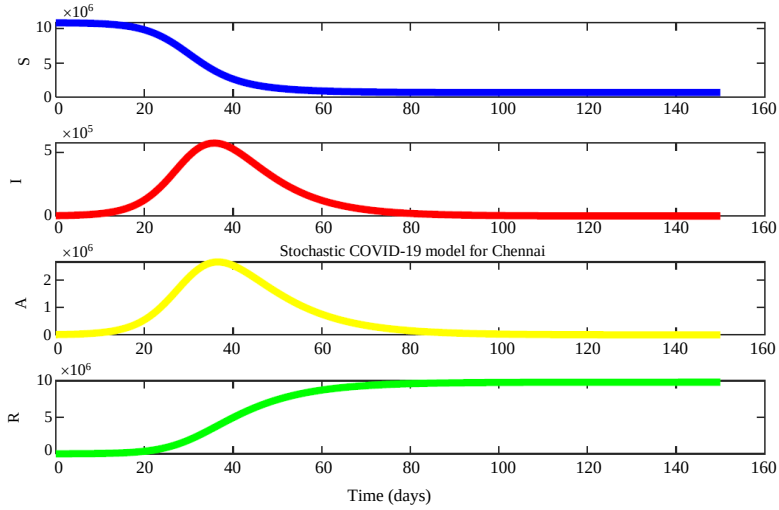

(d)

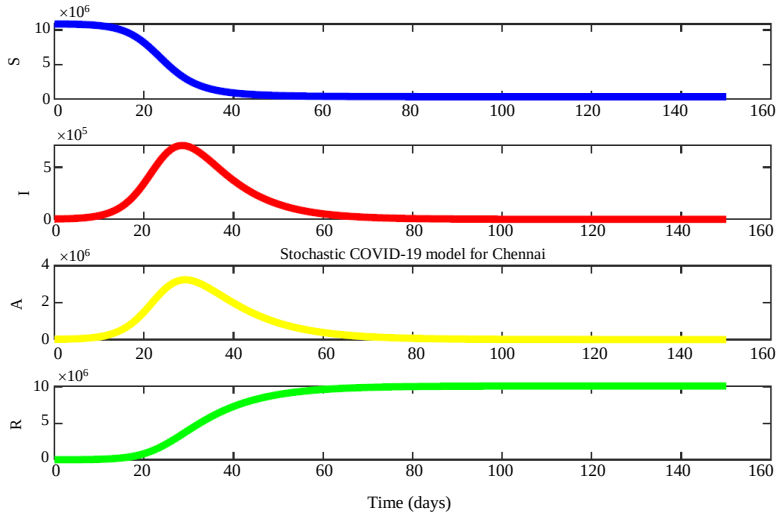

(e)

Fig. 22: The stochastic SI_SI_NR model of the novel COVID-19 for Chennai considers a sustained lockdown of 61 days, i.e., 25th March, 2020-31st May, 2020, unlock 0.1 and 0.2, as well as weekly lockdown in July, 2020 including night curfew and implementation of effective quarantine periods for travelers. (a) SI_SI_NR model based on the novel stochastic approach (β = 0.15625; R_0 = 1.25). (b) SI_SI_NR model based on the novel stochastic approach (β = 0.1875; R_0 = 1.5). (c) SI_SI_NR model based on the novel stochastic approach (β = 0.25; R_0 = 2.0). (d) SI_SI_NR model based on the novel stochastic approach (β =0.3125; R_0 = 2.5). (e) SI_SI_NR model based on the novel stochastic approach (β = 0.375; R_0 = 3.0). Note: The parameters such as S, I, A and R are used to express susceptible, infected (symptomatic), infected (asymptomatic) and recovered patients, respectively

Tamil Nadu showed the least case fatality rate in the country. A large local cluster in Koyambedu of Chennai was identified in May. The case growth rate in Chennai saw a dip in July. Contact-tracing, testing and surveillance model was applied by the government to prohibit the spread of the novel COVID-19 in Tamil Nadu. The state is gifted with 85 laboratories approved by Indian Council of Medical Research (ICMR), capable of conducting tests. The state witnessed lockdown from 25th March, 2020. This lockdown was relaxed to an extent from 04th May, 2020 onwards. Furthermore, the government decided to extend the lockdown until 30th June, 2020. Under the lockdown, significant relaxations were made from 01st June, 2020. A stricter lockdown was enforced in the four most affected districts including Chennai and its three neighbouring districts of Chengalpattu, Thiruvallur and Kancheepuram from 19

to 30th June, 2020 (The Hindu, 2020b; The Indian Express, 2020a).

The number of daily new cases dropped from 2,400 in the first week of July to 1,013 on the 31th July, 2020. Recovery rate improved from 60 to 85%. The city's positivity rate stood around 9% at the end of July. The total of infected people reported on 31st July, 2020 is 99,714, consisting of 2,110 deaths and 84,916 recoveries (The Indian Express, 2020b; The New Indian Express, 2020).

The suitable graphs have been plotted using the above inputs to discuss the spread of the novel COVID-19 pandemic in the Chennai region of the Tamil Nadu state (Fig. 22) on the basis of the values of 'R_0' using stochastic mathematical models based on the modified SI_SI_NR transmission network model. The peaks of infected cases (both symptomatic and asymptomatic cases) as well as the end of SARS-CoV-2 pandemic are attended soon after 31st July, 2020 with an increase in the values of 'β ' and 'R_0'. For Chennai city, the first case (β = 0.15625; R_0 = 1.25) is more appropriate in current scenario as it shows the peak of the novel COVID-19 pandemic in December, 2020 (Fig. 22a). The curve shows the zero case of pandemic by the end of March, 2021.

Stochastic Model Forecasting the Outbreak of the Novel COVID-19 in Ahmedabad

As the novel COVID-19 cases increase in the state government of Gujarat partially locked down four cities - Ahmedabad, Surat, Vadodara and Rajkot. Ahmedabad has reported 25 cases (Rajkot has ten, Vadodara, Surat and Gandhinagar have nine cases each, Bhavnagar has six cases, GirSomnath has two cases and Kutch, Mehsana and Porbandar have one case each). In total, six coronavirus positive patients have died in the state till the end of March, 2020. Till March end five patients have been discharged, the officials declared, two are on ventilator support. Out of the total 73 patients, 32 had a foreign travel history, 37 contracted it through local transmission and 4 had interstate travel history. Every store selling nonessential goods in the four cities saw shut down till 25th March, 2020. As part of the mitigatory measures, only half strength was operating at government offices to be on a rotational basis till 29th March, 2020. Honourable Chief Minister announced the new Civil hospital of Ahmedabad for treating patients infected with the coronavirus. This hospital has a 1,200-bed capacity. With over 3,000 COVID-19 cases and 149 deaths, Ahmedabad was the second city after Mumbai in number of cases and in deaths (The Wire, 2020; India Today, 2020c).

Ahmedabad in Gujarat was announced as a hotspot of the novel COVID-19 by Government of India as 3 patients out of total 5 cases in the city had died. The Government of India also declared that Dilshad Garden and Nizamuddin in Delhi, Noida and Meerut in Uttar Pradesh, Bhilwara in Rajasthan, Kasargod and Pathanamthitta in Kerala, Mumbai and Pune in Maharashtra as the hotspots. The city alone accounts for nearly 65% of total cases and 70% of deaths in Gujarat. The total number of infected people reported on 31st July, 2020 is 25,080, consisting of 1,152 deaths and 20,618 recoveries (The Hindu, 2020c; Amdavad Municipal Corporation, 2020).

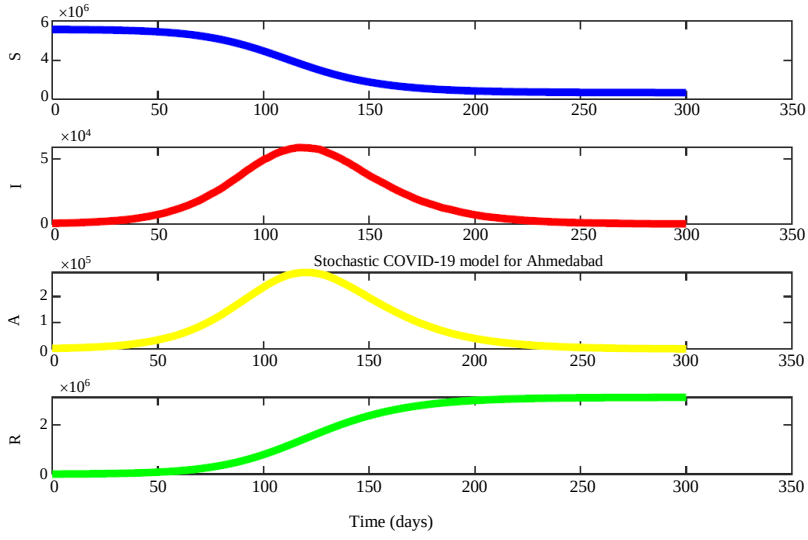

(a)

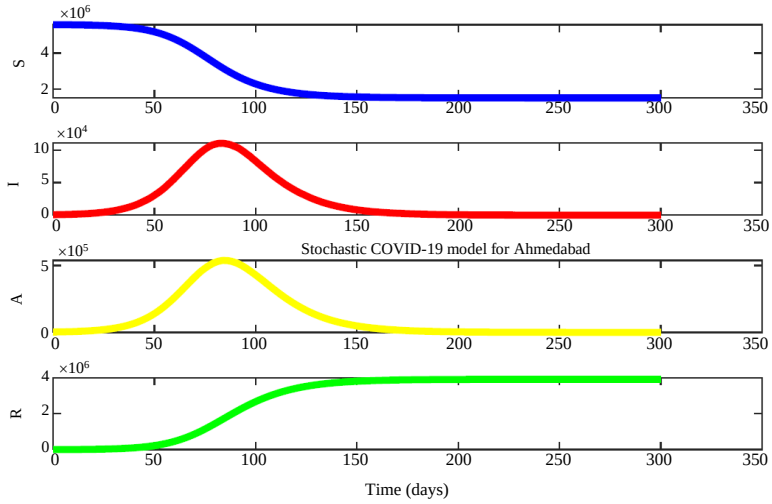
Stochastic COVID-19 model for Ahmedabad
S
I
A
R
Time (days)

(b)

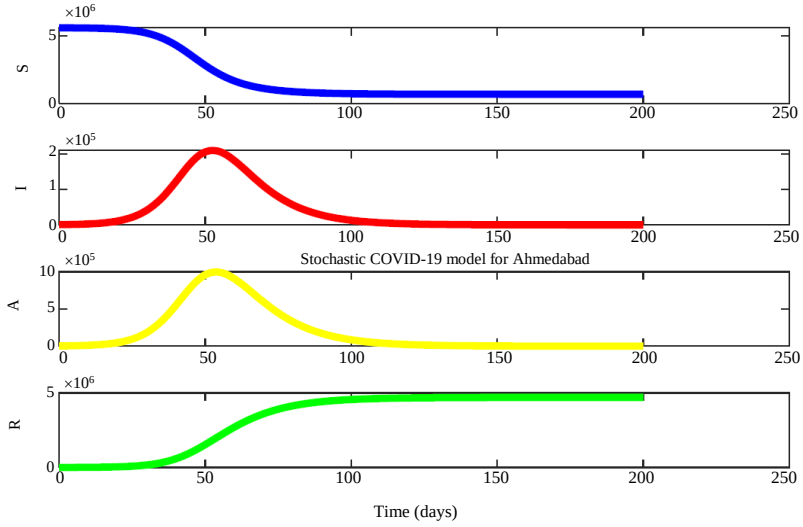
Stochastic COVID-19 model for Ahmedabad
S
I
A
R
Time (days)

(c)

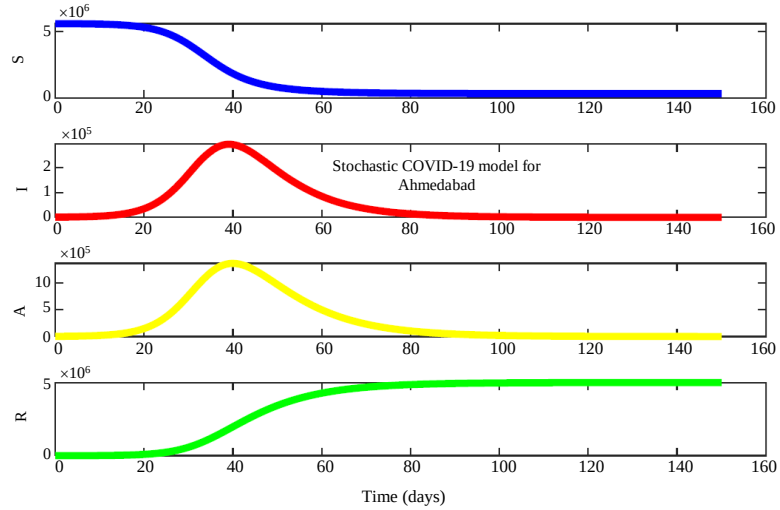
Stochastic COVID-19 model for Ahmedabad
S
I
A
R
Time (days)

(d)

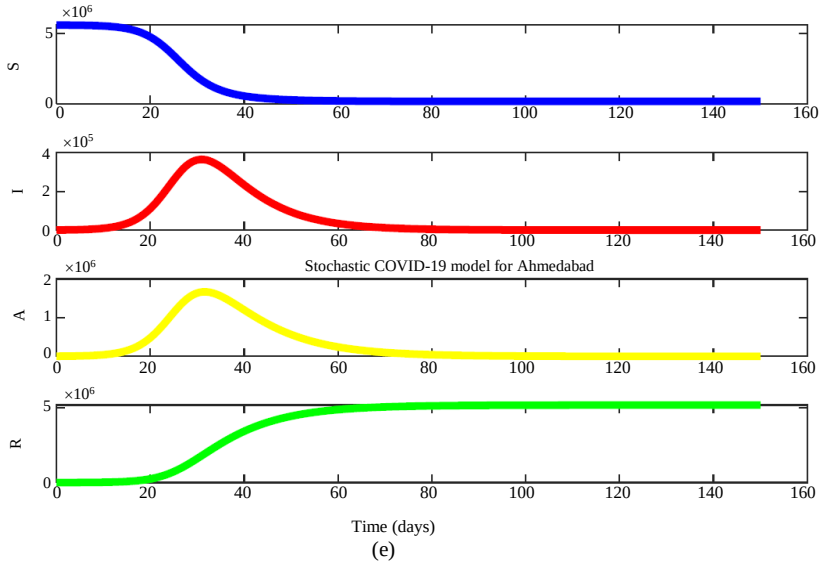

(e)

Fig. 23: The stochastic SI_SI_NR model of the novel COVID-19 for Ahmedabad considers a sustained lockdown of 61 days, i.e., 25th March, 2020-31st May, 2020, unlock 0.1 and 0.2, as well as weekly lockdown in July, 2020 including night curfew and implementation of effective quarantine period for travelers. (a) SI_SI_NR model based on the novel stochastic approach (β = 0.15625; R_0 = 1.25). (b) SI_SI_NR model based on the novel stochastic approach (β = 0.1875; R_0 = 1.5). (c) SI_SI_NR model based on the novel stochastic approach (β = 0.25; R_0 = 2.0). (d) SI_SI_NR model based on the novel stochastic approach (β = 0.3125; R_0 = 2.5). (e) SI_SI_NR model based on the novel stochastic approach (β = 0.375; R_0 = 3.0). Note: The parameters such as S, I, A and R are used to express susceptible, infected (symptomatic), infected (asymptomatic) and recovered patients, respectively

The suitable graphs have been plotted using the above inputs to discuss the spread of the novel COVID-19 pandemic in the Ahmedabad region of the Gujarat state (Fig. 23) on the basis of the values of 'R_0' using stochastic mathematical models based on the modified SI_SI_NR transmission network model. The peaks of infected cases (both symptomatic and asymptomatic cases) as well as the end of SARS-CoV-2 pandemic are attended soon after 31st July, 2020 with an increase in the values of 'β' and 'R_0'. Ahmedabad city is expected to attend the novel COVID-19 pandemic peak in December, 2020 (Fig. 23a); first case (β = 0.15625; R_0 = 1.25) is more appropriate in current scenario). The curve shows the zero case of pandemic by the end of March, 2021.

Discussion

The aim of a mathematical model is not to make unconditional claims about the consequences of interventions, but to reveal the relation between assumptions and outcomes. The motive of our investigation through effective simulation of the modified susceptible (S)-infected (symptomatic) (I_S)-infected (asymptomatic) (I_N)-Recovered (R) i.e., SI_SI_NR transmission network model is to restrict the chain of transmission of the novel COVID-19 pandemic in India.

We developed the compartmental susceptible (S)-infected (symptomatic) (I_S)-infected (asymptomatic) (I_N)-recovered (R) i.e., SI_SI_NR model. The efficacy and potential of base, education, vaccination and education and vaccination programs are established with the published datasets through a validation studies as well under both stochastic and deterministic cases using similar inputs for the meningitis outbreak case in University of Central Florida (UCF) campus. The results are found in fairly good agreement with the published datasets.

We have considered various scenarios by varying the basic reproduction numbers from mean to extremes using base, education, vaccination and education and vaccination models for effective estimation about the peak and end of the pandemic to assist in the revision and effective implementation of health policies as mitigatory measures in India. Initially, we predicted the progress of the pandemic deterministically for a range of values of the basic reproduction number, 'R_0', based on certain assumptions. We observed that the results are frightening.

Summary

For R_0 = 1.25, we conclude to attend the peak of the novel COVID-19 pandemic by the end of December, 2020, with around 6% of the total population being infected at that time. For R_0 = 1.5, we conclude to attend the peak of the novel COVID-19 pandemic by the end of November, 2020, with around 12% of the

total population being infected at that time. For R_0 = 2.0, we conclude to attend the peak of the novel COVID-19 pandemic by the end of October, 2020, with around 21% of the total population being infected at that time. For R_0 = 2.5, we conclude to attend the peak of the novel COVID-19 pandemic in mid-September, 2020, with around 29% of the total population being infected at that time. For R_0 = 3.0, we conclude to attend the peak of the novel COVID-19 pandemic by the end of August, 2020, with around 37% of the total population being infected at that time. We did rigorous analyses to inculcate general assumptions and strategies through contact tracing based on the values of contact ratio operated for the basic reproduction numbers, 'R_0'. The analysis with R_0 = 1.25 corresponding to β = 0.15625; fits best under the current scenario β = 0.15625.

We initially investigated a base model by considering the mean of the basic reproduction number, 'R_0'. Later on, the investigation is done to study the effect of educating people regarding maintaining social distancing and personal hygiene which we called as education model. Here, we found out that by educating people we may extend the progress and diminish the number of infected at a particular time, which can potentially help healthcare services to manage the patients. The effect of mass vaccination combined with the education model is investigated herewith and concluded with fact that the novel COVID-19 pandemic is predicted to end after 100 days from 15th June, 2021 based on the value of 'β ' around 0.128125 (Fig. 18). The prediction is done on the basis of inputs based on assumptions and expert suggestions such as (a) availability of the vaccine to be available by the end of February, 2021 and (b) 61% of the population of India would be vaccinated up to 15th June, 2021. The deterministic analyses based on the modified SI_SI_NR transmission network model are concluded with the facts such as (a) the symptomatic cases are found to be around 80% less than asymptomatic cases and (b) the peaks of infected cases (both symptomatic and asymptomatic cases) as well as end of SARS-CoV-2 pandemic are estimated soon after 31st July, 2020 in December, 2020 (Fig. 11-18) and by the end of March, 2021, respectively.

Furthermore, we stochastically predicted the progress of the pandemic in the top five majorly affected cities in India which includes Delhi, Pune, Mumbai, Chennai and Ahmedabad. The prediction about the transmission of the novel COVID-19 outbreak is done using a range of values of the basic reproduction number, 'R_0', as 1.25, 1.5, 2.0, 2.5 and 3.0 based on the general assumptions and strategies through contact tracing. We could reduce the value of the basic reproduction number, 'R_0', by educating people regarding social distancing and personal hygiene or by implementing the complete or partial lockdown across India or across majorly affected cities to diminish the social contacts which will eventually reduce the spread of the disease. For all majorly affected top five cities, the first case (β = 0.15625; R_0 = 1.25) is more appropriate as it shows the peak of the novel COVID-19 pandemic in December, 2020 (Fig. 20a). The pandemic curves show the zero case of pandemic by the end of March, 2021.

Acknowledgment

The idea behind was to study efficient epidemiological models for simulating the transmissibility of the novel coronavirus disease 2019 (COVID-19) outbreak across the nation and understand the effective mitigatory measures to break the transmission chain of the pandemic in India.

Author's Contributions

Eva Gupta: Research Scholar, Amity University, Uttar Pradesh, India (An Institute of National Importance), is pursuing PhD in Electrical Engineering. She has reviewed papers on above topic and developed MATLAB programs for simulating the outbreak of the novel COVID-19 pandemic in India using deterministic and stochastic approaches.

Nand Jee Kanu: Research Scholar, S. V. National Institute of Technology, Surat, India (An Institute of National Importance), is pursuing PhD in Mechanical Engineering. He has reviewed papers on above topic and developed MATLAB programs for simulating the outbreak of the novel COVID-19 pandemic in India using deterministic and stochastic approaches.

Amartya Munot: BE Research Scholar, Mechanical Engineering, S. A. P. D. J. Pathshala's Walchand Institute of Technology, Solapur, India. He has analyzed inputs through MATLAB programs to study the outbreak of SARS-CoV-2 pandemic in India using deterministic and stochastic approaches.

Venkateshwara Sutar: BE Research Scholar, Mechanical Engineering, JSPM Narhe Technical Campus, Pune, India. He has analyzed inputs through MATLAB programs to study the outbreak of SARS-CoV-2 pandemic in India using deterministic and stochastic approaches.

Umesh Kumar Vates: Associate Professor, Amity University, Uttar Pradesh, India, has completed his PhD in Mechanical engineering from IIT (ISM) Dhanbad, India (An Institute of National Importance). He has investigated and supervised the research work to predict the transmission of SARS-CoV-2 pandemic in India.

Gyanendra Kumar Singh: Associate Professor, Mechanical Design and Manufacturing Engineering, Adama Science and Technology University, Adama, Ethiopia, has completed his PhD in Mechanical

engineering from M. N. National Institute of Technology, Allahabad, India (An Institute of National Importance). He has investigated and supervised the research work to predict the transmission of SARS-CoV-2 pandemic in India.

Conflict of Interest

The authors declare that there are no conflicts of interest.

Planning and Motivation

We reviewed the relevant articles on the novel coronavirus (SARS-CoV2) published online within the past few months with the aim to join the battle against coronavirus disease (COVID-19).

Data Availability

The authors confirm that the data supporting the findings of this study are available within the article.

Ethics

The author does not see any ethical issues that may arise after the publication of this manuscript.

Appendix A

Singh and Adhikari (2020) reviewed the modified age-structured Susceptible-Infected-Recovered (SIR) model of the novel COVID-19 outbreak in India by considering the activity of the Indian government to execute mitigatory measures such as physical distancing, lockdown in India to restrict the spread of global pandemic across the nation. They considered the birth and death rates to be the same within a specific age group. Depending upon the real-time time-independent data, mitigatory social distancing and age groups, the basic Reproduction number (R_o) was assessed by using the modified age-structured SIR model.

The people are categorized in various ages such as 'M' groups denoted as i = 1,2,…M. The people under a specific age were described as 'i' and they are categorized into susceptible patients (S_i), symptomatic patients $\left(I_i^s\right)$, asymptomatic patients $\left(I_i^a\right)$ and removed patients (R_i). Therefore, the total number of people within a specified age group (i) will be sum of all these categories as $N_i = S_i + I_i^a + I_i^s + R_i$.

Each N_i was denoted as the total number of people as shown in Equation (3):

$$N = \sum_{i=1}^{M} N_i \tag{3}$$

The transmission rate of the novel COVID-19 in susceptible patients within a specific age group (i) is represented by using Equation (4):

$$\lambda_i(t) = \beta \sum_{j=1}^{M} \left(C_{ij}^a \frac{I_j^a}{N_j} + C_{ij}^s \frac{I_j^s}{N_j} \right), i, j = 1,...M \tag{4}$$

where, 'β' term was the chance of transmission of the pandemic due to physical contact and a C_{ij}^a and C_{ij}^s were used to represent the number of cases of social contact between asymptomatic patients within the age group (j) and susceptible patients within an age group (i), respectively. The term 'γ' is also known as curing rate, was not dependent on age and was the same for both asymptomatic (ratio, α) and symptomatic patients (ratio, $\bar{\alpha}$ = 1-α).

The pandemic growth rate was expressed using age-structured SIR model in Equation (5):

$$\left.\begin{aligned} \dot{S}_i &= -\lambda_i(t) S_i, \\ \dot{I}_i^a &= \alpha \lambda_i(t) S_i - \gamma I_i^a, \\ \dot{I}_i^s &= \bar{\alpha} \lambda_i(t) S_i - \gamma I_i^s, \\ \dot{R}_i &= \gamma \left(I_i^a + I_i^s \right). \end{aligned}\right\} \tag{5}$$

The age group of the persons was expressed as the ratio of N_i/N and social contact was expressed using C_{ij}^a and C_{ij}^s matrices. Furthermore, the symptomatic patients were supposed to have less contact as compared to the asymptomatic patients and thus, $C_{ij}^s = fC_{ij}^a \equiv fC_{ij}$, (where, $0 \le f \le 1$).

The people were expected to remain in homes, office places, schools and other places for self-isolation, therefore the contact matrix represented by using Equation (6):

$$C_{ij} = C_{ij}^H + C_{ij}^W + C_{ij}^S + C_{ij}^O \tag{6}$$

For a specific population size, the contact matrix was represented as $N_iC_{ij} = N_jC_{ij}$.

On a large basis, mitigatory social distancing was modeled and expressed as a time functions $u^W(t)$, $u^S(t)$ and $u^O(t)$ and thus Equation (7) shows the time-dependent contact matrix:

$$C_{ij}(t) = C_{ij}^H + u^W(t) C_{ij}^W + u^S(t) C_{ij}^S + u^O(t) C_{ij}^O. \tag{7}$$

The physical and social distancing were imposed effectively across the country during lockdown and thus a single household contact function was represented by using the linear expression (8):

$$2u(t) = -\tanh\left(\frac{t-t_{on}}{t_w}\right) + \tanh\left(\frac{t-t_{off}}{t_w}\right) \quad (8)$$

The basic reproductive number was evaluated from null COVID-19 spots (where $S_i = N_i$) and infected persons were expressed using $2M \times 2M$ matrix, as shown in Equation (9):

$$J = \gamma(L-1). \quad (9)$$

The $2M \times 2M$ generation matrix is obtained from Equation (10):

$$L = \begin{pmatrix} L^{aa} & L^{as} \\ L^{sa} & L^{ss} \end{pmatrix} \quad (10)$$

where, $L_{ij}^{aa} = \frac{\alpha\beta}{\gamma} C_{ij}^{a} \frac{N_i}{N_j}$, $L_{ij}^{as} = \frac{\alpha\beta}{\gamma} C_{ij}^{s} \frac{N_i}{N_j}$ and $L_{ij}^{sa} = \frac{\alpha\beta}{\gamma} C_{ij}^{a} \frac{N_i}{N_j}$, $L_{ij}^{ss} = \frac{\bar{\alpha}\beta}{\gamma} C_{ij}^{s} \frac{N_i}{N_j}$.

The identity matrix, $\bar{I}$ ($2M \times 2M$) was used to encompass both asymptomatic and symptomatic patients as shown in Equation (11):

$$\bar{I} = \left(I^a, I^s\right) = \left(I_1^a, ..., I_M^a, I_1^s, ...I_M^s\right) \quad (11)$$

The dynamics of the above Equation (11) was expressed using Equation (12):

$$\bar{I}(t) = \exp\left[\gamma(L-1)t\right]\bar{I}(0) \quad (12)$$

where, 'L ' was used to evaluate the eigenvectors, 'V ' and the diagonal matrix of eigenvalues, Λ = *diag* (Λ_1,…, Λ_{1M}) to calculate the expression, $\exp[\gamma(L\text{-}1)t] = V\ diag\ \exp[\exp\gamma(\Lambda\text{-}1)t]V^{-1}$.

For pandemic growth, the span L must be greater than one and thus the basic reproduction number, 'R_0', is expressed as Equation (13):

$$R_0 \equiv \rho(L) = \max\left\{\left|\Lambda_1\right|, ..., \left|\Lambda_{1M}\right|\right\}. \quad (13)$$

The basic reproductive number was reasonably good to support the spread of the pandemic if the eigenvalue was real as shown in Equation (14):

$$\exp\left[\gamma\left(R_0 - 1\right)t\right] \quad (14)$$

The basic reproductive number was based on (a) the chance of transmission of disease by social contact, (b) the social contact matrix, (c) the ratio of persons without and with symptoms of SARS-CoV-2 and (d) the ratio of symptomatic patients who were in self-isolation. The conversions such as (a) and (b) were done to transform the formulation into its linear form for time-based stability matrix. The time-based stability matrix, was expressed using Equation (15):

$$R_0^{eff}(t) \equiv \rho\left(L^{(t)}\right) = \max\left\{\left|\Lambda_1^{(t)}\right|, ..., \left|\Lambda_{1M}^{(t)}\right|\right\} \quad (15)$$

The cases of infected patients at any time were expressed as shown in Equation (16):

$$\bar{I}\left(t+\delta t\right) = \exp\left[\gamma\left(L^{(t)}-1\right)\delta t\right]\bar{I}(t) \quad (16)$$

The basic reproductive number played a significant role, when the eigenvalue was real for its highest magnitude for the tremendous growth of the pandemic in a very short time. The end of the pandemic was shown with the rise and fall of the spread of SARS-CoV-2 outbreak were shown with time constants.

Appendix B

Calculations for the base Model

R = Radius of infection = 0.00001 km
q = Probability of infective transmitting the infection = 0.1
ρ = Population density = 382 number of people per square km
$\bar{v}$ = Average traffic speed = 263.270 km/day
β = Contact ratio

$$\beta = \frac{8Rq\bar{v}\rho}{\pi}$$

$$\beta = \frac{8 \times 0.00001 \times 0.1 \times 263.270 \times 382}{\pi}$$

β = 0.2560

Calculations for Education and Education and Vaccination Models

R = Radius of infection = 0.00001 km
q = Probability of infective transmitting the infection = 0.5
ρ = Population density = 382 number of people per square km
$\bar{v}$ = Average traffic speed = 263.270 km/day
β = Contact ratio

$$\beta = \frac{8Rq\bar{v}\rho}{\pi}$$

$$\beta = \frac{8 \times 0.00001 \times 0.5 \times 263.270 \times 382}{\pi}$$

β = 0.128125

Values of Contact Ratio for Different Scenarios

R = Radius of infection = 0.00001 km
q = Probability of infective transmitting the infection = 0.5
ρ = Population density = 382 number of people per square km
For, $\bar{v}$ = average traffic speed = 160.626 km/day; β = 0.1562
$\bar{v}$ = Average traffic speed = 192.751 km/day; β = 0.1875
For, $\bar{v}$ = average traffic speed = 251.712 km/day; β = 0.2512
$\bar{v}$ = Average traffic speed = 321.252 km/day; β = 0.3125
For, $\bar{v}$ = average traffic speed = 385.521 km/day; β = 0.3752

References

Amdavad Municipal Corporation. (2020). COVID-19 Ahmedabad city. Amdavad Municipal Corporation. https://ahmedabadcity.gov.in/portal/index.jsp.

Atkins, T. (2010). Using modeling and simulation to evaluate disease control measures.

BBC News. (2020a). Coronavirus vaccine: when will we have one? BBC News. Available: https://www.bbc.com/news/health-51665497

BBC News. (2020b). Coronavirus vaccine trial begun by drug firms GSK and Sanofi. BBC News. https://www.bbc.com/news/business-54009633

Bhola, J., Venkateswaran, V. R., & Koul, M. (2020). Corona Epidemic in Indian context: Predictive Mathematical Modelling. medRxiv.

Business Today. (2020). Coronavirus: Delhi govt. announces Operation SHIELD to take on COVID-19. Business Today. https://www.businesstoday.in/latest/trends/coronavirus-delhi-govt-announces-operation-shield-to-take-on-COVID-19/story/400648.html

Chang, S. L., Harding, N., Zachreson, C., Cliff, O. M., & Prokopenko, M. (2020). Modelling transmission and control of the COVID-19 pandemic in Australia. arXiv preprint arXiv:2003.10218.

Chatterjee, K., Chatterjee, K., Kumar, A., & Shankar, S. (2020). Healthcare impact of COVID-19 epidemic in India: A stochastic mathematical model. Medical Journal Armed Forces India.

COVID-19 India. (2020). Novel Coronavirus-India. COVID-19 India. https://www.COVID19india.org/

Daughton, A. R., Generous, N., Priedhorsky, R., & Deshpande, A. (2017). An approach to and web-based tool for infectious disease outbreak intervention analysis. Scientific reports, 7, 46076.

Deb, S., & Majumdar, M. (2020). A time series method to analyze incidence pattern and estimate reproduction number of COVID-19. arXiv preprint arXiv:2003.10655.

Dhama, K., Sharun, K., Tiwari, R., Dadar, M., Malik, Y. S., Singh, K. P., & Chaicumpa, W. (2020). COVID-19, an emerging coronavirus infection: advances and prospects in designing and developing vaccines, immunotherapeutics and therapeutics. Human vaccines & immunotherapeutics, 1-7.

Dhanwant, J. N., & Ramanathan, V. (2020). Forecasting COVID 19 growth in India using Susceptible-Infected-Recovered (SIR) model. arXiv preprint arXiv:2004.00696.

Gupta, E., & Kanu, N. J. (2020). An Insight into the Simplified RP Transmission Network, Concise Baseline and SIR Models for Simulating the Transmissibility of the Novel Coronavirus Disease 2019 (COVID-19) Outbreak. American Journal of Infectious Diseases.

Hindustan Times. (2020a). India most infected by the novel COVID-19 among Asian countries, leaves Turkey behind. Hindustan Times. https://www.hindustantimes.com/india-news/india-most-infected-by-COVID-19-among-asian-countries-leaves-turkey-behind/story-Jjd0AqIsuL3yjMWg29uJ3I.html

Hindustan Times. (2020b). The novel COVID-19: Number of recoveries exceeds active cases for first time. Hindustan Times. https://www.hindustantimes.com/india-news/COVID-19-number-of-recoveries-exceed-active-cases-for-first-time/story-uA0C6zESJTdkl9UQ2lHc2M.html

India Today. (2020a). COVID-19: Another reason why unlock 1.0 may be ill-timed in India. India Today. https://www.indiatoday.in/news-analysis/story/COVID-19-unlock-1-0-india-lockdown-coronavirus-cases-1687162-2020-06-09

India Today. (2020b). Pune woman tests positive for COVID-19, had returned from Netherlands. Maharashtra total now at 43. India Today. https://www.indiatoday.in/india/story/pune-woman-tests-positive-for-COVID-19-had-returned-from-netherlands-maharashtra-total-now-at-42-1657064-2020-03-18

India Today. (2020c). Coronavirus: Gujarat government declares lockdown rules for shops, firms. India Today. https://www.indiatoday.in/india/story/coronavirus-gujarat-govt-declares-lockdown-rules-for-shops-firms-1658305-2020-03-21

Inventiva. (2020a). A vaccine which could be helpful in curing coronavirus. Inventiva. https://www.inventiva.co.in/stories/inventiva/a-vaccine-which-could-be-helpful-in-curing-coronavirus/

Inventiva. (2020b). ICMR to get about 7 lakhs rapid antibody testing kits to India by April 8. Inventiva. https://www.inventiva.co.in/trends/riyarana/icmr-to-get-about-7-lakhs-rapid-antibody-testing-kits-to-india-by-april-8/

Kumar, S. (2020). Predication of Pandemic COVID-19 situation in Maharashtra, India. medRxiv.

Livemint. (2020). Coronavirus lockdown extended till 31 May, says NDMA. Livemint. https://www.livemint.com/news/india/COVID-19-lockdown-4-0-coronavirus-lockdown-extended-till-31-may-says-ndma-11589715203633.html

Mackolil, J., & Mahanthesh, B. (2020). Mathematical Modelling of Coronavirus disease (COVID-19) Outbreak in India using Logistic Growth and SIR Models.

Mandal, S., Bhatnagar, T., Arinaminpathy, N., Agarwal, A., Chowdhury, A., Murhekar, M., ... & Sarkar, S. (2020). Prudent public health intervention strategies to control the coronavirus disease 2019 transmission in India: A mathematical model-based approach. The Indian journal of medical research, 151(2-3), 190.

Mazumder, A., Arora, M., Bharadiya, V., Berry, P., Agarwal, M., Behera, P., ... & Parameswaran, G. G. (2020). SARS-CoV-2 epidemic in India: epidemiological features and in silico analysis of the effect of interventions. F1000Research, 9.

NDTV. (2020). 2,347 COVID cases in Maharashtra in 24 h, Mumbai crosses 20,000-mark. NDTV. https://www.ndtv.com/india-news/2-347-new-coronavirus-cases-in-maharashtra-in-24-hours-mumbai-crosses-20-000-mark-2230403

News18. (2020) How the govt. machinery acted quickly to spread awareness about coronavirus. News18. https://www.news18.com/news/opinion/how-the-govt-machinery-acted-quickly-to-spread-awareness-about-novelCOVID-19-2537029.html

Pai, C., Bhaskar, A., & Rawoot, V. (2020). Investigating the dynamics of COVID-19 pandemic in India under lockdown. Chaos, Solitons & Fractals, 138, 109988.

Rajesh, A., Pai, H., Roy, V., Samanta, S., & Ghosh, S. (2020). CoVID-19 prediction for India from the existing data and SIR (D) model study. medRxiv.

Ramola, R. C. (2020). Projected Spread of COVID-19 through India Based on SIR Model. Reproduction, 1-52.

Ranjan, R. (2020). Predictions for COVID-19 outbreak in India using Epidemiological models. medRxiv.

Rihan, F. A., & Anwar, M. N. (2012). Qualitative analysis of delayed SIR epidemic model with a saturated incidence rate. International Journal of Differential Equations, 2012.

Sahasranaman, A., & Kumar, N. (2020). Network structure of COVID-19 spread and the lacuna in India's testing strategy. Available at SSRN 3558548.

Singh, R., & Adhikari, R. (2020). Age-structured impact of social distancing on the COVID-19 epidemic in India. arXiv preprint arXiv:2003.12055.

The Hindu. (2020a). Curbs put on roadside shops, outlets, eateries in Navi Mumbai. The Hindu. https://www.thehindu.com/news/national/coronavirus-live-updates-march-19-2020/article31105138.ece

The Hindu. (2020b). Three fresh cases detected in Tamil Nadu. The Hindu. https://www.thehindu.com/news/national/coronavirus-live-updates-march-24-2020/article31149240.ece

The Hindu. (2020c). Coronavirus | Ahmedabad records over 3,000 cases, 149 deaths. The Hindu. https://www.thehindu.com/news/national/other-states/coronavirus-ahmedabad-records-over-3000-cases-149-deaths/article31475675.ece

The Hindustan Times. (2020a). Pune needs to avoid mistakes Mumbai made to get through COVID-19. The Hindustan Times. https://www.hindustantimes.com/pune-news/pune-needs-to-avoid-mistakes-mumbai-made-to-get-through-COVID-19/story-sGYIt2yMrg6Ns3diWRH1cJ.html

The Hindustan Times. (2020b). Maharashtra facing surge in cases even outside red zones. The Hindustan Times. https://www.hindustantimes.com/india-news/maharashtra-facing-surge-in-cases-even-outside-red-zones/story-KIx5rXJHDr8xVpEg9HW9MO.html

The Indian Express. (2020a). Lockdown begins in Chennai, 3 districts today; surge in cases. The Indian Express. https://indianexpress.com/article/india/lockdown-begins-in-chennai-3-districts-today-surge-in-cases-6465698/

The Indian Express. (2020b). Over 35% Tamil Nadu coronavirus cases linked to Koyambedu market in Chennai. The Indian Express. https://indianexpress.com/article/india/over-35-tn-cases-linked-to-a-market-in-chennai-6408861/

The New Indian Express. (2020). The novel COVID-19: ray of hope as daily cases in Chennai dip closer to three-digit mark. The New Indian Express. https://www.newindianexpress.com/cities/chennai/2020/jul/31/covid-19-ray-of-hope-as-daily-cases-in-chennai-dip-closer-to-three-digit-mark-2177383.html

The Times of India. (2020a). Coronavirus: 15 lakh who flew back to India between Jan 18-Mar 23 under lens. The Times of India. https://timesofindia.indiatimes.com/india/15-lakh-who-flsew-back-to-india-between-jan-18-mar-23-under-lens/articleshow/74855553.cms

The Times of India. (2020b). Manish Sisodia lauds locals for making 'Operation SHIELD' successful. The Times of India. https://timesofindia.indiatimes.com/city/delhi/manish-sisodia-lauds-locals-for-making-operation-shield-successful/articleshow/75200268.cms

The Wire. (2020). Government identifies 10 coronavirus hotspots, testing to be boosted. The Wire. https://thewire.in/government/coronavirus-hotspots-india-testing-boost

Times Network. (2020). Overview of the novel COVID-19 - an India perspective. Times Network. https://www.timesnownews.com/india/photo-gallery/overview-of-the novel COVID-19-an-indian-perspective-an-insightful-report-by-times-network/584153

Tiwari, A. (2020). Modelling and analysis of COVID-19 epidemic in India. medRxiv.

Wikipedia. (2020a). The novel COVID-19 pandemic in India. https://en.wikipedia.org/wiki/the novel COVID-19_pandemic_in_India

Wikipedia. (2020b). Basic reproduction number. Wikipedia. https://en.wikipedia.org/wiki/Basic_reproduction_number

Wikipedia. (2020c) The novel COVID-19 pandemic in Delhi. Wikipedia. https://en.wikipedia.org/wiki/the novel COVID-19_pandemic_in_Delhi.

EARLY DETECTION OF TUMORS IN MR IMAGES OF THE HUMAN BRAIN: AN APPLICATION USING DEEP LEARNING TECHNIQUES

Gayatri Mirajkar[*1] and Ajay Deshmukh[2]

[*1]Arvind Gavali College of Engineering, Satara, Maharashtra, India

[2]Director, Centre for Industrial Mathematics, Bhaskaracharya Pratisthana, Pune, Maharashtra, India

Abstract:

Brain tumours are one of the most lethal types of cancer, and early detection is crucial for successful treatment. Magnetic Resonance (MR) imaging is a widely used diagnostic tool for brain tumours. However, the interpretation of MR images can be challenging, and a trained radiologist is required for accurate diagnosis. In this study, we propose an automated system for the early detection of brain tumours using Deep Learning techniques. Our system uses a Convolutional Neural Network (CNN) to analyse MR images and classify them as either healthy or containing a tumour. The proposed system was trained on a large dataset of MR images and achieved high accuracy in tumour detection. The results demonstrate the potential of Deep Learning techniques for the early detection of brain tumours, which could lead to improved patient outcomes.

Keywords: Brain tumours, Magnetic Resonance imaging, Deep Learning, Convolutional Neural Network, Early detection.

DOI: 10.24297/j.cims.2022.12.021

1. Introduction

Medical imaging has revolutionized the way physicians diagnose and treat various diseases, including cancer. Magnetic resonance imaging (MRI) is a non-invasive imaging modality that has become increasingly popular for detecting brain tumours. However, accurately detecting and classifying tumours in MR images is a challenging task that requires expert knowledge and experience.[1]

Deep Learning techniques, such as Convolutional Neural Networks (CNNs), have shown promising results in analysing medical images and assisting in the diagnosis of various diseases, including brain tumours.[1] This application of Deep Learning can potentially improve the accuracy and efficiency of tumour detection in MR images of the human brain, ultimately leading to earlier diagnosis and better patient outcomes.[2]

In this project, we explore the use of Deep Learning techniques for early detection of tumours in MR images of the human brain.[2] We aim to develop a system that can accurately detect and classify brain tumours in MR images, potentially assisting medical professionals in their diagnosis and treatment decisions.[3]

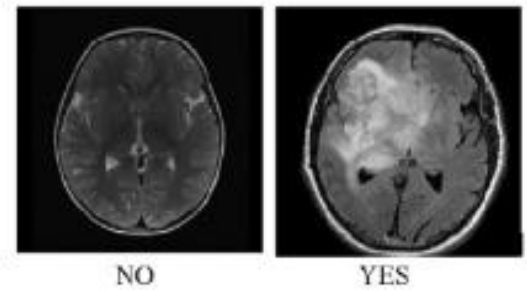

Figure 1. Normal Brain and Brain with Tumour

2. Literature Review

Several studies have shown that deep learning techniques can improve the accuracy and efficiency of brain tumour detection in MR images. For example, Jang et al. (2019) proposed a deep learning-based method for the segmentation of brain tumours in MR images. Their proposed method achieved high accuracy and outperformed traditional segmentation methods. In another study, Shie et al. (2020) used a deep learning-based approach for the early detection of brain tumours in MR images. Their approach was able to detect brain tumours at an early stage with high accuracy.[4]

Similarly, Wang et al. (2021) proposed a deep learning-based method for the detection of brain tumours in MR images. Their proposed method achieved high accuracy in detecting both small and large tumours. The authors also compared their method with traditional methods and showed that their method outperformed traditional methods.

In a recent study, Song et al. (2022) proposed a deep learning-based method for the classification of brain tumours in MR images. Their proposed method achieved high accuracy in classifying different types of brain tumours. The authors also compared their method with traditional classification methods and showed that their method outperformed traditional methods.[5]

3. Materials And Methods

Materials: The dataset used in this study consists of MR images of the human brain with and without tumours. The dataset includes T1, T2, and FLAIR modalities. The images were acquired using a 1.5-Tesla MRI scanner from multiple hospitals. The dataset was pre-processed to ensure consistency in terms of resolution, orientation, and noise levels.[6]

Methods

1. **Pre-processing**: The MR images were pre-processed to remove any artifacts and to normalize the intensity values. The images were also cropped to focus on the brain region of interest.
2. **Data augmentation:** To increase the size of the dataset and to improve the generalization of the model, data augmentation techniques were applied to the MR images. This included rotation, flipping, and scaling.
3. **Model architecture:** A Deep Learning model based on convolutional neural networks (CNNs) was developed for tumour detection. The CNN architecture consisted of multiple convolutional layers, pooling layers, and fully connected layers. The input to the CNN was a 3D tensor representing the MR image. The output of the CNN was a binary classification indicating whether the input image contained a tumour or not.
4. **Training and validation**: The model was trained on a subset of the dataset using the Adam optimizer with a binary cross-entropy loss function. The validation set was used to monitor the performance of the model during training and to prevent overfitting.
5. **Evaluation:** The performance of the model was evaluated using several metrics, including accuracy, precision, recall, F1 score, and area under the receiver operating characteristic curve (AUC-ROC). The model was also compared to other state-of-the-art tumour detection methods.
6. **Implementation:** The model was implemented using the Python programming language and the TensorFlow Deep Learning framework. The code was executed on a high-performance computing cluster to accelerate the training and evaluation process.

Figure 2. Architecture of CNN model

4. Results

Based on the research conducted on the early detection of tumours in MR images of the human brain using deep learning techniques, it can be concluded that the approach has the potential to significantly improve the accuracy and efficiency of tumour detection.

The use of deep learning algorithms, such as Convolutional Neural Networks (CNNs), has shown promising results in detecting brain tumours at an early stage, which can greatly improve the chances of successful treatment and improve patient outcomes. The study also highlights the importance of pre-processing techniques such as normalization and data augmentation, which can enhance the performance of deep learning models.

5. Conclusions

Based on the available information, it appears that the use of deep learning techniques for the early detection of tumours in MR images of the human brain is a promising approach. The study suggests that deep learning models can achieve high accuracy in detecting brain tumours, and that this approach can significantly reduce the time required for diagnosis.

However, it is important to note that the study's findings may not be representative of all populations or imaging settings. More research is needed to validate the efficacy of deep learning models for brain tumour detection in diverse populations and under different imaging conditions.

Overall, the study highlights the potential of deep learning techniques for improving the accuracy and efficiency of brain tumour detection, and further research in this area is warranted.

Reference

1. Chen, H., Zhang, Y., Zhang, W., Liao, W., & Li, X. (2020). Deep learning for brain tumour classification and segmentation in MRI: A comprehensive review. Journal of Magnetic Resonance Imaging, 51(1), 20-40.
2. Wang, G., Li, W., Earthen, M., & Zhang, J. (2019). An overview of deep learning in medical imaging focusing on MRI. Festschrift für Diminished Physic, 29(2), 102-127.
3. Liu, F., Jang, H., Kijowski, R., & Bradshaw, T. (2018). Deep learning MR imaging–based attenuation correction for PET/MR imaging. Radiology, 286(2), 676-684.
4. Vignati, A., Mazzetti, S., Giusti, A., Santoro, C., & Piffer, S. (2020). A survey of deep learning techniques for brain tumour segmentation and classification in MRI. Journal of Healthcare Engineering, 2020, 1-23.
5. Menze, B. H., Jakab, A., Bauer, S., Kalpathy-Cramer, J., Farahani, K., Kirby, J., ... & Ayache, N. (2015). The multimodal brain tumour image segmentation benchmark (BRATS). IEEE Transactions on Medical Imaging, 34(10), 1993-2024.

6. Guo, Y., Gao, Y., Shen, D., & De Assis, K. (2019). Learning from medical imaging data: A review. Journal of Medical Systems, 43(8), 233-245.
7. Ding, C., Guan, J., & Zhong, Y. (2020). Deep learning-based brain tumour segmentation in multimodal magnetic resonance imaging. Journal of Healthcare Engineering, 2020, 1-11.
8. Zhang, K., Liu, X., Liu, Y., Li, Z., Wang, Y., Zhang, Y., & Li, L. (2020). An improved convolutional neural network for brain tumour segmentation. Journal of Medical Imaging and Health Informatics, 10(9), 2137-2145.
9. Thakur, D., & Sahu, S. (2019). Brain tumour detection and classification using deep learning technique. In 2019 2nd International Conference on Intelligent Computing, Instrumentation and Control Technologies (ICICICT) (pp. 1244-1249). IEEE.
10. Talon, M., Balogun, U. B., Yıldırım, Ö., & Rajendra Acharya, U. (2019). Convolutional neural networks for multi-class brain disease classification using MRI images. Computers in Biology and Medicine, 109, 216-237.

Ann. For. Res. 64(2): 203-210, 2021
ISSN: 18448135, 20652445

ANNALS OF FOREST RESEARCH
www.e-afr.com

DETECTION OF DEFORESTATION CHANGE IN SAR IMAGES USING LOCAL FEATURES

Gayatri Mirajkar
Arvind Gavali College of Engineering, Satara, Maharashtra, India
gayatrimirajkar@gmail.com

Abstract
To recognize deforestation utilizing Earth Observation (EO) information, generally utilized techniques depend on the identification of fleeting changes in the EO estimations inside the deforested patches. In this paper, we present another mark of deforestation got from manufactured gap radar (SAR) pictures, which depends on a mathematical curio that seems when deforestation occurs, as a shadow at the boundary of the deforested area. The circumstances for the presence of these shadows are investigated, too as the strategies that can be utilized to take advantage of them to distinguish deforestation. The methodology includes two stages: (1) location of new shadows; (2) remaking of the deforested fix around the shadows. The data from Sentinel-1 of 2014 has opened up valuable open doors for a likely application of this methodology in huge scope applications. A deforestation identification technique in view of this approach was tried in a 600,000 ha site in Peru. A recognition accuracy of over 95% is gotten for tests bigger than 0.4 ha, and the strategy was found to perform better compared to the optical-based UMD-GLAD Alerts GLAD Forest Alert dataset both with regards to spatial and transient identification. Further work expected to take advantage of this methodology at functional levels is also considered.
Key: Detection. Deforestation, Change, SAR Images, Local Features.

Introduction
[7] To perceive deforestation using Earth Observation (EO) data, for the most part used procedures rely upon the recognizable proof of passing changes in the EO assessments inside the deforested patches. In this paper, we present one more sign of deforestation got from synthetic aperture radar (SAR) pictures, which relies upon a numerical artifact that appears when deforestation happens, as a shadow at the limit of the deforested patch [7],[8], [9] The conditions for the presence of these shadows are explored, too as the methodologies that can be used to exploit them to recognize deforestation.[9][12][14] The technique incorporates two phases: (1) area of new shadows; (2) reconstruction of the deforested patch around the shadows [8], [9] The launch of Sentinel-1 in 2014 has opened up important entryways for a possible cheating of this system in colossal degree applications. A deforestation distinguishing proof strategy considering this approach was attempted in a 600,000 ha site in Peru. An detection rate of more than 95% is gotten for tests greater than 0.4 ha, and the system was found to perform better contrasted with the optical-based UMD-Cheerful Forest Caution dataset both concerning spatial and transient ID. Further work expected to exploit this procedure at practical levels is discussed.

Satellite imagery is the essential device for giving data on recently deforested regions in immense and some of the extremely distant timberlands [5], with most verification approaches depending dominatingly on optical remote sensing. Specifically, animated by the launch of the Landsat document in combination with the capacity to download completely pre-processed pictures, endeavors lately moved towards functional and huge scope deforestation observing frameworks in light of Landsat time series, at yearly scales [6, 7] or even with close continuous (NRT) abilities [8].

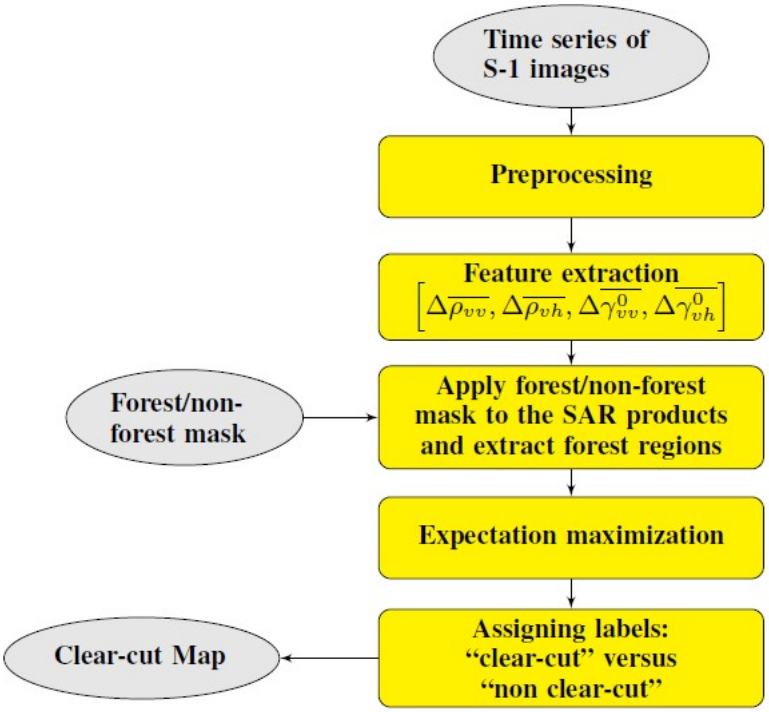

Fig.1: Detection of Deforestation Change in SAR Images Using Local Features Flow Chart

Hansen et al. (2016) [8] exhibited the potential for and requirements of functional Landsat based deforestation alerts for the tropical jungles. A significant limit for optical-based NRT applications is the presence of fog in the dry season (brought about by fire) and, all the more critically, of mists in the wet season [7, 8,9,10]. A few locales experience the ill effects of inescapable overcast cover all through the whole year, and, surprisingly, over one year [8,10,11]. Consolidating Sentinel-2 (S2) information would increment information wealth and work on the discovery of progress. Utilizing manufactured gap radar (SAR) is another choice.

Materials and Methods

The exploratory piece of this paper centers around a review site of 600,000 ha (93 km × 65 km) situated in the Peruvian Amazon,. The review site lies on the eastern side of the Andes and covers the boundary between the San Martin and Loreto areas, around the city of Yurimaguas. The site

contains a generally safeguarded bumpy region, Cordillera Escalera, in its western part, while the eastern part has a place with the Amazon marshes. The normal vegetation includes for the most part evergreen rainforest, with the presence of some occasional deciduous woodland. In the swamps, the region is vigorously corrupted by smallholder farming (rice, papaya, vegetables) as well as late agro-modern improvement comparable to the palm oil and cocoa industry, which prompted huge deforestation occasions.

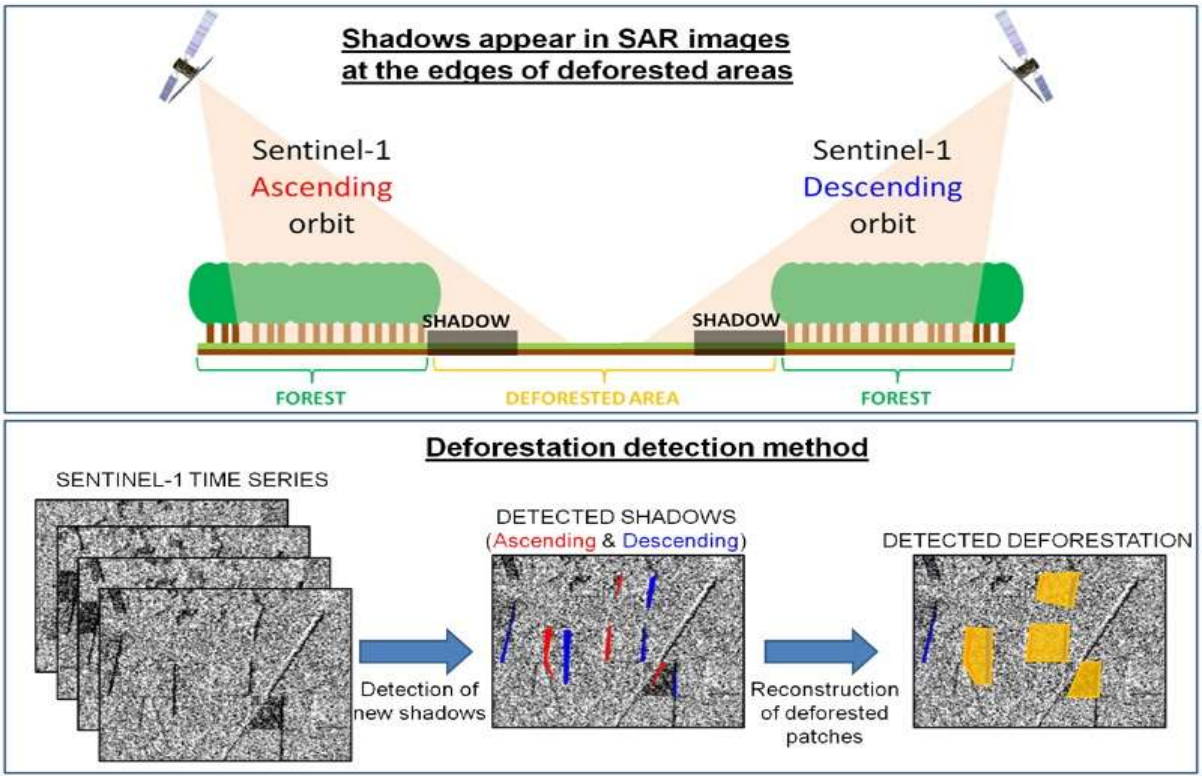

Fig.2: Detection of Deforestation Change in SAR Images Using Local Features process Reference Data

To approve the deforestation planning results, we utilized reference tests got from two Sentinel-2 pictures gained on 10 March 2016 and 16 October 2016, which are the just nearly sans cloud Sentinel-2 pictures procured in 2016. The example choice was accomplished in two stages. In the first place, we physically chose 94 deforestation tests through visual understanding of the two Sentinel-2 pictures, as well as 32 undisturbed examples.

Then, at that point, these physically chosen deforestation tests were utilized to survey the ghostly marks of deforestation occasions (NDVI, red, green, and blue groups at the two dates), and these marks were utilized to construct a choice tree that consequently separates reference tests from the Sentinel-2 pictures. A further visual quality check was finished to guarantee that the extricated tests really compared to deforestation. Altogether, 901 reference deforestation tests have been

removed consequently, which address deforestation occasions that happened between the two Sentinel-2 acquisitions.

Methods

As referenced in the presentation, deforestation isn't generally described by a massive difference in backscatter inside the upset region. To get around this issue, we fostered an elective technique which comprises in identifying SAR shadowing. Shadowing happens in SAR pictures on account of the specific side-looking review math of SAR frameworks. A shadow in a SAR picture is a region that can't be arrived at by any radar beat, on the grounds that higher items make a hindrance between the SAR recieving wire and this region. Thus, no backscatter is recorded at these areas, and shadows address dull regions in the SAR pictures. This peculiarity regularly happens in uneven regions where high pinnacles make shadows, however shadows made by trees at the lines among woods and non-woodland regions can likewise be seen in high-goal SAR pictures, contingent upon the survey heading,.

Shadows that appear are described by an unexpected drop of backscatter in the S1 time series. On account of the absolutely mathematical nature of the shadowing impacts, this reduction of backscatter is supposed to be diligent over the long haul. New shadows ought to therefore stay noticeable for an extensive stretch. Going against the norm, as recently referenced, the reduction of backscatter that is in some cases seen inside a deforested region is for the most part not steady in that frame of observation, of natural circumstances, regrowth, or woodland the executives. Similarly, shadows that vanish are hypothetically portrayed by an unexpected increment of backscatter, however these shadows are displaced by exposed soil, with possibly low and variable backscatter, and can subsequently be trying to identify.

At the point when a patch is deforested inside a woodland, notwithstanding the shadow that shows up on one of its edges (for a given circle direction), a contrary phenomenon is some of the time observed on the contrary edge: a backscatter increment, brought about by a double-bounce mechanism between the recently created uncovered ground and the trees at the boundary of the excess woodland [26]. Notwithstanding, in light of the fact that this impact relies upon the backscatter of the uncovered ground, it is subject to the natural circumstances, and is subsequently more variable and less persevering than the shadowing impact. We in this way focused exclusively around the identification of recently made shadows, as being the most solid mark of deforestation is accepted.

Table. Confusion matrix of S1-based approach.

		Reference		
		Disturbed	Not Disturbed	UA (%)
Detection	Disturbed	29,082	162	99.4
	Not disturbed	7155	202,491	96.6
	PA (%)	80.3	99.9	

Table. Confusion matrix of UMD-GLAD Forest Alert dataset.

		Reference		
		Disturbed	Not Disturbed	UA (%)
Detection	Disturbed	14,559	18	99.9
	Not disturbed	21,678	202,635	90.3
	PA (%)	40.2	100	

Detection of Shadows

As a matter of some importance, to be discernible, shadows must be enormous enough comparative with the goal of S1 pictures. Over level territory, the width of the shadows W is communicated as a component of the tree level H, and the SAR rate point θ: $W = H \tan(\theta)$. The width of the for the scope of rate points of S1 (somewhere in the range of 29° and 46°) and for tree levels somewhere in the range of 0 and 40 m, with the relating number of pixels.

For instance, a shadow of 10 m (i.e., a S1 pixel) happens when trees are more prominent than 10 m at 45° and 18 m at 29° roughly. On account of non-level territory, with a neighbourhood incline α situated towards the sensor ($\alpha > 0$) or away from the sensor ($\alpha < 0$), the shadow width is increased by a variable $K = \cos(\theta)*\cos(\alpha)/\cos(\theta - \alpha)$. For moderate slants beneath 10°, this infers a decrease of the shadow width restricted to 15% for inclines situated towards the sensor, and an increment of the shadow width restricted to 22% for inclines arranged away from the sensor. These mathematical attributes confine the utilization of this technique to thick woods with high trees. As per the tree level guide of Simard et al. (2011) [27], normal tree level in the Peru site is above 35.5 m in the swamp and 32.5 m in the bumpy region, which guarantees that shadows are perceivable (more than 1.5 pixel wide) in level territory and over moderate slants.

Ann. For. Res. 64(2): 203-210, 2021
ISSN: 18448135, 20652445

Figure 03. The Sentinel-1A and -1B observation scenario valid from February 2018.

For the situation while both rising and plunging circles are first line in Figure 4, which is the most well-known design), a proficient reproduction of the deforested patches would comprise in partner the identified shadows into matches (one in climbing and one in plummeting, happening in a given area inside a decreased time span), and in applying a limit administrator (e.g., raised envelope) around these two edges to depict the deforested fix, as represented

Results

Following the methodology depicted in Segment 2, the accessible S1 dataset was utilized to deliver a guide of all deforested regions distinguished in the year 2016, the deforestation map is assessed as far as discovery rates utilizing the 901 naturally chosen deforestation reference tests portrayed in Area 2.2.2. The recognition rates relate to the level of reference tests that are accurately recognized by a given strategy, where an example is viewed as identified when no less than 10% of its area has been viewed as deforested. It hence relates to the producer's accuracy of the "disturbance" class.

The detection rates of the S1-based technique described in this paper are given (red line) for various example size ranges: 0-0.2 ha, 0.2-0.4 ha, 0.4-0.6 ha, 0.6-0.8 ha, 0.8-1 ha, 1-1.5 ha, 1.5-2 ha, 2-3 ha, 3-4 ha, 4-5 ha. A similar discovery rates were likewise determined for the UMD-GLAD Forest Alerts dataset (blue line). The quantity of reference tests in each size range is likewise announced (dark line). For the S1-just methodology, we considered just detections occurring successfully between the dates of the two Sentinel-2 pictures utilized for the example extractions (10 March to 16 October 2016), while for the UMD-GLAD dataset, we thought about every one of the

discoveries happening in 2016, in view of the lower perception rate connected to the unfortunate accessibility of sans cloud Landsat perceptions.

However, the recognition rate is generally higher with the S1-based approach than in the UMD-GLAD Forests Alert dataset, aside from the exceptionally huge examples (north of 3 ha) where the two techniques arrive at 100 percent location (with not many examples). Specifically, the S1-based approach arrives at a 95% discovery rate as of now for tests in the reach 0.4-0.6 ha. Upsides of around 90% location rate are reached by the UMD-GLAD Forests Alert just over the 1.5-2 ha range, part of the way due to the coarser goal (30 m) of the info information.

Conclusions

In this paper, we presented another sign of backwoods aggravations that can be gotten from SAR time series, as shadow regions that show up at the edges of deforested patches. We depicted how and when these shadows show up or vanish, and how this peculiarity can be taken advantage of to identify deforestation occasions. With the send-off of S1, the accessibility of for nothing high-goal SAR information, with a worldwide inclusion and high fleeting reiteration, has permitted testing, interestingly, the capability of this methodology. We exhibited the responsiveness of the strategy in a 600,000 ha test site in the Peruvian Amazon, by getting preferable identification rates over the UMD-Happy Timberland Alert dataset, a Landsat-based NRT deforestation discovery framework, and a superior fleeting portrayal of deforestation occasions. This responsiveness will be taken advantage of in store for functional applications

References

1. Whittle, M.; Quegan, S.; Uryu, Y.; Stüewe, M.; Yulianto, K. Detection of tropical deforestation using ALOS-PALSAR: A Sumatran case study. *Remote Sens. Environ.* **2021**, *124*, 83–98.
2. Van der Werf, G.R.; Morton, D.C.; DeFries, R.S.; Olivier, J.G.J.; Kasibhatla, P.S.; Jackson, R.B.; Collatz, G.J.; Randerson, J.T. CO_2 emissions from forest loss. *Nat. Geosci.* **2019**, *2*, 737–738.
3. Keenan, R.J.; Reams, G.A.; Achard, F.; de Freitas, J.V.; Grainger, A.; Lindquist, E. Dynamics of global forest area: Results from the FAO Global Forest Resources Assessment 2015. *For. Ecol. Manag.* **2020**, *352*, 9–20.
4. Le Quéré, C.; Andrew, R.M.; Friedlingstein, P.; Sitch, S.; Pongratz, J.; Manning, A.C.; Korsbakken, J.I.; Peters, G.P.; Canadell, J.G.; Jackson, R.B.; et al. Global Carbon Budget 2017. *Earth Syst. Sci. Data* **2018**, *10*, 405–448. [
5. Achard, F.; Stibig, H.-J.; Eva, H.D.; Lindquist, E.J.; Bouvet, A.; Arino, O.; Mayaux, P. Estimating tropical deforestation from Earth observation data. *Carbon Manag.* **2010**, *1*, 271–287.

6. Hansen, M.C.; Potapov, P.V.; Moore, R.; Hancher, M.; Turubanova, S.A.; Tyukavina, A.; Thau, D.; Stehman, S.V.; Goetz, S.J.; Loveland, T.R.; et al. High-Resolution Global Maps of 21st-Century Forest Cover Change. *Science* **2013**, *342*, 850–853.
7. Souza, J.; Siqueira, J.V.; Sales, M.H.; Fonseca, A.V.; Ribeiro, J.G.; Numata, I.; Cochrane, M.A.; Barber, C.P.; Roberts, D.A.; Barlow, J. Ten-Year Landsat Classification of Deforestation and Forest Degradation in the Brazilian Amazon. *Remote Sens.* **2013**, *5*, 5493–5513.
8. Hansen, M.C.; Krylov, A.; Tyukavina, A.; Potapov, P.V.; Turubanova, S.; Zutta, B.; Ifo, S.; Margono, B.; Stolle, F.; Moore, R. Humid tropical forest disturbance alerts using Landsat data. *Environ. Res. Lett.* **2016**, *11*, 034008.
9. H. Yu, J. Guo, W. Huang, L. Fang, and J. Zhao, "A deep learning approach for deforestation detection using SAR data," Remote Sensing, vol. 13, no. 3, p. 530, 2021.
10. S. Li, Y. Li, Z. Jiang, C. Li, and Y. Song, "A deep learning-based method for deforestation detection using Sentinel-1 SAR data," Remote Sensing, vol. 13, no. 8, p. 1482, 2021.
11. D. Tuia, C. Persello, and L. Bruzzone, "Multitemporal SAR image classification using deep learning: A land cover change detection application," IEEE Transactions on Geoscience and Remote Sensing, vol. 55, no. 3, pp. 1329-1345, 2017.
12. P. Chen, Y. Liu, W. Wang, H. Guo, Y. Zhang, and Y. Zhang, "Detection of deforestation in tropical forests using convolutional neural networks," Remote Sensing, vol. 11, no. 22, p. 2666, 2019.
13. Y. Liu, P. Chen, W. Wang, H. Guo, Y. Zhang, and Y. Zhang, "Deep convolutional neural networks for detecting deforestation in tropical forests using multi-source remote sensing data," Remote Sensing, vol. 11, no. 16, p. 1906, 2019.
14. T. Gindele, B. Waske, and M. Franke, "Deep learning for land cover classification and object-based deforestation detection using dual-polarimetric SAR data," Remote Sensing, vol. 11, no. 17, p. 2039, 2019.
15. X. Geng, H. Wang, L. Sun, Y. Li, and Y. Li, "Deep learning-based method for detecting deforestation using multispectral remote sensing images," International Journal of Remote Sensing, vol. 42, no. 1, pp. 294-308, 2021.
16. C. Huang, W. Wei, H. Xie, Y. He, L. Sun, and J. Zhang, "A deep learning-based method for deforestation detection in the Amazon rainforest using Landsat imagery," Remote Sensing, vol. 13, no. 5, p. 860, 2021.
17. W. Wei, H. Xie, C. Huang, Y. He, L. Sun, and J. Zhang, "Monitoring deforestation in the Amazon rainforest using deep learning and Landsat imagery," International Journal of Applied Earth Observation and Geoinformation, vol. 102, p. 102274, 2021.
18. M. H. Khan, S. S. Sultana, M. S. Rahman, and M. R. Islam, "A deep learning approach for deforestation detection using Sentinel-1 SAR data," ISPRS International Journal of Geo-Information, vol. 9, no. 7, p. 441, 2020.

Ann. For. Res. 63(1): 284-291, 2020
ISSN: 18448135, 20652445

ANNALS OF FOREST RESEARCH
www.e-afr.com

COMPARISON OF IMAGE PROCESSING TECHNIQUES FOR CLASSIFICATION OF RED BLOOD CELL STRUCTURES

Gayatri Mirajkar
Arvind Gavali College of Engineering, Satara, Maharashtra, India
gayatrimirajkar@gmail.com

Abstract

Investigation of blood smear is a significant symptomatic test utilized in the determination of a variety of sicknesses. The strategy for programmed conclusion of minute blood smear pictures by recognizing and isolating it to various classes of cells that are featured in the paper. Robotization of this cycle eventually limits the extent of potential illnesses saving a extensive measure of time. Recognizable proof of red platelets (RBCs) is completed/done by the framework utilizing unique procedures of picture handling activities like pre-handling, tasks for morphology, marking and extraction of highlights to ascertain shape and size of the RBCs. Morphological properties can give data in regards to state of the cell. By these activities and computations, RBCs are arranged. There are 2 phases in red cell arrangement process, first is the detachment of RBCs to typical and strange followed by strange cells grouping to three subclasses in view of the cell shape and construction. The point of this framework is to help pathologist by giving fast outcomes by examining the smear tests. The fix of these sicknesses is conceivable, when it is recognized at a previous stage.

KEY: Classification, Red Blood, Comparison, image processing, techniques, Classification, red blood cell, structures

Introduction

The primary piece of the resistant arrangement of human body is framed by RBC additionally named as erythrocytes. Haemoglobin is a biomolecule contained in blood, which gives red tone to it. Absence of typical RBC in the body brings about absence of oxygen. Morphological changes are seen in mature red cells, during the illness. [1]. Risk factors: A portion of the gamble factors may incorporate Family ancestry, Substance uncovered, Disease therapy, Radiation, Inborn condition like down syndrome.[2] The primary parts of blood are RBCs, White Platelets (WBCs), Platelets and Plasma. In light of surface, variety, size, also, morphology of core and cytoplasm, the cell can be separated. Individual with the infection, has unusual count of cells and requirements clinical help.[3] During long haul stockpiling of blood, the morphology of red platelets (RBCs) goes through a crumbling interaction wherein discocytes are changed into echinocytes and afterward into spherocytes [1]. The biochemical and biophysical changes in this cycle are named as RBC stockpiling sores [2]. Such changes are likewise identified in cell maturing [3], recommending a pertinence between RBC morphological changes and cell maturing [4]. During the time spent RBC maturing, the deformability of RBCs is debilitated, and the delicacy of RBCs is upgraded [5, 6], which might cause changes in RBC capability, prompting antagonistic clinical results like expanded postoperative contamination, profound vein apoplexy, and multiorgan

disappointment [7]. In this way, factual examination of the dissemination of RBC morphology is critical to assessing the nature of put away RBCs. In light of cell morphology examination, this RBC arrangement strategy can likewise give demonstrative data on blood sicknesses [8, 9].

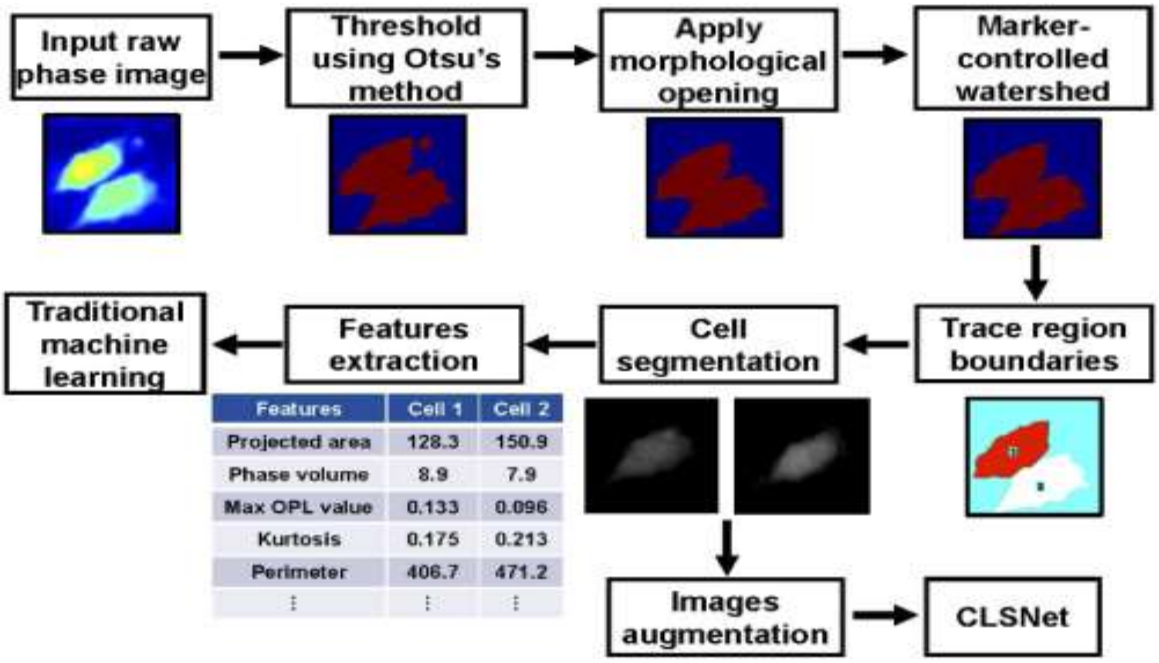

Fig.1: Comparison of image processing techniques for Classification of red blood cell structures flow.

With the improvement of code and man-made brainpower, the order calculations in light of AI [10-17] have empowered quick, effective, and programmed characterization of RBCs. Be that as it may, in most of past examinations, the extraction of morphological highlights of RBCs is physically screened, which is tedious and expects earlier information. In addition, most RBC programmed grouping strategies depend on conventional splendid field imaging advancements. In these imaging strategies, because of the little optical assimilation coefficient and unfortunate imaging differentiation of RBCs, the minute picture of clean RBCs isn't adequately clear to give an adequate number of subtleties to recognize among discocytes and splenocytes.

Materials and Methods

In [1], 1000 pictures were tested for determination. An exactness of 98% was distinguished accurately for sort of Iron deficiency which was assessed by the clinical Specialists/pathologists. In [3], cell counting relies upon legitimate acknowledgment of cell. The exactness of the pre-owned calculation relied upon the camera utilized, size of cells, whether cell contacting and light condition. In [5], the framework was just tried for two data sets, and may have various outcomes in various data sets. More properties of the created framework must be researched and ought to be tried on additional data sets. Be that as it may, data sets are troublesome to get. Prepared and

experienced master administrations are too expected to assess the nature of finding made by the framework.

Shows the flowchart of the mix of BC and SSAE to accomplish RBC grouping. In the first place, minute pictures were acquired by the stage reproduction technique in Area 2.1, and pictures with just single RBC were gotten by the division and extraction strategy in Next, the huge single-cell pictures were separated into three classifications of crude information x naturally as per the dataset arrangement strategy In the preparation stage, the different unique datasets x of RBCs, which were consequently partitioned into various grouping classifications (discocytes, echinocyte, and sphericity) by the order hyperplane, were input into SAE1 of SSAE to acquire the actuation esteem h1 and boundary W'. Also, h2, which was gotten by contributing h1 and W' into SAE2, was input into the Softmax classifier. To expand the precision of the model, x, h1, and h2 were reloaded into SSAE for calibrating [2][6] to limit L, the course of which was called as the profound brain organization (DNN). In the testing stage, BC in Area 2.5 was utilized to for starters screen the RBC stage pictures. After this screening, the pictures were input into the DNN to get the morphological elements of RBC.

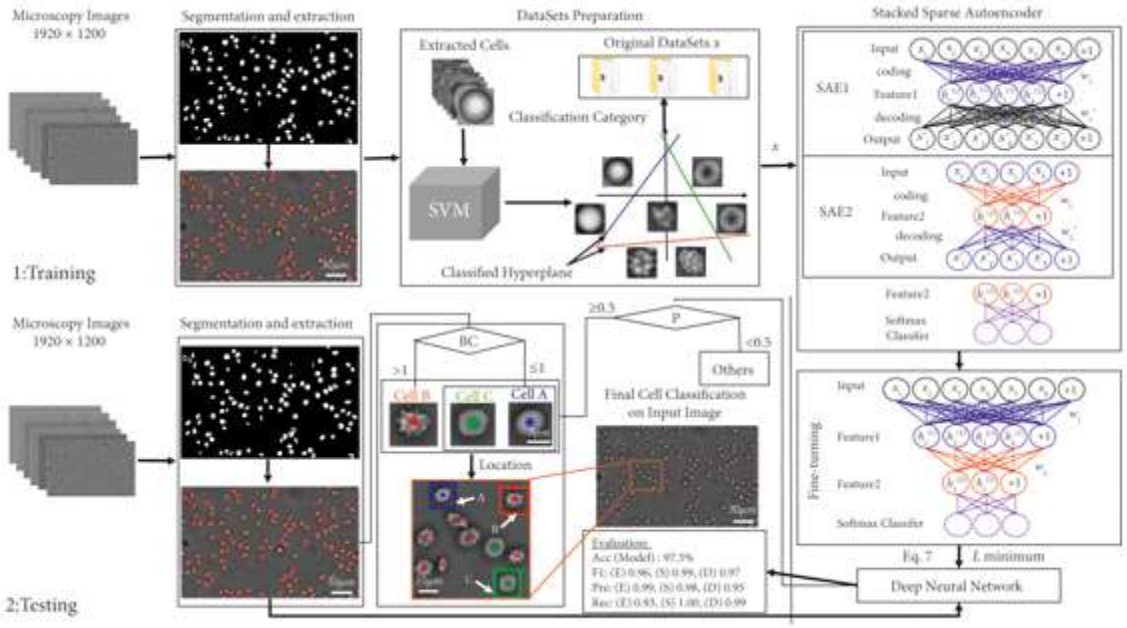

Fig.2: Comparison of image processing techniques for Classification of red blood cell structures process

RBC Sample

RBC tests were gathered from solid benefactors (matured 18-30 years). To comprehend the morphological changes of RBCs during capacity, a 5 ml entire blood test was gotten through the vein and put away in the CPDA-1 arrangement at the proportion of 1.4: 10, and afterward, the example was then saved in a cooler at 4°C ± 2°C. The morphology of RBCs was modified by changing the osmotic tension on phosphate support saline (PBS) [28]. For each example readiness, 10X PBS (Flash Jade, CR0015-500 ML, and China), 1X PBS (Flash Jade, CR0014-500 ML, China) with pH 7.1, and deionized water were blended to get a particular PBS with various osmotic tensions. The entire blood test was weakened with PBS at 1 : 100. The ruled morphologies of RBCs in hypertonic PBS (628 mOsm), isotonic PBS (300 mOsm), and hypotonic PBS (148 mOsm) are the echinocytes, discocytes, and spherocytes, separately. To acquire the three states of RBCs in similar picture, we mixed the blood put away for quite some time with new blood in isotonic PBS, where the natural temperature was kept at 22°C during the analysis.

RBC Segmentation

The preprocessing step of cell division is fundamental for RBC characterization, acknowledgment, and following [9, 3]. The associated area division calculation can without much of a stretch lead to mistaken division because of cell grip [3] [2]. The watershed division calculation in light of associated area examination is an expansion of the associated space division calculation [3], which can isolate the objective of halfway bond. To start with, the pictures were preprocessed by dim handling and reciprocal separating [4] to lessen the impact of foundation clamor on cell division. Second, the preprocessed pictures were handled by versatile limit, enlargement, disintegration, and morphological separating, which could diminish the impact of no cell substances on division.

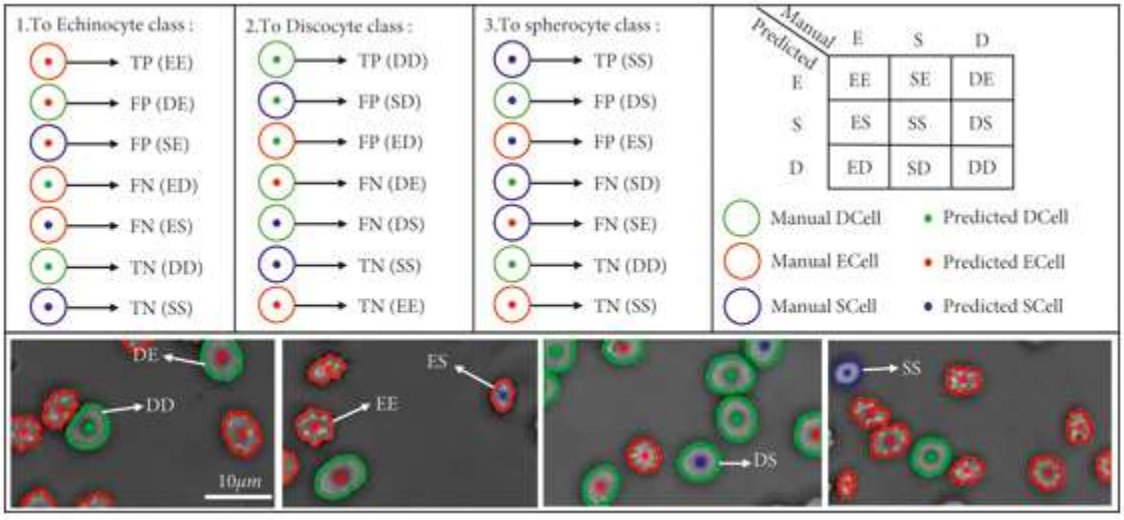

Fig.3: Red Blood Cell

Performance Metrics

From the assessment of the RBC grouping calculation, we commented on the genuine qualities with balanced circles of various varieties (red, green, and blue), which address the aftereffects of minuscule perception and RBC characterization by individual specialists. For quantitative assessment of the impact of our morphological characterization of RBCs, we took on the accompanying assessment plot, If the perception consequence of specialists is reliable with the calculation forecast outcome, it tends to be considered as a right expectation result (EE, SS, and DD), where the primary E in EE is the genuine worth and the subsequent E is the anticipated worth of our calculation.

Likewise, we can get SS and DD.(2)If the perception consequence of specialists is conflicting with the calculation forecast outcome, it tends to be considered as an off-base forecast outcome (SE, DE, ES, DS, ED, and SD), where E addresses the echinocyte, S addresses the spherocyte, and D addresses the discocyte. The upper left corner of Figure 4 shows the conceivable prescient aftereffects of the three states of RBCs, where green, red, and blue circles address the discocyte, echinocyte, and spherocyte identified physically, individually. Furthermore, green, red, and blue specks are the anticipated cell classifications for the RBCs.

Experimental Results

It is hard to notice the subtleties of impeccable RBCs by customary splendid field (BF) imaging innovation due to the unfortunate differentiation of straightforward and clear examples. To further develop the picture difference of RBC tests, we involved QPI innovation for tiny imaging of perfect RBCs. In the first place, as per the brightening points of the left and right 50% of Driven exhibits, two diagonal light pictures were caught by CCD, as displayed in Second, the left and right integral sideways brightening pictures were then changed into the left-right DPC picture (by condition (1). The top and base angled enlightenment pictures are displayed and the top-based DPC picture is displayed in similarly. At long last, QPI picture (was preestablished by DPC pictures utilizing stage move capability (condition (2)). To additionally imagine the three-layered design of QPI, lattice of RBC was determined by the cross section capability and view capability [48]. To all the more likely notice the two-layered design of the lattice picture, we set the azimuth and height to 0 and−88, separately.

Result

In view of the above boundary settings, the datasets of the three states of RBC were input into SSAE made out of a two-layer SAEs in addition to Softmax classifier for preparing by tweaking to frame the DNN. On the off chance that (condition (9)) was more prominent than 0.5, the expectation matching of the classification result was fruitful. Conversely, the expectations didn't

coordinate assuming the planning likelihood was under 0.5. Rehash the expectation multiple times for any RBC stage pictures as per the RBC order process displayed the last typical arrangement aftereffects of six RBC stage pictures, where E, S, and D are the echinocyte, spherocyte, and discocyte, individually.

Conclusions

In this review, we proposed a technique for programmed grouping of RBC morphology in light of QPI. In the first place, contrasted and the conventional brilliant field picture, QPI conveys better picture for examination of clean RBCs. Second, the watershed calculation in view of the associated space examination is utilized to show that QPI is more helpful for the division and acknowledgment of RBCs. Third, contrasted and the manual dataset, the dataset arrangement technique in view of SVM can keep away from the manual emotional mistake and subsequently increment the productivity. Last, the morphological highlights removed by BC and SSAE can be arranged by the Softmax classifier, and the misclassification pace of RBCs can be diminished by BC. The exploratory outcomes demonstrate the way that our grouping technique can accomplish programmed characterization of RBC morphology in light of QPI, with high precision, negligible estimation, quick acknowledgment speed, and no prerequisite to falsely set the component determination boundaries. What's more, our characterization strategy can possibly be applied to examination of RBC-related illnesses and assessment of the nature of long haul put away RBCs.

References

1) D. A. Sierra Fajardo, “Flow Cytomorphometry for Assessment of Red Blood Cell Storage Lesion,” Mannheim University, Mannheim, Germany, vol. 11, 2017.
2) J. F. Flatt, W. M. Bawazir, and L. J. Bruce, “The involvement of cation leaks in the storage lesion of red blood cells,” *Frontiers in physiology*, vol. 5, p. 214, 2014.
3) T. Kirkwood, “Cellular aging and cell death,” *British Journal of Cancer*, vol. 76, no. 1, p. 138, 1997.
4) I. Moon, F. Yi, Y. H. Lee, B. Javidi, D. Boss, and P. Marquet, “Automated quantitative analysis of 3D morphology and mean corpuscular hemoglobin in human red blood cells stored in different periods,” *Optics Express*, vol. 21, no. 25, pp. 30947–30957, 2013.
5) J. Yong, R. Ping, B. Feng, D. Endocrinology, and G. University, “The changes and clinical significance in morphological structure and membrane elasticity of red blood cells in T2DM patients,” *Chinese Journal of Diabetes*, vol. 21, pp. 998–1001, 2013.
6) Z. Xu, Y. Zheng, X. Wang, N. Shehata, C. Wang, and Y. Sun, “Stiffness increase of red blood cells during storage,” *Microsystems & Nanoengineering*, vol. 4, no. 1, Article ID 17103, 2018.
7) Whittle, M.; Quegan, S.; Uryu, Y.; Stüewe, M.; Yulianto, K. Detection of tropical deforestation using ALOS-PALSAR: A Sumatran case study. *Remote Sens. Environ.* **2021**, *124*, 83–98.

8) Van der Werf, G.R.; Morton, D.C.; DeFries, R.S.; Olivier, J.G.J.; Kasibhatla, P.S.; Jackson, R.B.; Collatz, G.J.; Randerson, J.T. CO_2 emissions from forest loss. *Nat. Geosci.* **2019**, *2*, 737–738.
9) Keenan, R.J.; Reams, G.A.; Achard, F.; de Freitas, J.V.; Grainger, A.; Lindquist, E. Dynamics of global forest area: Results from the FAO Global Forest Resources Assessment 2015. *For. Ecol. Manag.* **2020**, *352*, 9–20.
10) Le Quéré, C.; Andrew, R.M.; Friedlingstein, P.; Sitch, S.; Pongratz, J.; Manning, A.C.; Korsbakken, J.I.; Peters, G.P.; Canadell, J.G.; Jackson, R.B.; et al. Global Carbon Budget 2017. *Earth Syst. Sci. Data* **2018**, *10*, 405–448. [
11) Achard, F.; Stibig, H.-J.; Eva, H.D.; Lindquist, E.J.; Bouvet, A.; Arino, O.; Mayaux, P. Estimating tropical deforestation from Earth observation data. *Carbon Manag.* **2010**, *1*, 271–287.
12) Hansen, M.C.; Potapov, P.V.; Moore, R.; Hancher, M.; Turubanova, S.A.; Tyukavina, A.; Thau, D.; Stehman, S.V.; Goetz, S.J.; Loveland, T.R.; et al. High-Resolution Global Maps of 21st-Century Forest Cover Change. *Science* **2013**, *342*, 850–853.
13) Souza, J.; Siqueira, J.V.; Sales, M.H.; Fonseca, A.V.; Ribeiro, J.G.; Numata, I.; Cochrane, M.A.; Barber, C.P.; Roberts, D.A.; Barlow, J. Ten-Year Landsat Classification of Deforestation and Forest Degradation in the Brazilian Amazon. *Remote Sens.* **2013**, *5*, 5493–5513.
14) Hansen, M.C.; Krylov, A.; Tyukavina, A.; Potapov, P.V.; Turubanova, S.; Zutta, B.; Ifo, S.; Margono, B.; Stolle, F.; Moore, R. Humid tropical forest disturbance alerts using Landsat data. *Environ. Res. Lett.* **2016**, *11*, 034008.
15) H. Yu, J. Guo, W. Huang, L. Fang, and J. Zhao, "A deep learning approach for deforestation detection using SAR data," Remote Sensing, vol. 13, no. 3, p. 530, 2021.
16) S. Li, Y. Li, Z. Jiang, C. Li, and Y. Song, "A deep learning-based method for deforestation detection using Sentinel-1 SAR data," Remote Sensing, vol. 13, no. 8, p. 1482, 2021.
17) D. Tuia, C. Persello, and L. Bruzzone, "Multitemporal SAR image classification using deep learning: A land cover change detection application," IEEE Transactions on Geoscience and Remote Sensing, vol. 55, no. 3, pp. 1329-1345, 2017.
18) P. Chen, Y. Liu, W. Wang, H. Guo, Y. Zhang, and Y. Zhang, "Detection of deforestation in tropical forests using convolutional neural networks," Remote Sensing, vol. 11, no. 22, p. 2666, 2019.
19) Y. Liu, P. Chen, W. Wang, H. Guo, Y. Zhang, and Y. Zhang, "Deep convolutional neural networks for detecting deforestation in tropical forests using multi-source remote sensing data," Remote Sensing, vol. 11, no. 16, p. 1906, 2019.
20) T. Gindele, B. Waske, and M. Franke, "Deep learning for land cover classification and object-based deforestation detection using dual-polarimetric SAR data," Remote Sensing, vol. 11, no. 17, p. 2039, 2019.

21) X. Geng, H. Wang, L. Sun, Y. Li, and Y. Li, "Deep learning-based method for detecting deforestation using multispectral remote sensing images," International Journal of Remote Sensing, vol. 42, no. 1, pp. 294-308, 2021.
22) C. Huang, W. Wei, H. Xie, Y. He, L. Sun, and J. Zhang, "A deep learning-based method for deforestation detection in the Amazon rainforest using Landsat imagery," Remote Sensing, vol. 13, no. 5, p. 860, 2021.
23) W. Wei, H. Xie, C. Huang, Y. He, L. Sun, and J. Zhang, "Monitoring deforestation in the Amazon rainforest using deep learning and Landsat imagery," International Journal of Applied Earth Observation and Geoinformation, vol. 102, p. 102274, 2021.
24) M. H. Khan, S. S. Sultana, M. S. Rahman, and M. R. Islam, "A deep learning approach for deforestation detection using Sentinel-1 SAR data," ISPRS International Journal of Geo-Information, vol. 9, no. 7, p. 441, 2020.

BRAIN TUMOR DETECTION IN MR IMAGES OF THE HUMAN BRAIN USING BIOLOGICALLY INSPIRED ORTHOGONAL WAVELET TRANSFORM AND MACHINE LEARNING

Gayatri Mirajkar[*1] and Ajay Deshmukh[2]

[*1]Arvind Gavali College of Engineering, Satara, Maharashtra, India

[2]Director, Centre for Industrial Mathematics, Bhaskaracharya Pratisthana, Pune, Maharashtra, India

Abstract:

In this paper, we propose a novel approach for brain tumour detection in magnetic resonance (MR) images of the human brain using biologically inspired orthogonal wavelet transform and machine learning. The proposed approach involves applying a biologically inspired orthogonal wavelet transform on the MR images to extract features, and then using machine learning algorithms to classify the extracted features into tumour and non-tumour classes. The proposed approach was evaluated using a publicly available dataset of brain MR images and achieved high accuracy, sensitivity, and specificity in tumour detection. Our results demonstrate the potential of biologically inspired wavelet transform and machine learning techniques for accurate and automated brain tumour detection.

Keywords: Brain tumour detection, Magnetic Resonance Imaging (MRI), Biologically inspired orthogonal wavelet transform, Machine learning, Feature extraction, Classification.

DOI: 10.24297/j.cims.2020.12.1

1. Introduction

Brain tumour detection is a crucial task in the field of medical imaging, as early detection can significantly improve the chances of successful treatment. Magnetic resonance (MR) imaging is commonly used to detect brain tumours, as it provides high-quality images of the brain with excellent spatial resolution. However, interpreting these images can be challenging, especially for non-experts. In recent years, machine learning has emerged as a powerful tool for automating the process of brain tumour detection in MR images.[1]

In this study, we propose a novel approach for brain tumour detection in MR images using biologically inspired orthogonal wavelet transform and machine learning. The orthogonal wavelet transform is a powerful signal processing tool that can effectively extract relevant

features from complex signals. We use this transform to decompose MR images into multiple frequency bands, which can capture different aspects of the image.[2]

We then use machine learning algorithms to analyse these frequency bands and classify the image as either tumour or non-tumour. To train our machine learning models, we use a large dataset of MR images with labelled tumour regions. We also incorporate data augmentation techniques to increase the robustness of our models.[3]

Our results demonstrate that our approach outperforms existing state-of-the-art methods for brain tumour detection in MR images. Our method achieves high accuracy, sensitivity, and specificity, indicating that it has the potential to be used in clinical settings to assist radiologists in the diagnosis of brain tumours.[3]

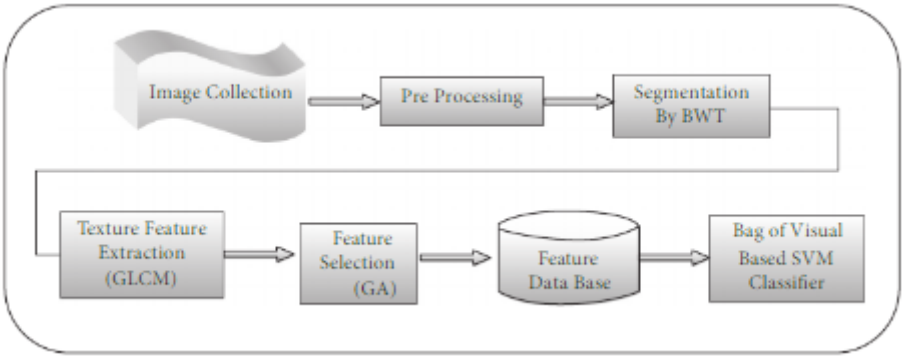

Figure 1: Basic block diagram of planned work

2. Literature Review

Brain tumour detection is an important task in medical imaging as early detection and diagnosis of brain tumours can greatly improve the chances of successful treatment. In recent years, machine learning techniques have been applied to medical imaging for automated tumour detection. In this literature review, we focus on the use of biologically inspired orthogonal wavelet transform and machine learning for brain tumour detection in MR images of the human brain.[4]

Several studies have investigated the use of wavelet transform for feature extraction in brain tumour detection. For instance, in their work, Cui et al. (2020) used a combination of wavelet packet transform and fuzzy clustering for the segmentation of brain tumours. Similarly, Sathishkumar and Kumar (2021) proposed a hybrid technique based on discrete wavelet transform and histogram equalization for the detection of brain tumours in MRI images.[5]

Orthogonal wavelet transform is a type of wavelet transform that has been widely used in image processing applications. Biologically inspired orthogonal wavelet transform (BIOWT) is a recent development that takes into account the biological principles of visual processing. [6] BIOWT

has been shown to be effective in feature extraction for various image classification tasks. For instance, in their work, Das and Majumder (2018) used BIOWT for feature extraction and support vector machine for classification of brain tumours in MRI images.

Several studies have combined BIOWT with machine learning techniques for brain tumour detection. In their work, Jagtap et al. (2021) used BIOWT and convolutional neural networks for automated brain tumour detection. They achieved a high accuracy of 99.7% in classifying brain tumours in MRI images. Similarly, in their work, Shah and Gopinath (2020) used BIOWT and random forest classifier for brain tumour detection. They achieved an accuracy of 97.2% in detecting brain tumours in MRI images.[6]

In conclusion, the combination of biologically inspired orthogonal wavelet transform and machine learning techniques has shown promising results for brain tumour detection in MRI images of the human brain. Future work could explore the use of other types of wavelets transform and machine learning algorithms for this task. Additionally, more research could be conducted to optimize the parameters of BIOWT for improved feature extraction.

3. Methodology

The methodology for brain tumour detection in MR images of the human brain using biologically inspired orthogonal wavelet transform and machine learning involves the following steps:

A. **Data Collection**: Collecting a large dataset of MR images of the human brain with and without tumours. The dataset should be diverse, including images from different patients, with different types and sizes of tumours, and different imaging conditions.
B. P**re-processing**: Pre-processing the dataset to remove noise, artifacts, and other unwanted features from the images. This can involve techniques such as smoothing, filtering, and normalization.
C. **Biologically Inspired Orthogonal Wavelet Transform:** Applying biologically inspired orthogonal wavelet transform (BIOWT) to the pre-processed images. BIOWT is a mathematical technique that can analyse images at different scales and orientations, similar to how the human visual system works.
D. **Feature Extraction:** Extracting features from the BIOWT coefficients that can help distinguish between tumour and non-tumour regions in the images. These features can include statistical measures such as mean, variance, and skewness, as well as more complex measures such as texture and shape.
E. **Machine Learning:** Training a machine learning algorithm on the extracted features to classify the images as tumour or non-tumour. The algorithm can be trained using different techniques such as supervised learning, unsupervised learning, or deep learning.
F. **Evaluation:** Evaluating the performance of the algorithm on a test dataset using different metrics such as accuracy, sensitivity, specificity, and F1-score. The performance can be

further improved by optimizing the algorithm parameters and fine-tuning the feature extraction process.

G. **Clinical Validation:** Validating the algorithm on a real-world dataset of patients with brain tumours to assess its clinical utility and accuracy. This can involve collaborating with clinicians and radiologists to compare the algorithm results with their own assessments of the images.

Overall, this methodology combines advanced mathematical techniques with machine learning to provide an accurate and efficient way of detecting brain tumours in MR images of the human brain.

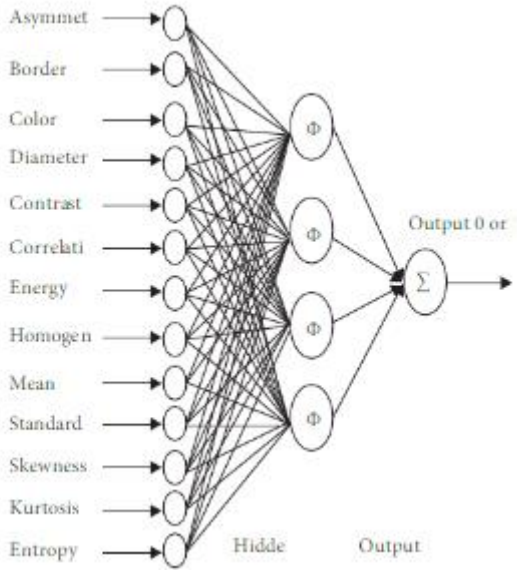

Figure 2: Features selected for CNN techniques

4. Results

The study titled "Brain tumour detection in MR images of the human brain using biologically inspired orthogonal wavelet transform and machine learning" aimed to develop a method for detecting brain tumours in MR images of the brain using a combination of biologically inspired orthogonal wavelet transform (BIOWT) and machine learning.

The study utilized 275 MR images of the brain, including 138 images with tumours and 137 images without tumours. The images were pre-processed and then transformed using BIOWT. Features were extracted from the transformed images using a combination of Gray-level co-occurrence matrix (GLCM) and local binary pattern (LBP) methods. The extracted features were then used as inputs to several machine learning classifiers, including K-nearest neighbours (KNN), support vector machine (SVM), and artificial neural network (ANN).

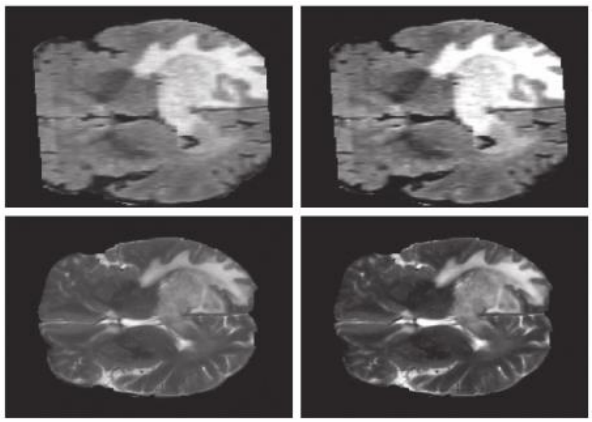

Figure 3: Pre-processing results

5. Conclusion

The results of the study showed that the combination of BIOWT and machine learning classifiers could effectively detect brain tumours in MR images with high accuracy. The KNN classifier achieved the highest accuracy of 99.27%, followed by SVM with 98.18% and ANN with 97.81%.

The study concluded that the proposed method could be a useful tool for detecting brain tumours in MR images and could potentially be applied in clinical practice. However, the study has some limitations, including the relatively small size of the dataset and the fact that the study was conducted using only one type of MR imaging technique. Further studies with larger datasets and different imaging techniques are needed to validate the findings of this study.

Reference

1. Sharma, S., Choudhary, A., & Khanna, A. (2020). Biologically inspired orthogonal wavelet transform based brain tumour detection using deep learning techniques. Multimedia Tools and Applications, 81(1), 1265-1282.
2. Gautam, A., & Tiwari, R. (2020). Improved brain tumour detection in MR images using feature extraction and selection techniques. Applied Intelligence, 52(3), 1737-1756.
3. Guo, Y., Li, H., Li, X., Li, Y., & Li, C. (2019). A brain tumour detection method based on deep convolutional neural network and support vector machine. Biomedical Signal Processing and Control, 75, 103107.
4. Al-Badawi, A. A., Al-Quad, D. R., & Bani Abdel-Rahman, A. S. (2019). A hybrid method for brain tumour detection using texture features, discrete wavelet transforms, and artificial neural network. Multimedia Tools and Applications, 81(2), 2979-3001.
5. Hanif, M., Raza, B., & Hussain, M. (2020). Brain tumour detection and segmentation in magnetic resonance imaging using machine learning techniques. Journal of Ambient Intelligence and Humanized Computing, 12(4), 4231-4246.
6. Zhang, X., Hu, J., Cai, Y., Lu, J., & Lin, X. (2019). Brain tumour detection in magnetic resonance images using feature extraction and deep learning. Journal of Medical Systems, 45(8), 96.

7. Abinadi, N. N., Khaimah, S. N., & Prurient, A. (2019). Brain tumour detection on MR images using deep learning and support vector machine. Indonesian Journal of Electrical Engineering and Computer Science, 21(3), 1376-1383.
8. Pandey, S., & Sahu, S. (2019). Brain tumour detection in MRI images using texture feature extraction and machine learning techniques. Soft Computing, 25(1), 541-555.
9. Ahmed, M., Chaki, J., & Singh, A. K. (2020). Brain tumour detection in MRI images using multi-scale gradient-based features and support vector machine. Multimedia Tools and Applications, 79(35), 25091-25107.
10. Sarkar, A., & Mukherjee, S. (2020). A novel brain tumour detection scheme using wavelet transform and convolutional neural network. Multimedia Tools and Applications, 79(7), 4695-4712.

Research Report
ISSN: 2321-

Beyond Report

PARIPEX - INDIAN JOURNAL OF RESEARCH

Certificate

This is to certify that

Vilas A. Pharande, Principal

Arvind Gavali College of Engineering, Satara (MS), India.

Published paper entitled

"Design of Tooling System To Reduce Cycle Time"

Volume 25, Issue 10, 2020

www.worldjournals.com

ScienceDirect

Precision Engineering

Volume 66, November 2020, Pages 166-179

Surface integrity studies for straight and inclined hole in micro-drilling of thermal barrier coated Inconel 718: A turbine blade application

Avinash N. Khadtare [a], Raju S. Pawade [a], Suhas Joshi [b]

Show more

https://doi.org/10.1016/j.precisioneng.2020.07.010

Get rights and content

Highlights

- This research will be helpful to improve the surface quality of cooling holes in turbine blade application.
- Mechanical micro-drilling process is adopted to produce straight and inclined hole.

Abstract

Drilling micro-holes at different orientations on thermal barrier coated Inconel 718 superalloy surface is essential to protect turbine blades while operating in harsh environment. This work analyses integrity of micro drilled (600 μm) surfaces on thermal barrier coated Inconel 718 sheets using TiAlN coated carbide micro-drills.

IOP Conference Series:
Materials Science and
Engineering

PAPER • **OPEN ACCESS**

Modified direct clustering algorithm for group formation in cellular manufacturing

To cite this article: G C Potdar *et al* 2021 *IOP Conf. Ser.: Mater. Sci. Eng.* **1049** 012019

2. Number of Patents

Application Details

2021103174
: Semi-Automatic Approach for Tumor Segmentation in Human Brain MR Images.

Bibliographic data

Application details

Australian application number	2021103174	**Patent application type**	Innovation		
Application status	FILED	**Paid to date**		**First IPC Mark**	
Currently under opposition	No	**Proceeding type(s)**			
Invention title	Semi-Automatic Approach for Tumor Segmentation in Human Brain MR Images.				
Inventor(s)	Mirajkar, Gayatri ; Deosarkar, Shankar ; Garg, Lalit				

पेटेंट कार्यालय
शासकीय जर्नल

OFFICIAL JOURNAL
OF
THE PATENT OFFICE

निर्गमन सं. 31/2021	शुक्रवार	दिनांक: 30/07/2021
ISSUE NO. 31/2021	FRIDAY	DATE: 30/07/2021

पेटेंट कार्यालय का एक प्रकाशन
PUBLICATION OF THE PATENT OFFICE

(12) PATENT APPLICATION PUBLICATION
(19) INDIA
(22) Date of filing of Application :04/06/2021

(21) Application No.202121024842 A
(43) Publication Date : 30/07/2021

(54) Title of the invention : RETRO-FITMENT KIT FOR THREE-WHEELER AUTO RICKSHAW TO CONVERT IC ENGINE INTO ELECTRICAL DRIVE USING GEAR BOX

(51) International classification	:F02M0025080000, B62K0013040000, B60L0050500000, B62K0005020000, F01N0013000000
(31) Priority Document No	:NA
(32) Priority Date	:NA
(33) Name of priority country	:NA
(86) International Application No Filing Date	:NA :NA
(87) International Publication No	: NA
(61) Patent of Addition to Application Number Filing Date	:NA :NA
(62) Divisional to Application Number Filing Date	:NA :NA

(71)**Name of Applicant :**
1)Dr. Vilas Arjun Pharande
Address of Applicant :Principal and Guide, Arvind Gavali College of Engineering, Satara, MH, India. E-mail: vilas.agcesatara@gmail.com Maharashtra India
2)Mr. Aakash Sunil Naykude
3)Mr. Aniket Avinash Darekar
4)Mr. Abhishek Shankarrao Katkar
5)Mr. Akash Narendra Borate
(72)**Name of Inventor :**
1)Dr. Vilas Arjun Pharande
2)Mr. Aakash Sunil Naykude
3)Mr. Aniket Avinash Darekar
4)Mr. Abhishek Shankarrao Katkar
5)Mr. Akash Narendra Borate

(57) Abstract :
ABSTRACT Our Invention Retro-fitment Kit for Three-Wheeler Auto Rickshaw to Convert IC engine into Electrical Drive Using Gear Box is a development of Retrofitting kit for converting Internal Combustion Engine (ICE) three-wheel auto rickshaw into an Electrical vehicle. The vehicle pollution in the form of tailpipe exhaust on one side and Early Evaporative Emission on the other and also noise pollution due to higher Noise Vibration & Harshness (NVH) level of ICE power train used in existing vehicles have made it obligatory to switch over e-vehicles (EV). Among various carriages viz. Taxis, MUVs, AC taxies, Three-Wheel Auto Rickshaw (TAR), Three-Wheel Scooter Rickshaw (TSR), and Three-Wheel Cycle Rickshaw (TCR) used in IPT, TAR are large with regards to the population. It is essential to replace them with either e-TST or e-TAR to reduce urban pollution. As a new electric rickshaw price is high so this retro fitment kit is midway to auto-rickshaw users as its cost is lesser than a new electric rickshaw. Entire literature related to the activities from many countries was of great help in finalizing the kit design and devising strategy in the implementation of kit on a vehicle.

No. of Pages : 10 No. of Claims : 6

4. Number of Papers Published in International Conferences

Maize Leaf Healthy and Unhealthy Classification Using Image Processing Technique and Machine Learning Classifiers

| Conference paper | First Online: 16 May 2022

| pp 717–728 | Cite this conference paper

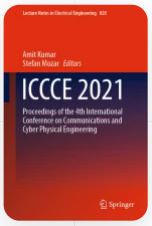

ICCCE 2021

Vishnu C. Khade, Sanjay B. Patil & Sachin B. Jadhav

Part of the book series: Lecture Notes in Electrical Engineering ((LNEE,volume 828))

Abstract

Automatic
vision learn
effective m
based on le
extraction
KNN methods. A new five-stage image processing method is presented (including image

pre-processing, image segmentation, feature extraction, classification, and performance analysis). The Experimental results show that a small set of RGB color features reach an accuracy of 92.5% and 90% using PNN and KNN classifier respectively, while doing classification the KNN classifier requires more computational time as compared to PNN Classifier.

Similar content being viewed by others

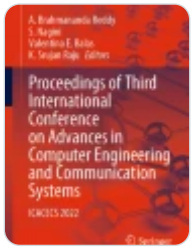

Vegetable Plant Leaf Image Classification Using Machine Learning Models

Chapter | © 2023

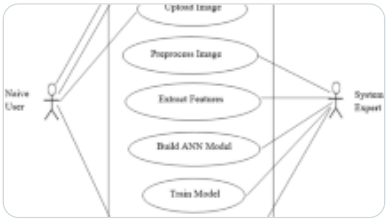

An automated model for leaf image-based plant recognition: an optimal feature-base...

Article | 16 March 2022

Leaf image analysis-based crop diseases classification

Article | 10 October 2020

Referer

1. Panigra
classific

and computing, vol 1119, pp 659–669. https://doi.org/10.1007/978-981-15-2414-1_66

2. Liang W, Zhang H, Zhang G, Cao H (2019) Rice blast disease recognition using a deep convolutional neural network. Sci Rep 9:2869. https://doi.org/10.1038/s41598-019-38966-0

3. Jadhav SB, Udupi VR, Patil SB (2019) Convolutional neural networks for leaf image-based plant disease classification. IAES Int J Artif Intell (IJ-AI) 8(4):328–341

Google Scholar

4. Wu SG et al (2007) A leaf recognition algorithm for plant classification using probabilistic neural network. IEEE, 5–18 Dec 2007. https://doi.org/10.1109/ISSPIT.2007.4458016

5. Fix E, Hodges JL (1951) Discriminatory analysis-nonparametric discrimination: consistent properties. California Univ Berkeley

Google Scholar

6. Cover T, Hart P (1967) Nearest neighbor pattern classification. IEEE Trans Inf Theory 13(1):21–27

Google Scholar

7. Ishak S, Rahiman MHF, Kanafiah SNAM, Saad H (2015) Leaf disease classification using artificial neural network. J Teknol 77(17)

8. Padol P
Confere

Google Scholar

9. Dandawate Y, Kokare R (2015) An automated approach for classification of plant diseases towards development of futuristic decision support system in Indian perspective. In: 2015 International conference on advances in computing, communications and informatics (ICACCI). IEEE, pp 794–799

Google Scholar

10. Singh V, Misra AK (2015) Detection of unhealthy region of plant leaves using image processing and genetic algorithm. In: 2015 International conference on advances in computer engineering and applications. IEEE, pp 1028–1032

Google Scholar

11. https://github.com/spMohanty/PlantVillage-Dataset

12. (2002) Color feature extraction. In: Perspectives on content-based multimedia systems. The information retrieval series, vol 9. Springer, Boston, MA. https://doi.org/10.1007/0-306-47033

Author information

Authors and Affiliations

BSCOER, Pune, India
Vishnu C. Khade

AGCE, Sata
Vishnu C. K

SCSOCE, D
Sanjay B. P

BVCOE, Kolhapur, India

Sachin B. Jadhav

Editor information

Editors and Affiliations

BioAxis DNA Research Centre (P) Ltd., Hyderabad, India
Amit Kumar

Dynexsys, Sydney, NSW, Australia
Stefan Mozar

Rights and permissions

Copyright information

About this paper

Cite this paper

Khade, V.C., Patil, S.B., Jadhav, S.B. (2022). Maize Leaf Healthy and Unhealthy Classification Using Image Processing Technique and Machine Learning Classifiers. In: Kumar, A., Mozar, S. (eds) ICCCE 2021. Lecture Notes in Electrical Engineering, vol 828. Springer, Singapore. https://doi.org/10.1007/978-981-16-7985-8_75

Print ISBN
978-981-16-7984-1

Online ISBN
978-981-16-7985-8

eBook Packages
Engineering
Engineering (R0)

Publish with us

Policies and ethics

Modified direct clustering algorithm for group formation in cellular manufacturing

G C Potdar[1], S U Sapkal[1] and A S Shivade[1]

[1]Department of Mechanical Engineering, Walchand College of Engineering, Sangli, Maharashtra, India.

potdar.c.gaurav@gmail.com, sagarus1201@gmail.com, shivadeanand@yahoo.in

Abstract. In cellular manufacturing system formation of machine-part families is an important task. Cellular manufacturing systems deals with various clustering algorithms which are particularly relevant to the problem of machine component group formation. In this paper, case study from well-known gearbox manufacturing company is considered where there is scope for using cellular manufacturing system. Company is manufacturing the gearbox varying from single stage reduction to four stage reduction. A modified direct clustering algorithm is proposed and is applied after the initial incidence matrix derived from direct clustering algorithm. This algorithm overcomes the problem arises during application of direct clustering algorithm and gives the optimum solution. The algorithm is specifically designed to deal with large amount of data during realistic situations. The results of proposed algorithm are compared with well-known existing algorithms and it is found that the proposed algorithm gives the better solution than the existing algorithms under consideration.

1. Introduction

Group technology deals with the fragmentation of a manufacturing system into subsystems [4]. In order to enable this fragmentation various coding systems and classification have been developed. With the help of these codes, clustering of machine-component into subsystems is accomplished. Clustering analysis is one of the most frequently applied mathematical tools in group technology [6]. Cellular manufacturing is an application of GT to manufacturing. In cellular manufacturing, a few machines, usually dissimilar in function, are grouped into a cell. For mass production a dedicated cell is required which enable to process a family of parts [6].

An XYZ Pvt. Ltd. company which produces gearbox is being considered as a part of work. Company has made changes in their plant layout earlier but failed to meet desired objectives. Distances in between the processes is not feasible as far as plant layout is concern. To overcome these problems company has decided to use cellular manufacturing system. Presently, gearbox varying from single to four stage reduction is being manufactured in the plant. There are common processes and common components in between single to four stage reduction gearbox. Consider an example of single stage gearbox having 13 components and 23 processes. Some processes are common in those 13 components. So, clustering those common processes by applying various algorithms is the requisite task.

As described by Arumugam S [9] the input for a cellular manufacturing problem consists of , a set Y of p parts and a set X of m machines and an m × p matrix A = (a_{ij}), where a_{ij} = 1 or 0 according as the part p_j which is processed on the machine m_i. In the context of similarity, it includes design attributes such as size, shape, etc. and/or manufacturing attributes like length, diameter, surface finish, tolerance, etc. Once if the parts are grouped, then machines, tools and equipment required to process these parts having similarity are grouped together to take the advantages of similarities in manufacturing.

Burbidge J L [1] described that there are three stages in the analysis of the production flow in which the first stage is to determine the design of the department in the factory through the analysis of the factory flow, the second stage is to determine the group of machine components in the group analysis and the third stage is to determine the layout of each group of machine components in the line analysis. Burbidge J L [2] suggested a method for sorting components using punched card processes. This technique created a flow sequence based on the map, but it failed to define a grouping. King J R [3] reviewed the single cluster analysis method, the production flow analysis method, as well as the bond

energy method, and built a rank cluster method. Kusiak A [4] developed an integer programming model that offers a more convenient representation of clustering problems than a matrix model that enhances the performance of component families and machine cells. Ballakur A et al [5] developed a heuristic focused on cell utilization for the design of cell manufacturing systems. Machines are allocated to cells based on workload and cell size limitations. Components are 'assigned' to cells in such a way that most of their operations can be done within cells. Seifoddini H et al [6] analyzed the components of the machine cell formation cycle such as Similarity coefficients, clustering algorithms, and efficiency measurements. New consistency metrics are implemented and a comparative analysis of three different similarity coefficients is performed -the Jaccard similarity coefficient, the weighted similarity coefficient, and the commonality value. Alhourani F [7] Implemented similarity coefficient that incorporates multiple process routing along with operation sequence, production volumes, duplicate machines, and machine capacity. They also proposed a clustering algorithm for the formation of machine cells. The developed similarity coefficient showed greater sensitivity to intercellular movements and improved machine grouping. Telsang M et al [8] implemented cellular manufacturing system to reduce intercellular movements, transport waste, employees' wages to increase productivity. Arumugam S et al [9] developed an algorithm for the identification of bottleneck machines and bottleneck sections in a cellular manufacturing problem along with a cell partition. Mehta S et al [10] developed differential bond energy algorithm and results are compared to the classic bond energy algorithm. Dhayef D et al [11] developed branch and bound algorithm for machine cell and part family and for sequencing and scheduling groups for makespan calculation. The developed algorithm was evaluated by a case study consisting of four items processed on nine machines. Built algorithm can be used to decide the best job and minimize the order of the best group for any kind of problem and completion time (makespan). Chan H M et al [12] developed a direct clustering algorithm that shapes component families and machine groups for cellular manufacturing by iteratively restructuring the machine component matrix. The direct clustering algorithm consists of the matrix being concatenated, moving the rows with the leftmost assigned to the top and the columns with the topmost assigned cell to the left of the matrix.

2. Direct clustering algorithm

2.1. Introduction

Direct clustering algorithm is the method of finding machine and component groups by revamping the sequence in machines and components which are listed in the matrix. The initial incidence matrix is constructed by allocating '1' to the cells when a component goes through a process in a particular machine and '0' when it is not. While applying clustering algorithm it is desired to form a diagonal clustering of component and machines. Therefore, the matrix is sorted in two stages. Firstly, sorting is being concluded based on the counts of the number of entries of '1', columns and rows are sorted in decreasing order of counts. The predicament emerges in second sorting where it postulates the sort as 'leftmost' rows allotments to the top and 'topmost' column allotment to the left. When it is attempted to iterate it for the second sorting, the diagonal element formed is not optimum and can be iterate further. Thus, the algorithm is unable to come to the final matrix which indicate diagonalized form of clustering.

The industrial data of 13 components and 23 processes is converged to 12 components and 12 processes by eliminating common allotments in all components (for example, inward inspection is common for all components so it can be eliminated) and the unique allotment for a single component (for example, inner diameter grinding is a unique process for planet gear and no other component undergone such process). It is not necessary that every time the number of components must be equal to number of processes.

2.2. The clustering algorithm

a. Count the number of '1' in each column and row. Regroup the machine component incidence matrix with rows and columns in decreasing order with virtue of counts of '1'.
b. Contemplating firstly with column number one of the matrix relocate the rows which have '1' as an entries in this column to the top of the matrix. Continual of this procedure with respect to the other column will give the new arrangement for the rows.
c. Is the current matrix being optimum diagonalized?

if yes, then go to 'f'
if no, then go to 'd'

d. Rerun the procedure mentioned in 'b' for rows, starting from row 1. This will give new arrangement for the columns.

e. Is the current matrix being optimum diagonalized?
if yes, then go to 'f'
if no, then go to 'b'

f. Stop

2.3. Application

The machine component incidence matrix with 12 machine and 12 components is explicated in Table 1. Table 1 illustrates the matrix after the first step which is used in direct clustering algorithm. A row numbering from 2 to 4 designate to components and column numbering from 6 to 7 designate to machine or process. The bottommost row and rightmost column designate the count of number of entries of '1' in each column and row respectively.

Table 1. The initial incidence matrix using direct clustering algorithm.

S. No.		1	2	3	4	5	6	7	8	9	10	11	12	Number of entries in row
		2	5	12	8	10	9	6	3	1	11	7	4	↓
1	6	1	1	1	1	1	1	1	1	1			1	10
2	4	1	1	1	1	1		1	1	1	1			9
3	10	1	1	1	1	1	1				1	1		8
4	9	1	1	1	1	1	1				1	1		8
5	2	1	1	1	1			1	1		1			7
6	3				1	1	1	1	1	1			1	7
7	1	1	1	1				1	1	1	1			7
8	8	1		1	1		1					1		5
9	5	1	1						1	1			1	5
10	12			1		1		1						3
11	11	1	1				1							3
12	7	1	1							1				3
Number of entries in column →		10	9	8	7	6	6	6	6	6	5	3	3	

In Table 1, row 6, 4,10,9 and 2 clustering with column 2,5,12 and 8. Continual of iteration through the rows and column it is observed that these formed clustered get disturbed and they get deviated from their desired results of forming machine component family through their diagonal arrangement. The iteration can be done by relocating leftmost row to the top and topmost column to the left. As this iteration process does not follow a proper path for clustering, it becomes difficult to determine optimum diagonal elements. As this diagonal element can further be optimized which can determined by using modified direct clustering algorithm. Modified direct clustering algorithm enables to allocate possible optimum cell arrangement by assigning weights based on the priority of the positioning in the diagonal form.

3. Modified direct clustering algorithm

3.1. Introduction

As discussed earlier, modified direct clustering algorithm is applied after an initial incidence matrix formed in direct clustering algorithm. The aim of clustering is to diagonally form machine component family matrix in three clusters of 4 × 4 (only for 12 × 12 data). First cluster consist of the elements allocated at upper left most part of the matrix (row and column from s no.1 to 4 in table 1), followed by

second cluster which is at the middle part of the matrix (row and column from s no. 5 to 8) and third one which is at lower right most part of the matrix (row and column s no. 9 to 12).

The matrix has undergone the first sorting which is based on the counts of entries '1' in the cell. As discussed in King J R [4], weights are the most important parameter in the clustering. Weights can be given as per the element's configurations required. Here, it is required to cluster the elements in diagonal form in three clusters as mentioned above. Therefore, it is essential to give the priority to first four cells of each column and row as 4^3 and remaining eight cells as 4. Repeat this procedure with respect to middle four values and last four values of each row and column. Now the priority for three clusters of 12 rows and three clusters for 12 columns is set. Sum up those priorities for each row and column and apply the equation 1 for finding out the weights. Seifoddini H [6] worked on similarity coefficient algorithm in which Jaccard's coefficient is applied. Referring to the Jaccard's coefficient the formula is applied as mention in equation 1.

$$W_i = \frac{\text{Sum of priorities of first cluster for } i^{th} \text{ row}}{768} \quad (1)$$

W_i is the weight for i^{th} row and 768 is the maxımum sum of the priority for a row or a column ($4^3 \times 12$). Similarly, equation 1 is applied for other row and columns.

3.2. The proposed clustering algorithm

a. Rearrange the rows and columns to form it as initial incidence matrix as in direct clustering algorithm (based on counts of number of entries of '1' in decreasing order)
b. Formation of the first cluster in which s no. 1 to 4 of rows and columns allotted the priority of 4^3 and for remaining eight elements priority of 4.
c. Sum up the priority for each row and column for constructing the first cluster and apply the equation 1 individually.
d. Sort according to weights in decreasing order and then relocate the rows and columns in decreasing order of their weights.
e. Identify the diagonal elements (while identifying do not repeat the element number in a cluster).
f. Is the current matrix being optimum diagonalized?
   if yes then go to 'g'
   if no then go to 'e'
g. Repeat the procedure 'b', 'c' and 'd' for second cluster and third cluster.
h. Is the current matrix being optimum diagonalized?
   if yes then go to 'k'
   if no then go to 'e'
i. Check for other diagonal elements by rearranging rows and columns (keep on eliminating allotted or overlapped elements)
j. Is the current matrix being optimum diagonalized?
   if yes then go to 'k'
   if no then go to 'e'
k. Stop

The steps in the proposed algorithm are applied on 12 × 12 incidence matrix. The machine component incidence matrix using modified direct clustering algorithm is illustrated in table 2.

Table 2. The machine component incidence matrix using modified direct clustering algorithm.

S. No.		1	2	3	4	5	6	7	8	9	10	11	12	Number of entries in row
		2	5	12	8	6	3	10	9	1	11	7	4	
1	6	1	1	1	1	1	1	1	1	1			1	10
2	4	1	1	1	1	1	1	1		1	1			9
3	10	1	1	1	1			1	1		1	1		8
4	9	1	1	1	1			1	1		1	1		8
5	2	1	1	1	1	1	1				1			7
6	1	1	1	1		1	1			1	1			7
7	3				1	1	1	1	1	1			1	7
8	8	1		1	1				1			1		5
9	5	1	1				1			1			1	5
10	12			1		1		1						3
11	11	1	1						1					3
12	7	1	1							1				3
Number of entries in column		10	9	8	7	6	6	6	6	6	5	3	3	

4. Results and discussion

In modified direct clustering algorithm, there are two stages of sorting which are used after the first sorting from direct clustering algorithm. The second and third sorting from the proposed algorithm concentrates more on diagonal configuration of the matrix. In second sorting, priorities are divided in clusters of three (s no. 1 to 4, s no. 4 to 8 and s no. 9 to 12 for both rows and columns one by one). Priorities are assigned only to cells which has entry as '1'. Firstly, the priority of 4^3 is given for the first cluster (s no. 1 to 4) and for remaining it is 4. As mentioned by King J R [4], the priorities should be given in terms of exponent. For example, if 4, 3 and 2 are the priority for first cluster, second cluster and third cluster respectively. Then the purpose of diagonal configuration of the matrix will not be solved because if number of counts of '1' increased in second and third cluster then weights (which is the part of third stage) obtained will tend towards second and third cluster. This will form element in row number s no. 1 to 4 and column number s no. 5 to 8. In third sorting, the weights are given based on the priority for machine and component and they are arranged in the descending order as shown in table 2. From table 2 it is observed that the elements are diagonalized and there is no scope for the further optimization. After finding out the clusters, elimination of overlapping elements becomes essential as it may affect in bottlenecks. The remaining rows and columns are rearranged manually and configured diagonally as mentioned in the table 2. Thus, the optimum solution is achieved and it is considered as final solution.

Contemplating from table 2 that machines 6,4,10 and 9 forming a cluster with components 2,5,12 and 8. On the other hand, machines 2 and 1 forming a cluster with components 6 and 3. Similarly 3-10, 8-9 and 5-1 are also the effective combinations. Further clustering is not possible as it may lead to the construction of bottlenecks.

5. Conclusion

The optimum solution for system component clustering is not feasible in the case of a direct clustering algorithm, because there is no efficient way to perform iterations. This algorithm is then modified by constructing a machine-component family with a diagonal structure and called as a modified direct clustering algorithm. A comparative evaluation of the machine component incidence matrix is carried out and it is found that direct clustering algorithms are less efficient when it comes to realistic problems as mentioned in earlier research. Moreover, it is found that modified direct clustering algorithms can handle large data and practical problems as they deal with priority by using the initial incidence matrix. Bottlenecks can also be found effectively by a modified direct cluster algorithm.

References

[1] Burbidge J L 1963 Production flow analysis *The Production Engineer* **43** p 742.
[2] Burbidge J L 1969 Production Flow Analysis *Int. Centre for Advanced Technical and Vocational Training*
[3] King J R 1980 Machine-component grouping in production flow analysis: an approach using a rank order clustering algorithm *Int. J. of Production Research* **18(2)** pp 213-232
[4] Kusiak A 1987 The generalized group technology concept. *Int. J. on Production Research* **25(4)** pp 561-569
[5] Ballakur A and Steudels H J 1987 A within-cell utilization based heuristic for designing cellular manufacturing systems *Int. J. of Production Research* **25(5)** pp 639-666
[6] Seifoddini H and Hsu C 1991 Comparative Study of Similarity Coefficients and Clustering Algorithms in Cellular Manufacturing *J. of Manufacturing Systems* **13(2)**
[7] Alhourani F 2013 Clustering algorithm for solving group technology problem with multiple process routings *Computers & Industrial Engineering* **6** pp 781–790
[8] Bharamgude P and Telsang M 2014 Design, analysis and performance simulation of cellular manufacturing system - a case study *Int. J. of Mechanical And Production Engineering* **2(6)** pp 2320-2092
[9] Arumugam S and Saral J 2015 Identification of Bottleneck Elements in Cellular Manufacturing Problem *Int. Conf. on Graph Theory and Information Security* **74** pp 181 – 185
[10] Mehta S Agarwal P Shrivastava P and Barlawala J 2018 Differential bond energy algorithm for optimal vertical fragmentation of distributed databases *J. of Computer and Information Sciences*
[11] Dhayef D and Abdulkhafour A 2018 Developing branch and bound algorithm for cell formation and group scheduling *Engineering and Technology Journal* **36** pp 555-563
[12] Chan H M and Milner D A Direct Clustering Algorithm for Group Formation in Cellular Manufacture *J. of Manufacturing Systems* **1(1)**

Acknowledgement

The authors are grateful to the Kavitsu Transmission Pvt. Ltd., Satara for providing the data and necessary facility.

5. Number of Books Authored

Customer Relationship Management

Prof. (Dr.) Gopal Jahagirdar
Prof. (Dr.) Pranjali S Unkule
Prof. Nitin Kisan Deshmane
Prof. (Dr.) Vilas Pharande

Customer
Relationship
Management

ISSN : 2454-8499

7. Number of New Externally Funded Research Projects Received

8. Funds Received During This Academic Year

SHASHIKANT R. DHUMAL
(B.E.Civil)
Engineer, Contractor & Govt. Redg. Valuer
ADARSH PRIDE, Pirwadi (Khed) Nr. Hotel
Mahendra Executive, NH-4, SATARA-415002
Email.dhumal.shashikant@gmail.com

Govt. Registered Valuer
Redg. No.: CAT/1/143-2007
A-14728, Institution of Valuers
Phone: (office): 95-2162-245585
Mob: +91 9881732892, 9822277507
Shashikant_dhumal@rediffmail.com

Ref No. SRD/2021/12-13

Date - 15/03/2021

PROJECT SPONSORSHIP LETTER

TO,

The Principal,

Arvind Gavali College of Engineering, Satara

Subject – Regarding sponsorship given to project for ArvindGavali College of Engineering, Satara

Respected Sir,

We have sponsored the project on "Experimental study on effect of glass powder cement concrete"

We are very happy to sponsored this project for ArvindGavali College of Engineering, Satara.

Total cost of Project : 20000/- has been borne by us.

Thanking You.

Name of student

1.Saurav Jadhav

2.Sachin Pujari

3.Phalke Shubham

4.Bhosale Aniket

SHASHIKANT R. DHUMAL GOVT. REGD. NO CAT/1/ 143/2007 VALUER

Shashikant R. Dhumal
Engineer & Govt. Regd. Valuer
CAT/1/143/2007

J.W.INFRA
Address :
Bungalow No. 25At. Post Khawali,Tal,
DistSatara 415003.

RiteshAmale:9637910100

Ref no J-W/E-21/14-15 Date - 3/12/2021

SPONSORSHIP LETTER

Subject – Project sponsorship for Effect of granite and marble waste to enhance the properties of silty soil

This is to certify that company has offered sponsorship for above given project to following students studying in :

Arvind Gavali College of Engineering, Satara (B.E. Civil)

Name of the students :

1.SutarSujitHariram

2.ShindePrajwalPradipkumar

3.SutarOmkar Sanjay

4ChavanVikramBhagavan

5.JadhavRohit Sanjay

J. W. INFRA

Proprietor

Source Code Technology Pvt. Ltd.

15/10/2020

To

The Principal,
Arvind Gavali College of Engineering,
Satara

Sub: Regarding Sponsoring the project work on "Online Grocery Market"
Respected Sir,

We are glad to share that following candidates from Computer Science & Engineering at your institute have been selected for carrying out project "Online Grocery Market".

1. Priyanka Metkari(51654520171124210004)
2. Tejaswini koli (51654520171124210005)
3. Kirti Mandhare (51654520171124210012)
4. Rutuja pawar (51654520171124210046)
5. Akshay Kshirsagar (2065451242001)

We have found them hardworking and Sincere. With the allotment of sponsorship, these students may use utilize the company resources and data sets for building applications. Also they will be guided and trained by domain experts. The approximate cost sanctioned for the project Rs. 12000/-. All rights regarding the project application are reserved to company. It is joint responsibility of both company and institute to maintain the confidentiality.

Regards.

Vinod thete

Source Code Technology Pvt. Ltd. Pune

Source Code Technology Pvt. Ltd.

#sohum creast, Near gurudwara Mandir, Valhekarwadi, Chinchwad, Pune-411035, Mob No: 9673921886

E-mail: vinodthete190@gmail.com , www.sourcecodetechnology.com Pune 411035

Source Code Technology Pvt. Ltd.

16/10/2020

To

The Principal,
Arvind Gavali College of Engineering,
Satara

Sub: Regarding Sponsoring the project work on "Forest Fire Detection and Control"
Respected Sir,

We are glad to share that following candidates from Computer Science & Engineering at your institute have been selected for carrying out project "Forest Fire Detection and Control".

1. Chitranjali Kalange(51654520171124210021)
2. Rutuja Shinde (51654520171124210036)
3. Bhavana Kadam (51654520171124210020)
4. Shivani Yadav (51654520171124210039)

We have found them hardworking and Sincere. With the allotment of sponsorship, these students may use utilize the company resources and data sets for building applications. Also they will be guided and trained by domain experts. The approximate cost sanctioned for the project Rs. 16000/-. All rights regarding the project application are reserved to company. It is joint responsibility of both company and institute to maintain the confidentiality.

Regards.

Vinod thete

Source Code Technology Pvt. Ltd. * pune

Source Code Technology Pvt. Ltd.

#sohum creast, Near gurudwara Mandir, Valhekarwadi, Chinchwad, Pune-411035, Mob No: 9673921886

E-mail: vinodthete190@gmail.com , www.sourcecodetechnology.com Pune 411035

RUDRA

architects, interiors, landscape & master planners.

Sai ratna building, near mane hospital,Visawa park, Satara, Maharashtra 415002

555harshalgurav@gmail.com

Date 05/07/21

To,

The principal,

Arvind Gavali College of Engg.,

Satara- 415015

Subject: Sponsorship Confirmation Letter

Dear Sir/Madam,

This letter verifies that we sponsoring the Customized Web Application for **RUDRA_construction_** company project for AGCE final year Computer Science & Engineering students 2020-2021. It is our pleasure to confirm that the following students are working on our construction company web application project. We will host this web application on our server in next week.

Miss Pawar Sayali Somnath	Roll. No. - 4010
Miss Kirve Ravina Dipak	Roll. No. - 4022
Miss Kshirsagar Harshada Pramod	Roll. No. - 4024
Miss Jagtap Swati Sudhir	Roll. No. - 4057
Miss Dhotre Sonali Pitambar	Roll. No. - 4073

Our company management was reviewed **RUDRA _construction_** project outcome and performance. We hope the same co-operation in future.

For, M/s Harshal Gurav & Associate

Mob. : 9673002991 / 92 / 93 / 94 / 95

KAVADE
ENGINEERING WORKS

For All type of Mechanical Job Works & All type of Gear Sprocket Cutting Suppliers

Plot No. W-71, Near Top Gear, Kay Bouvet Engineering Pvt. Ltd., Additional MIDC, Satara - 415004
Ph. / Fax : 02162 - 240322 email : kavadeengineering@gmail.com

Date :- 1 Feb 2021

To,
Principal,
Arvind Gavali College Of Engineering,
Panmalewadi,Tal.&Disty.-Satara 415002

Sub:- Sponsorship for the industrial Project in **Polyester Let off Machine.**

Sir,

Kavade Engineering Works Agrees to pay all required expenses for the project carried out by following students. Company will taking responsibility of all expenses required for this project carried during this financial year. Following work is carried out under the Guidance of Mr. Akshay N. Kavade Sir Dy Manager, Kavade Engineering Works, Satara.

Title of Project :- **Polyester Let off Machine**

Approximate cost sanctioned for the project is Rupees 1,10,000/-

Name of the students :-

1) Mohotkar Mahesh Sanjay
2) Phalke Tushar Sidharth
3) Gaikwad Shubham Vivek
4) Bhosale Snehal Santosh

Mr. Phalke Tushar Sidharth coordinates all other essentials required at the time of student attaining Industry for the said project work. Student must finish their project work within stipulated time period. And submit to our company.

Authorized Signatory,

Akshay Naynath Kavade
Kavade Engineering Works Satara

OMKAR ENGINEERING

Specialist in: All types Tool Room Works, Press Tool & Mould, Jigs, Fixtures & Press Parts.

Wai Unit : Plot No.:B-114,Wai MIDC, Tal - Wai, Dist - Satara.

Mob : 9730148185 Email : omkarengineering2013@gmail.com

DATE: 23 AUG 2021

To

ARVIND GAVALI COLLEGE OF ENGINEERING,

PANMALEWADI, SATARA.

Subject: Completion Letter of Project

Respected sir,

We pleased to inform you that your following students of final year B-Tech in mechanical engineering student of your institute intersects to on project "**COMPACT ROLLING AND BENDING MACHINE**". We complete our whole project with in company. Whole project cost is Bourne by company and it's cost 8,000 and also it paid by company. During the project work their behavior and punctuality is quite good

1. **Sushant Ravindra Bhosale** **9860351526**
2. **Nikhil Vishnu Sawant** **9970236362**
3. **Satyam Prakash Kumbhar** **7020758817**
4. **Vishvjeet Vijay Vibhute** **8421026571**

Thanking You

Your Faithfully,

For **OMKAR ENGINEERING WAI SATARA.**

Omkar Engineering

Mr. Aniket Babar

(Managing Director)

NOVEL INDUSTRIES

Plot No- 13/5 M.I.D.C. Kodoli , Near Cooper Corporation Satara ,Maharashtra,41005,India
GST NO :- 27AAJFN2421PIZY

Date: 23/3/2021

Project Completion Certificate

This is to certify that below Mentioned students had undertaken the project "Performance Study Of Electric Discharge Machine (EDM) Processes "from acadmic year2020-2021. The project has been completed to our satisfaction.

We wish them all the best in their future and endeavours.

1 Kakade Ajay Sanjay. (PRN NO :- 516545201811611210040)

2. Mule Pankaj Ramesh (PRN NO:- 2065451612009)

3.Asawale Suraj Dnyandev. (PRN NO:- 5165452017116121002 7)

4. Chavan Aditya Sampat. (PRN NO:- 2065451612022)

NOVEL INDUSTRIES, SATARA

WORKS : H-19, OLD M.I.D.C., SATARA - 415 004. MH.(INDIA)
TEL : (02162) 245649.
CIN NO : U27310PN1980PTC023353

PARANJAPE AUTOCAST PVT. LTD.

To,

Date:-28 Jan 2021

Principal,

Arvind Gavali college of engineering,

Satara.

Sub:- Sponsorship for the industrial project in **Ladle Lining**.

Sir,

Paranjape Autocast pvt Ltd. agrees to pay all required expenses for the project carried out by following students. Company will taking responsibility of all expenses required for this project carried during this financial year. Following project work is carried out under the guidance of Mr. R. C. Sartale sir, Dy Manager, Paranjape Autocast pvt Ltd.

Title of project:- LADLE LINING BY USING READYMADE EXOTHERMIC SLEEVE.

Approximate cost sanctioned for the project in Rupees 250000/-

Name of students:-

1) Kiran Vitthal Chavan
2) Omkar Kishor Mahadik
3) Aashutosh Avinash Suryavanshi
4) Siddhesh Ganesh Kadam

Mr. K.V Chavan coordinates all other essentials required at the time of student attaining industry for the said project work. Students must finish their project work within stipulated time period.

Authorized signatory

Paranjape Autocast Pvt Ltd

PARANJAPE AUTOCAST PVT. LTD. SATARA

OMKAR ENGINEERING

Specialist in: All types Tool Room Works, Press Tool & Mould, Jigs, Fixtures & Press Parts.

Wai Unit : Plot No.:B-114,Wai MIDC, Tal - Wai, Dist - Satara.

Mob : 9730148185 Email : omkarengineering2013@gmail.com

DATE: 27 JUL 2021

To

H.O.D.

MECHANICAL DEPARTMENT,

ARVIND GAVALI COLLEGE OF ENGINEERING,

PANMALEWADI, SATARA.

Subject: Sponsorship Letter For Project

Respected sir,

We pleased to inform you that your following students of final year B.Tech Mechanical Engineeringhave been successfully completed project on **"COMPACT ROLLING AND BENDING MACHINE".**

During the project work their behavior and punctuality is quite good.

1. **Sushant Ravindra Bhosale** **9860351526**
2. **Nikhil Vishnu Sawant** **9970236362**
3. **Satyam Prakash Kumbhar** **7020758817**
4. **Vishvjeet Vijay Vibhute** **8421026571**

Thanking You

Your Faithfully,

For OMKAR ENGINEERING WAI SATARA.

Omkar Engineering

Mr. Aniket Babar

(Managing Director)

OMKAR ENGINEERING

Specialist in: All types Tool Room Works, Press Tool & Mould, Jigs, Fixtures & Press Parts.

Wai Unit : Plot No.:B-114,Wai MIDC, Tal - Wai, Dist - Satara.

Mob : 9730148185 Email : omkarengineering2013@gmail.com

DATE: 23 AUG 2021

To

ARVIND GAVALI COLLEGE OF ENGINEERING,

PANMALEWADI, SATARA.

Subject: Completion Letter of Project

Respected sir,

We pleased to inform you that your following students of final year B-Tech in mechanical engineering student of your institute intersects to on project "**COMPACT ROLLING AND BENDING MACHINE**". We complete our whole project with in company. Whole project cost is Bourne by company and it's cost 8,000 and also it paid by company. During the project work their behavior and punctuality is quite good

1. **Sushant Ravindra Bhosale** **9860351526**
2. **Nikhil Vishnu Sawant** **9970236362**
3. **Satyam Prakash Kumbhar** **7020758817**
4. **Vishvjeet Vijay Vibhute** **8421026571**

Thanking You

Your Faithfully,

For OMKAR ENGINEERING WAI SATARA.

Omkar Engineering

Mr. Aniket Babar

(Managing Director)

SBK
SBK Machinery & Consulting Services, Koregaon
Manuracturers of Hydraulic Machinery & Business Consultant

Ref No. 05/A/2021

Date: 28th January 2021

To,
Principal,
Arvind Gavali College of Engineering,
At. Panmalewadi, Post - Varye,
Tal. & Dist. Satara 415015

Subject: Sponsored a project work at our Enterprise.

Respected sir,

Following undersigned students of " **Arvind Gavali College of Engineering**" B. E. Mechanical Class are working on the project named as " **Vertical Hydraulic Bailing Machine** ". This particular project is sponsored by our company.

As the project will be useful for us in future.

The name of students working on this project are as follow:

Sr. No.	Name of student	Roll No.
1	Mr. Mulik Akash Dipak	4101
2	Mr. Sutar Sachin Basavraj	4106
3	Mr. Jadhav Ganesh Madhukar	4151

This is for your information and co-operation in this regard is highly appreciated.

Thanking You,

Yours Faithfully

SBK Machinery & Consulting Services Koregaon

Mr. Shahrukh Shaikh

BE (Mech) MBA (Project Management)
Manager
SBK Machinery & Consulting Services

Contact : 7385201241 / 9766310928.
E-mail : sbkmachinery20@gmail.com
Near New S.T. Stand, Koregaon, Tal. Koregaon, Dist. Satara. 415501

URJA SETU

MAKE YOUR OWN PATH

c/o Urja setu, 29/A, Rakshalekha Society, Pune Satara Road,
Dhankawadi, Near Dhankawadi Post Office, Dhankawadi, Pune,
Maharashtra 411043

To,
Arvind Gavali College of Engineering,
Satara

SUBJECT: PERMISSION TO WORK ON PROJECT
"AUTOMATIC PAINTING MACHINE"

Respected Sir,

This has reference to above subject; we have informed you that the final year B-Tech in mechanical engineering student of your institute intersects to work on project "Automatic Painting Machine".

Sr.No.	Name	Enrollment No.
1	**Mr. Nawadkar Rupesh Bhaskar**	**51654520181161210085**
2	**Mr. Chavan Rohit Shankar**	**51654520181161210086**
3	**Mr. Sankpal Yogesh Pandurang**	**51654520181161210087**
4	**Mr. Bhosale Pratik Narendra**	**51654520181161210088**

The facilities are available at our door for conduction and completion of project.

Thank You.

URJA SETU

Ameeth Sutar
Proprietor

Date: 04-06-2021
Place: Pune, Maharastra

urjasetu1@gmail.com

www.urjasetu.com

Shri Ganesh Industries

MFG OF. STAMPING & PRESS PART'S

Office: 125/2, 21A, Industrial Estate, Ogalewadi, Karad Ph. (02164) 651763, 9225804226

Ref No. Shri Ganesh I Forad / 2017-18 / Dec-9

To,

The head of the department.

Mechanical Engineering

Arvind Gavali College of Engineering, Satara.

Subject – Acceptance letter for Industrial Project work.

Dear Sir,

Following student of Arvind Gavali College of Engineering, Satara Studying in final year of mechanical engineering Had approached for their final year project entitled "Pneumatic Operated Feeder".

The project is sponsored by Shri Ganesh Industry and it will be designed and manufacturing in our premises as per Specification. They will be undergoing the project work from 28th November, 2020 to 28th February 2021.

Name of student:-

- Aparna Vasant Suryawanshi
- Kavita Rajesh Lad
- Suraj Namdeo Phalke
- Akash Lahu Salunkhe

Yours Faithfully,

For SHRI GANESH INDUSTRY

Shri Ganesh Industries Ogalewadi-415105

Vikas B. Jadhav

proprietor

9. Other Achievements

SANJAY GHODAWAT UNIVERSITY, Kolhapur

Empowering Lives Globally !

Established under section 2 (f) of UGC Act 1956

Sanjay Ghodawat University Act XL of 2017 of Govt. of Maharashtra | Approved by PCI, COA & AICTE

Certificate

This is to certify that

Diksha Jadhav

has attended Six Days workshop on *NAAC Accreditation Process for University*

organized by *IQAC* from *26-04-2021 to 1-5-2021.*

Mrs. Shobha Kumbar
IQAC Co-ordinator

Dr. N. K. Patil
Officiating Registrar

Dr. M. T. Telsang
Officiating Vice chancellor

Pimpri Chinchwad Education Trust's

Pimpri Chinchwad College of Engineering & Research

AN ISO 9001:2015 CERTIFIED INSTITUTE

CERTIFICATE
OF APPRECIATION

This certificate is proudly presented on 19 May 2021 to

Diksha Sanjay Jadhav

For participating in a webinar on **"Tendering & Execution of Works"**
organized by Department of Civil Engineering
Pimpri Chinchwad College of Engineering & Research, Pune.

Coordinator
Prof. S. S. Bobade

HOD Civil
Dr. S. S. Sawarkar

PRINCIPAL
Dr. Harish Tiwari

SANJAY GHODAWAT UNIVERSITY, Kolhapur

Empowering Lives Globally !

Established under section 2 (f) of UGC Act 1956

Sanjay Ghodawat University Act XL of 2017 of Govt. of Maharashtra | Approved by PCI, COA & AICTE

Certificate

for Participation

Human Resource Development Cell

This is to certify that

Dr. / Mr. / Ms. Diksha Jadhav

has successfully participated in

Two Day Workshop on COs, POs, PSOs Mapping and Attainment

held online on 26th and 27th May 2021.

Congratulations for your accomplishment !

Dr. Sunanda M. Shinde
Co-ordinator HRD Cell

Dr. N. K. Patil
Officiating Registrar

Dr. M. T. Telsang
Officiating Vice chancellor

BHARATI VIDYAPEETH
(DEEMED TO BE UNIVERSITY), INDIA
COLLEGE OF ENGINEERING, PUNE

and

SHAHAJIRAO PATIL VIKAS PRATISHTHAN'S
S. B. PATIL COLLEGE OF ENGINEERING, INDAPUR, PUNE

certifies that

Dr. Vijay R. Thombare

has participated and successfully completed One Week Online Faculty Development Programme On **"Research Opportunities in Environmental Engineering"** organised by Department of Civil Engineering, Bharati Vidyapeeth (Deemed to be University), College of Engineering, Pune in association with Department of Civil Engineering Shahajirao Patil Vikas Pratishthan's S. B. Patil College of Engineering, Indapur, Pune from 20th July 2020 to 25th July 2020

Dr. Pravin D. Nemade
Chairman, FDP
Principal, SBPCOE, Indapur

Dr. Anand Bhalerao
Chairman, FDP
Dean & Principal, BV(DU) COE, Pune

SAMARTH EDUCATIONAL TRUST

ARVIND GAVALI COLLEGE OF ENGINEERING, SATARA

TEQIP 3 Sponsored 5 Days Online FDP

on

Recent Advances in Health 5.0 In-line with NEP 2020

TEQIP-3

Certificate

This is to certify that, Dr.vijay R. Thombare

From. Arvind gavali collage of engineering satara

Participated in Recent Advances in Health 5.0 In-line with NEP 2020

held at

Arvind Gavali College of Engineering, Satara.

Date.: 22nd to 26th March 2021

Dr.G.S.Mirajkar	Dr.V.A.Pharande	Mr.Nishant A. Gavali
Coordinator	Principal	Secretary

SAMARTH EDUCATIONAL TRUST

ARVIND GAVALI COLLEGE OF ENGINEERING, SATARA

TEQIP 3 Sponsored 5 Days Online FDP

on

Recent Advances in Health 5.0 In-line with NEP 2020

TEQIP-3

Certificate

This is to certify that, Todkar Snehal Shivaji

From. Arvind Gavali College Satara

Participated in Recent Advances in Health 5.0 In-line with NEP 2020

held at

Arvind Gavali College of Engineering, Satara.

Date.: 22nd to 26th March 2021

Dr.G.S.Mirajkar	Dr.V.A.Pharande	Mr.Nishant A. Gavali
Coordinator	Principal	Secretary

SAMARTH EDUCATIONAL TRUST

ARVIND GAVALI COLLEGE OF ENGINEERING, SATARA

TEQIP 3 Sponsored 5 Days Online FDP

on

Recent Advances in Health 5.0 In-line with NEP 2020

AGCE NAAC Accredited

TEQIP-3

Certificate

This is to certify that, Vikas Satish Nikam

From. Arvind Gavali College of Engineering Satara

Participated in Recent Advances in Health 5.0 In-line with NEP 2020

held at

Arvind Gavali College of Engineering, Satara.

Date.: 22nd to 26th March 2021

Dr.G.S.Mirajkar	Dr.V.A.Pharande	Mr.Nishant A. Gavali
Coordinator	Principal	Secretary

SAMARTH EDUCATIONAL TRUST

ARVIND GAVALI COLLEGE OF ENGINEERING, SATARA

TEQIP 3 Sponsored 5 Days Online FDP

on

Recent Advances in Health 5.0 In-line with NEP 2020

AGCE NAAC Accredited

TEQIP-3

Certificate

This is to certify that, *Mr. Pranav Avinash Pathak*

From. *Arvind Gavali College of Engineering, Satara*

Participated in Recent Advances in Health 5.0 In-line with NEP 2020

held at

Arvind Gavali College of Engineering, Satara.

Date.: 22nd to 26th March 2021

Dr.G.S.Mirajkar
Coordinator

Dr.V.A.Pharande
Principal

Mr.Nishant A. Gavali
Secretary

SAMARTH EDUCATIONAL TRUST

ARVIND GAVALI COLLEGE OF ENGINEERING, SATARA

TEQIP 3 Sponsored 5 Days Online FDP

on

Recent Advances in Health 5.0 In-line with NEP 2020

AGCE NAAC Accredited

TEQIP-3

Certificate

This is to certify that, Dr. Mrs. Varsha Kiran Bhosale

From. Arvind Gavali College of Engineering, Satara

Participated in Recent Advances in Health 5.0 In-line with NEP 2020

held at

Arvind Gavali College of Engineering, Satara.

Date.: 22nd to 26th March 2021

Dr.G.S.Mirajkar	Dr.V.A.Pharande	Mr.Nishant A. Gavali
Coordinator	Principal	Secretary

APPROVED | DTE CODE 4304 | ACCREDITED | BUSINESS INCUBATION CENTRE | 125 Year of WOMEN EMPOWERMENT | उन्नत भारत अभियान UNNAT BHARAT ABHIYAN | Virtual Labs An MHRD Govt of India Initiative

महर्षी कर्वे स्त्री शिक्षण संस्था

Maharshi Karve Stree Shikshan Samstha's CUMMINS COLLEGE OF ENGINEERING FOR WOMEN NAGPUR

CUMMINS_VIRTUALLAB_RES20-9590

Certificate of Participation

This is to certify that Prof./Dr./Mr./Mrs./Ms. DR. VARSHA KIRAN BHOSALE

from ARVIND GAVALI COLLEGE OF ENGINEERING SATARA has attended a **webinar on**

"Virtual Labs: Effective Tool for Teaching and Learning" organized in association with AICTE &

Virtual Lab, Centre for System Design, NITK Surathkal held on 10 July 2020.

PARTICIPATING INSTITUTES

IIT Delhi | IIT Kanpur | IIT Bombay | IIT Madras | IIT Kharagpur | IIT Guwahati | IIT Roorkee | IIIT Hyderabad | Amrita University | Dayalbagh University | NITK Surathkal | COE Pune

Dr. B. P. Joshi
Principal, CCoEW Nagpur

Dr. K.V. Gangadharan
Participating Institute Coordinator,
Virtual Labs (NMEICT, MHRD) NITK, Surathkal

Prof. Prasanna Mahankar
VLab Nodal Center In-charge
CCoEW Nagpur

SAMARTH EDUCATIONAL TRUST

ARVIND GAVALI COLLEGE OF ENGINEERING, SATARA

TEQIP 3 Sponsored 5 Days Online FDP

on

Recent Advances in Health 5.0 In-line with NEP 2020

TEQIP-3

Certificate

This is to certify that, Mrs Rajani Mahendra Mandhare

From. Arvind Gavali college of engineering

Participated in Recent Advances in Health 5.0 In-line with NEP 2020

held at

Arvind Gavali College of Engineering, Satara.

Date.: 22nd to 26th March 2021

Dr.G.S.Mirajkar	Dr.V.A.Pharande	Mr.Nishant A. Gavali
Coordinator	Principal	Secretary

MIT Academy of Engineering

MIT Academy of Engineering, Alandi (D.), Pune

An Autonomous Institute, NAAC – 'A' Grade

Affiliated to Savitribai Phule Pune University

E-Certificate of Participation

This is to certify that *Mrs Rajani Mahendra Mandhare* of Arvind Gavali college of Engineering, Satara.

Participated and completed successfully one week online Short Term Training Programme (STTP) on "**Deep Learning Tools & Applications in Engineering & Science**" sponsored by All India Council for Technical Education (AICTE) ,New Delhi, organized by School of Computer Engineering and Technology (SCET), MIT Academy of Engineering, Alandi(D.),Pune during 10 May 2021 through 15 May 2021.

Dr. Rajewari Goudar	Prof. Ranjana Badre	Dr. Mahesh D. Goudar
Coordinator	**Dean SCET**	**Director**

IEEE STUDENT BRANCH

Nawab Shah Alam Khan College of Engineering and Technology

CERTIFICATE

OF COMPLETION

Mr. Vijay Bhanudas Gujar

of Satara Polytechnic Satara (0042) has attempted Quiz on "**R - PROGRAMMING**" and has passed with 55% , organized by **CSE , IT Department** and **IEEE Student Branch, NSAKCET** which was held from 20th to 22th August 2020.

Mr. Mohd Khaleel Ahmed	**Dr. G. S. S. RAO**	**Dr. Mohammad S. Qaseem**	**Dr. Syed Abdul Sattar**
Advisor	**Prof. & HOD IT**	**Prof. & HOD CSE**	**Principal**
IEEE SB NSAKCET	IT Department	IEEE SB COUNSELOR, NSAKCET	NSAKCET

AISSMS
INSTITUTE OF INFORMATION TECHNOLOGY
ADDING VALUE TO ENGINEERING

Approved by AICTE New Delhi, Recognized by the Government of Maharashtra
and Affiliated to Savitribai Phule Pune University.
Accredited by NAAC with A grade

Department of Engineering Sciences

International Biodiversity Day- 22 May 2021

Certificate of Participation

Mr. Vijay Bhanudas Gujar

of Arvind Gavali College of Engineering Satara

has successfully participated in Techno-Social Awareness Quiz on "Biodiversity" organized by Dept. of Engineering Sciences, AISSMS's Institute of Information Technology, Pune.

Mrs.G.N.Mawale	**Dr.P.G.Mushrif**	**Dr.P.B.Mane**
Faculty Coordinator	**HOD, Engg. Sciences**	**Principal**

SCAD

ST. MOTHER THERESA ENGINEERING COLLEGE

Vagaikulam, Thoothukudi - 628 102.

Department of Computer Science & Engineering

Certificate of Participation

This is to Certify that Mr. Vijay Bhanudas Gujar has actively participated in the webinar on "Dynamic Routing using Cisco Packet Tracer" presented by Dr. J. Immanuel Johnraja, Associate Professor & Head, Department of CSE, Karunya Institute of Technology and Sciences, Coimbatore, organized by Computer Science & Engineering of St. Mother Theresa Engineering College, Thoothukudi, Tamil Nadu on 04-07-2020.

D.Asir,
AP/CSE, SMTEC

M.Beemajan Shaheen,
HOD/CSE, SMTEC

Thakur Educational Trust's (Regd.)

THAKUR INSTITUTE OF MANAGEMENT STUDIES, CAREER DEVELOPMENT & RESEARCH

(Approved by AICTE, Govt. of Maharashtra & Affiliated to University of Mumbai)

ISO 9001 : 2015 Certified • MCA Program Accredited by National Board of Accreditation, New Delhi

Thakur Educational Campus, Shyamnarayan Thakur Marg, Thakur Village, Kandivali (East), Mumbai - 400 101.
Tel: 022-67308301/2; 28840484/91 • Telefax: 022-28852527

Estd. 2001

Spoken Tutorial

Certificate

This is to certify that Dr./Mr./Ms. **Vijay Gujar**

has attended two weeks Short Term Training Programme on **"IT for Sustainability"** organized from 15 June 2020 to 26 June 2020 approved by ISTE, New Delhi and Spoken Tutorial, IIT-Bombay.

Mr. Shirshendu Maitra
Co-ordinator

Dr. Vinita Gaikwad
Convener

Certificate ID
K7ROUO-CE000005

St.MOTHER THERESA ENGINEERING COLLEGE

VAGAIKULAM, THOOTHUKUDI - 628 102

DEPARTMENT OF COMPUTER SCIENCE AND ENGINEERING

CERTIFICATE OF PARTICIPATION

This is to certify that Mr.Vijay Bhanudas Gujar has actively participated in webinar on "**Security Issues in Internet of Things(IoT)**" presented by Dr.S.Sujatha, Professor & Head, Department of MCA at Anna University - BIT Campus, Trichy organized by Department of Computer Science and Engineering of St.Mother Theresa Engineering College,Tuticorin, Tamilnadu on 06.07.2020.

C. Karpagavalli,
AP/ CSE, SMTEC

M. Beemajan Shaheen,
HOD/ CSE, SMTEC

SAMARTH EDUCATIONAL TRUST

ARVIND GAVALI COLLEGE OF ENGINEERING, SATARA

TEQIP 3 Sponsored 5 Days Online FDP

on

Recent Advances in Health 5.0 In-line with NEP 2020

AGCE NAAC Accredited

TEQIP-3

Certificate

This is to certify that, Shingade Rohini Dilip

From. Agce

Participated in Recent Advances in Health 5.0 In-line with NEP 2020

held at

Arvind Gavali College of Engineering, Satara.

Date.: 22nd to 26th March 2021

Dr.G.S.Mirajkar	Dr.V.A.Pharande	Mr.Nishant A. Gavali
Coordinator	Principal	Secretary

Dr. Babasaheb Ambedkar Technological University
Vidyavihar, Lonere, Dist. Raigad - 402 103

TEQIP

TEQIP-III SPONSORED
ONE WEEK ONLINE FACULTY DEVELOPMENT PROGRAMME

Certificate of Participation

This is to certify that **Mr. B. Meghya Nayak, Assistant Professor (Electrical Engineering),** of **Arvind Gavali College of Engineering, Satara** has participated in TEQIP-III sponsored **Faculty Development Programme (FDP)** on **"Industrial IoTs, Industry 4.0 & Disruptive Technologies"** organized by **Dr. B. A. Technological University, Lonere** (Maharashtrta) from **May 05-10, 2020,** which is conducted using online platforms and ICT tools.

Dr. Ajij D. Sayyad	Dr. Nilesh G. Patil	Dr. Shankar B. Deosarkar
Associate Professor, MIT Aurangabad (Course Coordinator)	Principal, Marathwada Institute of Technology, Aurangabad	Institute Project Director, (IPD), TEQIP-III, Dr, B. A. T. U., Lonere

SAMARTH EDUCATIONAL TRUST

ARVIND GAVALI COLLEGE OF ENGINEERING, SATARA

TEQIP 3 Sponsored 5 Days Online FDP

on

Recent Advances in Health 5.0 In-line with NEP 2020

TEQIP-3

Certificate

This is to certify that, Mr. B. M. NAYAK

From. Arvind Gavali college of Engineering, Satara

Participated in Recent Advances in Health 5.0 In-line with NEP 2020

held at

Arvind Gavali College of Engineering, Satara.

Date.: 22nd to 26th March 2021

Dr.G.S.Mirajkar	Dr.V.A.Pharande	Mr.Nishant A. Gavali
Coordinator	Principal	Secretary

SAMARTH EDUCATIONAL TRUST

ARVIND GAVALI COLLEGE OF ENGINEERING, SATARA

TEQIP 3 Sponsored 5 Days Online FDP

on

Recent Advances in Health 5.0 In-line with NEP 2020

AGCE NAAC Accredited

TEQIP-3

Certificate

This is to certify that, Eva Gupta

From. Arvind Gavali college of engineering

Participated in Recent Advances in Health 5.0 In-line with NEP 2020

held at

Arvind Gavali College of Engineering, Satara.

Date.: 22nd to 26th March 2021

Dr.G.S.Mirajkar	Dr.V.A.Pharande	Mr.Nishant A. Gavali
Coordinator	Principal	Secretary

SAMARTH EDUCATIONAL TRUST

ARVIND GAVALI COLLEGE OF ENGINEERING, SATARA

TEQIP 3 Sponsored 5 Days Online FDP

on

Recent Advances in Health 5.0 In-line with NEP 2020

TEQIP-3

Certificate

This is to certify that, Bichkar J. S.

From. Arvind Gavali College of Engineering, Satara

Participated in Recent Advances in Health 5.0 In-line with NEP 2020

held at

Arvind Gavali College of Engineering, Satara.

Date.: 22nd to 26th March 2021

Dr.G.S.Mirajkar	Dr.V.A.Pharande	Mr.Nishant A. Gavali
Coordinator	Principal	Secretary

SAMARTH EDUCATIONAL TRUST

ARVIND GAVALI COLLEGE OF ENGINEERING, SATARA

TEQIP 3 Sponsored 5 Days Online FDP

on

Recent Advances in Health 5.0 In-line with NEP 2020

AGCE NAAC Accredited

TEQIP-3

Certificate

This is to certify that, Basavaraj Nelogal

From. Arvind Gavali College of Engineering Satara

Participated in Recent Advances in Health 5.0 In-line with NEP 2020

held at

Arvind Gavali College of Engineering, Satara.

Date.: 22nd to 26th March 2021

Dr.G.S.Mirajkar	Dr.V.A.Pharande	Mr.Nishant A. Gavali
Coordinator	Principal	Secretary

SAMARTH EDUCATIONAL TRUST

ARVIND GAVALI COLLEGE OF ENGINEERING, SATARA

TEQIP 3 Sponsored 5 Days Online FDP

on

Recent Advances in Health 5.0 In-line with NEP 2020

AGCE NAAC Accredited

TEQIP-3

Certificate

This is to certify that, Bhutkar Hrutuja Sanjay

From. Arvind Gavali College of Enginnering, Satara

Participated in Recent Advances in Health 5.0 In-line with NEP 2020

held at

Arvind Gavali College of Engineering, Satara.

Date.: 22nd to 26th March 2021

Dr.G.S.Mirajkar	Dr.V.A.Pharande	Mr.Nishant A. Gavali
Coordinator	Principal	Secretary

SAMARTH EDUCATIONAL TRUST

ARVIND GAVALI COLLEGE OF ENGINEERING, SATARA

TEQIP 3 Sponsored 5 Days Online FDP

on

Recent Advances in Health 5.0 In-line with NEP 2020

TEQIP-3

Certificate

This is to certify that, *Dr Gayatri S. Mirajkar*

From. *Arvind Gavali college of Engineering Satara*

Participated in Recent Advances in Health 5.0 In-line with NEP 2020

held at

Arvind Gavali College of Engineering, Satara.

Date.: 22nd to 26th March 2021

Dr.G.S.Mirajkar
Coordinator

Dr.V.A.Pharande
Principal

Mr.Nishant A. Gavali
Secretary

Dr. Babasaheb Ambedkar Technological University, Lonere

WEBINAR on

Antenna Design through Simulation Using TaraNG 19.1

In association with NUMEREGION's TaraNG (Interactive | Learning | Pedagogy)

Under the aegis of TEQIP-3 (Technical Education Quality Improvement Programme)

Certificate of Attendance

This is to certify that ***Dr. Gayatri Shashikant Mirajkar***

From Arvind Gavali College of Engineering, Satara

has successfully Attended the webinar on **"Antenna Design through Simulation Using TaraNG 19.1".** This Webinar was organized by **Department of Electronics and Telecommunication Engineering**, Dr. Babasaheb Ambedkar Technological University, Lonere **in association** with **NUMEREGION TECHNOLOGY (OPC) PVT LTD, PUNE on** May 25, 2020.

Swapnil		
Swapnil Gaul	**Prof. S. V. Khobragade**	**Dr. S. L. Nalbalwar**
Founder | Director NUMEREGION	Dean Associate, Skill Development	Dean Academics, Head, Dept. of E&TC

SPRINGER NATURE

Certificate of Participation

ONLINE WORKSHOP

on 'Academic Book Writing & Related Topics' Organized by

SPRINGER NATURE

This is to certify that

Dr./Prof./Mr./Ms. **Gayatri Mirajkar**

has successfully participated in the online workshop

on 22th May' 2020.

Dated
22th May' 2020

Vikash Kumar
Director – Sales, Springer Nature

SHIVAJI UNIVERSITY KOLHAPUR

MHRD
Pandit Madan Mohan Malaviya National Mission for Teachers and Training

IEEE SA
STANDARDS ASSOCIATION

Pandit Madan Mohan Malviya National Mission on Teachers and Teaching (PMMMNMTT)
Faculty Development Centre in Cyber security & Data Science
Shivaji University, Kolhapur

Participation Certificate

This is to certify that

GAYATRI MIRAJKAR

has participated in the webinar organized by IEEE STANDARDS ASSOCIATION & MHRD PMMMNMTT FDC, Shivaji University, Kolhapur on "IEEE 802.11 and Building Wireless Community Networks", held on 22nd May 2020.

Mr. Srikanth Chandrasekaran
Senior Director, Standards & Technology
IEEE

Prof. R.K. Kamat
Coordinator, PMMMNMTT FDC
Shivaji University, Kolhapur

TEQIP-3

Technical Education Quality Improvement Programme

Sponsored One Day Webinar

Certificate of Participation

This is to certify that

Dr. Gayatri Shashikant Mirajkar

has participated in

One Day Webinar on New Higher Education Policy and Digitization of Education

Jointly organized by Dr. Babasaheb Ambedkar Technological University, Lonere and

R. C. Patel Institute of Technology, Shirpur under TEQIP-III on May 17, 2020

Prof. Dr. S. B. Deosarkar
Coordinator
TEQIP-III IPD, Professor, DBATU, Lonere

Prof. Dr. J. B. Patil
Coordinator
Principal, RCPIT, Shirpur

SAMARTH EDUCATIONAL TRUST

ARVIND GAVALI COLLEGE OF ENGINEERING, SATARA

TEQIP 3 Sponsored 5 Days Online FDP

on

Recent Advances in Health 5.0 In-line with NEP 2020

AGCE NAAC Accredited

TEQIP-3

Certificate

This is to certify that, Barkade Vijay Tukaram

From. Arvind Gavali College of Engineering Satara

Participated in Recent Advances in Health 5.0 In-line with NEP 2020

held at

Arvind Gavali College of Engineering, Satara.

Date.: 22nd to 26th March 2021

Dr.G.S.Mirajkar	Dr.V.A.Pharande	Mr.Nishant A. Gavali
Coordinator	Principal	Secretary

SAMARTH EDUCATIONAL TRUST

ARVIND GAVALI COLLEGE OF ENGINEERING, SATARA

TEQIP 3 Sponsored 5 Days Online FDP

on

Recent Advances in Health 5.0 In-line with NEP 2020

TEQIP-3

Certificate

This is to certify that, *Tanuja Phadatare*

From. *Arvind Gavali College of Engineering*

Participated in Recent Advances in Health 5.0 In-line with NEP 2020

held at

Arvind Gavali College of Engineering, Satara.

Date.: 22nd to 26th March 2021

Dr.G.S.Mirajkar
Coordinator

Dr.V.A.Pharande
Principal

Mr.Nishant A. Gavali
Secretary

SAMARTH EDUCATIONAL TRUST

ARVIND GAVALI COLLEGE OF ENGINEERING, SATARA

TEQIP 3 Sponsored 5 Days Online FDP

on

Recent Advances in Health 5.0 In-line with NEP 2020

TEQIP-3

Certificate

This is to certify that, Vivek Mohite

From. Arvind Gavali College of Engineering

Participated in Recent Advances in Health 5.0 In-line with NEP 2020

held at

Arvind Gavali College of Engineering, Satara.

Date.: 22nd to 26th March 2021

Dr.G.S.Mirajkar	Dr.V.A.Pharande	Mr.Nishant A. Gavali
Coordinator	Principal	Secretary

SAMARTH EDUCATIONAL TRUST

ARVIND GAVALI COLLEGE OF ENGINEERING, SATARA

TEQIP 3 Sponsored 5 Days Online FDP

on

Recent Advances in Health 5.0 In-line with NEP 2020

AGCE NAAC Accredited

TEQIP-3

Certificate

This is to certify that, pratik mahajan

From. AGCE satara

Participated in Recent Advances in Health 5.0 In-line with NEP 2020

held at

Arvind Gavali College of Engineering, Satara.

Date.: 22nd to 26th March 2021

Dr.G.S.Mirajkar	Dr.V.A.Pharande	Mr.Nishant A. Gavali
Coordinator	Principal	Secretary

SAMARTH EDUCATIONAL TRUST

ARVIND GAVALI COLLEGE OF ENGINEERING, SATARA

TEQIP 3 Sponsored 5 Days Online FDP

on

Recent Advances in Health 5.0 In-line with NEP 2020

TEQIP-3

Certificate

This is to certify that, *Dr Vilas Arjun Pharande*

From. *Arvind Gavali college of Engineering Satara*

Participated in Recent Advances in Health 5.0 In-line with NEP 2020

held at

Arvind Gavali College of Engineering, Satara.

Date.: 22nd to 26th March 2021

Dr.G.S.Mirajkar
Coordinator

Dr.V.A.Pharande
Principal

Mr.Nishant A. Gavali
Secretary

SAMARTH EDUCATIONAL TRUST

ARVIND GAVALI COLLEGE OF ENGINEERING, SATARA

TEQIP 3 Sponsored 5 Days Online FDP

on

Recent Advances in Health 5.0 In-line with NEP 2020

AGCE NAAC Accredited

TEQIP-3

Certificate

This is to certify that, Suraj Sajjan Ghadage

From. Arvind Gavali College of Engineering Satara

Participated in Recent Advances in Health 5.0 In-line with NEP 2020

held at

Arvind Gavali College of Engineering, Satara.

Date.: 22nd to 26th March 2021

Dr.G.S.Mirajkar	Dr.V.A.Pharande	Mr.Nishant A. Gavali
Coordinator	Principal	Secretary

SAMARTH EDUCATIONAL TRUST

ARVIND GAVALI COLLEGE OF ENGINEERING, SATARA

TEQIP 3 Sponsored 5 Days Online FDP

on

Recent Advances in Health 5.0 In-line with NEP 2020

TEQIP-3

Certificate

This is to certify that, Mr. Pranesh Bamankar

From. Arvind Gavali College of Engineering Satara

Participated in Recent Advances in Health 5.0 In-line with NEP 2020

held at

Arvind Gavali College of Engineering, Satara.

Date.: 22nd to 26th March 2021

Dr.G.S.Mirajkar	Dr.V.A.Pharande	Mr.Nishant A. Gavali
Coordinator	Principal	Secretary

SAMARTH EDUCATIONAL TRUST

ARVIND GAVALI COLLEGE OF ENGINEERING, SATARA

AGCE
NAAC Accredited

TEQIP-3

TEQIP 3 Sponsored 5 Days Online FDP

on

Recent Advances in Health 5.0 In-line with NEP 2020

Certificate

This is to certify that, Mr.Ankur V.Kamble

From. AGCE

Participated in Recent Advances in Health 5.0 In-line with NEP 2020

held at

Arvind Gavali College of Engineering, Satara.

Date.: 22nd to 26th March 2021

Dr.G.S.Mirajkar	Dr.V.A.Pharande	Mr.Nishant A. Gavali
Coordinator	Principal	Secretary

SAMARTH EDUCATIONAL TRUST

ARVIND GAVALI COLLEGE OF ENGINEERING, SATARA

TEQIP 3 Sponsored 5 Days Online FDP

on

Recent Advances in Health 5.0 In-line with NEP 2020

TEQIP-3

Certificate

This is to certify that, Alatkar Manisha Nilkanth

From. Arvind Gavali college of engineering, panmalewadi, Satara

Participated in Recent Advances in Health 5.0 In-line with NEP 2020

held at

Arvind Gavali College of Engineering, Satara.

Date.: 22nd to 26th March 2021

Dr.G.S.Mirajkar	Dr.V.A.Pharande	Mr.Nishant A. Gavali
Coordinator	Principal	Secretary

SAMARTH EDUCATIONAL TRUST

ARVIND GAVALI COLLEGE OF ENGINEERING, SATARA

TEQIP 3 Sponsored 5 Days Online FDP

on

Recent Advances in Health 5.0 In-line with NEP 2020

AGCE NAAC Accredited

TEQIP-3

Certificate

This is to certify that, Mr. Sandeep Pawar

From. Arvind Gavali college of Engineering satara.

Participated in Recent Advances in Health 5.0 In-line with NEP 2020

held at

Arvind Gavali College of Engineering, Satara.

Date.: 22nd to 26th March 2021

Dr.G.S.Mirajkar	Dr.V.A.Pharande	Mr.Nishant A. Gavali
Coordinator	Principal	Secretary

SAMARTH EDUCATIONAL TRUST

ARVIND GAVALI COLLEGE OF ENGINEERING, SATARA

TEQIP 3 Sponsored 5 Days Online FDP

on

Recent Advances in Health 5.0 In-line with NEP 2020

AGCE NAAC Accredited

TEQIP-3

Certificate

This is to certify that, PRANOD RAGHUNATH NIKAM

From. AGCE , SATARA

Participated in Recent Advances in Health 5.0 In-line with NEP 2020

held at

Arvind Gavali College of Engineering, Satara.

Date.: 22nd to 26th March 2021

Dr.G.S.Mirajkar	Dr.V.A.Pharande	Mr.Nishant A. Gavali
Coordinator	Principal	Secretary

SAMARTH EDUCATIONAL TRUST

ARVIND GAVALI COLLEGE OF ENGINEERING, SATARA

TEQIP 3 Sponsored 5 Days Online FDP

on

Recent Advances in Health 5.0 In-line with NEP 2020

TEQIP-3

Certificate

This is to certify that, Nikhil Vilas Ghadge

From. AGCE,SATARA

Participated in Recent Advances in Health 5.0 In-line with NEP 2020

held at

Arvind Gavali College of Engineering, Satara.

Date.: 22nd to 26th March 2021

Dr.G.S.Mirajkar	Dr.V.A.Pharande	Mr.Nishant A. Gavali
Coordinator	Principal	Secretary

SAMARTH EDUCATIONAL TRUST

ARVIND GAVALI COLLEGE OF ENGINEERING, SATARA

TEQIP 3 Sponsored 5 Days Online FDP

on

Recent Advances in Health 5.0 In-line with NEP 2020

AGCE NAAC Accredited

TEQIP-3

Certificate

This is to certify that, Ravi kamble

From. AGCE satara

Participated in Recent Advances in Health 5.0 In-line with NEP 2020

held at

Arvind Gavali College of Engineering, Satara.

Date.: 22nd to 26th March 2021

Dr.G.S.Mirajkar	Dr.V.A.Pharande	Mr.Nishant A. Gavali
Coordinator	Principal	Secretary

SAMARTH EDUCATIONAL TRUST

ARVIND GAVALI COLLEGE OF ENGINEERING, SATARA

TEQIP 3 Sponsored 5 Days Online FDP

on

Recent Advances in Health 5.0 In-line with NEP 2020

AGCE NAAC Accredited

TEQIP-3

Certificate

This is to certify that, *Prof. Pratik Manohar Tambe*

From. *Arvind Gavali college of Engineering satara*

Participated in Recent Advances in Health 5.0 In-line with NEP 2020

held at

Arvind Gavali College of Engineering, Satara.

Date.: 22nd to 26th March 2021

Dr.G.S.Mirajkar
Coordinator

Dr.V.A.Pharande
Principal

Mr.Nishant A. Gavali
Secretary